Investigation of chloride transport mechanisms in *Arabidopsis thaliana* root

Jiaen Qiu
M.Biotech

A dissertation submitted for the degree of
Doctor of Philosophy
School of Agriculture, Food and Wine
Faculty of Sciences
The University of Adelaide

2015

Declaration

This work contains no material which has been accepted for the award of any other degree or diploma in any university or other tertiary institution to Jiaen Qiu and, to the best of my knowledge and belief, contains no material previously published or written by another person, except where due reference has been made in the text.

I give consent to this copy of my thesis when deposited in the University Library, being made available for loan and photocopying, subject to the provisions of the Copyright Act 1968.

I also give permission for the digital version of my thesis to be made available on the web, via the University's digital research repository, the Library catalogue, the Australasian Digital Theses Program (ADTP) and also through web search engines, unless permission has been granted by the University to restrict access for a period of time.

…… ……

Jiaen Qiu **Date**

Acknowledgements

I wish to thank my supervisors Assoc Prof. Matthew Gilliham and Dr. Stuart Roy for your guidance, inspiration and support. Your knowledge, patience and encouragement have helped me throughout my PhD. Matt and Stuart are always available for discussions on my interesting data and enthusiastic about my project. I really enjoyed my PhD, it is a wonderful and memorable time.

I am also grateful to my co-supervisor Prof. Mark Tester for your contributions. Your ideas and guidance have been vital for me to complete my project. Thank you for your support.

I would like to thank the financial support provided by the University of Adelaide during my PhD through the provision of Adelaide Graduate Research Scholarship, and further thank Grain Research and Development Corporation and IWPMB2013 organizing committee for provision of the financial support to attend IWPMB2013 in Japan.

I also would like to thank those people that have contributed to my research. Dr Aurelie Evrard and Dr Ute Baumann from ACPFG for providing microarray data, Dr Maroru Okamoto and Ms Karen Francis for teaching nitrate concentration analysis, Ms Jodie Kretschmer from ACPFG for kindly donating expression vectors, Ms Asmini Athman for assisting CO_2 measurement, Dr Yuan Li from ACPFG for assisting qRT-PCR analysis, Dr Zhengyu Wen for teaching me radioactive flux assay and all the lab crew, Dr Sam Henderdon, Dr Sunita Ramesh, Dr Caitlin Byrt, Dr Bo Li, Dr Bo Xu, Dr Caitlin Byrt, Mr Maclin Dayod, Mr Qu Yue, Dr Brad Hocking and my friend Dr Jin Zhang and Dr Wenmian Huang.

Finally, I would like to thank my parents for their support throughout all of my studies as well as my partner Mr Jia Jiang for helping me get through the tough times.

Table of Contents

Table of Figures

List of Tables

Abbreviations and symbols

Abbreviation	Full term
#	Number
%	Percentage
±	Plus and minus
×	Times
°C	Degree celsius
µg	Microgram(s)
µl	Microliter(s)
µM	Micromolar
µmol	Micromole(s)
β	Beta
3´	Three prime end
3-D	Three dimensional
5´	Five prime end
A-9-C	Anthracene-9-carboxylic acid
ABA	Abscisic acid
ABARE	Australian Bureau of Agricultural and Resource Economics
ABRC	Arabidopsis Biological Resource Centre
ABS	Australian Bureau of Statistics
ACPFG	Australian Centre for Plant Functional Genomics
AGRF	Australian Genome Research Facility
amiRNA	Artificial micro ribonucleic acid
At	Arabidopsis thaliana
BLAST	Basic Local Alignment Search Tool
BNS	Basal Nutrient Solution
bp	Base pair
BSA	Bovine serum albumin
Ca^{2+}	Calcium ion
CaMV	Cauliflower mosaic virus
CCC	Cation chloride co-transporter
cDNA	Complimentary deoxyribonucleic acid
CFP	Cyan florescent protein
Cl^{-}	Chloride ion
CLCs	Chloride channel proteins
cm	Centimeter
Col-0	Columbia-0
cRNA	Capped ribonucleic acid
dH_2O	Deionised water

DIDS	4,4'-Diisothiocyano-2,2'-stilbenedisulfonic acid
DNA	Deoxyribonucleic acid
dNTP	Mixture of equal equivalents of dATP, dTTP, dCTP and dGTP
dS	Decisiemens
DTT	Dithiothreitol
E.coli	Escherichiacoli
ECe	Electrical conductivity
EDTA	Ethylenediaminetetraacetic acid
FAO	Food and Agriculture Organization
FW	Fresh weigh
g	Gravity
g	Gram(s)
gDNA	Genomic deoxyribonucleic acid
GFP	Green fluorescent protein
GOI	Gene of interest
GUS	β-glucuronidase protein
H^+	Hydrogen ion
H^+- ATPase	Proton-ATPase
ha	Hectare
HCl	Hydrochloric acid
HEPES	4-(2-hydroxyethyl)-1-piperazineethanesulfonic acid
HKT	High-affinity K+ transporter
hr	Hour(s)
Hv	Hordeum vulgare
IBSC	International Barley Genome Sequencing Consortium
ICP-AES	Inductively Coupled Plasma Optical Emission Spectrometry
K^+	Potassium ion
kb	Kilo base pairs
KBr	Potassium bromide
KCl	Potassium chloride
KD	Knock down
kD	Kilo dalton
KF	Potassium fluoride
KOH	Potassium hydroxide
LB	Left border (of T-DNA)
LBmedia	Luria betanimedia
Ler	Lands bergerecta
M	Molar
MES	2-(N-morpholino) ethanesulfonic acid
mg	Milligram (s)
$MgCl_2$	Magnesium chloride
Min	Minute (s)
ml	Millilitre (s)
mol	Mole

MS	Murashige and Skoog media
mV	Micro voltage
MYTH	Membrane Yeast Two-Hybrid
nA	Nanomolar
Na^+	Sodium ion
NaBr	Sodium bromide
NaF	Sodium fluoride
$NaNO_3$	Sodium nitrate
NaOH	Sodium hydroxide
NASC	European Arabidopsis Stock Centre
NCBI	National Centre for Biotechnology Information
ng	Nanogram (s)
nl	Nanolitre
NLWRA	National Land & Water Resource Audit
nM	Nanomolar
nm	Nanometer
NMDG	N-Methyl-D-glucamine
NO_3^-	Nitrate ion
NRTs	Nitrate transporters
NUE	Nitrogen use efficiency
OD	Optical density
OEX	Over- expression
OR	Outward rectifying
Os	Oryzasativa
P/B	Peak/background ratio
PEG	Polyethylene glycol
PBS	Phosphate buffered saline
PCR	Polymerase chain reaction
PM	Plasma membrane
POT	Protodependent oligo-peptide transporter
qRT-PCR	Quantitative reverse transcription polymerase chain reaction
QTL	Quantitative trait loci
RIL	Recombinant inbred lines
RNA	Ribonucleic acid
RO	Reverse osmosis treated
rpm	Rotation per minute
RT-PCR	Reverse transcription polymerase chain reaction
SDS	Sodium dodecyl sulfate
SEM	Standard error of the mean
SKOR	Stelar k^+ outwardly-rectifying channel
SLAC	Slowly activated anion conductance
SSC	Saline sodium citrate
TAE	Tris-acetate-EDTA
TAIR	The Arabidopsis Information Resource

Taq	Polymerase identified from T. aquaticus
T-DNA	Transfer deoxyribonucleic acid
TEVC	Two electrode voltage clamp
Tm	Melting temperature
TMD	Trans-membrane domain
Tris	tris(hydroxymethyl)aminomethane
Tx	Transgenic plants of generation x
U	Unite(s)
UAS	Upstream activation sequence
UTR	Untranslated region
w/v	Weight per volume
Ws	Wassilewskija
WT	Wildtype
X-IRAC	Xylem-inwardly rectifying anion conductance
X-KORC	Xylem-K+outward rectifying channel
X-QUAC	Xylem-quickly activating anion conductance
X-SLAC	Xylem-slow activating anion conductance
YFP	Yellow fluorescent protein

Abstract

Salinity tolerance is correlated with shoot chloride (Cl^-) exclusion in many horticultural and crop species (e.g. grapevine, soybean). It is hypothesized that the key regulatory step in root-to-shoot transfer of Cl^- is conferred by plasma membrane-localised anion transporters associated within the root vasculature. Reducing long-distance Cl^- transport by manipulating the regulation of anion transporters in the root vasculature is therefore a strategy that promises to increase plant tolerance to saline environments. However, the information of which candidate genes are responsible for this process is limited. To gain a greater knowledge of the long distance Cl^- movement from a molecular aspect, a number of candidate anion transporters from *Arabidopsis thaliana* were identified from a preliminary microarray study. Quantitative PCR was used to indicate transcriptional levels of candidate anion transporters that decreased upon NaCl and ABA treatment. Based on this analysis, *AtSLAH1*, *AtSLAH3* and *AtNRT1.5* were selected as genes of interest (GOI) that were likely to be involved in the Cl^- movement between the root stele symplast and the xylem vessels.

To functionally characterize the transport properties of all GOIs at a protein level, various heterologous systems were used to investigate the anion (Cl^- and NO_3^-) transport capacity. Two-electrode voltage clamp electrophysiology was used to measure the currents that were generated by the target anions crossing oocyte membranes. A yeast expression system was also used to further study the anion transport properties *in vitro*.

AtSLAH1 cRNA injected oocytes were not able to produce significant anion currents. Also, no evident anion currents were generated from a site-directed mutant of AtSLAH1 in a putative phosphorylation site injected into oocytes. Although there was evidence that anion currents were elicited from *AtSLAH1* and *AtSnRk2.3* co-injected oocytes, due to difficulties in the ability to reproduce these results, it is uncertain whether AtSLAH1 can function as an anion transporter in the conditions tested. Both wild type and site-mutated *AtSLAH1* was also separately transformed into yeast for further examination without an observable phenotype.

In order to examine the effect of altered *AtSLAH1* expression on shoot anion accumulation, *AtSLAH1* amiRNA knockdown and constitutive over expression of *AtSLAH1* mutant plants were generated. *AtSLAH1* knockdown lines (T_2) exhibited strong repression in transcript abundance in low salt environments and resulted in a significant reduction in shoot Cl^- when compared to nulls. Constitutive over expression of *AtSLAH1* showed increased shoot Cl^- contents under high salt stress. These results indicated the potential role of AtSLAH1 in Cl^- transport in plants.

Electrophysiological characterization of AtSLAH3 in oocytes showed that AtSLAH3 was able to produce significant NO_3^- but not Cl^- currents suggesting a role in the efflux of NO_3^- out of cells in most of circumstances. Similar results were gained in *AtSLAH3*- transformed yeast. However, *AtSLAH3* over-expression lines showed a decreased shoot Cl^- without an effect on shoot NO_3^- under high salt stress compared to null plants. The potential reasons for this are discussed and further experiments are proposed to test these hypotheses.

Although AtNRT1.5 has been reported to transport NO_3^-, electrophysiological characterization of AtNRT1.5 in *X. Laevis oocytes* was not able to detect any anion currents induced by the gene. Interestingly, AtNRT1.5 transformed yeast showed a significant inhibited phenotype (grow less well than empty vector control) when challenged with high concentration of Cl^- and NO_3^- within the growth media, indicating a role the transport of both anions. Constitutive over- expression lines showed a potent shoot Cl^- reduction under high salt stress compared to nulls. Interestingly, no significant NO_3^- accumulation in shoot was identified. These results might suggest that AtNRT1.5 was able to regulate both Cl^- and NO_3^- transport from root to shoot; however, the mechanism by which this occurs is unclear.

Previous findings indicated the possibilities that Cl^- and NO_3^- can be transported through the same anion channel/transporter. To further study the regulation of Cl^- and NO_3^- uptake, an anion blocker (DIDS) was used to test the anion shoot accumulation under different salt conditions. Under high salt stress, DIDS was able to reduce the Cl^- accumulation and increase

the NO_3^- contents in shoots. Further experiments are required at both a physiological and molecular level to further understand how plants recognize and respond to this blocker, as the molecular targets of this blocker are a potential way to improve the plant salt tolerance and nitrogen use efficiency under high salt stress.

In summary, new information was revealed on several candidates that affect root-to-shoot loading of chloride and new research avenues have been proposed based on the findings of this study.

Chapter 1 Introduction, literature review and research aims

1.1 Introduction

High concentrations of sodium chloride (NaCl) in soils reduces crop yield (Tester and Munns 2008, Rengasamy 2010, Roy *et al*., 2014. Sodium chloride, a dominant salt in saline soils, dissociates in the soil solution into Na^+ and Cl^-. Most salinity research has concentrated on the toxic effect of Na^+ on plant growth as most cereals are more sensitive to Na^+ compared to Cl^- (Munns and Tester 2008). As such, Na^+ toxicity and transport has been relatively well documented at both a physiological and molecular level in a variety of plant species (Davenport *et al*., 2005, Apse and Blumwald 2007, Munns and Tester 2008, Plett and Møller 2010, Roy *et al*., 2014). In barley and wheat, Na^+ is the main ion which causes salt-induced damage (Tester and Davenport 2003). However, in other economically important crop plants, like soybean, grapevine, citrus and lotus it is leaf Cl^-accumulation, not Na^+, that is most closely and most frequently correlated with salt toxicity symptoms such as decreased plant growth and photosynthesis (Mass and Hoffman 1977, Downton *et al*. 1990, Walker *et al*., 1997, Storey and Walker, 1999, Walker *et al*., 2002, Zhang *et al*., 2002, Tregeagle *et al*., 2006, Teakle *et al*., 2007, Teakle and Tyerman 2010, Gong *et al*., 2011). However, it has been proposed that the regulation of both Na^+ and Cl^- transport is significant for salt tolerance, even in species where one ion is more overtly toxic than the other (Teakle and Tyerman 2010).

Previous studies have highlighted the importance of controlling shoot Cl^- accumulation in improving plant salinity tolerance. As such, the identification of the molecular determinants that underpin root-to-shoot transfer of Cl^- and the related-signaling pathways will help provide a better understanding of general plant Cl^- transport mechanisms as well as provide information that could one day be used to alleviate the Cl^- toxicity in commercial crop plants. The following review will focus firstly on the transport pathways of Cl^- in roots and secondly, the molecular basis of root-to-shoot Cl^- transport. It will also serve to identify knowledge

gaps related to the control of shoot Cl^- concentration under salinity stress and candidate anion transporters for that underpin this process.

Most biochemical and electrophysiological evidence suggests that the loading of Cl^- and Na^+ into the xylem from root stelar cells, by proteins on the plasma membrane, is a dominant factor controlling both shoot Cl^- and Na^+ concentrations (reviewed in sections 1.6-1.8). The linkage between the control of Cl^- transport and salt tolerance has been identified in *Medicago* and suggests that plants which accumulate less Cl^- in the shoot are more salt tolerant (Rogers *et al*. 1997). Under saline conditions (40 mM NaCl), salt-tolerant *Medicago* (cv. Haifa) maintained a lower level of Cl^- concentration in the shoot compared to salt-sensitive *Medicago Trifolium repens L.* (Rogers *et al*., 1997). It has also been shown that salt tolerant wheat was able to accumulate less Cl^- within the xylem-sap when compared to salt sensitive genotypes of wheat (Lauchli *et al*., 2008). Taken together, it is suggested that reduced Cl^- in the transpiration stream improves plant salinity tolerance. Therefore, salt tolerance is correlated with the control of shoot Cl^- accumulation.

Charge balance is another issue that needs to be considered in salinity studies. When one ion is accumulated, a counter ion of opposite charge must also be accumulated by the plant for osmotic and charge balance. The most readily available ions in the environment and that accumulate in the plant for these purposes are generally K^+ or Na^+ and Cl^- or NO_3^- (Teakle and Tyerman 2010). Therefore, in addition to Na^+ and Cl^- transport, K^+ and NO_3^- transport are involved in a plant's response to salt stress. In addition, if Na^+ tolerance is improved in wheat and barley, it may reveal Cl^- toxicity symptoms that have been masked by the effects of Na^+ toxicity (Tavakkoli *et al*., 2012). Thus, studies of salt tolerance should focus on Na^+ and Cl^-, as well as the counter ions K^+ and NO_3^- (Teakle and Tyerman 2010).

Shoot Na^+ exclusion is an important component of salinity tolerance (Tester and Davenport 2003, Hauser and Horie 2010, Roy *et al*., 2014). Several ion transporters have been functionally characterized as being involved in shoot Na^+ exclusion. *Arabidopsis thaliana*

High-affinity K^+ transporter 1;1 (HKT1;1) is responsible for retrieving Na^+ from the root metaxylem into xylem parenchyma cells (Davenport *et al*., 2007). Plants with reduced or no *AtHKT1;1* expression have increased root-to-shoot Na^+ translocation and increased leaf Na^+ (Rus *et al*. 2006, Davenport *et al*., 2007). Overexpression of *AtHKT1;1* in Arabidopsis root stele cells significantly reduced the shoot Na^+ and therefore increase salt tolerance (Møller *et al*., 2009). Salt Overly Sensitive 1 (SOS1), a plasma membrane localised Na^+/H^+ antiporter, has also been hypothesised to retrieve Na^+ from the xylem stream under severe salt stress but under Na^+ gradients in non-saline conditions is believed to load Na^+ into the xylem (Shi *et al*., 2003). However, genes encoding proteins involved in loading or the retrieval of Cl^- from the xylem are still to be definitively identified.

Recently, genes encoding anion transporters, such as those within the nitrate transporter NPF (NRT1/PTR Family) (Léran *et al*., 2014), the chloride channel (CLC) and the slow activating anion channels (SLAC) families, have been identified (De Angeli *et al*., 2009, Li *et al*., 2010, Lin *et al*., 2008, Negi *et al*., 2008, Geiger *et al*., 2009, Geiger *et al*., 2010, Hedrich 2012, Krapp *et al*., 2014). Functional characterization of these transporters indicates that most of these transporters are permeable to both NO_3^- and Cl^- to varying degrees. As Cl^- and NO_3^- are both monovalent anions and can often be transported by the same proteins, identification of the anion selectivity of transporters expressed within the root stele may help with the understanding of Cl^- transport pathways that control accumulation of Cl^- in the shoot.

1.2 Soil salinity and Australian agricultural production

Improving the salinity tolerance of crop plants is widely advocated as key in maintaining world food security (Rengasamy 2006, Tester and Langridge 2010, Schroeder *et al*., 2013). Both nationally and internationally, the increasing incidence of salinity-affected agricultural land is decreasing the productivity of conventional crop species (Tester and Davenport 2003). With the global population predicted to increase from 6.1 billion to 9.3 billion by 2050 (http://www.unfpa.org/swp/2001/), food shortages will be inevitable unless crop yields can

be increased and marginal lands reclaimed for cultivation (Tester and Langridge 2010). In Australia 5.7 million ha of agricultural soils are currently affected by dryland salinity. It is predicted this area will increase to 17 million ha by 2050 (http://www.anra.gov.au/topics/salinity/risk-hazard/index.html#risk). Strategies to increase crop productivity on such soils include better soil management and crop improvement (Tester and Langridge 2010). Compared to the long term gains presented by intensive soil amelioration strategies, crop improvement offers an attractive sustainable alternative (Munns *et al.*, 2012). Huge untapped natural variation exists within the plant kingdom with respect to salinity tolerance and this potential has only recently been exploited to increase productivity within the field (reviewed in Sanchez *et al*., 2008, Roy *et al*., 2011, Roy *et al*., 2013).

1.3 Plant response to salinity

The plant's response to salinity has been classified into three main components (Figure 1.1): 1) response to the shoot ion independent stress imposed by decreased water availability from the soil by building up high concentrations of osmotically active solutes within tissues; 2) exclusion of Na^+ and Cl^- ions from the shoot by altering the transport of ions in both the root and stems of plants to ensure that ions are not accumulated to toxic concentrations in leaves; and 3) tissue tolerance, compartmentalization of Na^+ and/ or Cl^- in intracellular compartments (such as vacuoles) to avoid the accumulation of Na^+ or Cl^- in the cytoplasm or apoplast to a toxic level (Munns and Tester 2008, Roy *et al*., 2014, Munns and Gilliham 2015). Studies on cereals have suggested that Na^+ exclusion from the shoot is a primary component of salinity tolerance in wheat, rice and barley, as the yield of cereal crops is often negatively correlated with shoot Na^+ concentrations (James *et al*., 2006, Plett and Møller 2010, Tester and Davenport 2003). In some Cl^- sensitive species, particularly for legumes, such as *Lotus tenuis* (Teakle *et al*., 2007), Cl^- exclusion from shoot is positively correlated with salt tolerance (Teakle and Tyerman 2010). However, the mechanism that controls Cl^- exclusion is not fully understood.

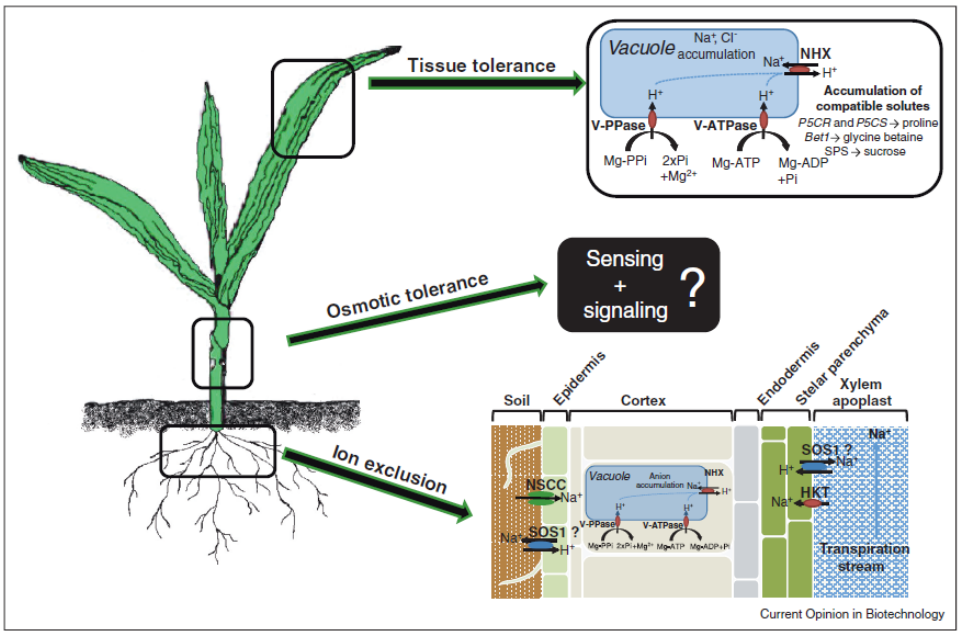

Figure 1.1 Three major components of a crop plant responses to salt tolerance. 1) Osmotic tolerance; 2) Ion exclusion; 3) Tissue tolerance (Adapted from Roy *et al*., 2014)

1.4 Chloride as a plant micronutrient

Chlorine is an essential micronutrient, it is usually present within plants as Cl^-, and contributes to the regulation of a variety of physiological processes under normal conditions (Rognes 1980, Teakle *et al*., 2010, Teakle and Tyerman 2010, White and Broadley 2001). A deficiency of Cl^- reduces leaf growth rate of plants and suppresses the development of lateral roots (White and Broadley 2001). Cl^- deficiency in plants is rare as the inputs of Cl^- from rain or irrigation water, sea spray, dust and air pollution make the Cl^- concentration in soils on average 4 to 8 kg ha^{-1} (White and Broadley 2001) whereas the minimum requirement of plants for crop growth is around 0.2- 0.4 g kg^{-1} dry matter (Marschner 1995). Chloride regulates activities of several enzymes in the cytoplasm, for instance, asparagine synthetase, which shows an increase in the affinity for its substrate (glutamine) in the presence of Cl^- (Rognes 1980). Furthermore, Cl^- is required for water-splitting at the oxidizing site of photosystem II and therefore facilitates plant oxygen release and aids photosynthesis (Izawa *et al*., 1969). In addition, the plasma membrane localised H^+- ATPase, which is involved in regulation of proton-pumping (from the cytoplasm to apoplast) and membrane potential, is

also a key enzyme directly regulated by Cl^- (Churchill and Sze 1984). Chloride efflux out of cells, as it provides a current that is equal and opposite to the H^+ flux carried by the H^+-ATPase can prevent stabilize the membrane potential from becoming too negative (Lorenzen *et al*. 2004). Chloride is also co-transported into the plant across the plasma membrane by a $Cl^-/ 2H^+$ symport mechanism (Sanders 1980). Therefore, Cl^- transport can help regulate the electrochemical potential difference across membranes (Teakle and Tyerman 2010, Tyerman 1992, White and Broadley 2001).

1.5 Chloride toxicity varies in plants

Normally, the Cl^- concentration of plant tissues is about 4-7 mg g^{-1} dry weight in Cl^--sensitive plants (glycophytes) and 15-50 mg g^{-1} dry weight in Cl^--tolerant plants (some halophytes) (Xu *et al*., 2000). Although Cl^- is an essential micronutrient, it can be toxic to plants if Cl^- accumulates at high concentrations in the cytoplasm (Teakle and Tyerman 2010). Too much Cl^- accumulation in the leaves will inhibit the production of chlorophyll and accelerate the production of proline (Storey and Walker 1999). Therefore, plant growth will be affected and yield will be reduced.

Interestingly, differences in sensitivity to Cl^- is often related to restricting Cl^- transport to the shoot between species and cultivars (Munns and Tester 2008, White and Broadley 2001, Henderson *et al*., 2014), which has been demonstrated in many plants, such as barley (*Hordeum vulgare*) (Greenway and Munns 1980), *Citrus* spp. (Storey and Walker 1999) and grapevine (*Vitis* spp.) (Fort *et al*., 2013). Several *Citrus* spp. rootstocks, such as Cleopatra mandarin (*Citrus reshni Hort. ExTan*.) and Rangpur lime (*Citrus limonia Osbeck*), have been classified as shoot Cl^- excluders (non-sensitive) due to the better capability to restrict Cl^- uptake and transport from root-to-shoot, compared to other Cl^- sensitive and poor Cl^- excluding rootstocks (for example Carrizo citrange) (Brumos *et al*., 2010). Similar Cl^- excluding differences are also found in grapevine, for instance, 140 Ruggeri (good shoot Cl^- excluder), K51-40 (poor shoot Cl^- excluder) and Cabernet Sauvignon (intermediate shoot Cl^- excluder) under 50 mM NaCl treatment (Henderson *et al*., 2014). Hence, Cl^- toxicity can vary

in plants because of the different ability to reduce Cl^- loading to the shoot.

In this project, Arabidopsis will be used to further investigate the mechanisms of shoot Cl^- exclusion. Although Arabidopsis is a salt-sensitive plant species (Cramer 2002), and as such may not be a good model for salinity tolerance studies, it is a good model for transport studies (Møller and Tester 2007). Some important Na^+ transporters, such as AtHKT1; 1 (Rus *et al*., 2004) localised to the plasma membrane (PM), and AtNHX1 (Apse *et al*., 1999) a tonoplast localised $(Na^+/K^+)/H^+$ antiporter (which was also recently shown to be involved in controlling K^+ homeostasis) (Bassil *et al*., 2011), have already been characterised in Arabidopsis and many of these results have been extrapolated to other species and shown to affect salt tolerance i.e. rice HKT1; 5 (Ren *et al*., 2005), wheat HKT1;5 (Munns *et al*., 2012) and tomato NHX1 (Barragan *et al*., 2012). Thus, knowledge about shoot Cl^- exclusion in Arabidopsis could eventually be extrapolated to crop plants. Furthermore, the small size and well mapped and sequenced genome, rapid life cycle and well-established gene expression databases for Arabidopsis offer advantages in investigating the mechanisms of Cl^- transport (Møller and Tester 2007).

1.6 Chloride loading pathways

Like many other solutes, once Cl^- enters root from the soil solution it will be transferred mainly through symplastic and apoplastic pathways to the xylem (White and Broadley 2001). In the symplastic pathway, Cl^- will enter into root cells across the plasma membrane, and transfer between cells through plasmodesmatal connections (Davenport *et al*., 2007, White and Broadley 2001).

In the apoplastic pathway, the movement of most ions is restricted before they enter into the stele due to the presence of the casparian band (formed from hydrophobic suberin lamellae and lignin), which is deposited on the endodermal cell walls that separate the root cortex from the stele (Vanfleet 1961, White and Broadley 2001). However, substantial evidence suggests that Na^+ can move from root-to-shoot through apoplastic pathways under salt

stress (Yeo et al. 1987). In rice, Na^+ uptake is primarily through the apoplastic leakage (bypass flow) into the xylem (Koyama *et al*., 2001). In Arabidopsis, radial flow of ions can also occur through the apoplastic pathway (White and Broadley 2001). However, more suberin was formed in the Arabidopsis mutant (enhanced suberin 1, *esb1*), which resulted in less accumulation of Ca^{2+}, Mn^{2+} in shoot, with a greater amount of Na^+ indicating this ion may be transported more through the symplast in Arabidopsis (Baxter *et al*., 2009). It is possible that Cl^- can reach to the root xylem by both pathways. However, the symplastic pathway is believed to be the predominant path in most situations, followed by passive unloading of Cl^- into the xylem across the plasma membrane (xylem parenchyma cells) (Pitman 1982, White and Broadley 2001).

1.7 Chloride transport across the plasma membrane

Since Cl^- is dominantly transported via the symplastic pathway, Cl^- has to cross the plasma membrane at least twice before loading to the xylem. Under normal conditions, a large potential difference exists across the plasma membrane due to the proton pump activity. Thus, a 2 Cl^-/H^+ symporter (located on plasma membrane) actively transports Cl^- from the extracellular space into root cells against its electrochemical gradient (Felle 1994, Sanders 1980). When the external concentration of NaCl is relatively high, the membrane potential becomes more positive than the anion equilibrium potential and passive entry of Cl^- can also occur (Tyerman 1992). An outward rectifying (OR) anion channel responsible for this anion influx has been identified in barley (Kohler & Raschke 2000), maize (Pineros & Kochian 2001) and wheat root protoplasts (Skerret & Tyerman 1994). Several Cl^- efflux anion conductances that are likely to function in xylem loading have been identified in root cells in many plant species. These anion conductances are discussed in Section 1.8.3. In addition, many root cell plasma membrane located anion transporters have been discovered in higher plants recently; these are reviewed in Section 1.10.

1.8 Regulation of chloride transport within plants

Many salt tolerant plants accumulate less Cl^- in the shoot under salt stress (Teakle and

Tyerman 2010). To reduce shoot Cl^- there are several mechanisms involved in the transport of Cl^- from the root to the shoot that can be modified.

1.8.1 Reducing net Cl^- uptake from the soil

Plants acquire the majority of their Cl^- from the soil (White and Broadley 2001). The net uptake of Cl^- in the root depends on both Cl^- efflux and influx as the movement of Cl^- within the plant is a dynamic process (Teakle and Tyerman 2010). Therefore, decreasing the Cl^- influx into the plant or and/or increasing the Cl^- efflux from the plant are key steps for reducing the net Cl^- uptake into roots. Very limited evidence exists to suggest that salt tolerant plants have a better Cl^- efflux ability to prevent Cl^- build up in roots (White and Broadley 2001). Significant Cl^-efflux from the root apex was identified in a salt tolerant poplar (*Populus euphratica*) when treated with 100 mM NaCl for 15 day. However, with the same treatment, a Cl^- efflux was not identified in a salt sensitive poplar (*Populus popularis*) (Sun *et al*., 2009). As a result the salt tolerant poplar was hypothesised to maintain better ion homoeostatic control within root cells under salt stress (Sun *et al*., 2009). Reducing Cl^- influx from the soil to root can also be managed through decreasing the soil Cl^- concentrations, but soil management is not the aim of this research. Due to the limited evidence with respect to reducing the net Cl^- uptake from soil to the root as a primary mechanism for salt tolerance the targeting of this process is not a primary aim of this thesis.

1.8.2 Chloride compartmentalization in roots

Partitioning of Cl^- between different cell types at the whole plant level is thought to contribute to salinity tolerance (Teakle and Tyerman 2010). The ability to keep more Cl^- in the root instead of transferring it to the shoot is an effective way to increase salt tolerance. For instance, salt tolerant genotypes (Cleopatra mandarin and Rangpur lime) of citrus are estimated to have higher Cl^- concentration in the root and lower in the shoot (Moya *et al*., 2003). In the grapevine rootstock 140 Ruggeri (*Vitis berlandieri* × *Vitis rupestris*) (shoot Cl^- excluder, salt-tolerant), reduced Cl^- loading to the root stele (xylem) was hypothesised to contribute to the improvement of its salt tolerance over salt- sensitive rootstocks (Gong *et*

al., 2011). Secondly, within the root, sequestration of Na^+ and Cl^- in vacuoles contributes to reducing shoot Cl^- concentration as well as preventing high levels of Cl^- in the root causing tissue toxicity within the cytoplasm (Storey *et al*., 2003, Teakle and Tyerman 2010). Analogous results show in both lotus and grapevine that the vacuole in xylem-associated cells of the root are involved in efficient compartmentation of Cl^-, thereby reducing the amount of Cl^- loaded into the xylem (Storey and Walker 1999, Teakle *et al*., unpublished data). In grapevine roots (*Vitis*), a salt-tolerant genotype, produced from a backcross population between *Vitis berlandieri* and *Vitis vinifera* exhibited 20 % higher vacuolar Cl^- in root pericycle cells than salt-sensitive genotypes (Storey *et al*., 2003). Indeed, it appears that plants selectively accumulate Cl^- in their pericycle as they exhibit 50 % greater vacuolar concentrations of Cl^- than in endodermal cells from the same plant (Storey *et al*., 2003). By accumulating Cl^- in pericycle cells, the amount of Cl^- transported through the root will be restricted and this will reduce Cl^- transport to the shoot. Preferential accumulation of Cl^- in different cells types of fourteen-day-old Arabidopsis seedlings stressed with 50 mM NaCl for 7 days was also observed, however, it was cortical and parenchyma cells which accumulated Cl^- (Figure 1.2) (unpublished data from M. Gilliham). Under saline conditions, the accumulation of Cl^- was higher in xylem parenchyma and cortical cells (Figure 1.2). It is possible that different membrane transporters are located in different cell-types and may help to accumulate Cl^- selectively into cells.

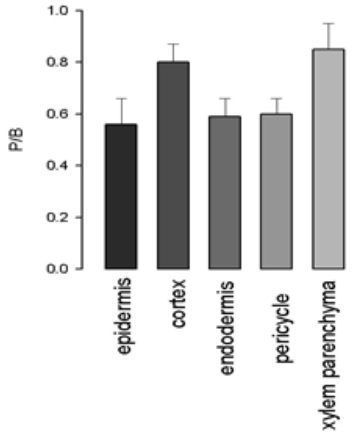

Figure 1.2 Scanning electron microscopy and X-ray microanalysis was used to provide a qualitative measure of Cl^- accumulation in different root cell types of cryo-fixed wild-type (Col-0) *Arabidopsis thaliana* seedlings. Arabidopsis were grown in hydroponics (14 days) and treated with 50 mM NaCl for another 7 days (Unpublished data, M Gilliham). P/B: peak/background ratio

1.8.3 Xylem loading through anion conductances

A key pathway in reducing the amount of Cl^- accumulation in the shoot is tight control of the loading of Cl^- from parenchyma cells into the transpiration stream (Teakle and Tyerman, 2010). Several key steps have been identified as being closely involved in loading Cl^- into the xylem. Many anion conductances have been found in higher plants by using electrophysiology, but fewer studies have examined the relationship between the anion conductances and salt stress (Teakle and Tyerman 2010).

Three anion conductances have been identified in barley root xylem parenchyma protoplasts including an inwardly rectifying anion channel (X-IRAC), a quickly activating anion conductance (X-QUAC) and a slowly activating anion conductance (X-SLAC) (Köhler and Raschke 2000, Roberts 2006) (Figure 1.3). Similar results were found in maize root stelar cells (Gilliham and Tester 2005) and Arabidopsis root pericycle cells (Kiegle *et al*., 2000). X-QUAC is the most prevalent xylem loading conductance observed in parenchyma cells and is likely to load the majority of Cl^- (and NO_3^-) ions in to the xylem under non-saline conditions (Gilliham and Tester 2005, Köhler *et al*., 2005). X-IRAC and X-SLAC are both of smaller magnitude and are present in fewer parenchyma cells (Gilliham and Tester 2005, Köhler and Raschke 2000, Roberts 2006). The estimation of Cl^- fluxes through these three conductance have been compared with the value of Cl^- release from the xylem vessels using a $^{36}Cl^-$ tracer (Köhler and Raschke 2000, Pitman 1982). The results suggested that any of these conductances are able to regulate the Cl^- loading into the xylem vessels, but it is most likely that the major Cl^- loading pathway is through X-QUAC as it has the highest current magnitude and is the most commonly found conductance (Köhler *et al*., 2005).

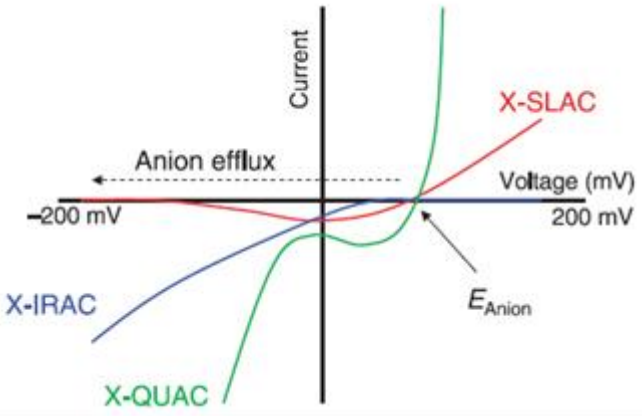

Figure 1.3 Representative current-voltage curves for three anion transporter conductances observed in barley root parenchyma cells. X-SLAC (red): slowly activating anion conductance; X-QUAC (green): quickly activating anion conductance; X-IRAC (blue): inwardly rectifying anion conductance (Adapted from Roberts 2006).

1.8.4 ABA regulates xylem loading

Abscisic acid (ABA), an important plant hormone, is recognized as being responsible for regulating many critical processes in plants, including germination, plant root and shoot elongation and stomata aperture (Leung and Giraudat 1998). ABA has also been shown to be important when a plant is experiencing an environmental (drought and salt) stress (Zhu 2003). ABA has been shown to regulate solute (K^+) loading from root to shoot in barley and maize (Cram and Pitman 1972), as well as inhibiting the transport of Cl^- from root to shoot, leading a root Cl^- accumulation (Cram and Pitman 1972). Excised barley roots treated with 0.4 to 1.9 $\times 10^{-5}$ M ABA for 2 hours accumulated significantly more Cl^- than roots that had no ABA treatment. The efflux of Cl^- to the xylem was also reduced due to the ABA treatment but Cl^- influx to the root was unaffected (Cram and Pitman 1972). These results indicate that ABA down-regulates the loading of Cl^- into the xylem but not the movement of Cl^- into the root. As a consequence, ABA is considered as a significant factor which regulates Cl^- loading to shoots. In addition, anion conductances found in the stele of maize, barley and Arabidopsis, such as X-QUAC as well as potassium conductances through the stelar K^+ outwardly-rectifying channel (SKOR), were also shown to have down-regulated activity by ABA. In Arabidopsis, *AtSKOR* was transcriptionally down-regulated by ABA (Cram and Pitman 1972,

Gaymard *et al*., 1998, Gilliham and Tester 2005, Roberts and Snowman 2000). It may be possible to identify candidate genes for Cl^- loading into the xylem by characterising those genes encoding putative anion transporters that are expressed in the stele and down-regulated (either transcriptionally or post-translationally) by ABA.

1.9 Chloride and nitrate

NO_3^- is one of the main nitrogen sources for plant growth, when NO_3^- uptake is reduced, nitrogen use efficiency (NUE) will be affected (less N will be transferred from soil to plant). High concentrations of Cl^- within soils suppress root nitrate uptake (Crawford and Glass 1998, Dluzniewska *et al*., 2007). There are several linkages between Cl^- and NO_3^- which possibly can explain why NO_3^- uptake is closely correlated with Cl^- transport. First of all, it is a common characteristic of anion conductances (i.e. X-IRAC, X-QUAC and X-SLAC) that they not only share similar features in xylem loading, but are also permeable to both Cl^- and NO_3^- (Roberts 2006, Teakle and Tyerman 2010). For instance, an anion conductance discovered in wheat root protoplasts was shown to be permeable to both Cl^- and NO_3^- (Skerrett and Tyerman 1994). Similarity, X-IRAC in the xylem parenchyma cells of barley was equally permeable to Cl^- and NO_3^- (Köhler and Raschke 2000). The maize X-QUAC, identified as having a conductance which was most likely to be responsible for the majority of anion loading into the xylem, was also highly permeable to both Cl^- and NO_3^- (Gilliham and Tester 2005, Kohler *et al*., 2002). This evidence suggests a correlation between the Cl^- and NO_3^- fluxes which may relate to the control of solute loading from the root to shoot, and that they may occur through the same protein.

In Arabidopsis, a slow–type (S type) anion channel (SLAC1) and its homolog, SLAH3 which functions in regulating stomatal opening and closure (Negi *et al*., 2008, Vahisalu *et al*., 2008) has been found to be more permeable to NO_3^- than Cl^- (Barbier-Brygoo *et al*., 2011, Roberts 2006, Geiger *et al*., 2009; Geiger *et al*., 2011). Chloride channel a (AtCLCa), was initially identified as a nitrate transporter (De Angeli *et al*., 2006). However, recent research suggested that the AtCLCa can be modified to transport Cl^- through a site mutation in a

specific signature sequence (Wege *et al*., 2010, Wege *et al*., 2014). These results further indicate that Cl^- and NO_3^- can be transported through the same anion transporters.

Since an anion transporter or channel might have the capacity to transport Cl^- and NO_3^- simultaneously (Figure 1.4) (Barbier-Brygoo *et al*., 2011, Kollist *et al*., 2011, Wang *et al*., 2012, Hedrich 2012), competition for the transport of the two anions must exist. An attempt to manipulate Cl^- transport, through misexpression of anion transport genes, may result in the reduction of NO_3^- transport and negatively affect plant growth. Therefore, if the eventual aim is to find ways of reducing shoot Cl^- without reducing NO_3^- uptake, it would be necessary to manipulate only Cl^- movement through manipulation of Cl^- specific transporters (if they do exist) or find a way to modify a Cl^-/ NO_3^- transporter so that it only transports one of the two substrates. A lot more is known about NO_3^- transport than Cl^- transport in plants (Tsay *et al*., 2007, Miller *et al*., 2007, Wang et al., 2012, Krapp *et al*.,2014) (Figure 1.5). As NO_3^- permeable transporters may also transport Cl^-, the nitrate transport network can be used as a model for further identifying mechanisms of Cl^- transport.

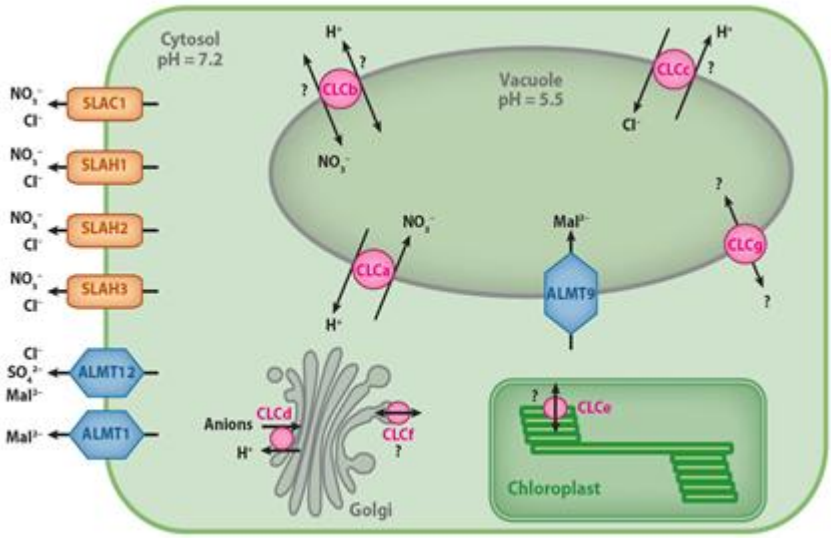

Figure 1.4 Subcellular localization of the SLAC/SLAH, ALMT, and CLC families in Arabidopsis. SLAC1/SLAH (1, 2 and 3) and ALMT (1 and 12) are localized to the plasma membrane. SLAC1/SLAH can transport Cl^- and NO_3^-. ALMT12 also can transport more than one type of anion, including Cl^-, SO_4^{2-} and Mal^{2-}. AtCLCa-c, g and ALMT9 are localized to the tonoplast, AtCLCd and AtCLCf are localized to the Golgi vesicles, and AtCLCe are localized to the thylakoid membranes (Adapted from Barbier-Brygoo *et al*., 2011).

Cytosolic K^+/Na^+ ratio is one of the key determinants (high K^+/Na^+ ratio indicates high salinity tolerance) in plant salt tolerant research (Maathuis and Amtmann 1999). Under salt stress, competition between K^+ and Na^+ exists. Excess Na^+ in the cytosol can inhibit K^+ uptake and these results in K^+ deficiency (Maathuis and Amtmann 1999). Thus, maintenance a high cytosolic K^+/ Na^+ ratio is a key element in salinity tolerance (Yeo 1998). As the relation between NO_3^- and Cl^- is analogous to the interactions between K^+ and Na^+, it is likely that further identification of NO_3^-/ Cl^- selectivity will increase the understanding of salt tolerance. Therefore, manipulation of Cl^- transport without negatively impacting on the NUE of plants will be a concern of this project.

1.10 Gene families responsible for Cl^- transport in plants

While genes encoding for Cl^- transporters have now been identified, those responsible for the loading of Cl^- into the root xylem from the parenchyma cells have still to be determined. Possible candidate gene family encoding for these channels will now be described.

1.10.1 *AtCLC* family

Chloride channel proteins (CLCs) were originally discovered in animals and function as 2 Cl^-/ 1 H^+ antiporters within intercellular compartments (from cytosol to vesicular lumen) (Bergsdorf *et al*., 2009, Lisal and Maduke 2008). There are seven homologues of Arabidopsis CLC (AtCLC), AtCLCa to AtCLCg, which are localised to different organelles within the plant cell (De Angeli *et al*., 2006, De Angeli *et al*., 2009). AtCLCa-c and AtCLCg have been localized to the tonoplast, AtCLCe to the thylakoid membrane of chloroplasts and AtCLCd and AtCLCf to the Golgi vesicles (De Angeli *et al*., 2009) (Figure 1.4). Recently, functional characterization of AtCLCc indicated that it is involved in Cl^- homeostasis and contributes to salt tolerance (Jossier *et al*., 2010). It is likely to impart increased salt tolerance by sequestering Cl^- to the vacuole to avoid high concentrations of Cl^- in the cytoplasm. An *Atclcc* T-DNA knockout line also showed hypersensitivity to NaCl (Jossier *et al*., 2010). Functional characterization of

another CLC in Arabidopsis, AtCLCa, showed that it is responsible for nitrate accumulation in the vacuoles and behaves as a NO_3^-/ H^+ exchanger (De Angeli *et al*., 2006, Wege *et al*., 2010, Wege *et al*., 2014), which displaying a higher selectivity for nitrate than for chloride. Interestingly, when a serine is modified to a proline within the selectivity filter (GXGIP) of the AtCLCa protein, it becomes more selective for Cl^- instead of NO_3^- (Wege *et al*., 2010). This indicates possibilities of producing transgenic plants with modified transgenes that increase Cl^- tolerance. As other *AtCLC* homologues could be good candidates for improving salt tolerance in plants, further characterization of their roles in Cl^- transport is needed. However, this project is focusing on controlling how Cl^- moves across the plasma membrane and enters into the xylem, rather than loading into the vacuole. Therefore, *AtCLC* is not a key candidate gene in this research.

1.10.2 *AtSLAC/SLAH* family

Early electrophysiological studies on stomata guard cells discovered the slowly activated anion conductance (SLAC) (Linder and Raschke 1992) and more recently, the gene encoding the protein responsible for this conductance, *SLAC1* was identified (Negi *et al*., 2008, Vahisalu *et al*., 2008). Further characterisation of SLAC1 located the protein to the plasma membrane and demonstrated that *slac1* mutants have increased accumulation of Cl^- in their guard cells (Negi *et al*., 2008, Vahisalu *et al*., 2008). There are four homologous of SLAC1: SLAH1-4 that, have been identified. These localise to the plasma membrane and are predicted to be involved in anion transport (Negi *et al*., 2008, Vahisalu *et al*., 2008). SLAH1, exhibits strong expression in the root vascular cylinder (Negi *et al*., 2008, Vahisalu *et al*., 2008) and therefore has been hypothesised to encode a protein involved in anion xylem loading (Köhler and Raschke 2000). SLAH3 is highly expressed in root and was shown to be involved in both NO_3^- and Cl^- transport (Geiger *et al*., 2009, Geiger *et al*., 2011, Demir *et al*., 2013). Compared to SLAH3, SLAH2 was also found permeable to NO_3^- and Cl^- (NO_3^-/ Cl^- permeability ratio of 82) (Maierhofer *et al*., 2014). There is little published work on the role of SLAH1-SLAH4 on long distance NO_3^- and Cl^- transport has the potent contribution towards restricting Cl^- uptake from root to shoot under saline environments for any of this family, so

the activities and roles of these proteins are of interest.

1.10.3 *AtNRT* family

Research has hypothesised that Cl^- may be transported through nitrate channels and transporters. Three classes of nitrate transporters (NRTs) have been discovered in higher plants, NRT1s, NRT2s and PTRs or NPF (Figure 1.5) (Segonzac *et al*., 2007, Tavares *et al*., 2011, Tsay *et al*., 2007, Krapp *et al*., 2014, Le´ran et al., 2014). Although many of these proteins have been shown to transport a range of substrates (including other anions and amino acids) this discussion will focus on their role in NO_3^- transport (Krapp *et al*., 2014). NRT1s are low affinity transporters which function when there is a sufficient nitrate supply, NRT2s are high affinity transporters that are active during nitrate starvation and NAXTs are a NO_3^- transporter responsible for NO_3^- efflux to external medium under acid stress (Segonzac *et al*., 2007).

Previous research suggested that two NRT1 transporters, AtNRT1.5 and AtNRT1.8 not only functions in NO_3^- transport, but are also involved in Cl^- homeostasis (Teakle and Tyerman 2010). Functional analysis of NRT1.5 in *X. laevi*s oocytes indicated that it is a low-affinity, pH-dependent nitrate transporter (Lin *et al*., 2008). AtNRT1.5 has been shown to be located on the plasma membrane and expressed in the root, particularly in pericycle cells which are near to the xylem. Arabidopsis mutants which have NRT1.5 knocked out show reduced nitrate transport from root to shoot suggesting that the protein is involved in xylem loading (Lin *et al*., 2008). Interestingly the expression of NRT1.5 is decreased under salt stress (Genevestigator) (Zimmermann *et al*., 2004) suggesting that this transporter may have a direct or indirect role in shoot Cl^- accumulation. AtNRT1.8, which has also been identified as being expressed in xylem parenchyma cells, with the protein localised to the plasma membrane (Li *et al*., 2010). AtNRT1.8 has also been hypothesised to retrieve NO_3^- from the xylem (Li *et al*., 2010) and unlike NRT1.5 its expression is up- regulated under salt stress, perhaps aiding retrieval of Cl^- from the xylem. Given the evidence for both of these genes

might involve in Cl^- transport, it is worthwhile to further characterize their functions and the anion selectivity.

1.10.4 *AtCCC*

Cation chloride co-transporters (CCC) were originally identified in animal cells, and are hypothesised to play a significant role in cellular ionic and osmotic regulation (Gamba 2005). A homologue of CCC was identified in Arabidopsis that may be responsible for the retrieval of Cl^- from the xylem (Colmenero-Flores *et al*., 2007). AtCCC promoter GUS fusions suggest the gene is expressed in xylem parenchyma cells (Colmenero-Flores *et al*., 2007). Shoot Cl^- concentrations in the knockout mutants (*ccc-1* and *ccc-2*) are 40% higher than wildtype (Colmenero-Flores *et al*., 2007). In addition, *X. laevis* oocytes transformed with AtCCC demonstrated the ability to transport Cl^- (and K^+ and Na^+) (Colmenero-Flores *et al*., 2007). However, for AtCCC to directly function in Cl^- retrieval from the xylem, it would be localised to the plasma membrane. Based on the thermodynamic analysis (Teakle and Tyerman 2010) and results from AtCCC:YFP fusions expressed in Arabidopsis mesophyll protoplasts, it has been suggested that AtCCC is not localised to the plasma membrane but some other intracellular location, like the trans-Golgi network and not directly involved in xylem ion transfer or improving salinity tolerance (Henderson *et al*., 2015).

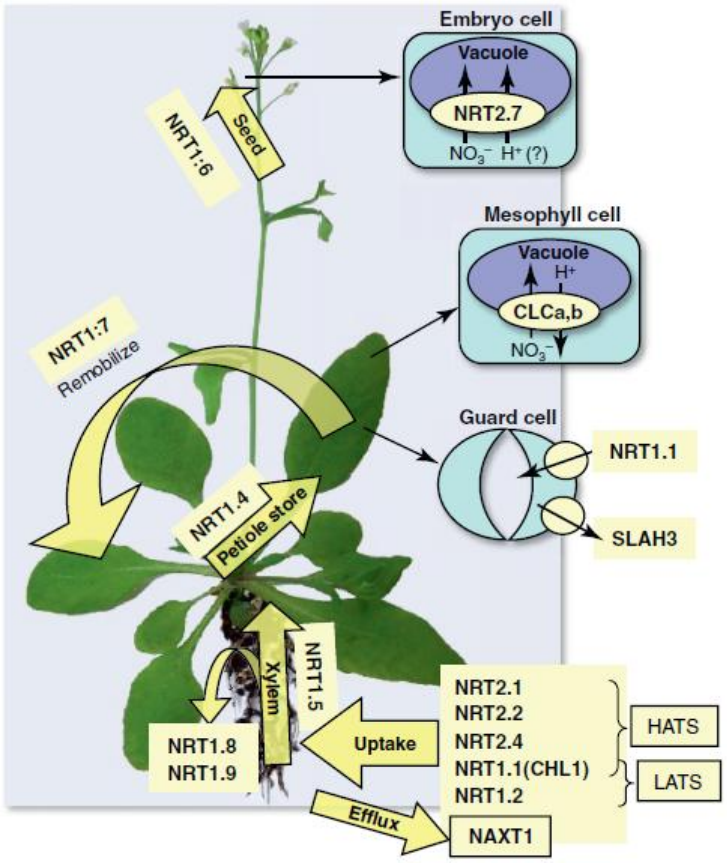

Figure 1.5 A summary of nitrate transporters have been identified in Arabidopsis. Nitrate transporter 1 (NRT1), NRT2, chloride channel (CLC) a/b, and slow anion channel-associated 1 homolog 3 (SLAH3) are involved in nitrate uptake and allocation in different tissue types (Adapted from Wang *et al*., 2012).

1.11 Regulation of anion transporters/ channels

Several gene and protein families that are likely to be involved in root- to- shoot anion transport are reviewed above. Misexpression (over- expression, knockout and knockdown) of the candidate genes in plants could potentially be employed to manipulate the anion transporters/channel activity improve the plant salinity tolerance. However, there are other strategies that have focused on molecular structure and regulation that have been intensively used for investigating of anion transporters regulation (Roelfsema *et al*., 2012, Hedrich 2012, Kollist *et al*., 2011). The following review will summarize how the activities of anion transporters are affected by their selectivity filters and by regulatory partners.

1.11.1 The selectivity filter of anion transporters

The selectivity of anion transporters can be modified through the genetic manipulation of their selectivity motif (Wege *et al*., 2010). The mutated anion transporters listed below had a greater Cl^- transport capacity than wildtype (Chen *et al*., 2010, Rudiger and Oesterhelt 1997, Wege *et al*., 2010, Maierhofer *et al*., 2014). Therefore, shoot Cl^- exclusion might be controlled through the misexpression of mutated anion transporters.

- ***CLCs***

Sequence alignment of CLC proteins from both bacteria and animals has identified four highly conserved amino acid sequences (selectivity filter motifs), GSGIP (106-110), G (K/R) EGP (146-150), GXFXP (355-359) and Y445 (Dutzler *et al*., 2002). Using X-ray structural analysis of two prokaryotic CLCs indicated that these conserved amino acid sequences form a central ion-binding site (Dutzler *et al*., 2002). The presence of a proline and a serine in these selectivity filter motifs has been shown to be linked to anion selectivity (Estevez and Jentsch 2002). In an *E. Coli* CLC (EcCLC-ec1) a serine/ proline substitution at serine 107 (S107) changed the ion selectivity of EcCLC-ec1 towards greater selectivity for NO_3^- over Cl^- (Dutzler *et al*., 2002, Picollo *et al*., 2009). By contrast, the selectivity of AtCLCa can be altered from NO_3^- to Cl^- when a proline was replaced by serine (P160S) (Wege *et al*., 2010) which indicates that the serine in the selectivity filter is critical for Cl^- selectivity. AtCLC, which is localized to the tonoplast, has a serine in the CLC- specific ion binding site, lending weight to this hypothesis.

- ***SLAC1***

Although there is no crystal structure of plant SLAC1, the crystal structure of a bacterial homologue (*Haemophilus influenza*) of SLAC1, HiTehA, has been determined which was used to model the plant SLAC1 (Chen *et al*., 2010). The structure suggested that the three subunits of the protein each form a pore and combined together as a 'triple barrel' structure in the membrane (Figure 1.6). This pore is suggested to neither have the ability to select between anions nor have an ion binding site. It has been hypothesised that a phenol side chain of

phenylanlaine is responsible for anion selectivity in both TehA and SLAC1 model through size exclusion (Chen *et al*., 2010, Thomine and Barbier-Brygoo 2010, Dreyer *et al*., 2012).

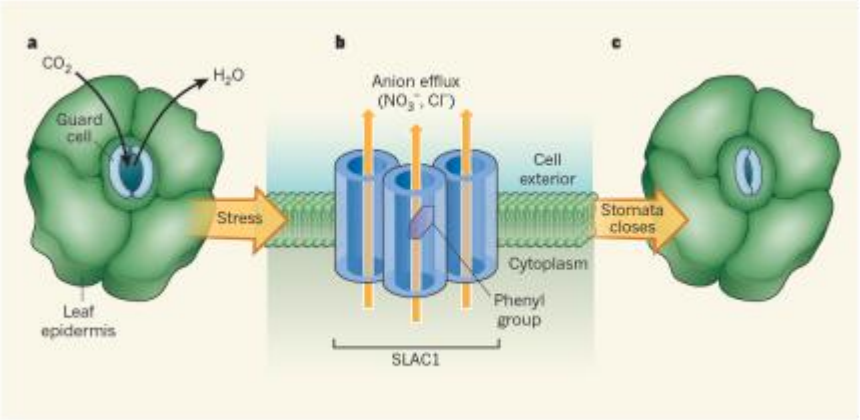

Figure 1.6 Role of SLAC1 channels in stomatal closure. **a**, stomata regulates CO_2 uptake and water loss; **b**, SLAC1 is responsible for NO_3^- and Cl^- efflux from the cells, a process which is triggered by stress (loss water). According to the crystal structure of TehA, three individual subunits of the protein combine with each forming a pore in a 'triple barrel' structure in the membrane. A phenyl group (only shown on one of the pores in this figure) is involved in regulating anion transport through the pore; **c**, efflux of NO_3^- and Cl^- triggers K^+ influx into cell (not shown) and results the stomatal closure (Adapted from Thomine and Barbier-Brygoo 2010).

- ***SLAH2***

SLAH2 was also found to be involved in anion transport in *X. laevis* oocytes, and was much more selective for nitrate over chloride when both substrates were available (Maierhofer *et al*., 2014). To identify why SLAH2 showed a distinctive anion selectivity compared to SLAC1, the 3D homology model of SLAH2 was established based on the crystal structure of Hi-TehA (Figure 1.7). The Phe-402 residue in SLAH2 was replaced by an alanine to examine whether this site was also crucial to open SLAH2 in a similar manner to SLAC1. The mutation of SLAH2 in F402A did result in a greater conductance of the channel without the need of activation through a protein kinase (Maierhofer *et al*., 2014). Interestingly, when Phe- 231 was replaced with Ala in SLAH2, chloride currents were identified when the mutated SLAH2 was co-expressed with CIPK23/CBL1 complex in oocytes (Maierhofer *et al*., 2014). These sites that located in SLAH2 pore not only controls the opening of the channel but are also involved in changing the anion selectivity between NO_3^- and Cl^-. This strategy could potentially be used

in the future to identify the anion channel regularly mechanisms.

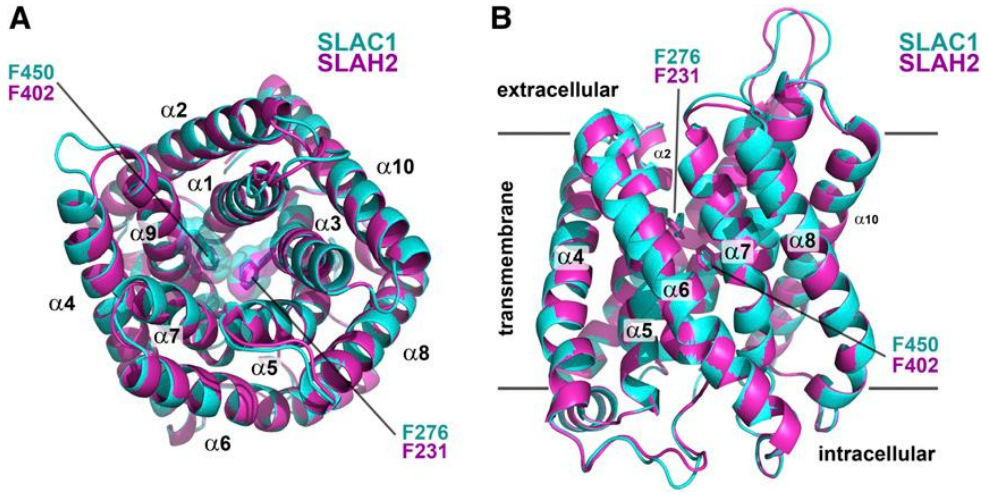

Figure 1.7 3D homology structure of SLAC1 and SLAH2 established based on the crystal structure of Hi-TehA. (**A**) and (**B**) Ribbon plot of the homology models of SLAC1 (cyan) and SLAH2 (magenta). (**A**) Channel seen from the extracellular side, with the side chains of the conserved Phe-450/402 and Phe-276/231 occluding the pore. (**B**) Same as in (**A**) but shown as a side view (Adapted from Maierhofer *et al*., 2014).

- **Halorhodopsin (HR) chloride binding site**

The light –driven chloride pump halorhodopsin (HR) is a halobacterial retinal protein (Rudiger and Oesterhelt 1997). Within the HR protein, arginine and threonine residues have been shown to control anion binding and transport (Rudiger and Oesterhelt 1997). Interestingly, mutants, where threonine was site mutated to a valine (T203V), showed a strong inhibition of Cl^- transport and did not affect NO_3^- transport when compared to wildtype (Figure 1.8) (Rudiger and Oesterhelt 1997). This result may suggest that threonine is a key site for Cl^- selectivity in HR. The crystal structure of HR further indicates the significance of arginine and threonine residues for Cl^- binding (Kolbe *et al*., 2000). Collectively, the above evidence may suggest that arginine and threonine are good candidates within a selectivity motif for chloride transport.

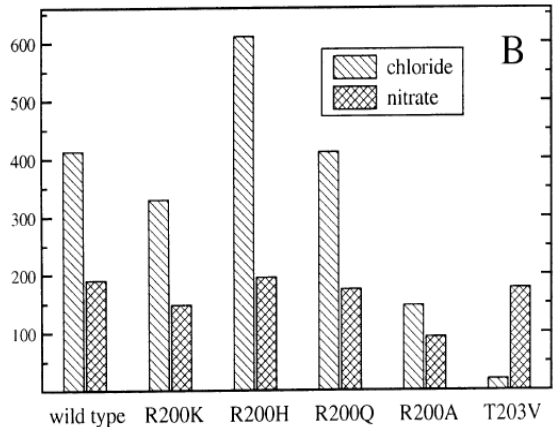

Figure 1.8 The anion transport activities of different mutants of HR. Compared to the wildtype, T203V exhibits reduced Cl^- transport activity, while the NO_3^- transport activity is less affected (Adapted from Rudiger and Oesterhelt 1997). Y-axis: ion translocation activities

1.11.2 Anion transporters/channels regulated by protein kinases

Anion transporters/channels can also be activated by protein kinase through phosphorylation. These types of regularly mechanisms have been intensively studied and the published results suggested that anion channel/transporters, especially those from the same gene family can be regulated by several protein kinases from the same family. In addition, the interactions between anion channel/transporter and protein kinases are tightly manipulated by ABA signalling and availability of cytosolic Ca^{2+} (Table 1.1).

Table 1.1 Summary of anion transporters/ channels regulating mechanisms in SLAC1 family

Gene family	Physiological function	Regulating mechanisms	Important sites	References
SLAC1 Slow Anion Channel-Associate 1 AT1G12480	Required for stomatal closure induced by ozone, CO_2, ABA, calcium, light/dark transitions and reduction in air humidity; Encodes S- type anion channel and involves in anion transport ($NO_3^- > Cl^-$); Involved in ABA siganlling; Play roles in regulating Ca^{2+} sensitive K^+ uptake channel in stomata.	calcium-dependent protein kinase 21 (CPK21), CPK23, CPK6 and Open Stomata 1 kinase (OST1) **positively activates** SLAC1 directly through phosphorylation; SLAC1 is **negatively regulated** by PP2C-type phosphatases ABI1, ABI2 and PP2CA (through inactivation of OST1 and CPK); ABA can **recovery** the inhibition of ABI1/2 to CPK6/OST1- dependent SLAC1 channel; CIPK23+ CBL1 postively activates SLAC1 for both NO_3^- and Cl^- transport.	**S120** (S120A prevents channel activation by OST1); **S59** (S59A abolish the channel activation by CPK6); **F450** (F450A resulted in large Cl^-currents without the activation of OST1);	Geiger *et al*., 2009; Geiger *et al*., 2010; Vahisalu *et al*., 2010; Negi *et al*., 2008; Vahisalu *et al*., 2008; Brandt *et al*., 2012; Chen *et al*., 2010; Laanemets *et al*., 2012; Maierhofer et al., 2014
SLAH2 SLAC1 Homologue 2 AT4G27970	Encodes an nitrate- permeable anion channel; Expressed in root stelar tissue and might be involved in transporting anions from root to shoot.	calcium-dependent protein kinase 21 (CPK21) and CBL-interacting protein kinase 23 (CIPK23) physically interacts with SLAH2 and **positively regulates** SLAH2 through phosphorylation when nitrate was presented;	**F402** (F402A activates SLAH2 without protein kinase); **F231** and **F276** (F231A and F276A converts SLAH2 from a nitrate-permeable channel to chloride- permeable channel;	Maierhofer *et al*., 2014
SLAH3 SLAC1 Homologue 3 At5G24030	Contributes to the release of chloride and nitrate during stomatal closure; Involved in ABA signalling response to drought stress; Functions in nitrate-dependent alleviation of ammonium toxicity in Arabidopsis.	calcium-dependent protein kinase 21 (CPK21) /CPK23 **positively regulates** SLAH3 through phosphorylation when nitrate was presented; CPK21-dependent SLAH3 phosphorylation and activation were **blocked** by ABI1; ABA promotes SLAH3 phosphorylation in the presence of ABI1 and RCAR1; CPK2/20 physcially interacts with SLAH3 and regualtes pollen tube growth.	**T187** (T187D mutated SLAH3 was fully activated without CPK21);	Geiger *et al*., 2011 Demir *et al*., 2013 Zhang *et al*., 2015 Gutermuth *et al*., 2013

- SLAC1:

In the absence of ABA, the ABA receptor, PYR/PYL/RCAR inhibits the protein phosphatase 2Cs (PP2Cs), such as ABI1/2, which then inactivates OST1 (SnRK2.6). In the presence of ABA, PP2Cs are inhibited, which allows the activation of OST1 (Geiger *et al*., 2009, Geiger *et al*., 2010). Therefore, OST1 activates SLAC1 through phosphorylation when ABA is presented (Vahisalu *et al*., 2010). CPK21 and CPK23 were also found to be controlled by PP2Cs, which only activate SLAC1 in an ABA- dependent manner (Geiger *et al*., 2009, Geiger *et al*., 2010). Additionally, CPK21 activates SLAC1 in a Ca^{2+}- dependent manner; however CPK23 could also activate SLAC1 in a Ca^{2+}- independent fashion (Geiger *et al*., 2009, Geiger *et al*., 2010). Moreover, CPK6 was also found to interact with SLAC1 in a Ca^{2+}- dependent but not ABA dependent manner (Brandt *et al*., 2012). Recently, SLAC1 was found to be activated by CIPK23/CBL1 and CIPK23/CBL9 complex in the oocytes in both Ca^{2+}- dependent or independent manner, which suggests there is a very complex network of CIPK/CBL proteins involved in regulating anion transport during stomatal closure (Maierhofer *et al*., 2014).

- SLAH3:

Similar to SLAC1, when ABA was available, the ABA receptor RCAR1 inhibits ABI1/2 which allows CPK21 to activate SLAH3 in a Ca^{2+}- dependent manner. In the absence of ABA, CPK21 was inactivated by ABI1/2 and cannot interact with SLAC1 (Geiger *et al*., 2011, Demir *et al*., 2013). Later, SLAH3 was also found to be activated by CPK2/20 in a Ca^{2+}- dependent way, however, whether CPK2/20 are both involved in the ABA signalling pathway is not yet known (Gutermuth *et al*., 2013). Interestingly, SLAH3 activity was also found to be triggered by CIPK23/CBL1 in oocytes (Maierhofer *et al*., 2014).

- SLAH2:

CPK21 and a CIPK23/CBL1 complex were found to interact with SLAH2 and activate its function (nitrate transport) through phosphorylation in oocytes (Maierhofer *et al*., 2014). However, no evidence has suggested that CPK21 or CIPK23/CBL1 are involved in ABA signalling pathways (i.e. controlled by ABI1/ABI2)

The knowledge summarized above suggests that SLAC1/SLAHs are activated and regulated by protein kinases from CPKs, CIPKs/CBLs and SnRK2s families, which indicates that different protein kinases regulate anion channel/transporter in a similar fashion, and may be involved

in the response to slightly different environmental signals. The CPKs and SnRK2s families are heavily involved in regulating plant anion channels/transporters especially under abiotic stress (Kulik *et al*., 2011, Schulz *et al*., 2013). Therefore, it would be interesting to examine whether the GOIs in this project could be activated by protein kinases from the same family through phosphorylation. The identification of upstream regulatory partners of anion channel/ transporter would also be crucial to understand the entire anion regulation network in plants.

1.12 Thesis outlines/ hypothesis

Knowledge gaps exist in the understanding of anion (chloride and nitrate) transport mechanisms in plants with respect to improving salinity tolerance through manipulating long-distance anion transport. Previous knowledge regarding anion loading pathways, channels/transporters involved in anion transport and their molecular regularly mechanisms is valuable for attempting to understand if manipulation of candidate anion channels/transporters can improve plant salt tolerance.

In summary, the key relevant facts and gaps identified in this review are:

a) Salt tolerance in plants can be associated with Cl^- exclusion from shoots and higher plants regulate the accumulation of shoot Cl^- by limiting its transfer from the root symplast into the xylem apoplast.

b) ABA was shown to significantly inhibit xylem loading of Cl^- by down-regulating the anion conductance (X-QUAC) in plants, therefore the major anion channels/transporters may be transcriptionally and post-translationally down-regulated by ABA as occurs for root-to-shoot transport of K^+ through SKOR.

c) While some candidate proteins, such as AtCCC and AtNRT1.5 have been proposed to be involved in retrieving Cl^- from xylem transpiration stream, unresolved questions still remain regarding their role in this process. Also, there are likely to be, as yet, unidentified PM-localised anion channels/transporters that are expressed in root xylem-associated cells that are potential candidates for contributing to anion transport.

These knowledge gaps have led to the following hypothesis:

a) PM-localised, root xylem expressed candidates that are transcriptionally down- regulated by ABA and NaCl are likely to be involved in root- to- shoot anion transport.

b) Functional characterization of selected candidate genes in heterologous systems will lead to the discovery of their anion transport properties and selectivity.

c) Misexpression of these candidate genes in plants will give a better understanding of their potential role in improving plant salt tolerance by manipulation of anion transporters.

Although a great deal of research has been carried out into the role of cations (such as sodium and potassium) in plants under salt stress, the role and transport mechanisms of anions (such as chloride and nitrate) is less well understood. The aim of this project is to discover and characterise putative candidate genes that control anion loading to the shoot of Arabidopsis. Also, as high concentrations of chloride in the soil suppress plant nitrate uptake and affect NUE, another object of this project is to manipulate the mechanism of shoot chloride exclusion under salt stress while maintaining adequate nitrate uptake.

Chapter 2: General materials and methods

All chemicals and reagents were obtained from Sigma-Aldrich (Castle Hill, Australia) unless stated.

2.1 Growing Arabidopsis

2.1.1 Plant materials

Arabidopsis thaliana ecotype Columbia-0 (Col-0), obtained from Gilliham laboratory stocks but originally sourced from the Arabidopsis Biological Resource Centre (ABRC), were used for studying candidate genes (Chapter 3), and to generate the transgenic plants used in Chapter 5. T-DNA knockout lines (SALK lines) were ordered from the ABRC to characterize candidate gene function *in planta* (Chapter 5). In addition, an Arabidopsis (Col-0 background) enhancer trap line which had strong GFP expression in the root stele tissue, E2586 (Møller *et al*., 2009) was used for generating root cell- specific expression lines (Chapter 5).

2.1.2 Plant growth

Plants were grown within growth rooms in the Plant Research Centre (Waite Campus, University of Adelaide) in soil, hydroponics or on sterile agar based media. Arabidopsis plants that were grown in soil were kept in long day conditions with 16-h day/8-h night. Arabidopsis germinated and grown in hydroponics (or on sterile media) were kept in short day conditions with 10 h day/ 12-h night period. In both long day and short day conditions the temperature was maintained between 21 to 23 °C, the humidity was maintained between 60%- 75%, and the irradiance during the light period was 120 µmol m^{-2}. s^{-1}.

2.1.3 Hydroponically grown Arabidopsis

Arabidopsis was grown in hydroponics following the protocol of Conn *et al*. (2013). In brief, seeds were first sown on a 1.5 mL microcentrifuge tube's cap (a hole was created in the centre of the lid) (Astral Scientific, New South Wales, Australia) with 0.7 % (w/v) agar (Difco ™ Agar, BD Diagnostic System, Australia) containing germination solution (Table 2.1). The lid containing solidified germination solution and seed were placed in germination tank (Scientific Specialties Inc., Hanover, Maryland, USA) and stratified in the dark at 4 °C for at least 48 h. The germination tank was transferred to a short day growth room for another

week, which allowed the roots of seedlings to emerge from the agar. After seven days, the germination solution was replaced by modified Hoagland's solution (Basal Nutrient Solution, BNS) (Conn *et al*., 2013) and the growth media was changed weekly for another 3 weeks. At 21 days post-germination, each single plant was transferred into a large aerated hydroponics tank (432 mm × 324 mm × 127 mm, Nally Limited, NSW, Australia) with an aquarium pump (AAPA 15 L air pump, Hydrofarm, Petaluma, California, USA). Finally, 4-5 week old Arabidopsis plants were ready for the treatment.

Table 2.1 The composition of the germination solution and Basal Nutrient Solution (BNS) (Conn *et al*., 2013) **used for the Arabidopsis hydroponic experiments**

	Germination solution	Basal Nutrient Solution (BNS)
	Final Concentration (mM)	Final Concentration (mM)
Macronutrients		
NH_4NO_3	0	2
KNO_3	0	3
$CaCl_2$	0.75	0.1
KCl	1	2
$Ca(NO3)_2 \cdot 4H_2O$	0.25	2
$MgSO_4 \cdot 7H_2O$	1	2
KH_2PO_4	0.2	0.6
NaCl	0	2
Micronutrients		
NaFe(III)EDTA	0.05	0.05
H_3BO_3	0.05	0.05
$MnCl_2 \cdot 4H_2O$	0.005	0.005
$ZnSO_3 \cdot 7H_2O$	0.01	0.01
$CuSO_4 \cdot 5H_2O$	0.0005	0.0005
$Na_2MoO_4 \cdot 2H_2O$	0.0001	0.0001

pH 5.6, adjusted by 1M KOH.

2.1.4 Soil grown Arabidopsis

Arabidopsis seeds were sown on a plant pots (PunTPX, Garden City Plastics, Victoria, Australia) containing sterilized coco-peat based soil , which was completely saturated with reverse osmosis treated (RO) water. A clear plastic cover (Smoult, Kersbrook, SA, Australia) was used to keep the humidity high after sowing. Covered pots/trays were kept in dark at 4°C for at least 48 h stratification before being transferred to long day growth conditions. High humidity was maintained until plants were 2-3 weeks old. The plastic cover was removed and plants were regularly watered until 5-6 weeks old. At this point they were ready for treatment.

2.2 Selection of transgenic plants

2.2.1 Selection of transgenic plants on solid MS media

Transgenic Arabidopsis seeds were sterilized in 30 % bleach for 5 min with gentle shaking and washed with autoclaved Milli-Q (MQ) water 4–5 times. Sterilized seeds were dried on filter paper (Whatman). Half-strength Murashige & Skoog Media (MS) media with 0.75 % (w/v) agar was autoclaved at 121°C for 20 min, and when cooled to 55-60 °C the appropriate antibiotic for the selectable marker in the destination vector was added (details are specified in Chapter 5). The media and then poured into round petri dishes (145 diameter × 20 deep mm; Greiner Bioone, Germany). Seeds of the primary transformants (T_0) were placed on the selective media. All the procedures described above were performed in a laminar flow hood to preventing bacterial infection. Plates with seeds sealed with micropore tape were kept in dark at 4 °C for 48 hours. After stratification, growth was stimulated for rapid selection following the protocol of Harrison *et al.*, (2006). Plates containing plants were illuminated under light (150 µmol m^{-2}. s^{-1}) at 25 °C for 6 hours and placed back in the growth chamber (in the dark for 48 hours) to accelerate the hypocotyl growth. Plates were then exposed to light in the growth chamber again for another 2 days. Seedlings that had longer hypocotyls were deemed transgenic and transferred to another plate containing 1/2 strength MS medium plus 0.75 % (w/v) agar without antibiotics for further growth in short day growth room. To confirm whether these seedlings were positive transformants containing the gene of interest, genomic DNA (gDNA) was extracted (section 2.3) and a standard PCR was performed using primers designed to amplify a fragment specific to the binary vector which is incorporated into the plant genome (see section 2.5 for further details).

2.2.2 Select transgenic plants in soil

Transformants that contained a bar (BASTA resistant gene) selection marker were selected on soil with the application of the herbicide glufosinate (BASTA; Bayer Crop Science, Australia). Positive transgenic plants containing the BASTA resistance gene should survive in such conditions and the non-transformants should die. In brief, seeds were evenly sown on the top of autoclaved coco-peat soil (Section 2.1.4) and stratified in dark at 4 °C for 48 h under high humidity. Once the seedlings started to produce the first true leaf, approximately 10 days after sowing, 100 µg/mL of BASTA was sprayed evenly to all the seedlings. This process was repeated 3 times every two days. The surviving seedlings were carefully transferred to

another pot with coco-peat soil, and plants were watered regularly. Plant gDNA was extracted and a PCR assay used to confirm the insertion by amplifying a fragment specific to the binary vector (see section 2.5.1).

2.3 Plant genomic DNA extraction

A number of gDNA extraction methods were used in this project depending on the downstream application. A rapid extraction protocol was used to quickly screen the DNA of mutant plants by PCR as this procedure has lower quality and purity requirements for the gDNA. For gDNA that was used for checking the insertion number in transgenic lines by Southern Blot, a more involved extraction protocol was employed for isolating high quality gDNA.

2.3.1 Quick gDNA isolation method

A simple method used for gDNA extraction from young Arabidopsis was used. A leaf from a young Arabidopsis plant (3- weeks old) was harvested into a microcentrifuge tube (stored at 4 °C) and homogenized with a plastic pestle at room temperature. To this 10 µL of 0.5 M NaOH was added and the centrifuged at 12, 000 × *g* in a desktop microcentrifuge for 1 minute at room temperature. Five microliters of the supernatant were transferred to another microcentrifuge tube containing 50 µL 100 mM Tris-HCl and mixed well by vortex. This mixture was used directly in the PCR (see section 2.5.1). However, this method is not suitable for tissue that was stored in -80 °C before isolation.

2.3.2 Edwards method

The method of Edwards *et al*. (1991) was used to extract gDNA quickly from a limited amount of tissue. In brief, one Arabidopsis leaf (5 weeks old) was harvested into a 1.5 mL microcentrifuge tube (stored at 4 °C) and grounded with a disposable pestle at room temperature. Edwards extraction buffer (200 mM Tris-HCl pH 7.5, 250 mM NaCl, 25 mM EDTA, 0.5% SDS, pH 7.5) (400 µL) was added to the tube and the sample vortexed for 5 seconds. The sample was then centrifuged at 16, 000 × *g* in a desktop microcentrifuge for 5 minutes and the supernatant was carefully decanted into a fresh microfuge tube. To the supernatant 300 µL 100% isopropanol was added and the mixture was incubated at room temperature for 2 minutes. A DNA pellet was collected at the bottom of the tube after centrifuging (11,000 × *g*) of the sample for 10 minutes at room temperature. The

supernatant was discarded and the pellet was dried in air before being dissolved in 100 µL DNase- free water and stored in -20 °C until further use.

2.3.3 Phenol/chloroform/iso-amylalcohol method

This method was used for extracting gDNA with high quality and purity. In this project, this protocol was used to isolate gDNA for Southern blotting. Large quantities of Arabidopsis tissue (0.5–2 g, fresh weight (FW)) were harvested and snap-frozen in the liquid nitrogen. Frozen tissue was ground into a fine powder with liquid nitrogen and combined with 600 µL of DNA extraction buffer (100 mM Tris-HCl, 100 mM NaCl, 10 mM EDTA, pH 8.5 and 1% w/v sarkosyl). To the extraction buffer 600 µL of a phenol/chloroform/iso-amyl alcohol (25:24:1) mixture was then added and this was centrifuged (11,000 × *g*) at room temperature for 10 minutes. The upper phase of the supernatant was transferred to another tube and 60 µL of 3 M Sodium acetate (pH 4.8) and 600 µL of 100% isopropanol were added and the samples incubated at room temperature for 10 minutes to precipitate DNA. Samples were centrifuged (12,000 × *g*) for another 15 minutes. After the centrifuge step, the supernatant was carefully discarded and the DNA pellet washed with 1 mL 70 % (v/v) ethanol. After the first wash, remnant ethanol was removed and the pellet washed again with fresh ethanol before the tube was vortexed for 30 seconds followed by centrifuge at 12,000 × *g* in a desktop microcentrifuge for 2 minutes. The supernatant was discarded and the washed pellet dried in air at room temperature and dissolved in 20–30 µL of R-40 (1x TE buffer containing 40 µg/mL RNaseA, pH 8.0). Isolated gDNA was then stored at -20 °C until further use.

2.4 Total RNA extraction and cDNA synthesis

2.4.1 Total RNA extraction

As RNA can be easily degraded by robust RNase found in the environment, all the bench areas and equipment used in the RNA extraction were cleaned and sprayed with RNase Zap (Ambion, Austin, USA) and washed with 70 % ethanol and RNase free water before proceeding to the isolation procedures.

Arabidopsis tissue was harvested and quickly snap-frozen in liquid nitrogen to prevent RNA degradation. Harvested tissue was ground into a fine powder in a 1.5 mL microcentrifuge tube with liquid nitrogen using a plastic pestle. To the ground powder, 1 mL of TRIZOL reagent (Invitrogen, USA) was added and mixed gently by inverting the tube upside down for

5 minutes. The sample was then centrifuged at 12, 000 × *g* in a desktop microcentrifuge for 10 minutes at 4 °C. The supernatant was transferred to a new tube which contained 200 µL of chloroform and was shaken vigorously by hand for 20 seconds. The mixture was incubated at room temperature for 5 minutes. The tube was centrifuged at 4 °C for 20 minutes at 16, 000 × *g* in a desktop microcentrifuge before the upper aqueous phase, containing nucleic acids was removed and transferred to a new tube. An equal volume (approximately 500 µL) of 100 % isopropanol was added and the sample mixed using a vortex. The tube was incubated at room temperature for 30 minutes to precipitate RNA and then was centrifuged at 12,000 g for 20 minutes at 4 °C in a desktop microcentrifuge to collect the RNA at the base of the tube. The supernatant was discarded and the pellet was washed twice using 70 % (v/v) ethanol and air-dried until the pellet's color turned transparent. RNase-free water (10-25 µL) was used to dissolve the pellet. DNA residues were removed from raw RNA extraction using the DNase treatment Kit and following the manufacturer's protocols (Ambion, Austin, USA). The purified RNA samples had their concentration measured using a NanoDrop spectrophotometer (Thermo Scientific, USA). To further examine the RNA quality, 0.5 µg of RNA was loaded on a 2 % agarose gel (see 2.5.2).

2.4.2 cDNA synthesis

In a 200 µl thin-walled microfuge tube purified total RNA (1-2 µg) was mixed with 1 µL of 50µM oligo$(dT)_{20}$, 1 µL of 10 mM dNTP and made up to a final volume of 13 µL with nuclease- free water. The tube was gently agitated by hand and incubated in a thermal cycler (Bio-Rad, USA) at 65 °C for 5 minutes. Once the heating procedure was finished, the tube was placed on ice immediately for 5 minutes. The following reagents from a Superscript III Reverse kit (Invitrogen, CA, USA), including 4 µL of 5× first strand buffer, 1 µl of 0.1 M DTT, 50 units of Reverse Transcriptase, 20 units RNaseOUT and nuclease- free water were added into the tube to a final volume of 20 µL. The tube was incubated in a thermal cycler machine at 50 °C for 60 minute followed by 72 °C for 15 min. The cDNA synthesized was stored at -20 °C until required.

2.5 Molecular cloning and plasmid constructions

2.5.1 Polymerase Chain Reaction (PCR)

2.5.1.1 Amplification PCR

PCR was widely employed in this project for various purposes. For instance, proof reading PCR was used to amplify DNA fragment from different templates for cloning; colony PCR was used to identify the insertion in *E.coli*, *Agrobacterium tumefaceiens* and *Saccharomyces cerevisiae* cultures; genotyping PCR was used for identify insertion events in transgenic plants. Each type of PCR was performed according to a similar procedure. A standard PCR using Phire^{TM} polymerase (Life Technology, NSW, Australia) was assembled as showed in Table 2.2. Specific primers for PCR were ordered from Geneworks (Adelaide, Australia) and details of the primers used will be given in the relevant chapters. The PCR cycling conditions were similar to the standard reaction shown in Table 2.3. The cycling conditions were modified as appropriate for each PCR, for example, the annealing temperature was adjusted according to each primer's nature and the extension time was adjusted according to the product length.

Table 2.2 The composition of a standard PCR

PCR components	Final Conc.
10 x Phire Buffer (with 2 mM $MgCl_2$)	1 x
dNTP	200 µM
Forward Primer	200 nM
Reverse Primer	200 nM
Phire polymerase	0.5 U/µL
Template	5-10 ng
H_2O	up to 10 µl

Table 2.3 standard PCR cycling conditions

Cycle Steps	Temperature	Time	Cycles
Initial denaturation	98 °C	30 s	1
Denaturation	98 °C	5 s	
Annealing	X °C	5 s	25-30
Extension	72°C	30 s/Kb	
Finalextension	72°C	1 min	1

Annealing temperature depends on the primer Tm value

2.5.1.2 Quantitative real-time RT- PCR (qRT-PCR)

Total RNA from Arabidopsis root tissue was isolated (Section 2.4.1) and cDNA was synthesised (Section 2.4.2) and used as a template for qPCR. Before performing qPCR the cDNA quality was tested by amplifying a section of the housekeeping gene (*AtActin2* (AT3G18780)) and the target gene using a standard PCR (20-25 cycles) (Section 2.5.1). qRT-PCR primers were carefully designed (GenScript, software for qPCR-PCR primer design) and

the specificity of the primers was tested. Primers which confirmed to be able to amplify the specific fragment of the transgene were used for qRT-PCR analysis. Primers used for analysing are listed in Chapter 3. The qRT-PCR experiments were conducted by Yuan Li (ACPFG, Adelaide, Australia). IQ SYBR green PCR reagent (Bio-Rad, Gladesville, Australia) was used to label amplified DNA and the fluorescence of the product was measured. Each qRT-PCR contained 5 µL IQ SYBR Green PCR reagent (Bio-Rad, CA, USA), 0.3 µL 10× SYBR Green (Bio-Rad, CA), 1.2 µL of each primers (4 µM), 2 µL of cDNA (DNase/RNase- free water was used as control) and 0.3 µL of water. Every sample had three technical replicates. An RG6000 Rotogene real time PCR cycler (QIAGEN, Hilden, Germany) was used to perform the qRT-PCR analysis. The cycling conditions followed the protocol described in Burton *et al*., (2008) using primers designed to the housekeeping genes were listed in Chapter 3. Normally, at least a region of four housekeeping genes were amplified along with the samples, and the three with the most consistent expression levels were used. To calculate the mean value of expression and standard errors, the selected housekeeping genes were used to normalize the mRNA level of each GOI with respect to the biological replicates that were treated under same conditions.

2.5.2 Agarose gel electrophoresis

The gel tank was cleaned and sprayed with RNase Zap before 1 x TAE buffer was transferred into it as running buffer. Agarose (1–2 % (g/mL)) was dissolved into 1 x TAE buffer (40 mM Tris-acetate, 1 mM EDTA) using a microwave. SYBR-safe (0.005 % (v/v)) (Invitrogen, Mulgrave, Australia) was added to the cooling gel to visualise DNA. PCR products or RNA (10 µL) was mixed with 6 x gel loading dye (New England BioLabs, USA) and loaded into the gel. A 1Kb or 100 bp DNA ladder or RNA ladder (ssRNA) was also loaded into the gel for indicating the product size. The gel was run at 70–110 V for at least 20 minutes. The gel was visualized with a UV transilluminator (Bio- Rad, NSW, Australia).

2.5.3 DNA extraction from agarose gel

When necessary, DNA products were extracted from the agarose gel in order to separate the target fragment from non-specific bands. The protocol for the Gel extraction Kit (Bioline, Australia) was strictly followed. Isolated DNA was run on the agarose gel (Section 2.5.2) for

further confirmation of the size of target fragment.

2.5.4 Cloning PCR products into a Gateway®entry vector

PCR products were amplified with Phusion™ Hot Start High-Fidelity DNA polymerase (FINNZYMES). However, due to the nature of this polymerase, the final product does not contain an overhanging 3' deoxyadenosine (A) residues that are required to compliment the overhanging 3' deoxythymidine (T) residues of the linearized entry vector pCR8/GW/TOPO (Invitrogen) which is required for ligation. Therefore, an A-tailing reaction was performed before the ligation. To ligate the desired DNA fragment into the pCR8 vector, 50-100 ng of A-tailed PCR product, 1 µL salt solution, 0.5 µL of pCR8/GW/TOPO TA Gateway® entry vector and nuclease- free water to a final volume of 6 µL were mixed gently. The mixture was incubated at room temperature for 30 min before 2 µL of the solution was added to TOP10 *E.coil* competent cells (Invitrogen, USA) for transformation. The transformation protocol will be described in section 2.5.6.

2.5.5 Cloning PCR products into Gateway® destination vector through an LR reaction

The target fragment that was successfully cloned into an entry vector was recombined into Gateway® destination vector using LR Clonase (Invitrogen). Equal amounts (around 150 ng) of entry and destination vector were gently mixed by pipetting and made up to a final volume of 9 µL with nuclease- free water. One microliter of LR Clonase II enzyme was added to the mixture and incubated at 25 °C for at least 1 hour. To stop the reaction 1 µL of Protein Kinase A (Invitrogen, USA) was added and the samples incubated at 37 °C for 10 minutes. For transformation, 2 µL of the reaction was transferred into TOP10 *E. coli* competent cells (Invitrogen, USA) (Section 2.5.6). The name of various destination vectors will be described in Chapter 4, 5 and 6.

2.5.6 *E. coli* transformation

E. coli TOP 10 (50µL) (Invitrogen) competent cells were thawed on ice, and 50 ng of the desired plasmid DNA was mixed gently with the cells and incubated on ice for 30 minutes. The cells were heat shocked at 42 °C for 30 seconds to facilitate entry of the plasmid into the *E.coli* and transferred immediately to ice for 2 minutes incubation. Once cooled, 250 µL of Lysogeny broth (LB) medium was added and the samples incubated with shaking (200 rpm) at 37 °C for 1 hour. A 50-100 µL subsample of culture was spread evenly on LB Difco agar (15

g/L) plates containing the appropriate concentration of selection antibiotic. Once the culture was dried, the plates were incubated at 37 °C overnight.

2.5.7 Plasmid DNA extraction from transformed *E. coli*

A single colony from the LB medium plate (Section 2.5.6) was picked with a pipette tip and inoculated in 5 mL liquid LB with an appropriate antibiotic. The culture was incubated at 37 °C with shaking (200 rpm) overnight. A plasmid DNA extraction kit (Bioline, Australia) was used to isolate the DNA from the overnight culture following the manufacturers' instructions. The plasmid DNA concentration was determined using an ND-1000 NanoDrop spectrophotometer (NanoDrop Technologies, USA). Isolated DNA plasmid was stored at -20 °C.

2.5.8 Restriction digestion

To determine the success of transformation and the direction of the insertion in either the entry or destination vector, selected restriction enzymes (enzymes cut on gene and vector's backbone) which cut the inserted fragment and the backbone were used in the restriction digestion. Typically, 500 ng of plasmid DNA, 1–10 units of selected restriction enzyme, 2 µL of Reaction Buffer, 10 µg of BSA and water were added to a final volume of 10µL, these were well combined by gentle pipetting and incubated at 37 °C for 1 to 3 h. The digested plasmid DNA was visualized by running the digested products on agarose gel (Section 2.5.2), and observing fluorescence using a UV transilluminator.

2.5.9 DNA sequencing

DNA sequencing was heavily employed in this project for confirming the correct insertion of gene and examining the primer's (qRT-PCR primer) quality through sequencing of their amplicons. Plasmid DNA or PCR product (around 100 ng) were mixed with 1.5 µL BigDye (BigDye® Terminator V3.1 Cycle Sequencing Kit,Applied Biosystems, Mulgrave, Australia), 3.5 µL BigDye Reaction Buffer, 3.2 pmol primer (sequencing primer) and MQ water bring to a final volume of 10 µL. The reaction was then placed in a thermal cycler under following cycling conditions: initial denaturing at 96 °C for 2 min, followed by 35–40 cycles of 96 °C for 10 s, 50 °C for 10 s and 60 °C for 4 min. Once the reaction was finished, a sample (10 µL) was mixed with 75 µL washing buffer (made as a stock containing 5 mL of 70 % (v/v) ethanol and 10 µL of 1 M $MgSO_4$) and was incubated in the dark for 15 minutes. The sample was

centrifuged (16,000 × *g*) for 15 minutes before the supernatant was carefully removed and the DNA pellet was air-dried. The sequencing procedure was conducted by the Australian Genome Research Facility (Adelaide, Australia) by capillary separation and sequence determination.

2.6 *Agrobacterium tumefaciens*-mediated Arabidopsis transformation

Arabidopsis (6-7 weeks old, flowering) were transformed using the *A. tumefaciens* mediated flora-dip method (Zhang *et al*. 2006). In brief, the destination vector which contained the target gene was transformed into *A. tumefaciens* competent cells (strain AGL1) using a modified freeze-thaw method Höfgen and Willmitzer (1988). Two micrograms of plasmid DNA was inoculated into 50 µL of *A. tumefaciens* competent cells and incubated on the ice for 5 minutes, followed by freezing in liquid nitrogen for 5 minutes and then incubated at 30 °C for another 5 minutes. LB medium (1 µL) was added to sample which was then incubated at 37 °C with shaking (200 rpm) for 2 hours. The culture was then spread on a LB plate (with 2 % agar w/v) containing Rifampicin (25 µg/mL) and Kanamycin (50 µg/mL) and placed in a 37 °C incubator (Ratek Instruments, Australia) overnight. A single colony carrying the foreign gene was confirmed by colony PCR (Section 2.5.1) with gene specific primers. The appropriate colony containing the expression vector was inoculated in 10 mL LB medium containing the appropriate antibiotics at 30 °C for 2 days with constant shaking (200 rpm), before 2 mL of the culture was then transferred to another 500 mL fresh LB medium for a further 15 hours culturing at same conditions. The culture was collected by centrifugation at 400 × *g* for 10 minutes (ROTANTA 460R centrifuge, Hettich, Germany) and the pellet gently resuspended in 200 mL of 5% (w/v) sucrose solution with 0.025 % (v/v) Silwet L-77. Arabidopsis flowers were immersed into the culture for 30 s and wrapped with cling film to maintain moisture. The transformed plants were kept in dark at room temperature overnight before the cling wrap was removed afterwards. Plants were kept in long day growth with appropriate watering until the seeds were mature.

2.7 Genotyping transgenic plants

2.7.1 Identifying insertion lines

To confirm the presence of a transgene in Arabidopsis, a standard PCR (Section 2.5.1) was used with transgene specific primers. Details of the primers that were used to identify the insertion lines are listed in Chapter 6.

2.7.2 Southern-blotting

To determine the number of insertion events in T_1 lines Southern-blots were used (Southern 2006). High quality gDNA was isolated (section 2.3.3) from T_1 mutant plants and then completely digested with *HindIII* (New England Biolabs, USA) at 37 °C overnight. After digestion, the mixture was combined with 6 × Ficoll dye (New England Biolabs, USA) and loaded into a 1 % high quality agarose gel (Bioline, Australia). The gel was denatured in a denaturation buffer (0.5 M NaOH, 1.5 M NaCl) for 80 minutes with gentle shaking. After 40 minutes the buffer was removed and the denatured gel was then treated with a neutralization buffer (1.5 M Tris and 1.5 M NaCl, pH 7.5) twice for another 40 minutes (20 mins each). To transfer the DNA from the agarose gel to an N^+ bond membrane (GE Healthcare Life Sciences, Australia) the structure described in Figure 2.1 was assembled. The DNA was transferred to the membrane driven by the gradient established by the addition of 0.4 M NaOH. The transferring procedure was conducted overnight at room temperature. Instead of labeling the target fragment with 32P, a non-radioactive label method was used in this project. The Dig-11-dNTP (Roche, Germany) was used to label the probe with a standard PCR reaction (Table 2.4).

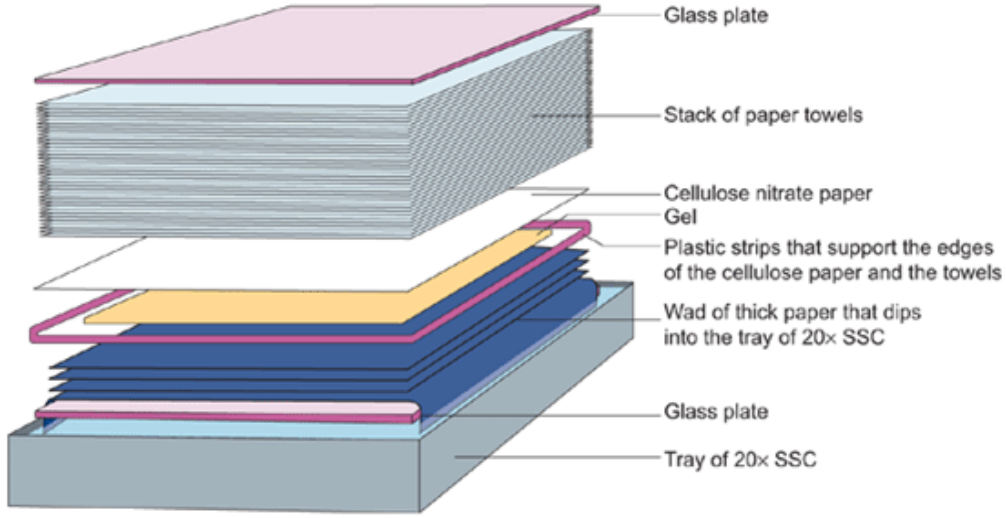

Figure 2.1 The assembly for a Southern blotting DNA transfer (Southern, 2006)

Table 2.4 the PCR composition used to produce the DIG-probe

PCR components	Final Conc.
10 x Buffer	1 x
dNTP	200 µM
Forward Primer	200 nM
Reverse Primer	200 nM
Dig-11-dNTP	50 µM
$MgCl_2$	2 mM
Taq polymerase	0.5 U/µL
Probe PCR fragment	1-5 ng
H_2O	up to 50 µL

After an overnight incubation, the DNA was transferred to the Hybond N^+ nylon membrane (Biodyne B, Pall Corporation). The membrane was immersed and washed in 6 × SSC (0.9 M NaCl and 90 mM trisodium citrate, pH 7.0) with shaking for 5 minutes at room temperature. The washed membrane was placed between 2 pieces of mesh and transferred into a hybridization bottle to which 20 mL DIG Easy Hyb Granules (Roche, Germany) for were added pre-hybridization. The bottle was closed and incubated with rolling for 2 hours at 42 °C. The hybridization solution (Hyb solution) was removed after the incubation and 10 mL Hyb solution containing a DIG labelled probe (10-25 ng/mL) was added for overnight incubation at 42 °C. The probe labelled membrane was firstly washed in 2× SSC / 0.1 % SDS for 5 minutes at room temperature and secondly washed with 0.5× SSC/0.1% SDS s at 68 °C for 15 minutes. The membrane was taken out from the hybridization bottle and immersed in 10 mM maleic acid (with 0.03 % Tween 20 and 15 mM NaCl) and incubated with gentle shaking for 15 minutes. The blocking solution (1×, 75 µL) (Roche, Germany) was applied to the membrane which was gently shaken for 45 minutes. The blocking solution was poured off and another 75 mL of 1 × blocking solution (containing 7.5 µL anti-digoxigen AP (Roche, Germany)) was added for one hour at room temperature. The membrane was transferred to a fresh container and washed with washing buffer (0.2 × SSC, 0.1% SDS) twice for 15 minutes. The washed membrane was immersed in 1× detection buffer and gently shaken for 5 minutes. Finally, the membrane was carefully placed in a clean plastic bag and 1–2 mL of detection buffer, containing 1:100 diluted CDP-star (Roche, Germany), was spread evenly onto the membrane. The plastic bag was sealed and incubated at room temperature in the dark for 5–10 minutes. The membrane was then placed in an autoradiography cassette (GE Healthcare Life Care, NSW, Australia) with Fuji medical X-ray film (Fujifilm) and stored at room temperature for 1-2 d to increase the film sensitivity. The film was developed using a

CP1000 automatic film processor (AGFA, Mortsel, Belgium).

2.8 Statistical analysis

Microsoft Excel 2010 (Microsoft Inc, USA) and GraphPad Prism 6 (GraphPad software Inc, USA) were used in this project to perform the statistical analyses described in the text of the relevant chapters.

Chapter 3: Selection of candidate proteins that catalyze root-to-shoot transfer of chloride

3.1 Introduction

Stressful conditions, such as drought and salinity, are widely observed worldwide and these environmental issues can significantly affect crop plant growth and limit their productivity. Plants employ a raft of sophisticated mechanisms to tolerate these stressful conditions. A major mechanism for tolerance to salinity stress in higher plants is the maintenance of ion homeostasis in cell-types and tissues. Previous studies have shown that both the regulation of Na^+ and Cl^- transport are involved in plant responses to salt stress, and toxicity occurs when either ion accumulates to high levels in the cytoplasm (Teakle and Tyerman, 2010). Particular emphasis is still largely placed, on the regulation of Na^+ but not Cl^- transport, despite Cl^- being the apparent cause of toxicity in many plant species undergoing salt stress (Teakle and Tyerman 2010). Na^+ exclusion from the shoot is positively correlated with salt tolerance and excluding Na^+ is critical to improve the salt tolerance (Munns and Tester, 2008; Plett and Møller, 2010; Munns *et al*., 2012; Roy *et al*., 2014). It has been suggested that exclusion of Cl^- from the shoot is also positively correlated with salt tolerance (Teakle and Tyerman, 2010). Therefore, it is likely that restricting Cl^- transport from the root to shoot may also contribute to improve the plant salt tolerance.

Under normal conditions, Cl^- efflux out of the cell is a passive event as the plasma membrane potential is usually highly negative (positive outside). An active influx of Cl^- can happen when it is transported along with protons (Felle 1994; Sanders 1980). Under saline conditions, Na^+ entry into cells affects membrane equilibrium and depolarizes the membrane potential, which allows passive entry of Cl^- through an anion channel down as electrochemical gradient (Skerret & Tyerman, 1994; Blumwald *et al*., 2000; Teakle and Tyerman, 2010). Physiological studies have showed a quick activating anion conductance (X-QUAC), identified in xylem parenchyma cells, which could catalyse xylem Cl^- transport within barley roots (Cram and Pitman, 1972).

Previous studies have shown that when plants were under salt/ drought stress, ABA significantly inhibits the loading of Cl^- (and other ions) into the xylem, whilst not affecting ion influx (Cram and Pitman, 1972). Under stress conditions, this means that Cl^- will accumulate in the root but not be transported to the shoot (Cram and Pitman 1972). Using patch clamp

electrophysiology, ABA was also found to significantly reduce the activity of stelar K^+ outwardly-rectifying channels (Gaymard *et al*. 1998; Roberts 1998) and the major Cl^- conductance in this tissue (Gilliham and Tester 2005). An Arabidopsis gene that encodes the stelar K^+ outwardly-rectifying channel (*AtSKOR*) has been isolated and shown to be strongly transcriptionally down-regulated by external ABA (Pilot *et al*. 2003), and there is physical evidence for a stelar Cl^- transporter, but no gene encoding a stelar Cl^- transporting protein has yet been identified.

Plant salinity tolerance studies often focus on the whole organ or plant level. This is not ideal to capture a full understanding of the roles of particular cell types in response to salt stress. Recently, evidence has been found to suggest that plant salinity tolerance is influenced by key types of ion transporters that are present in very specific cell types. The HKT family involved in the retrieval of Na^+ from the xylem is often highly expressed in the root stelar tissue (Byrt *et al.*, 2007, Davenport *et al.*, 2007, Munns and Tester, 2008, Møller *et al*. 2009, Munns *et al*., 2012) due to having a very specific role in ion transport – retrieval of Na^+ from the stele. Therefore, to investigate Cl^- transport mechanisms, especially under salt stress, a focus will be paid to root stelar tissue.

As most ion transport in higher plants is facilitated by membrane localized protein, to identify candidate genes encoding Cl^- transporters/channels, identification of genes that are expressed in the stele and are down-regulated by ABA could help to identify those genes encoding important proteins involved in Cl^- transport. Therefore, several preliminarily candidate genes were selected by reviewing published literature (Chapter 1), analyzing in-house microarray data of genes expressed in pericycle and cortical cells, and mining of the eFP browser (http://bar.utoronto.ca/efp/cgi-bin/efpWeb.cgi) and GENEINVESTIGATOR (https://genevestigator.com/gv/) Arabidopsis online databases. Candidate genes were selected on two criteria deemed critical for a protein likely to transport anions in the root: **1)** high expression in Arabidopsis root stelar tissue; and **2)** encoded proteins which were predicted to be localized to the plasma membrane. Once candidate genes were identified, quantitative real time PCR (q-RT-PCR) was performed on Arabidopsis root cDNA upon addition the NaCl and ABA treatment. Candidate genes that were both down- regulated by NaCl and ABA will be selected as the GOIs in this project for additional functional characterization to determine whether they are involved in the long distance transport of chloride from root to shoot.

3.2 Materials and methods

3.2.1 Mining of microarray data

A previous Affymetrix microarray experiment, studying the cell specific responses of Arabidopsis root to salt, was performed by Dr Aurelie Everard, Dr Alex Jonathon and Dr Ute Bauman at the Australian Centre for Plant Functional Genomics. The detailed methods and materials were described in Evrard (2013). In brief, two Arabidopsis *GAL4:GFP* enhancer trap lines with stelar and cortical cell specific expression of GFP (from C24 background) J2731* and J1551 were used to isolate specific cell types from which RNA could be extracted. Plants were grown under control conditions (2 mM NaCl) for seven days and were treated with NaCl for two days (25 mM NaCl on first day of treatment and 50 mM NaCl on second treatment day). After treatment, fluorescence-activated cell sorting (FACS) was used to rapidly separate root cells which had GFP fluorescence from the remainder of the root cells. RNA was then extracted from the isolated protoplasts, and cDNA was synthesised to perform the comparative microarray using the Affymetrix ATH1 chip (Evrard 2013). Standard protocols for microarray hybridisation and analysis were used (Evrard 2013).

3.2.2 *In silico* analysis using public database

Public databases such as GENEVESTIGATOR (Zimmermann *et al.*, 2004) and Arabidopsis eFP Browser database (Winter *et al*., 2007) that contain large quantities of Arabidopsis microarray data were used in this project to investigate gene expression profiles in various tissues and stress treatments (such as NaCl and ABA). Several candidate genes that meet the criteria (i.e. PM localized, expressed in root parenchyma cells) were initially selected according to the previous published literature (Chapter 1) and then searched in the public database.

3.2.3 Plant material and growth condition

Arabidopsis thaliana (Col-0) was used as plant material in this chapter. The details of seeds germination and Arabidopsis growth conditions can be found in Chapter 2 (Section 2.1.3). Arabidopsis were grown in hydroponics for 4 weeks (with basal nutrient solution (BNS) changed weekly). At the start of the 5th week, NaCl was added to the BNS solution to a final concentration of 50 mM or 100 mM and the plants grown for a further week. For the ABA treatment, solid +/- cis, trans ABA (Sigma) was initially dissolved in 99% ethanol to make a

100 mM stock. The appropriate amount of stock solution was added to the BNS solution to make a final concentration of 20 µM. Samples were taken 4h and 16h after treatment. After the appropriate amount of time, Arabidopsis root tissues were harvested at approximately midday and snap frozen in liquid N_2. Harvested tissues were stored in a - 80 °C freezer for further analysis. Each treatment contained 5 replicates.

3.2.4 Quantitative RT-PCR (qRT-PCR) of GOI expression analysis in Arabidopsis root

To determine the expression level of the GOI under NaCl and ABA treatment, qRT-PCR was performed to determine the relative transcriptional level in Arabidopsis root. RNA was extracted from NaCl or ABA treated Arabidopsis root tissue, and cDNA was synthesized following the method outlined in chapter 2. The gene specific qRT-PCR primers (Table 3.1) were designed using GenScript primer design software and the specificity of the primers was confirmed by sequencing the target product. Specific primers were then used for qRT-PCR analysis. The qRT-PCR was conducted by Yuan Li (Australian Centre for Plant Function Genomics, Adelaide, Australia) following the protocol described in Hackenberg *et al*., (2012). Four Arabidopsis housekeeping genes including *AtGAPDH*, *AtTublin*, *Atactin* and *AtCycophlin* were used to normalize the GOI's expression data.

Table 3.1 Primers used to qRT-PCR analysis in this chapter.

Gene Name	Forward Primer	Reverse Primer	Product Size (bp)	Tm * (℃)
AAP3	GCCGTTATGTCCTTCACTTATTCC	TGTCTCTGTTACTGCTCCTATGC	120	60
ABCB14	GCGTATCCCACTAGACCCGAAATC	GTCCGATCACTGTGCTCTTTCCC	118	62
CLCc	GGCACGAAGGAGACCATC	CGATTCCTAGCGAGAAGAG	127	57
NRT1.5	AGAGGATCACATGCCTGGT	TCGTTCCTCTTCACTCTCG	211	54
NRT1.8	CAAGCTCCAGCACTTTGAG	AGCCATGCACATCATCTGT	236	56
NRT1.9	ATCACGGCTGCGAAAGTC	ATCCATTGCCACCGAACC	150	60
SLAH1	TCTTCATGTCCCTGGTCTG	ATTGCTGTTTGCTGCTGTC	229	57
SLAH3	ATCTCTCGGTCGTTGGGAACTTTG	CTCGTTGGTCGGTAGCCTTTGG	146	56
SLAH4	CGCAAAGAGAGAAAGACTAAC	GCACCATAATCTTCCACAAC	136	56
CCC	TGGGAGAGATCAAGAGACAA	GGTGATTCAACGGAGGTG	186	57
NAXT5	TAGGAGTTGCGGATGCTTTT	CAAGCGGCTGCTATTAAGGT	215	58
GAPDH	TGGTTGATCTCGTTGTGCAGGTCTC	GTCAGCCAAGTCAACAACTCTCTG	262	65
Cyclophiln	TGGCGAACGCTGGTCCTAATACA	CAAAAACTCCTCTGCCCCAATCAA	223	66
Tublin	GAGTTCACGGAAGCGGAGAG	ATATCTTTCAGGCTCCACCGA	224	62
actin	GAGTTCTTCACGCGATACCTCCA	GACCACCTTTATTAACCCCATTTACC	180	63

3.3 Results

3.3.1 Candidate genes preferentially expressed in the root stele were selected from microarray analysis

To identify candidate proteins involved in anion xylem loading, a cell specific comparative microarray was performed between the Arabidopsis root pericycle and cortical cells (Evrard, 2013). The dataset was further interrogated to select candidate genes that encode potential anion transporters that were highly expressed in the root stelar tissue and down-regulated by salt treatment. More than 10 candidate genes were identified that may be involved in xylem Cl^- loading (data not shown), four of them (Table 3.2) were selected as they have the highest fold change, which suggesting preferentially expressed in the root stelar tissue ($p<0.05$). *AtNRT1.5* (At1g32450), already characterised as a $2H^+/NO_3^-$ symport transporter with a role in NO_3^- loading of the xylem, was highly expressed in the root stelar tissue compared to the cortex (Log Fold-change: 3.61, $P< 0.05$) (Table 3.2). The second candidate gene, *AtAAP3* (At1g77380), amino acid permease 3, a potential anion transporter had a relatively high and statistically significant preferential expression in the root stele and it was down-regulated upon salinity stress (Table 3.2). The third gene, *AtClCc* (At5g49890), a member of chloride channel was identified involved in nitrate transport and related to the chloride movement in shoot across the tonoplast membrane (Jossier *et al*., 2010). Although previous results indicated that *AtClCc* was preferentially expressed in shoot over root, the results from the microarray data results suggested that *AtClCc* has higher expression in stelar rather than cortex ($p< 0.05$). The last candidate gene, *AtNPF2.4* (At3g45700), a proton-dependent oligo-peptide transporter, was also shown to have higher expression in pericycle than cortex ($p< 0.05$) (Table 3.2).

Table 3.2 Candidate genes that preferentially expressed in root stelar than cortex were selected upon microarray data.

Affymetrix Identifier	Gene ID	Tair annotation	Fold Change (pericycle-cortex log2)	adj. p.value
260693_at	At1g32450	*AtNRT1.5*	3.61	0.01
246389_at	At1g77380	*AtAAP3*	1.77	0.01
248580_at	At5g49890	*AtCLCc*	1.66	0.047
252536_at	At3g45700	*AtNAXT5*	1.76	0.038

3.3.2 Candidate gene profiling using public database

The Affymetrics ATH1 microarray data only revealed four candidate genes that were

preferentially expressed in stelar tissue (Table 3.2). However, how the gene transcriptional level was changed upon salt and ABA treatments was yet unknown. To further explore more potential candidate genes that may be involved in long- distance anion transport, two public microarray databases (Arabidopsis eFP Browser database and GENEVESTIGATOR) were mined. These two databases integrate large numbers of microarray data regarding to Arabidopsis gene expression profiles in different organs and tissue types from many experiments. The transcriptional level of Arabidopsis genes were examined for response to environmental stresses (such as cold, salinity and drought) and hormone treatments (such as ABA, IAA and Cytokinin) Figure 3.1 and Figure 3.2. Based on the microarray study and candidates identified in the literature search, 11 candidates were selected (*AtSLAH1*, *AtSLAH3*, *AtSLAH5*, *AtNPF2.4*, *AtNRT1.5*, *AtNRT1.8*, *AtNRT1.9*, *AtCCC*, *AtAPP3*, *AtCLCc* and *AtABCB14*). Unfortunately, information on the expression of *AtSLAH4* and *AtCCC* was not available in both public microarray databases as they are not contained on the ATH1 chip. Figure 3.1 shows the transcriptional change of the nine selected candidate genes when Arabidopsis was challenged with 150 mM NaCl for 0- 24 hours. These results suggested that the expression level of *AtSLAH1* (Figure 3.1 A), *AtNPF2.4* (Figure 3.1 C), *AtNRT1.5* (Figure 3.1 D), *AtNRT1.9* (Figure 3.1 F) and *AtABCB14* (Figure 3.1H) in root were down-regulated with prolonged NaCl treatment. The rest of candidate genes were either up-regulated or did not respond to the salt treatment. For the ABA treatment in the databases, 10 µM of ABA was applied to the root from 30 minutes to 3 hours (Figure 3.2). The results suggested that *AtSLAH1* (Figure 3.2 A), *AtNRT1.5* (Figure 3.2 D), AtNRT1.9 (Figure 3.2 F) and *AtAAP3* (Figure 3.2 G) were down-regulated upon ABA treatment. In summary, only *AtSLAH1*, *AtNRT1.5*, *AtNRT1.9* and *AtNPF2.4* met the selection criteria of both being down-regulated by NaCl and ABA.

To further examine the gene transcript changes in different tissues and development stages, Genevestigator was used to profile the expression of all candidate genes. The microarray data suggested that all the candidate genes had medium to high expression with no significant expression differences between these candidatures in different development stages (Figure 3.3). *AtNRT1.5* (Figure 3.3 A), *AtNRT1.5* (Figure 3.3 B), *AtNPF2.4* (Figure 3.3 C), *AtNRT1.9* (Figure 3.3 D), *AtSLAH3* (Figure 3.3 E) and *AtAAP3* (Figure 3.3 G) were found to be strongly expressed in root pericycle. The expression change of all candidate genes upon the application of salt and ABA stress were also examined using GENEVESTIGATOR, similar results were identified in comparisons to the eFP database (data not shown).

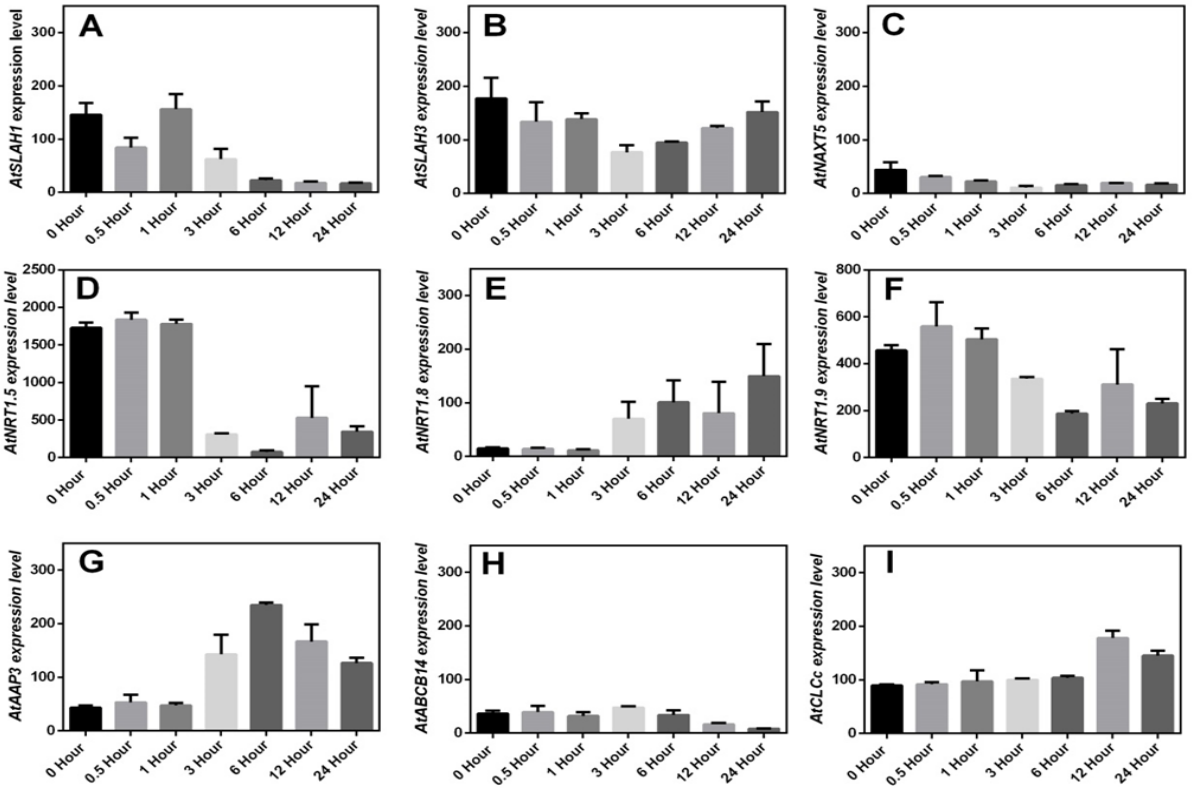

Figure 3.1 the transcript level changes of all candidate genes upon 150 mM NaCl treatment for 0-24 hours. (A) *AtSLAH1*; (B) *AtSLAH3*; (C) *AtNPF2.4*; (D) *AtNRT1.5*; (E) *AtNRT1.8*; (F) *AtNRT1.9*; (G) *AtAAP3*; (H) *AtABCB14*; (I) *AtCLCc*. Data was extracted from Arabidopsis eFP Browser database. Results were presented as mean ± SD (n= 3). Y axis: Gene chip operating software (GCOS) signal (adapted from Kilian *et al*., 2007)

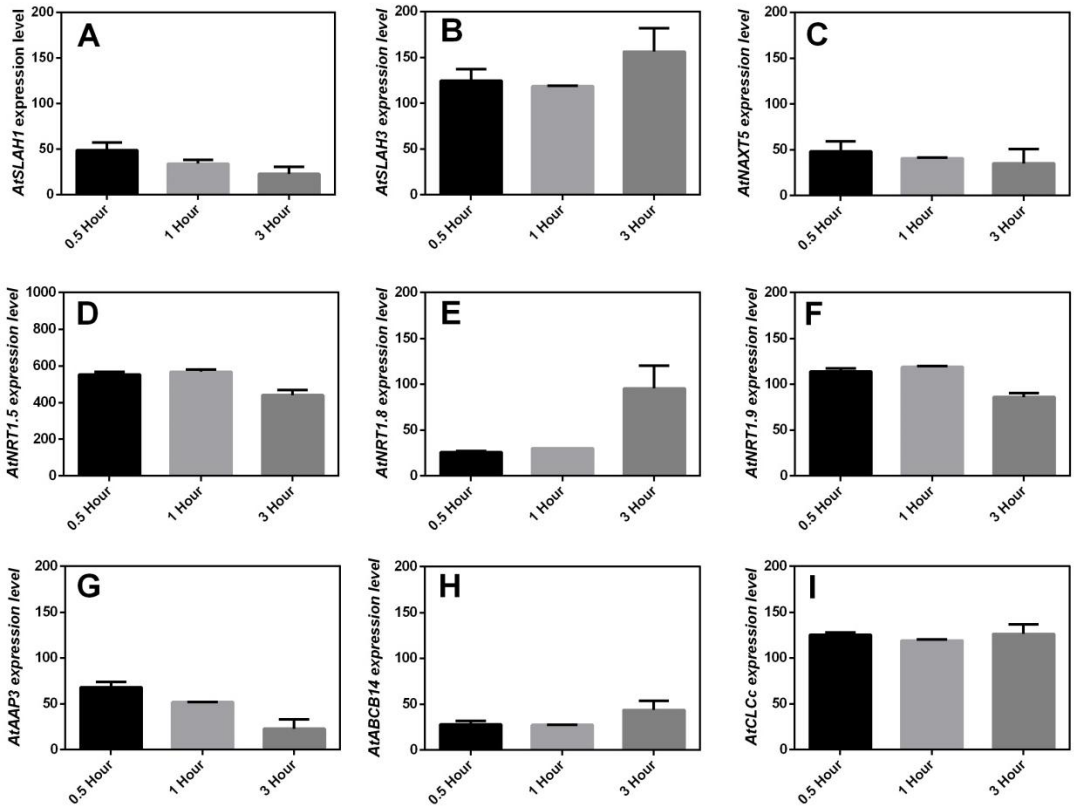

Figure 3.2 the transcript level changes of all candidate genes upon ABA (20 µM) treatment for 0.5-3 hours. (A) *AtSLAH1*; (B) *AtSLAH3*; (C) *AtNPF2.4*; (D) *AtNRT1.5*; (E) *AtNRT1.8*; (F) *AtNRT1.9*; (G) *AtAAP3*; (H) *AtABCB14*; (I) *AtCLCc*. Data was extracted from Arabidopsis eFP Browser database. Results were presented as mean ± SD (n= 3). Y axis: GCOS signal (adapted from Kilian *et al*., 2007)

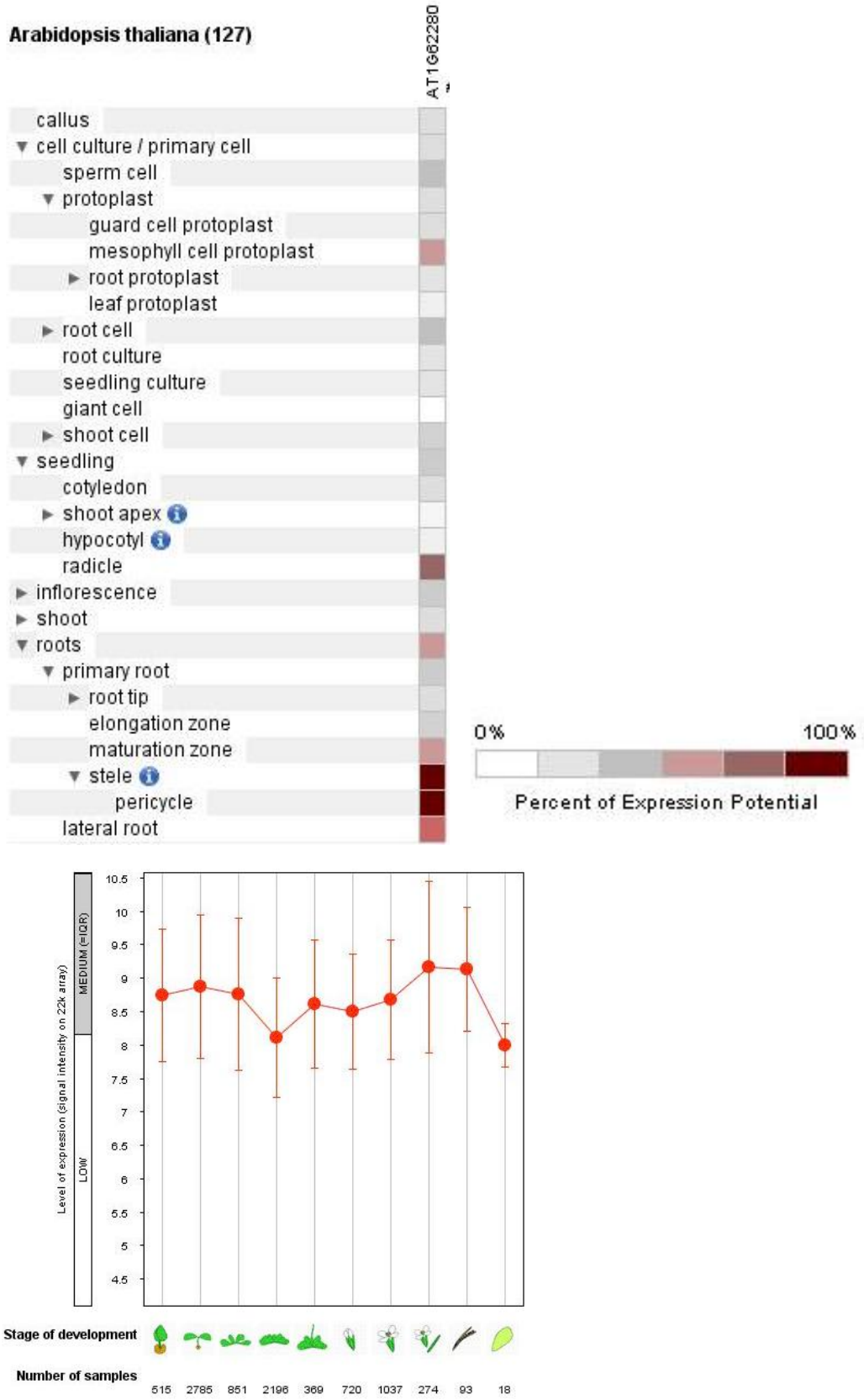

Figure 3.3 (A) Expression of *AtSLAH1* in different parts of Arabidopsis tissues and different development stages. Date and images were created by GENEVESTIGATOR.

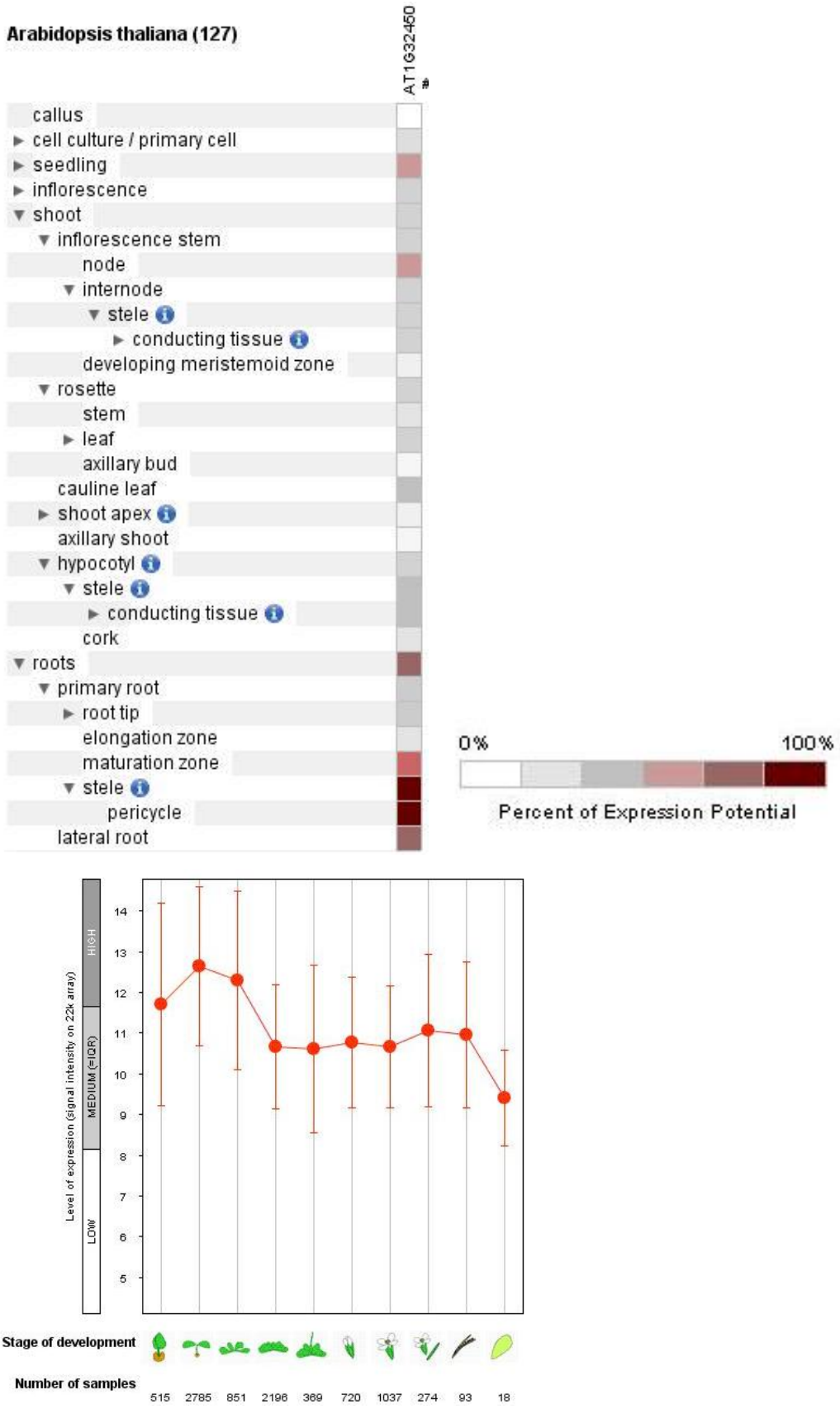

Figure 3.3 (B) Expression of *AtNRT1.5* in different parts of Arabidopsis tissues and different development stages. Date and images were created by GENEVESTIGATOR.

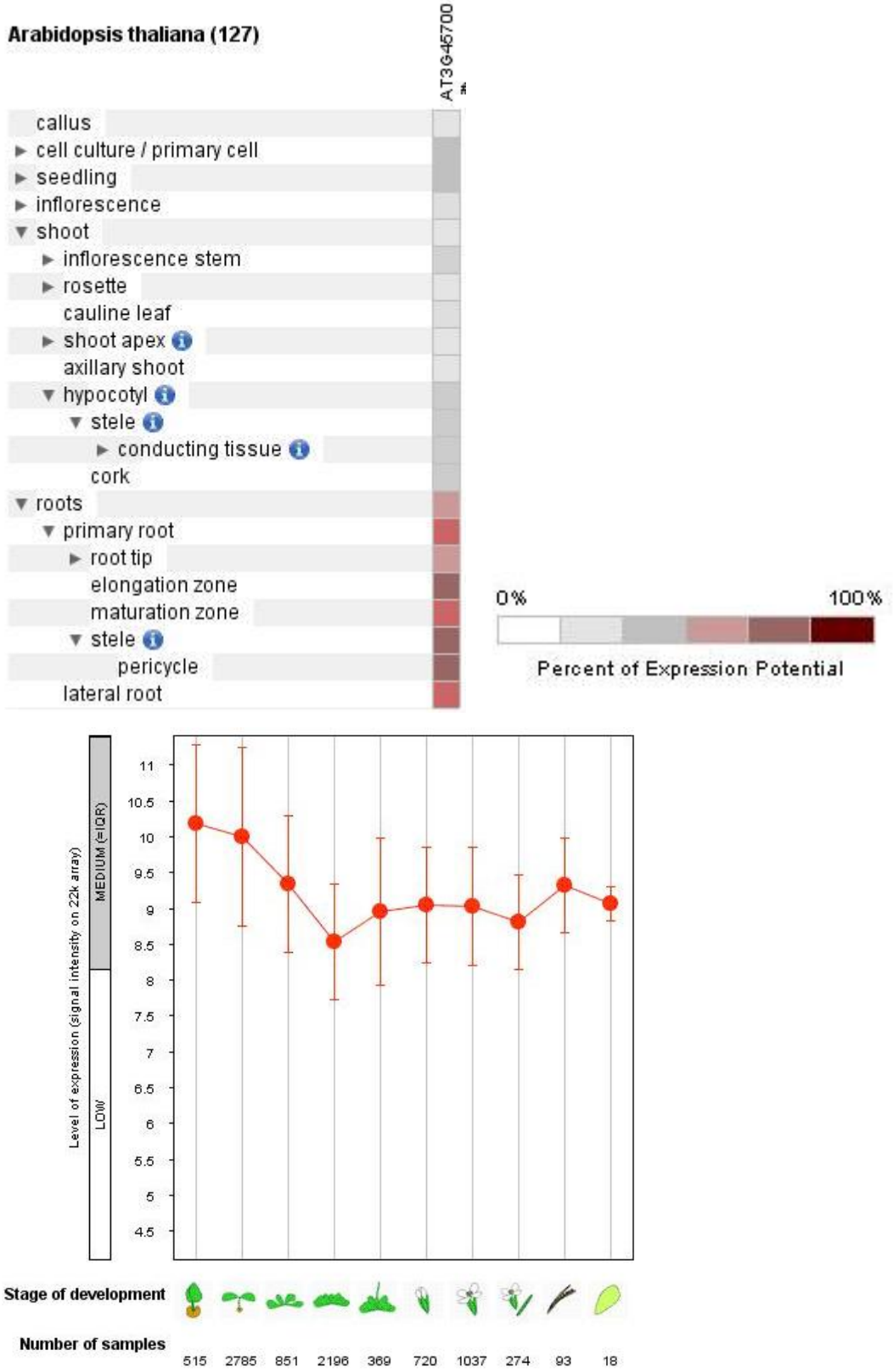

Figure 3.3 (C) Expression of *AtNPF2.4* in different parts of Arabidopsis tissues and different development stages. Date and images were created by GENEVESTIGATOR.

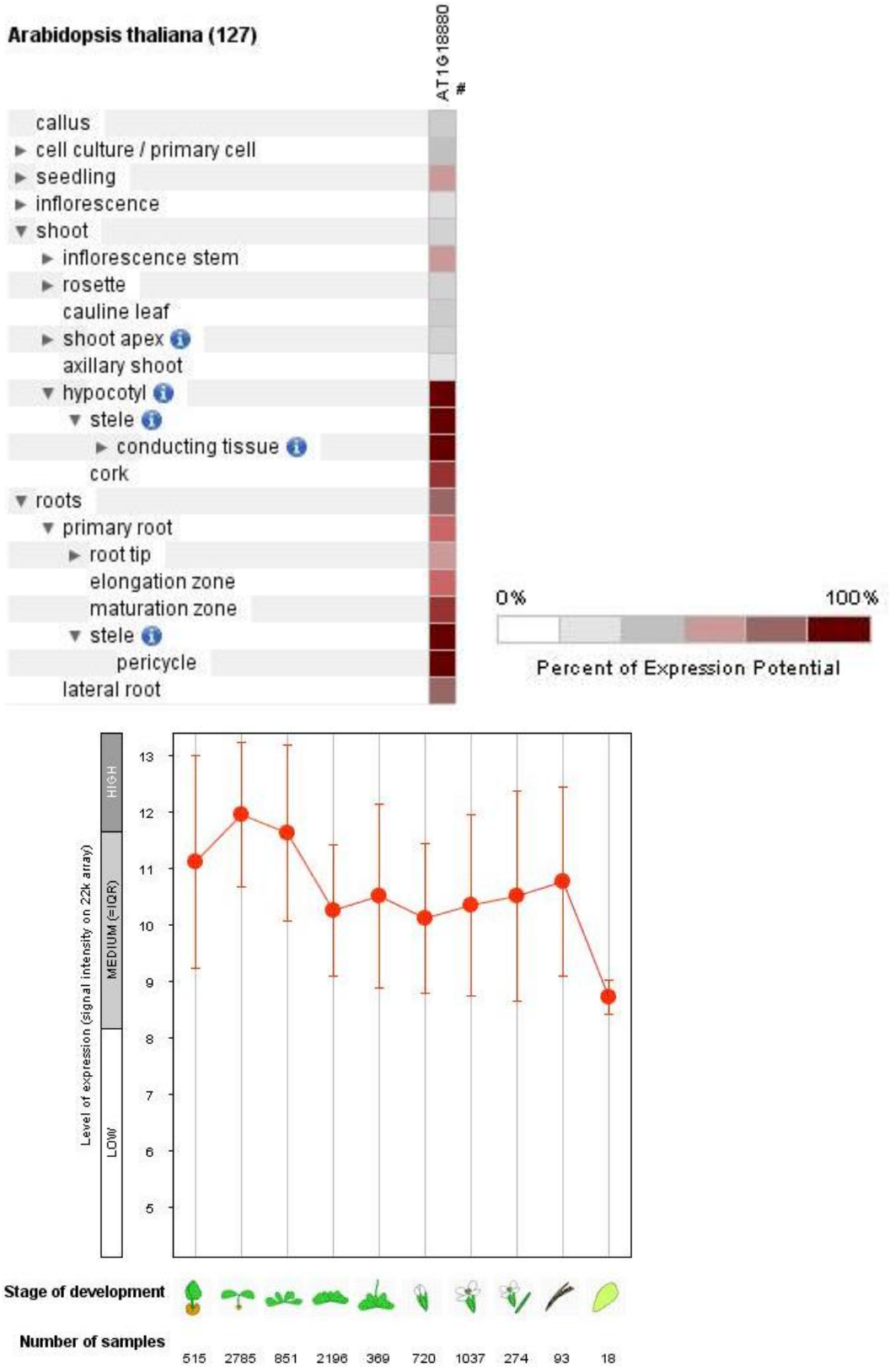

Figure 3.3 (D) Expression of *AtNRT1.9* in different parts of Arabidopsis tissues and different development stages. Date and images were created by GENEVESTIGATOR.

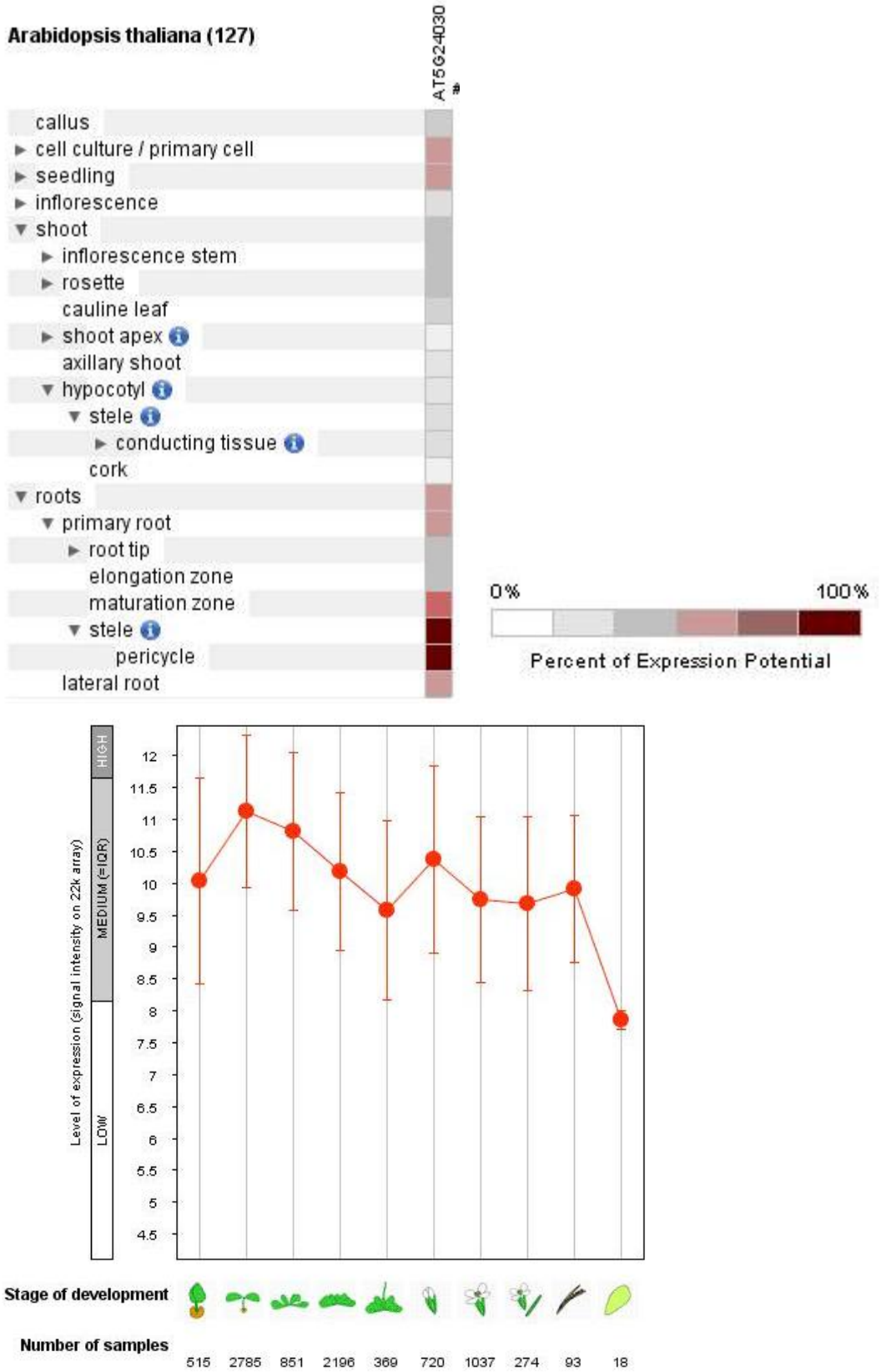

Figure 3.3 (E) Expression of *AtSLAH3* in different parts of Arabidopsis tissues and different development stages. Date and images were created by GENEVESTIGATOR.

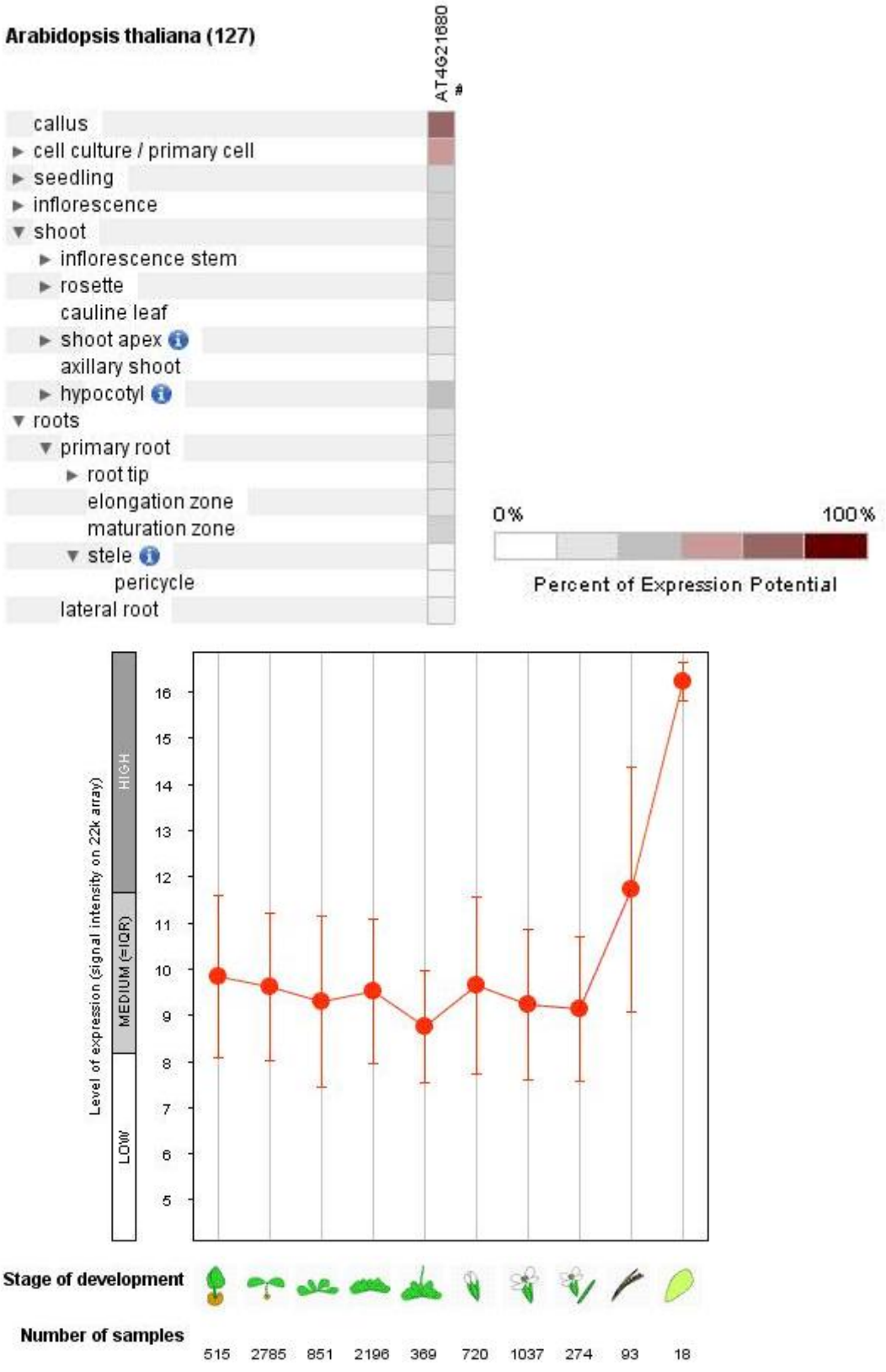

Figure 3.3 (F) Expression of *AtNRT1.8* in different parts of Arabidopsis tissues and different development stages. Date and images were created by GENEVESTIGATOR.

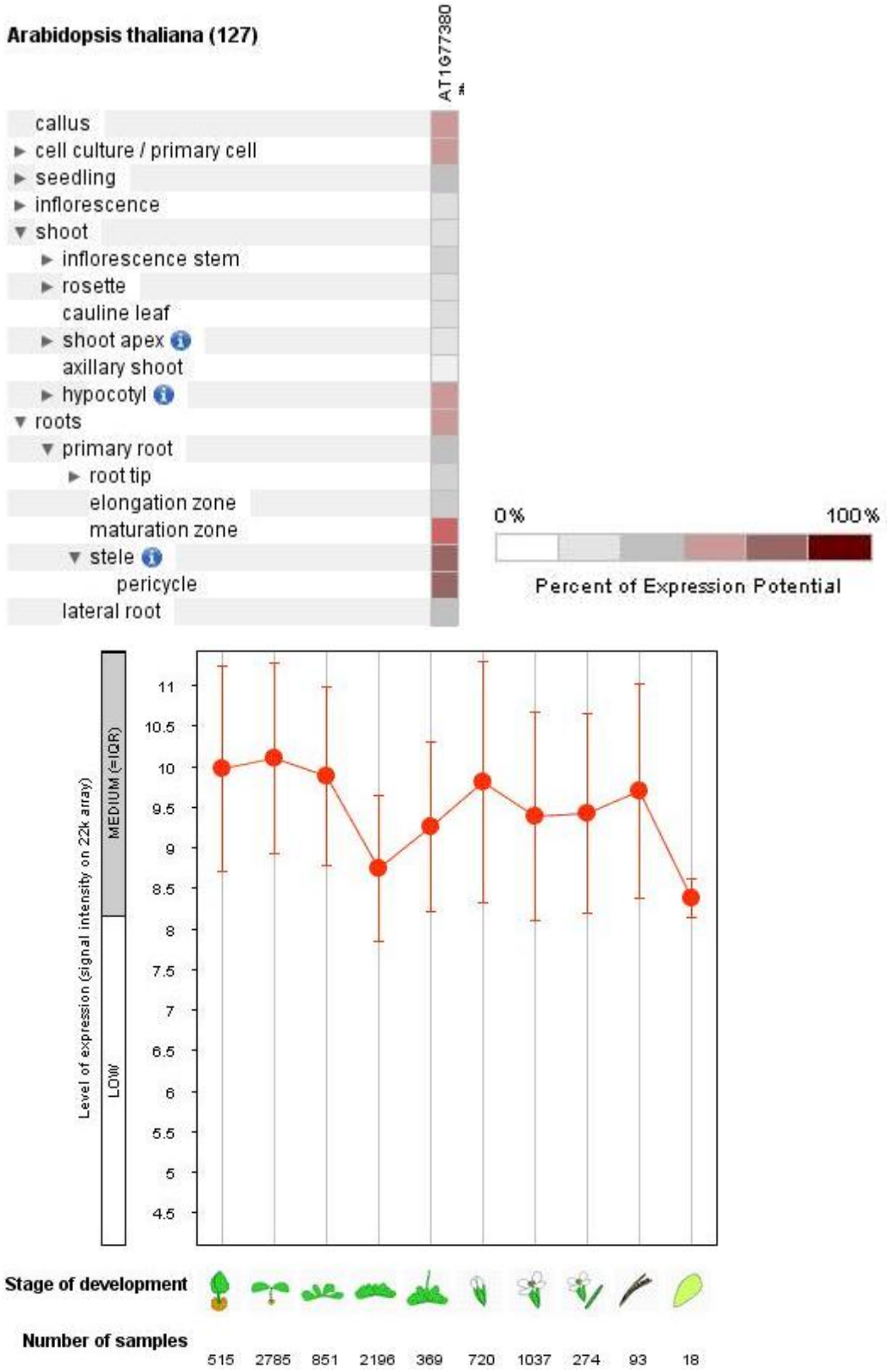

Figure 3.3 (G) Expression of *AtAAP3* in different parts of Arabidopsis tissues and different development stages. Date and images were created by GENEVESTIGATOR.

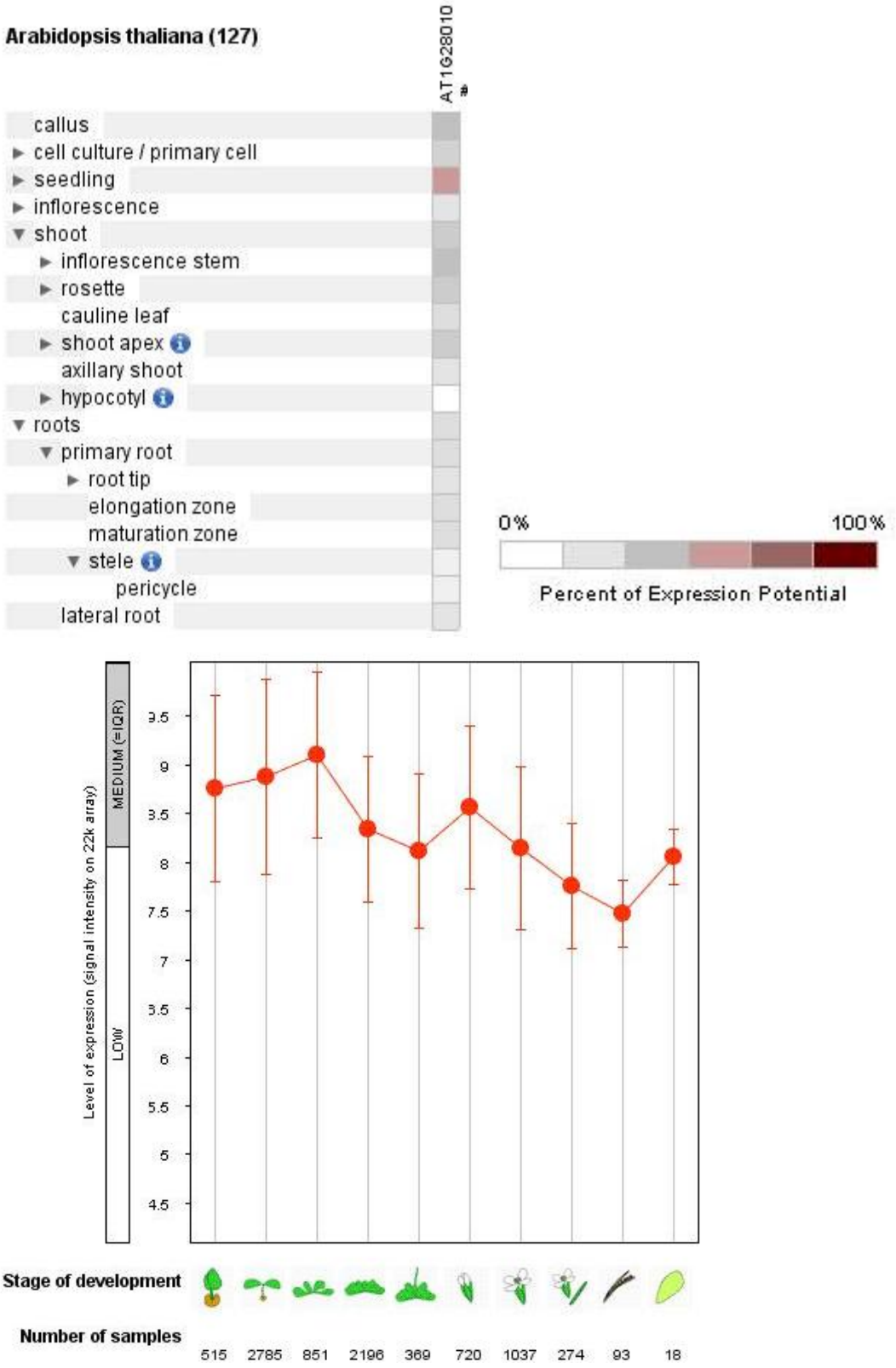

Figure 3.3 (H) Expression of *AtABCB14* in different parts of Arabidopsis tissues and different development stages. Date and images were created by GENEVESTIGATOR.

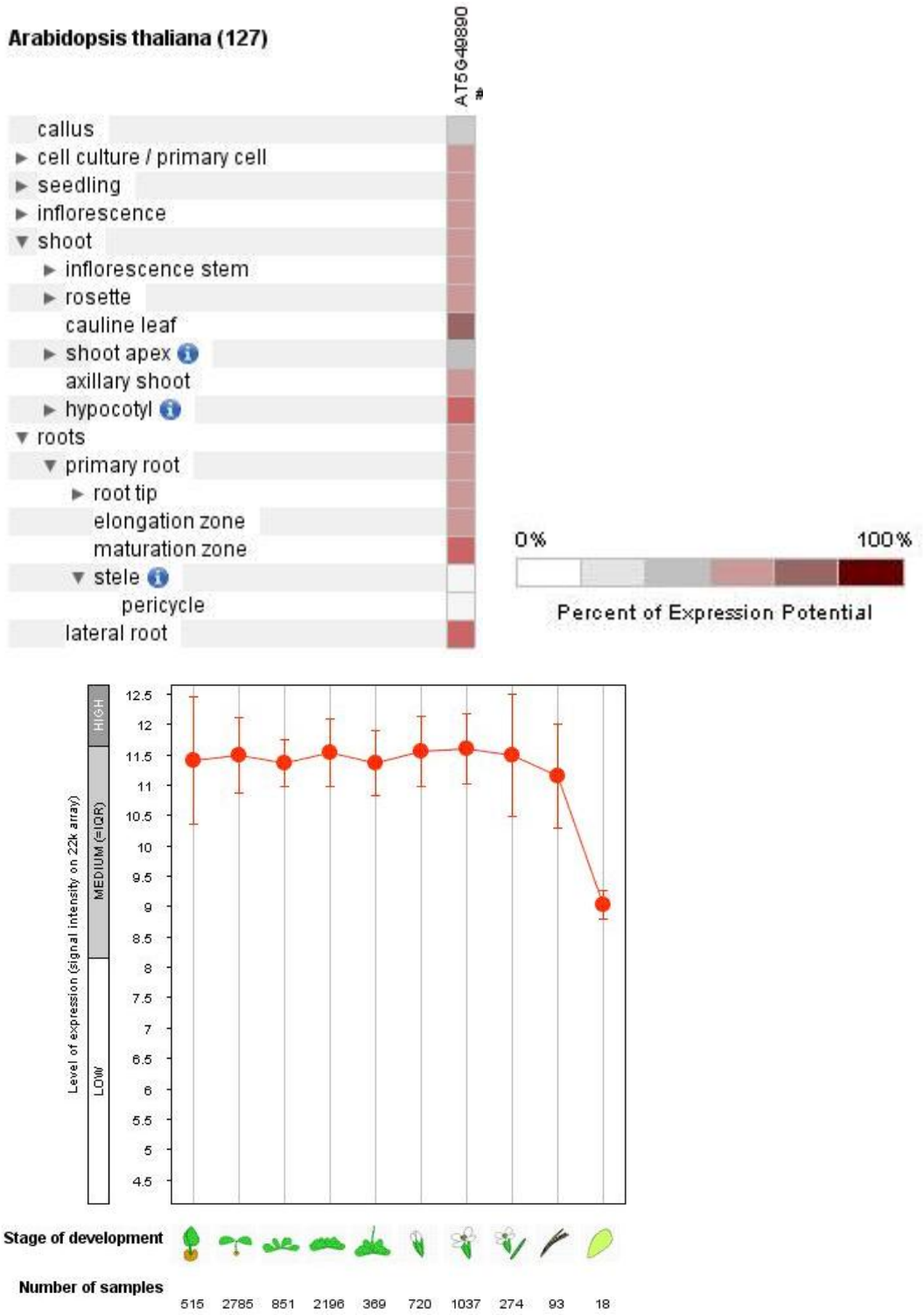

Figure 3.3 (I) Expression of *AtCLCc* in different parts of Arabidopsis tissues and different development stages. Date and images were created by GENEVESTIGATOR.

3.3.3 Candidate gene expression upon NaCl and ABA treatment

Root-pericycle specific microarray analysis and public microarray databases mining revealed that several candidate genes might encode proteins involved in xylem loading of Cl^- as they showed signs of being down- regulated by salt and ABA. However, results were inconsistent so to further validate the transcriptomic regulation of these genes to salt and ABA, a qRT-PCR was performed on Arabidopsis root cDNA to determine overall expression abundance and the transcript change with respect to the salt or ABA treatment. The expression level of *AtSLAH1*, *AtSLAH3*, *AtNRT1.5* and *AtABCB14* were significantly reduced by 91%, 48%, 76% and 78% respectively with 100 mM NaCl treatment (Figure 3.4 A, B, D and H), however, not all genes were expressed at the same level. For example, *AtSLAH1* and *AtNRT1.5* had 4000 fold higher copy numbers than *AtABCB14*. The expression of *AtSLAH4*, *AtNRT1.8*, *AtNRT1.9* and *AtCLCc* were up-regulated upon the NaCl treatment (Figure 3.4 C, E, F and G). The expression of the remaining candidate genes, including *AtAAP3* and *AtCCC*, appeared to not be altered by salt (Figure 3.4 I and J).

A pronounced reduction in gene expression was detected in *AtSLAH1* (97%) and *AtNPF2.4* (41%) after 16 hours of ABA treatment (Figure 3.4 A and K). The abundance of *AtNRT1.5* transcripts in the root was also reduced after exposure to ABA, however, this down-regulation was less (32%). Interestingly, *AtSLAH3* and *AtNRT1.8*, *AtNRT1.9* and *AtCLCc* were up-regulated by ABA (Figure 3.4 B, E, F and G). In summary, both *AtSLAH1* and *AtNRT1.5* were highly expressed in Arabidopsis root and were significantly down- regulated by both salt and ABA.

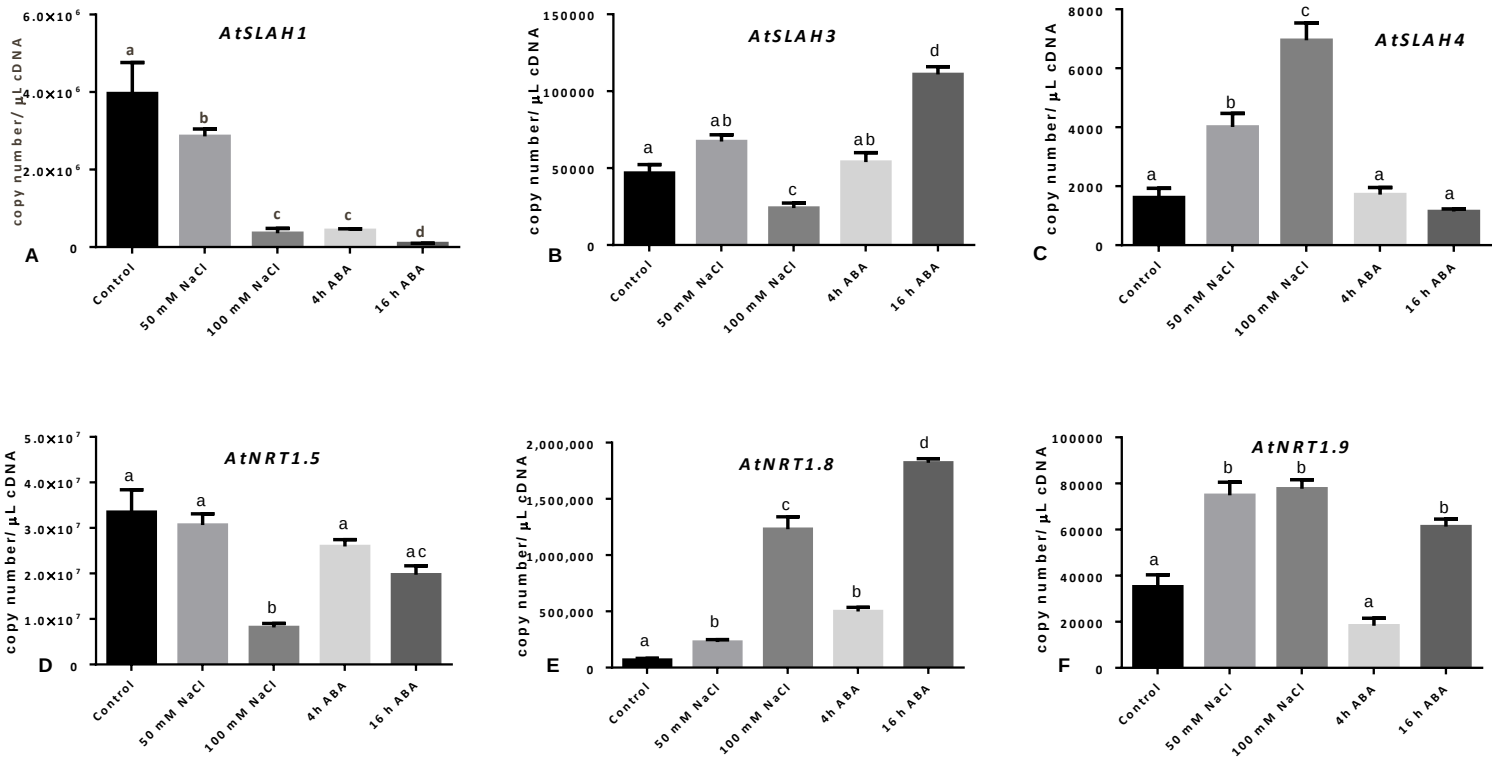
AtSLAH1
AtSLAH3
AtSLAH4
AtNRT1.5
AtNRT1.8
AtNRT1.9
copy number/ µL cDNA
A
B
C
D
E
F
Control
50 mM NaCl
100 mM NaCl
4h ABA
16 h ABA

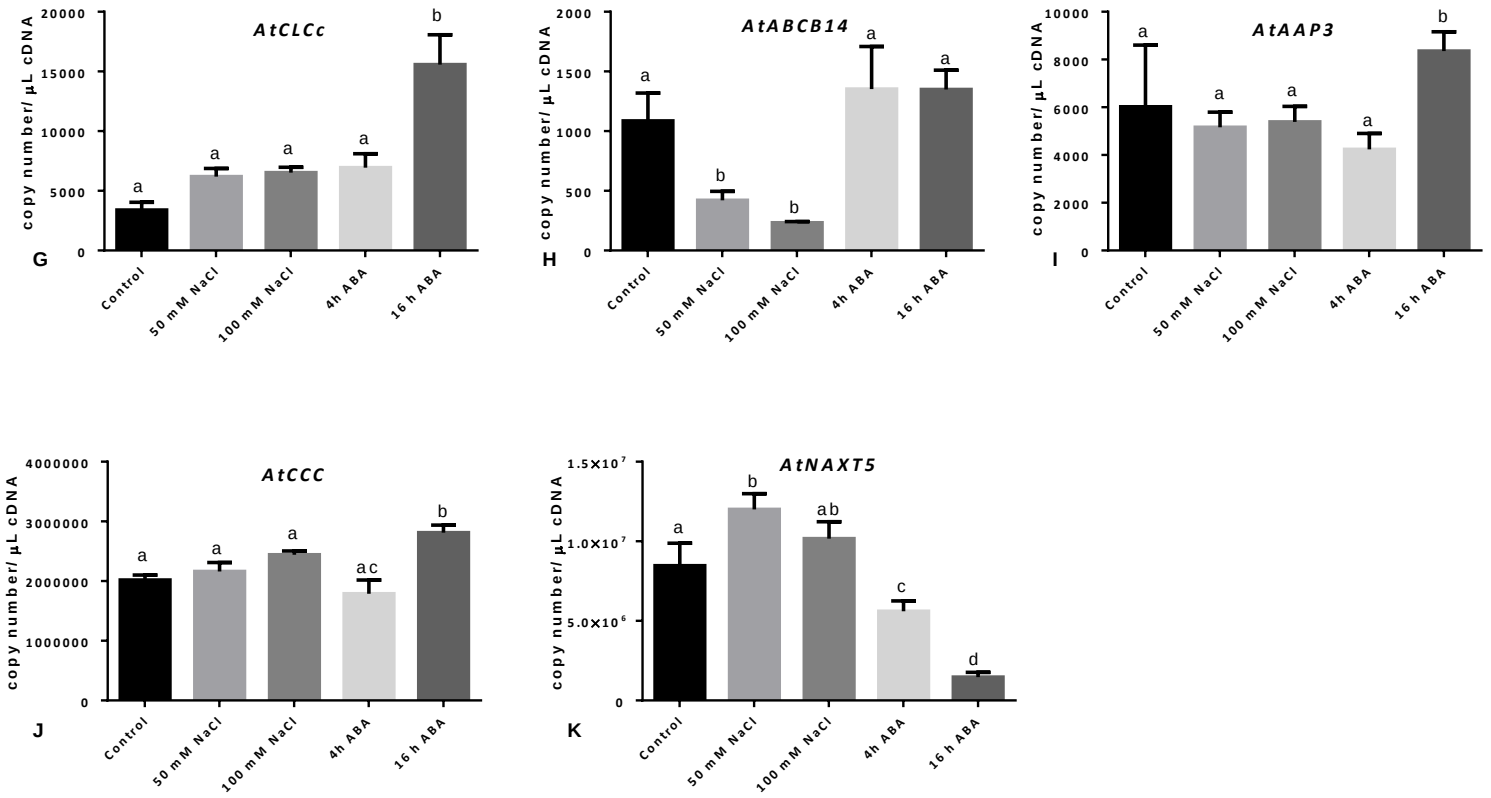

Figure 3.4 A-K. The transcript levels of candidate genes treated with control (2 mM NaCl), 50 mM and 100 mM NaCl for 7 days, or 20 µM +/- cis, trans ABA for 4/16 hours. Arabidopsis (Col-0) were grown in hydroponics for 4 weeks, NaCl treatment was started on 5th week. The ABA was applied 4/16 hours before harvest. Transcripts were detected in the whole root cDNA. Results are presented as means ± SD, n=5. The expression levels were normalized to four controls. (A) *AtSLAH1*. (B) *AtSLAH3*. (C) *AtSLAH4*. (D) *AtNRT1.5*. (E) *AtNRT1.8*. (F) *AtNRT1.9*. (G) *AtCLCc*. (H) *AtABCB14*. (I) *AtAAP3*. (J) *AtCCC*. (K) *AtNPF2.4*. Statistical significance was determined by one-way ANOVA ($P \leq 0.05$). a, b and c represent data groups that are not statistically different from each other.

3.4 Discussion

A number of candidate genes (Table 3.1) were initially selected from previous studies suggesting that the genes were found to be more abundant expression in stele and their proteins were found on the plasma membrane. The availability of microarray databases allows another opportunity to examine the expression profiles of a number of candidate genes under stress and their expression location in different tissues. However, these databases are not ideal. For example, the experimental conditions used (Arabidopsis ecotypes and age, light intensity and treatment length) vary so interpretation of these should be made with caution. Therefore, qRT-PCR was employed in our conditions so it was possible to precisely identify the candidate genes that strongly responded to salt and ABA treatment.

3.4.1 Selection of candidate genes

The Affymetrix microarray experiment performed by Evrard (2013) indicated that four candidate proteins were preferentially expressed in root stelar cells compared to the cortex. However, only one mild NaCl (50 mM) stress was applied and only one time point was taken, which is different compared to the treatment conditions used in eFP database. Therefore, it is not a surprise to observe the expression level difference between this root-pericycle-specific microarray analysis and public microarray databases. Moreover, it was also a different ecotype (C24) which has been shown to have different expression profile to Col-0 is mainly used in the database.

Using Arabidopsis eFP browser, five candidate genes, *AtSLAH1*, *AtANXT5*, *AtNRT1.5*, *AtNRT1.9* and *AtABCB14*, were found to be down-regulated by salt stress within 24 hours of application (Figure 3.1). The transcript of *AtSLAH1*, *AtNRT1.5*, *AtNRT1.9* and *AtAAP3* were also significantly down- regulated by ABA in the root. Only *AtSLAH1*, *AtNRT1.5* and *AtNRT1.9* met the criteria of genes which were down-regulation by both NaCl and ABA.

GENEVESTIGATOR showed that *AtSLAH1*, *AtNRT1.5*, *AtNRT1.9*, *AtSLAH3* and *AtAAP3* were preferentially expressed in root pericycle. These results are not consistent with the results that generated by Evrard (2013) using root-pericycle-specific microarray. GENEVESTIGATOR reports that *AtCLCc* was barely expressed in roots (Figure 3.3 I) however, a strong signal was evident in the root-pericycle-specific microarray (Table 3.2). Differences in the expression

profiles of the genes is most likely due to different Arabidopsis ecotypes being used, as well as differences in the stress treatment (both concentration of NaCl and treatment lengths). Research has shown that under salt stress, salt responsive proteins such SOS1 will be activated and then involved in regulating downstream targets, such as AVP1 (Undurraga *et al*., 2011). When salt stress is less strong, activation might not occur to trigger the transcriptional change of the candidate gene. Alternatively, if the salt stress is very strong, an osmotic shock will occur over a short period of time, which will potentially alter the gene expression. Therefore, the results extracted from these databases were only considered as a guide and will be used with caution as the differences between databases could be produced due to the experimental details. In addition, each experiment has used different growth conditions and growth solutions. Most experiments in the databases are in Col-0, whereas Evrard (2013) was using C24, an ecotype known to have a different response to salt stress than Col-0 (Jha *et al*., 2010). Without uniform experimental conditions, the comparisons between the microarrays must be taken carefully.

In the q-RT-PCR experiments, Arabidopsis was treated with salt treatments that were mild (50 mM) and strong (100 mM NaCl) for 7 days. qRT-PCR showed that *AtSLAH1* and *AtNRT1.5* were significantly ($p < 0.05$) down-regulated by salt stress and ABA, consistent with results from the Arabidopsis eFP browser and GENEVESTIGATOR. *AtSLAH3* was down- regulated by NaCl, but up- regulated by ABA but was still selected as a candidate for several reasons: SLAH3 was also found to be involved in NO_3^- transport in *X. laevis* oocytes and Arabidopsis (Geiger *et al*., 2012, Zhang et al., 2015). In addition, as NO_3^- and Cl^- are suggested to be transported through the same anion channels (Gilliham and Tester 2005), it would be interesting to examine whether or not SLAH3 is also plays a role in long distance Cl^- transport.

Together all the results that were gained from the root-pericycle-specific microarray analysis, public database and qRT-PCR analysis, *AtSLAH1*, *AtNRT1.5* and *AtSLAH3* were selected as GOI in this project.

3.4.2 *AtSLAH1*, *AtSLAH3* and *AtNRT1.5* were selected as GOI that might be involved in Cl^- xylem loading

Previous publications suggested that *AtSLAH1* and *AtSLAH3* are two homologs belonging to

the *AtSLAC1* family, which was discovered to be involved in anion efflux across the plasma membrane of stomatal guard cells in response to CO_2 and O_3 (Negi *et al.*, 2008; Vahisalu *et al*., 2008). The process is facilitated by the slow type anion conductance, also called the slow type (S-type) anion channel. Research shows this type of anion channel was highly permeable to NO_3^- and its activation is triggered by ABA (Schroeder and Hagiwara, 1989). Previous characterization of AtSLAC1 suggested that it was localized to plasma membrane and involved in anion transport in the guard cell. Therefore, it is possible that SLAC1 homologs (SLAH1 and SLAH3) have the similar functions in anion transport in roots, as both of them are found to be highly expressed in Arabidopsis root. qRT-PCR results (Figure 3.3 A) showed that *AtSLAH1* was highly expressed in the Arabidopsis root, suggesting that AtSLAH1 may be involved in chloride xylem loading in root stelar tissue. So far, no functional characterization has been published to confirm our hypothesis. Therefore, in this project, *AtSLAH1* was selected as a candidate gene for the long distance transport of Cl^- from root to shoot in Arabidopsis.

Another AtSLAC1 homolog, *AtSLAH3* was also highly expressed in Arabidopsis root and its expression significant reduced after salt stress (Figure 3.2 B). Although *AtSLAH3* was up-regulated by ABA, it was still selected as candidate gene because it belongs to the SLAC1 family that has been shown to be involved in anion transport. After the initiation of this project, *AtSLAH3* was functionally characterized in *X. laevis* oocytes and was found to require activation by a calcium dependent kinase, CPK21 , before NO_3^- mediated currents were detected (Geiger *et al*., 2011; Demir *et al*., 2013). Further research proposed AtSLAH3 was involved in the ABA signaling pathway in guard cells and that ABA was initially recognized by ABA receptors (RCAR/PYR/PYL), and the activation of ABI1 was then inhibited which enables the activation of CPK21 for phosphorylation of AtSLAH3 in the guard cells (Geiger *et al*., 2011). Since *AtSLAH3* was found highly expressed in the roots, and the regulation of AtSLAH3 by ABA in the roots has yet to be characterized, therefore, the increased transcript level upon the ABA treatment that observed in qRT-PCR might due to the regulation caused by unknown upstream regulators (protein kinase i.e. CIPKs and CDPKs). In addition, the qRT-PCR indicated that *AtSLAH3* was up-regulated by ABA in root; however, both whole plant and guard cell expression level was down regulated by 50 µM ABA. These results might suggest that the regulation mechanisms / functions of AtSLAH3 might vary in shoot and root. Taken together, AtSLAH3 might be responsible for anion transport from root to shoot. Therefore, AtSLAH3 was selected for characterization and more attention will be paid on

characterization of the function *in planta* by misexpression of the gene.

The third candidate gene, *AtNRT1.5* has previously characterized in Arabidopsis and encodes a NO_3^- transporter that is responsible for delivery NO_3^- to the root xylem (Lin *et al*., 2008). Consistent with its discovery in cell-specific microarrays (eFP microarray database), *AtNRT1.5* was also reported to be down-regulated by NaCl (Chen *et al*., 2012). The qRT-PCR results (Figure 3.2 D) suggested that *AtNRT1.5* was also significantly down-regulated by ABA. Combined with this evidence, it is reasonable to suggest that *AtNRT1.5* might be involved in long distance Cl^- transport in plants. It is often hypothesis that plant shares the same anion transporter to facilitate NO_3^- and Cl^- transport (Teakle and Tyerman, 2010) and the NO_3^- uptake was significantly decreased upon the salt stress (Figure 5.17). Therefore, it is interesting to discover the relationship between Cl^- and NO_3^- movement especially under salt stress.

3.4.3 Other candidate genes that may contribute to xylem loading of Cl^-

Among all the candidate genes, *AtNPF2.4* was also down-regulated by prolonged ABA treatment (Figure 3.2 K). However, the qRT-PCR results suggested that AtNPF2.4 was up-regulated by salt treatment after seven days of treatment. Another qRT-PCR was performed with different time length of salt treatment (see appendix, Li *et al.*, 2014) and the results indicated that *AtNPF2.4* was down-regulated by salt in a time dependent way. Therefore, it is likely to propose that AtNPF2.4 might also responsible for the Cl^- xylem loading. The characterizations of this candidate gene were carried out by another member in the lab (Li, 2013).

3.5 Conclusion

Microarray data analysis and qRT-PCR suggested that *AtSLAH1*, *AtSLAH3*, *AtNRT1.5* and *AtNPF2.4* responded to salt and ABA treatment and were highly expressed in Arabidopsis root. Previous research also showed that all of these proteins were localized to the plasma membrane, suggesting a potential role in long distance anion transport. Therefore, these four candidate genes are selected as the GOI in this project and were hypothesized to be involved in anion root- to- shoot transport in Arabidopsis.

Chapter 4 Functional characterization of candidate gene in heterologous systems

4.1 Introduction

Previous research has proposed the final loading of Cl^- into the xylem is a passive process and facilitated by plasma membrane localized anion transporters and/or channels localized within the stele (White and Broadley, 2001; Munns and Tester, 2008; Teakle and Tyerman, 2010; Kollist *et al*., 2011). However, little is known about the genes and proteins responsible for this phenomenon. To attempt to gain a better understanding of the mechanisms of Cl^- xylem loading in Arabidopsis, candidate genes of interest (GOI) were selected according to microarray and quantitative PCR analysis of Arabidopsis plants subjected to salt and ABA treatment (Chapter 3). Candidate genes were selected on the basis of being expressed in the root stelar tissue surrounding the vasculature and their transcript abundance in root tissue being significantly reduced when salt or ABA was applied (Chapter 3). Based on this analysis, *AtSLAH1*, *AtSLAH3*, *AtNRT1.5* and *AtNPF2.4* (which has undergone preliminary characterization by Li *et al*., 2014) were selected as GOI that encoded proteins likely to be involved in Cl^- movement between the root stele and the xylem vessels, which is essential for reducing Cl^- loading of the shoot when the plant is under NaCl stress.

To test the hypothesis that any of these GOI are responsible for xylem loading of Cl^-, the functional characterization of candidate genes must be examined at a protein level. Heterologous systems have been widely employed to characterize plant membrane ion transport proteins (Dreyer *et al*., 1999). In this chapter, *X. laevis* oocytes are used to investigate the anion (Cl^- and NO_3^-) permeability and selectivity of all candidate genes. First of all, the two- electrode voltage clamp (TEVC) technique was employed to examine the electrophysiological properties of plant ion transporters in *X. laevis* oocytes (Tester, 1997; Gilliham, 2007). Previously, with the aid of electrophysiological techniques, three types of anion conductances (X-QUAC, X-SLAC and X-IRAC) were successfully identified in maize and barley root xylem parenchyma cells that are likely responsible for regulating Cl^- loading of the xylem (Kohler and Raschke, 2000; Kohler *et al*., 2002; Gilliham and Tester, 2005). These studies identified that most of the Cl^- loading is likely to occur through the X-QUAC as it had the highest current density and was down-regulated by ABA. Therefore, it would be interesting to test whether any of the identified GOI can contribute to an X-QUAC-like conductance using X.Laevis oocytes as an expression system. Secondly, a unidirectional radioactive flux assay (^{36}Cl) was conducted as another assay to detect the anion transport

properties of candidate proteins expressed in *X. Laevis* oocytes.

When plant membrane anion transport proteins are heterologously expressed, there is the potential for them to not work as they would in the plant due to missing endogenous factors. Co-expression of a candidate protein with a putative regulatory protein (i.e. kinase or phosphatase) in *X. Laevis* oocytes has been used to identify signaling pathways involved in the control of transport (Geiger *et al*., 2009; Geiger *et al*., 2010). For instance, in the absence of the protein kinase OST1, the recently identified guard cell Cl^- channel, SLAC1, remains electrically silent when expressed in the heterologous systems (Geiger *et al*., 2009). There is the potential for the requirement for an interacting partner with SLAH1 and SLAH3[1]. Therefore, in addition to examining the anion selectivity of candidate protein by expressing them in the *X. Laevis* oocytes, several GOI will be co-expressed with potential regulatory factors. Furthermore, split YFP assays have been performed to confirm whether regulatory and transport proteins interact. For instance, OST1 and SLAC1 were co-expressed in Arabidopsis mesophyll protoplasts and showed it is likely that they physically interact when expressed in the same cell (Geiger *et al*., 2009). Therefore, this method is also used in this project to test the protein-protein interactions between candidate transport proteins and protein kinases.

Yeast is another popular heterologous expression system that is used to investigate the transport properties of membrane localized ion transporters (Dreyer *et al*., 1999; Uozumi *et al*., 2000; Munns *et al*., 2012). For instance, when *TmHKT1;5-A* was expressed in yeast, in the presence of 10 mM Na^+ in the growth media, the yeast growth rate was significantly slower than the control, which suggested that TmHKT1;5-A was involved in excessive Na^+ transport into the cell suppressing yeast growth (Munns *et al*., 2012). To further test whether the candidate transport proteins can facilitate anion (Cl^- and NO_3^-) transport, the growth inhibition phenotype of transformed yeast when grown on solid media containing high concentrations of Cl^- or NO_3^- salts (such as NaCl, $NaNO_3$, KCl and KNO_3) were recorded. Also, a modified liquid assay method that measures the OD value frequently over a period of at least 36 hours was developed in this project with the aim of distinguishing smaller differences between GOI and control yeast than possible on solid media, or of conventional liquid assays that use manual measurements of OD (Munns *et al*., 2012).

[1]After this study was initiated it was subsequently found that SLAH3 is regulated by CPK23 in Xenopus oocytes (Demir *et al*., 2013)

In summary, different heterologous expression systems, including *X. Laevis* oocytes, yeast and Arabidopsis mesophyll protoplasts were used to functionally characterize candidate proteins in this chapter. The aims of this chapter were to improve the understanding of the GOI function in terms of anion permeability, anion selectivity and potential post-regulation that might occur *in vivo*.

4.2 Materials and methods

4.2.1 Gene cloning and plasmid construction

All the GOI were cloned from Arabidopsis (Col-0) root cDNA with gene-specific primers (Table 4.1) using the method described in the chapter 2 (Section 2.5). Each PCR product was ligated into the Gateway® entry vector pCR8/GW/TOPO (Invitrogen) by TOPO cloning (Section 2.5.4) and transformed to TOPO 10 *E.coli* competent cells (Invitrogen) (Section 2.5.6). Colony PCR (Section 2.5.1) was performed to confirm the PCR product was correctly ligated into the entry vector. Primers used to perform the colony PCR are listed in Table 4.2. Colonies that tested positive using the PCR were inoculated in LB media and incubated in LB media overnight (Section 2.5.6). Plasmid DNA was isolated according the protocol outlined in section 2.5.7. Before sending for sequencing (Section 2.5.9), a restriction digestion was performed to confirm the direction of inserted fragment (Section 2.5.8). All the restriction enzymes that were used to determine the direction of the insert, and the primers used to sequence the plasmid are listed in Table 4.3. The target fragment that was successfully cloned into entry vector was recombined into different destination vectors (Table 4.2) followed the same transformation steps. In brief, the pGEM-HE (DEST) (Appendix 3) destination vector (Preuss *et al*., 2010) was used for driving foreign gene expression in *X. laevis* oocytes; the pYES2-52-DEST vector was provided by Dr Andrew Jacobs (ACPFG, Australia) to trigger the gene expression in yeast; and, the pUC-SPYCE/NE-DEST vectors were ordered from Institut für biologie und biotechnologie der Pflanzen, University of Würzburg, Germany (Anand *et al*., 2007) to perform the BiFC assay in Arabidopsis mesophyll protoplasts.

Table 4.1 Primers used to clone candidate gene coding sequence from Arabidopsis root cDNA.

Gene	Primers	Primer sequence (5'-3')	Tm (°C)*	Size of CDS (bp)
SLAH1	SLAH1_F	ATGGAAATTCCGAGGCAA	55.9	1158
	SLAH1_R	CTAGTTTTGGTTAGTCGCATTG	55.2	
SLAH1 w/o stop	SLAH1_F	ATGGAAATTCCGAGGCAA	55.9	1155
	SLAH1_R w/o stop	GTTTTGGTTAGTCGCATTGAG	53	
SLAH3	SLAH3_F	ATGGAGGAGAAACCAAACTAT	52.5	1908
	SLAH3_R	TTATGATGAATCACTCTCTTGAGT	53.9	
NRT1.5	NRT1.5_F	ATGTCTTGCCTAGAGATTTATAA	52.5	1845
	NRT1.5_R	TTAGACTTTAGAATCCTTCTCTC	53.1	
SnRK2.6 (OST1)	SnRK2.6_F	ATGGATCGACCAGCAGTGA	56.2	1089
	SnRK2.6_R	TCACATTGCGTACACAATCTCT	55.7	
SnRk2.2	SnRK2.2_F	ATGGATCCGGCGACTAAT	54.8	1110
	SnRK2.2_R	TCAGAGAGCATAAACTATCTCTCC	55.4	
SnRk2.2 w/o stop	SnRK2.2_F	ATGGATCCGGCGACTAAT	54.8	1107
	SnRK2.2_R w/o stop	GAGAGCATAAACTATCTCTCCACT	54.1	
SnRK2.3	SnRK2.3_F	ATGGATCGAGCTCCGGTG	58.5	1086
	SnRK2.3_R	TTAGAGAGCGTAAACTATCTCTCC	54.7	
SnRK2.3 w/o stop	SnRK2.3_F	ATGGATCGAGCTCCGGTG	58.5	1083
	SnRK2.3_R w/o stop	GAGAGCGTAAACTATCTCTCC	50.5	
SCS	SCS_F	ATGGACTTGAAAAGCAACAAC	52.6	1128
	SCS_R	TTAGTTTGAAGGCTCCTCTGTA	53.8	

***The Tm was calculated using NetPrimer (PRIMER Biosoft)(http://www.premierbiosoft.com/netprimer/)**

4.2.2 Mutagenesis PCR

Site-directed mutagenesis PCR was performed to introduce a single nucleotide polymorphism in the predicted phosphorylation site (S179D) of *AtSLAH1*. As a positive control, *AtSLAH3* was also mutated at a known phosphorylation site (T187D) which activates the transporter in *X. Laevi*s oocytes. It is electrically silent without according to Geiger *et al*. (2011). In brief, a pair of mutagenic primers to introduce the mutation were designed following the rules prescribed by Ke and Madison (1997) and as described below: (a) both forward and reverse primer contain the expected mutation site and should anneal to the same sequence on opposite strands of target plasmid; (b) the mutation site should be located in the middle of both primers with at least 10 bases of correct sequence at both ends; (c) the GC content of primer should have a minimum of 35%; and, (d) the Tm of the primers should be greater than 68 °C. The mutagenic primers used are listed in Table 4.4. *SLAH1* in the pCR8 entry vector was used as the target plasmid (DNA template, double strands), and a standard PCR (Section 2.5) that described conditions and cycles) was performed to amplify the entire plasmid with a pair of mutagenic primers using Phusion™ Hot Start High-Fidelity DNA Polymerase (FINNZYMES) (Figure 4.1 A). The PCR product was examined on an agarose gel before completely digesting it with 20 Units of *DpnI* (10 U/µL) at 37 °C overnight. Digested PCR products (10-20 ng) were transformed into DH5α competent

E.coli cells (Invitrogen). Plasmid DNA of site-mutated *SLAH1* in pCR8 was then confirmed by sequencing before it was recombined into different expression vectors, such as pYES2-DEST and pGEM-HE (DEST) using Gateway® LR Clonase® II Enzyme Mix (Invitrogen). All LR reactions were transformed into TOPO10 *E.coli* competent cells.

Table 4.2 Primers used to perform the colony PCR and the constructs generated for heterologously expressing candidate genes in *X. laevis* oocytes, yeast and Arabidopsis mesophyll protoplasts.

DNA Templates	Primers	Primer sequence (5'-3')	Tm (°C)*	Size (bp)	vecotr type
SLAH1 in pCR8	SLAH1_F	ATGGAAATTCCGAGGCAA	55.9	1326	Entry vector
SLAH1 w/o stop in pCR8	M13_R	GGAAACAGCTATGACCATG	55	1323	
SLAH3 in pCR8	M13_F	GTAAAACGACGGCCAGT	54	2054	
	SLAH3_R	TTATGATGAATCACTCTCTTGAGT	53.9		
NRT1.5 in pCR8	M13_F	GTAAAACGACGGCCAGT	54	1991	
	NRT1.5_R	TTAGACTTTAGAATCCTTCTCTC	53.1		
SnRk2.6 (*OST1*)in pCR8	M13_F	GTAAAACGACGGCCAGT	54	1235	
	SnRK2.6_R	TCACATTGCGTACACAATCTCT	55.7		
SnRK2.2 in pCR8	SnRk2.2_F	ATGGATCCGGCGACTAAT	54.8	1278	
SnRk2.2 w/o stop in pCR8	M13_R	GGAAACAGCTATGACCATG	55	1275	
SnRK2.3 in pCR8	SnRk2.3_F	ATGGATCGAGCTCCGGTG	58.5	1254	
SnRK2.3 w/o stop in pCR8	M13_R	GGAAACAGCTATGACCATG	55	1251	
SCS in pCR8	M13_F	GTAAAACGACGGCCAGT	54	1274	
	SCS_R	TTAGTTTGAAGGCTCCTCTGTA	53.8		
SLAH1 in pGEMHE	T7_F	TAATACGACTCACTATAGGG	53	1314	Destination vector for expreesion in xenopus oocyte
	SLAH1_R	CTAGTTTTGGTTAGTCGCATTG	55.2		
SLAH3 in pGEMHE	T7_F	TAATACGACTCACTATAGGG	53	2064	
	SLAH3_R	TTATGATGAATCACTCTCTTGAGT	53.9		
NRT1.5 in pGEMHE	T7_F	TAATACGACTCACTATAGGG	53	2001	
	NRT1.5_R	TTAGACTTTAGAATCCTTCTCTC	53.1		
SnRK2.2 in pGEMHE	T7_F	TAATACGACTCACTATAGGG	53	1266	
	SnRK2.2_R	TCAGAGAGCATAAACTATCTCTCC	55.4		
SnRK2.3 in pGEMHE	T7_F	TAATACGACTCACTATAGGG	53	1242	
	SnRK2.3_R	TTAGAGAGCGTAAACTATCTCTCC	54.7		
SnRK2.6 (*OST1*) in pGEMHE	T7_F	TAATACGACTCACTATAGGG	53	1245	
	SnRK2.6_R	TCACATTGCGTACACAATCTCT	55.7		
SCS in pGEMHE	T7_F	TAATACGACTCACTATAGGG	53	1284	
	SCS_R	TTAGTTTGAAGGCTCCTCTGTA	53.8		
SLAH1 in pYES2-DEST52	T7_F	TAATACGACTCACTATAGGG	53	1233	Destination vector for expression in yeast
	SLAH1_R	CTAGTTTTGGTTAGTCGCATTG	55.2		
SLAH3 in pYES2-DEST52	T7_F	TAATACGACTCACTATAGGG	53	1983	
	SLAH3_R	TTATGATGAATCACTCTCTTGAGT	53.9		
NRT1.5 in pYES2-DEST52	T7_F	TAATACGACTCACTATAGGG	53	1920	
	NRT1.5_R	TTAGACTTTAGAATCCTTCTCTC	53.1		
SLAH1 w/o stop in pUC-SPYNE	M13_F	GTAAAACGACGGCCAGT	54	2934	Destination vector for spilt YFP assay in mesophyll protoplasts
	M13_R	GGAAACAGCTATGACCATG	55		
SLAH1 w/o stop in pUC-SPYCE	M13_F	GTAAAACGACGGCCAGT	54	2720	
	M13_R	GGAAACAGCTATGACCATG	55		
SnRK2.2 w/o stop in pUC-SPYNE	M13_F	GTAAAACGACGGCCAGT	54	2886	
	M13_R	GGAAACAGCTATGACCATG	55		
SnRK2.2 w/o stop in pUC-SPYCE	M13_F	GTAAAACGACGGCCAGT	54	2672	
	M13_R	GGAAACAGCTATGACCATG	55		
SnRK2.3 w/o stop in pUC-SPYNE	M13_F	GTAAAACGACGGCCAGT	54	2862	
	M13_R	GGAAACAGCTATGACCATG	55		
SnRK2.3 w/o stop in pUC-SPYCE	M13_F	GTAAAACGACGGCCAGT	54	2648	
	M13_R	GGAAACAGCTATGACCATG	55		

***The Tm was calculated using NetPrimer (PRIMER Biosoft)**

(http://www.premierbiosoft.com/netprimer/)

Table 4.3 Restriction enzymes and primers used to confirm the direction of insertion and primers used for sequencing.

Constructs	Restriction Enzymes	Primers	Primer sequence (5'-3')	Tm (°C)*
SLAH1 in pCR8	BsrBI, NcoI			
SLAH1 w/o stop in pCR8	BsrBI, NcoI	M13_F	GTAAAACGACGGCCAGT	54
SLAH1 in pGEMHE	BsrBI, NcoI	M13_R	GGAAACAGCTATGACCATG	55
SLAH1 in pYES2-DEST52	PmeI, NcoI	T7_F	TAATACGACTCACTATAGGG	53
SLAH1 w/o stop in pUC-SPYNE	EcoRV, NcoI	SLAH1_internal_F	GGTTCACTATTTGGTTATCTTTG	52.5
SLAH1 w/o stop in pUC-SPYCE	EcoRV, NcoI			
SLAH3 in pCR8	BsrBI, NcoI	M13_F	GTAAAACGACGGCCAGT	54
SLAH3 in pGEMHE	BsrBI, HindIII	M13_R	GGAAACAGCTATGACCATG	55
SLAH3 in pYES2-DEST52	NcoI	T7_F	TAATACGACTCACTATAGGG	53
		SLAH3_internal_F	TCGTTCTACCAAATGATAAAAAG	56
SnRK2.2 in pCR8	BsrBI			
SnRk2.2 w/o stop in pCR8	BsrBI			
SnRK2.2 in pGEMHE	BsrBI			
SnRK2.2 w/o stop in pUC-SPYNE	BsrBI			
SnRK2.2 w/o stop in pUC-SPYCE	BsrBI	M13_F	GTAAAACGACGGCCAGT	54
SnRK2.3 in pCR8	BsrBI	M13_R	GGAAACAGCTATGACCATG	55
SnRK2.3 w/o stop in pCR8	BsrBI	T7_F	TAATACGACTCACTATAGGG	53
SnRK2.3 in pGEMHE	BsrBI			
SnRK2.3 w/o stop in pUC-SPYNE	EcoRV			
SnRK2.3 w/o stop in pUC-SPYCE	EcoRV			
SnRk2.6 (*OST1*) in pCR8	HindIII, NheI			
SnRK2.6 (*OST1*) in pGEMHE	BsrBI, XhoI			
SCS in pCR8	NheI, XhoI			
SCS in pGEMHE	BsrBI			
NRT1.5 in pCR8	BsrBI	M13_F	GTAAAACGACGGCCAGT	54
NRT1.5 in pGEMHE	BsrBI	M13_R	GGAAACAGCTATGACCATG	55
NRT1.5 in pYES2-DEST52	BsrBI	T7_F	TAATACGACTCACTATAGGG	53
		NRT1.5_internal_F1	CCTCGGATCGCTCTTTTC	55
		NRT1.5_internal_F2	CGTCGCTTTGTTCATATTCC	56

***The Tm was calculated using NetPrimer (PRIMER Biosoft)**

(http://www.premierbiosoft.com/netprimer/)

Table 4.4 Primers used to site-mutate the *SLAH1* and *SLAH3* in pCR8® entry vector.

Product name	Primers	Primer sequence (5'-3')	Tm (°C)*	product size (bp)
ΔAtSLAH1 in pCR8 (S179D)	SLAH1 M_F	ACGGAGAAGAGATTTTTGGATATGCTAGCA	69	3975
	SLAH1 M-R	CGGGTTTGCTAGCATATCCAAAAATCTCTT	70	
ΔAtSLAH3 in pCR8 (T187D)	SLAH1 M_F	GTACAACTCGTTCAAGGATTGGTCGGGGA	74	4725
	SLAH1 M-R	AGTTTCCCCGACCAATCCTTGAACGAGT	73	

***The Tm was calculated using NetPrimer (PRIMER Biosoft)**

(http://www.premierbiosoft.com/netprimer/)

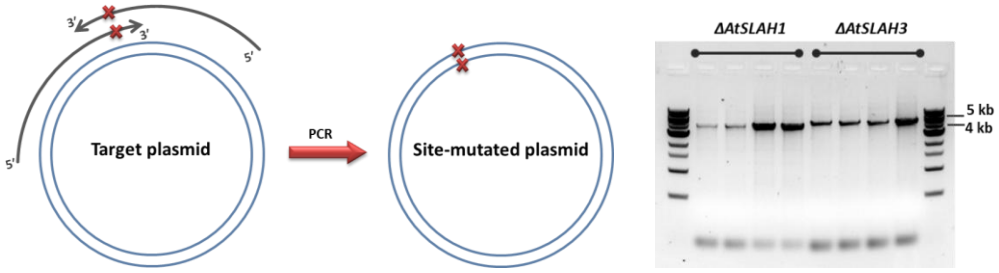

Figure 4.1 Site-mutation PCR process. (Left) a pair of mutagenic primers was used to amplify the entire target plasmid. **(Right)** amplified PCR products (site-mutated entire plasmid) was checked on agarose gel.

4.2.3 Expression of candidate genes in *X. laevis* oocyte

4.2.3.1 cRNA synthesis

The GOIs were cloned into the pGEM-HE (DEST) vector (Preuss *et al*, 2011), which contains the T7 promoter to drive the expression of the GOI in *X. laevis* oocytes. The plasmid DNA carrying the gene was linearized with a restriction enzyme that only cuts once downstream of the 3' untranslated region. The linearized plasmid DNA was precipitated using NaAc (0.5 M) and ethanol (70 % v/v). Purified DNA (1 µg) was used for cRNA synthesis using the mMESSAGE mMACHINE® Kit (Ambion, Australia). The transcription reaction was a modified version of the manufacturer's instructions. Briefly, the reaction mixture was assembled containing 10 µL 2x NTP/CAP, 2 µL 10x Reaction Buffer, 1 µg of linearized DNA, 2 µL of enzyme mix and topped up with nuclease- free water to 20 µL. The reaction was gently mixed by carefully vortexing and incubated at 37**°**C for 2 hours, followed by a TURBO DNase treatment (TURBO DNase (1 µL) was added and mixed well, followed by an incubation at 37°C for 15 min) to remove the template DNA. The RNA was recovered using the phenol: chloroform extraction and isopropanol precipitation methods described in the manufacturer's instruction manual. The cRNA was dissolved in 10 µL nuclease-free water and stored in –80 °C. The concentration of cRNA was measured using a Nanodrop ND1000 (Thermo Scientific, USA) and the quality was examined by loading on an agarose gel using instructions in the mMESSAGE mMACHINE® Kit manual.

4.2.3.2 Electrophysiological characterization of candidate genes expressed in *X. oocytes* using the two-electrode voltage-clamp (TEVC) method

Healthy stage IV-VI defoliculated oocytes (Taylor *et al*., 1985) were obtained through surgery and enzymatic digestion of ovaries from toads kept in a Xenopus colony at the Waite Campus (University of Adelaide). The cRNA were injected into oocytes at an appropriate concentration (46 nL/23 ng per oocyte) using a micro injector (Drummond 'Nanoject II'

automatic nanolitre injector, USA) with a glass microcapillary pipette following manufacturers procedures. The same volume of nuclease free water was injected into control oocytes. Injected oocytes were incubated at 18 °C for 2 days in a ND96 solution (96 mM NaCl, 2 mM KCl, 1 mM $MgCl_2$, 5 mM 4-(2-hydroxyethyl)-1-piperazineethanesulfonic acid (HEPES), 1.8 mM $CaCl_2$, pH 7.4 with 1 M Tris) combined with horse serine (50 ml/L), tetracycline (50 µg/ml) and penicillin (50 µg/ml), plus PGH solution (2.5 mM Na pyruvate, 100 mg mL^{-1} gentamycin and 1% w/v horse serum). After days , GOI cRNA injected oocytes were voltage clamped from + 40 mV to -120 mV in 20 mV decrements for 3 seconds perfusing in bath solution as previously used by Roy *et al.* (2008) (basal: 2 mM calcium-gluconate, 5 mM HEPES and 0.1 mM $LaCl_3$) plus 1 or 20 mM $CsNO_3$/CsCl at pH 5.5/7.5. TEVC was performed on oocytes as previously described in (Roy *et al.*, 2008) using an OC-725C amplifier (Warner Instruments Corporation), signals were digitized with a 1440A Digidata (Axon), and then the data were recorded and analyzed using pCLAMP 10.2 (Axon).

4.3.3.3 Radioactive $^{36}Cl^-$ flux uptake assay in *X. leavis* oocyte

cRNA of GOI or the same volume of nuclease free water was injected into oocytes and incubated in Ringer solution as described in section 2.9.1.2. After 2- day incubation, both cRNA and water injected oocytes were washed twice by in a Cl^- free media (96 mM sodium isethionate, 2 mM potassium gluconate, 1.8 mM calcium gluconate, 1 mM magnesium gluconate, 5 mM HEPES, 2.5 mM sodium pyruvate and 5% gentamicin, pH 7.4 with 1 M Tris) and then incubated for 2 hours. After the Cl^- was eliminated, the oocytes were assayed for Cl^- uptake for 1 hour in 100 mM NaCl (of which 1 µCi/mL was radioactive $Na^{36}Cl$) (The Radiochemical Centre Limited, Amersham, England), 2 mM calcium gluconate, 2 mM potassium gluconate and 5 mM MES, 240 mOsm kg^{-1} H_2O, to pH 7.5 with 1 M Tris. Once finished, the oocytes were washed three times using ice-cold Cl^- uptake solution without $Na^{36}Cl$ to remove all traces of $^{36}Cl^-$ left on the oocyte surface. Each of the washed oocytes were carefully transferred into a scintillation vial which containing 4 mL of Ecolume scintillation fluid (MP Biomedicals, Australia). The radioactivity of $^{36}Cl^-$ was detected using a Tri-Carb liquid scintillation counter (Perkin Elmer, LS 6500 Scintillation Counter, Beckman Coulter Inc., California, USA). Briefly, $^{36}Cl^-$ uptake in cRNA injected oocyte was calculated by converting the CPM ratio between sample and control using the following equation:

$^{36}Cl^-$ uptake (pmol/oocyte/h) = ([Cl^-] in control solution × input volume) / control's CPM × sample's CPM / incubation time length

4.2.4 Characterization of gene function in yeast

4.2.4.1 Yeast transformation

The GOI was cloned into the pYES-DEST52, a destination vector which has a GAL1 promoter to drive the expression of the gene only when galactose is the sole carbon source in the media (Flick and Johnston, 1990). Yeast strain InvSc2 (Invitrogen, USA) was used to express the GOI in this project. The GOI was transferred into yeast using the LiAc/SS carrier DNA/PEG method (Gietz and Schiestl, 2007).

In brief, the yeast strain InvSc2 was inoculated onto an agar plate containing SD media and incubated at 30 °C (Table 4.5). After 2 days incubation, a fresh colony was picked and cultured in 5 mL liquid SD media at 30 °C for 3- 5 hours. The cells were harvested by centrifuging at 500 × *g* for 5 minutes. The supernatant was removed and the pellet was resuspended in 1.5 mL TE/LiAc (150 µL 10 x TE, 150 µL 10 x LiAc and 1.2 mL H_2O). Plasmid DNA (0.5-1 µg) was added to 100 µL of the cell culture and 5 µL of pre-boiled single-stranded carrier DNA (2 mg/mL) in a 1.5 mL tube. The tube was gently mixed followed by adding 600 µL transformation mixture (1600 µL of 50 % PEG 3500, 200 µL of 1M LiAc and 200 µL of 10x TE) before incubated at 30 °C for 1 hour. DMSO (70 µL) was then added and incubated at 42 °C water bath for 15 minutes. The tube was immediately placed on ice for 2 minutes. The pellet was harvested by centrifuging at maximum speed (13,000 × *g*) for 5-10 seconds. The supernatant was discarded and resuspended by vortex mixing in 500 µL water. The pellet was re-extracted and resuspended in 250 µL 1x TE buffer. The culture (100 µL) was spread on an SD galactose media (without Uracil) plate (2 % Agar) and kept at 30 °C for 2-3 days. The single colony was picked and suspended in 0.1 M NaOH in order to carry out a yeast colony PCR with construct-gene specific primers (Table 4.3) and the protocol listed in Chapter 2 (section 2.4).

Table 4.5 The composition of SD media

Chemical	SD liquid media	SD solid media
0.67 % Nitrogen base w/o amino acids	√	√
2 % carbon * (Galactose or Glucose)	√	√
Uracil Drop-out amino acid mix	√	√
Uracli *	√	√
2 % Agar		√
H_2O	√	√
pH 5.6 with 1 M KOH		

* Uracli was only allpied to wide type yeast strain (without foreign gene)

* galactose was only applied if the expression of foreign gene needs to be trigerred

4.2.4.2 Yeast growth inhibition assay on solid media

To characterize the transport properties of the GOI expressed in yeast, a growth inhibition assay was initially performed on solidified SD media. Briefly, a successfully transformed yeast colony was suspended and cultured in liquid SD glucose media (without Uracil) for 2 days. The cells were harvested when in the exponential growth phase (when the OD_{600nm} value reached 0.5 – 0.6) by centrifuging at 800 × *g* for 1 minute. The pellet was resuspended in an appropriate amount of sterile water until the OD_{600nm} value was adjusted to 0.1. A serial dilution (1x, 10x, 100x, 1000x and 1000x) was made and 5 µL of each was spotted on solid SD galactose media (without Uracil) with various concentrations of NaCl, KCl, $NaNO_3$, KNO_3, NaBr and KBr. The plates were incubated at 37 °C and the plates were imaged after 2-3 days incubation.

4.2.4.3 Yeast growth assay performed in small volume of liquid media

A modified liquid assay method, which more frequently measures the OD value over the whole time course was optimized and used in this chapter to characterize the GOI's function in yeast. The detailed method was described in the (Section 2.8.1). To calculate the growth rate within log phase, a linear regression was generated based on the OD_{600nm} value within the log phase region, the calculated slope was used as the growth rate in this chapter. GraphPad Prism 6 was used to produce the calculation.

4.2.5 Transient expression in Arabidopsis mesophyll protoplasts

Arabidopsis mesophyll protoplasts were isolated according to the method described in Yoo *et al*. (2007). In brief, 5-6 week-old Arabidopsis (section 2.1.3) was used as the plant materials for protoplast isolation. Normally 15-20 leaves (from 3-5 plants) were cut into 1 mm strips

and immediately submerged into 10 mL enzyme solution (1.5% (w/v) Cellulase R10, 0.4% (w/v) Macerozyme R10, 20 mM MES, 0.4 M mannitol, 20 mM KCl, 10 mM $CaCl_2$, 0.1% (w/v) BSA, and pH adjusted to 5.6 by 1 M KOH). The enzyme solution that contains the leaf strips was vacuum-infiltrated 3 times over 30 minutes (1 minute per vacuum) using a desiccator in the dark at room temperature, this was followed by 3 hours incubation without vacuum to degrade the cell walls. After incubation, cell wall free protoplasts in the enzyme solution was mixed with ice-cold 10 mL W2 solution (4 mM MES, 15 mM KCl, 0.4 M mannitol, 10 mM $CaCl_2$ and 5 mM $MgCl_2$, pH 5.6 with 1 M KOH) to stop the reaction and transferred into a fresh 50 mL falcon tube through a 75 µm nylon mesh. Filtered protoplasts solution was centrifuged at 150 × *g* at 4°C for 2 minutes and the pellet was carefully resuspended in 2 mL ice-cold W2 solution. To transform the target DNA to protoplasts, 100 µL of protoplasts was mixed with 10-20 µg of plasmid DNA (total volume: 10 µL) and 110 µL PEG solution (30% (w/v) PEG 4000, 0.2 M mannitol and 100 mM $CaCl_2$) and incubated at room temperature for 5 minutes. To stop the reaction, 400 µL of W2 solution was added and centrifuged at 200 × *g* at room temperature for 4 minutes. Harvested pellet was gently resuspended in 500 µL W2 solution and then transferred into a 12-well plate (Iwaki, UK) for overnight incubation (16-20 hours) in the dark at room temperature.

4.2.6 Split yellow fluorescence complementation (split-YFP) assay

The split YFP assay is widely used to explore the interactions between proteins. The pUC-SPYNE/pUC-SYPNCE-gatewayDEST (N-terminal YFP) (Appendix 3) destination vector was used to study the potential protein-protein interaction (Waadt *et al*., 2008) in this project. Transient co-expression of pUC-SPYNE/pUC-SYPNCE with a candidate GOI in Arabidopsis mesophyll protoplasts was performed following the method outlined in section 4.2.5. The protoplasts transiently expressing the GOI were imaged by the confocal laser scanning microscope with a Zeiss Axioskop 2 LSM5 PASCAL fitted with an argon laser (Carl Zeiss) using the following wavelengths and filters for detection of YFP (excitation = 514 nm, emission BP = 570-590 nm), CFP (excitation = 458 nm, emission BP = 470-500 nm) and chlorophyll autofluorescence (excitation = 488 nm, emission = 640-670 nm).

4.3 Results

This section contains a large amount of results. To orientate the reader, the results were grouped and presented by the type of the heterologous system. The first part of results covered the characterization all GOIs in *X. Laevis* oocytes by voltage clamping and the radio-labelled flux assay, followed by the characterization of transport properties in yeast. Finally, the potential interaction between GOI and protein kinase was examined using transient expression in mesophyll protoplasts.

4.3.1 Electrophysiological characterization of GOI in *X. laevis* oocytes

4.3.1.1 No significant anion currents were attributable to *AtNRT1.5* when expressed in *X. laevis* oocytes

Previous functional characterization of AtNRT1.5 in *X. laevis* oocytes suggested that it is a low-affinity, pH-dependent bidirectional nitrate transporter (Lin *et al*., 2008). In this project, two-electrode voltage clamp analysis was used to test whether *AtNRT1.5* cRNA injected oocytes can also generate Cl^- mediated currents. No significant currents were stimulated in water-injected oocytes either in $CsNO_3$ or CsCl solution at either pH 5.5 or pH 7.5 (Figure 4.2 A and B). As such, oocyte injection with *AtNRT1.5* cRNA did not result in any observable NO_3^- mediated anion currents (Figure 4.2 C), which is not consistent with previous published results (Lin *et al*., 2008). It initially appeared that at both pH 5.5 and 7.5, with presence of 20 mM $CsNO_3$, the current at -120 mV was more negative compared to controls, however this is not statistically significant (Figure 4.2 E and F). Also, no significant current density differences were found when the different pH environment was applied, which is also not consistent with previous results (Lin *et al*., 2008). Interestingly, compared to the water injected control, the mean of *AtNRT1.5* cRNA injected oocytes were lower currents at -120 mV when 20 mM CsCl was present in the solution, but again these were not statistically significant. The experiment was repeated several times (33 eggs clamped from 5 batches of harvests); however, no Cl^- or NO_3^- responsible anion currents were identified via expression of *AtNRT1.5* in oocytes using a voltage step protocol.

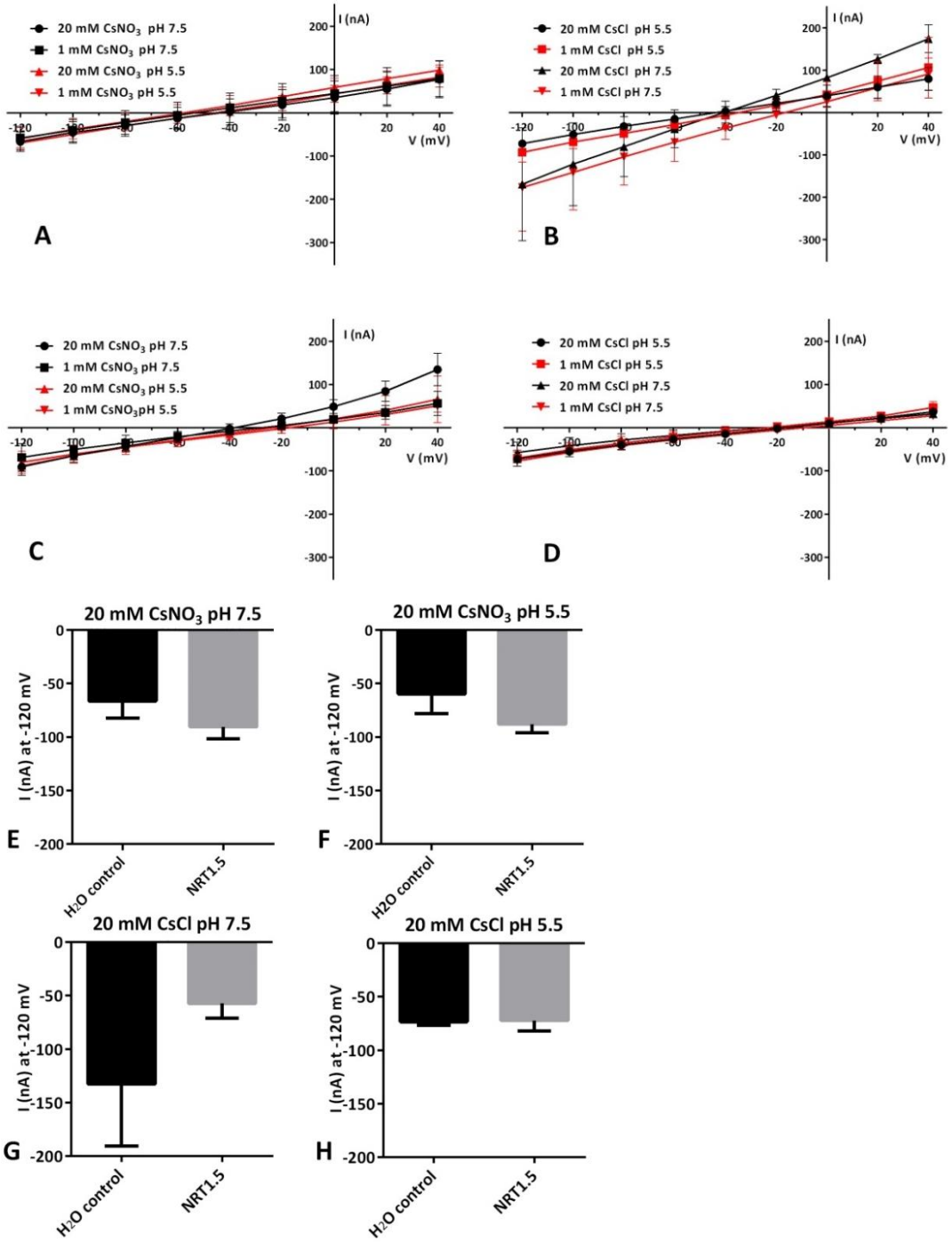

Figure 4.2 Electrophysiolocal characterization of *NRT1.5* in *X. Laevis* oocytes. (**A-D**) Whole cell currents in response to 3-second voltage pulse from +40 mV to -120 mV for *AtNRT1.5* cRNA and nuclease-free water injected oocytes were recorded. (**A-B**) water injected oocytes perfused with 1 and 20 mM $CsNO_3$ or CsCl at pH 5.5/7.5 (mean ± SEM, n=3); (**C-D**) *AtNRT1.5* injected oocytes (mean ± SEM, n=3); (**E-H**) Steady state currents were plotted at -120 mV; (**E**) *AtNRT1.5* perfused with 20 mM $CsNO_3$ at pH 7.5; (**F**) *AtNRT1.5* perfused with 20 mM $CsNO_3$ at pH 5.5; (**G**) *AtNRT1.5* perfused with 20 mM CsCl at pH 7.5; (**H**) *AtNRT1.5* perfused with 20 mM CsCl at pH 5.5. Data were presented without water subtraction.

4.3.1.2 Functional characterization of *AtSLAH1* in *X. laevis* oocytes

4.3.1.2.1 No consistent evidence for a direct role of AtSLAH1 in anion transport using *X. laevis* oocytes

AtSLAC1 was previously identified to encode a protein present in Arabidopsis guard cells that was responsible for a component of the S-type anion (Cl^- and NO_3^-) efflux. AtSLAH1, a homolog of AtSLAC1, may therefore also be capable of catalyzing an S-type anion conductance. The quantitative analysis of Arabidopsis root *AtSLAH1* also suggested that this gene was down-regulated by ABA and salt stress (Chapter 3), which suggesting it might be involved in mediating Cl^- and NO_3^- transport. To test our hypothesis, *AtSLAH1* cRNA was firstly injected alone in the Xenopus oocytes and its electrophysiological properties were examined using the TEVC technique. In the presence of NO_3^- or Cl^- at the external face, *SLAH1* injected oocytes did not generate significant anion currents (Figure 4.3 C and D). The current density was similar to the water injected oocytes (Figure 4.3 A and B). Similar results were obtained after using three batches of oocytes from three Xenopus (total 35 oocytes).

4.3.1.2.2 One exception for *AtSLAH1* injected oocytes having significant anion currents

Only one *AtSLAH1* injected oocyte showed Cl^- and NO_3^- mediated currents (Figure 4.3 E and F). Increased external $CsNO_3$ elicited increased outward anion currents (Figure 4.3 E). The membrane potential of this *AtSLAH1* cRNA injected oocyte in bath solution containing 1 mM $CsNO_3$ was near 38 mV, which is more positive than the estimated Nernst potential of NO_3^- at 17 mV (when internal NO_3^- concentration is estimated in oocytes to be > 0.01 mM (Léran *et al*., 2013). When external NO_3^- concentration was increased from 1 mM to 50 mM, a reversal shift of - 45 mV resulted, which is less negative than the estimated shift in reversal potential for NO_3^- (i.e. -75 mV) (Figure 4.3 E). In water injected control oocytes, the membrane potential was around -50 mV in 1 mM $CsNO_3$ solution and a slight shift of +12 mV (i.e. in the opposite direction with gene injected oocytes) was also discovered when NO_3^- concentration was increased from 1 to 50 mM (Figure 4.3 A). Taken together, these results might indicate that in *AtSLAH1* cRNA injected oocytes the influx (outward currents) of NO_3^- is favored especially when NO_3^- was abundant in the external environment.

When the concentration of CsCl within the bath solution was increased from 1 mM to 100 mM, *AtSLAH1* cRNA injected oocytes showed significant outward currents and this resulted in a -42 mV reversal potential shift (Figure 4.3 F). Compared to the estimated Nernst potential of Cl^- (when internal [Cl^-] in oocyte is around 40 mM (Sigel, 1990), the observed

membrane shift was away from the predicted value of -116 mV if the measured current was purely due to Cl movement. However, similar currents were not reproducible in any other *AtSLAH1* cRNA injected oocytes, these all showed similar current densities compared to the water injected controls, which suggested that *AtSLAH1* was most likely electrophysiological silent when expressed alone in oocyte – and the results in 4.3 E and F are likely to be the result of unique processing in that oocytes that allowed AtSLAH1 to work, or the induction of endogenous currents that were not present in other oocytes.

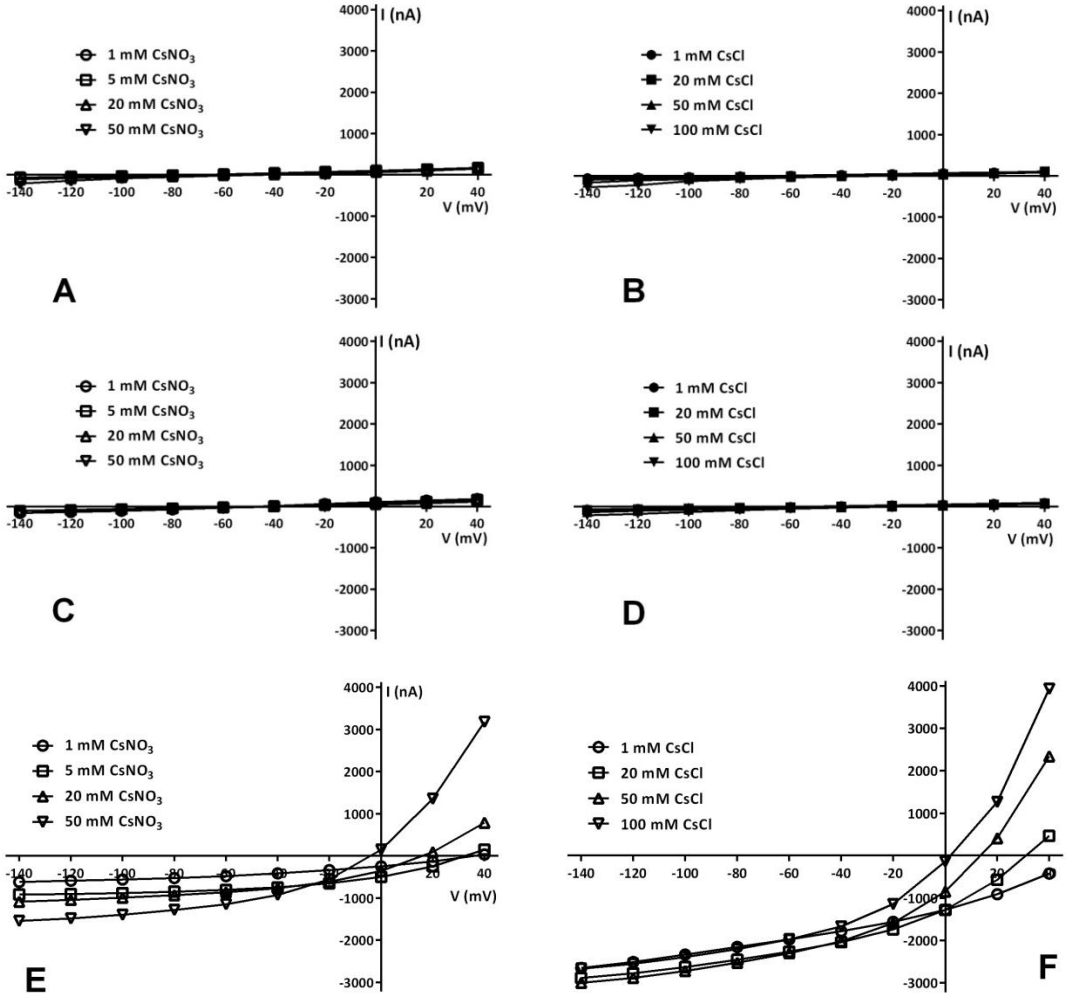

Figure 4.3 Electrophysiolocal characterization of *SLAH1* in *X. Laevis* oocyte. (**A-E**) Whole cell currents (steady states) in response to 3 second voltage pluses from +40 mV to -140 mV for *SLAH1* cRNA and nuclease-free water injected oocytes were recorded. (**A**) water injected oocytes perfused with 1, 5, 20 and 50 mM $CsNO_3$ at pH 7.5 (mean ± SEM, n= 4); (**B**) water injected oocytes perfused with 1, 20, 50 and 100 mM CsCl at pH 7.5 (mean ± SEM, n= 4); (**C**) *SLAH1* injected oocytes perfused with 1, 5, 20 and 50 mM $CsNO_3$ at pH 7.5 (mean ± SEM, n= 3); (**D**) *SLAH1* injected oocytes perfused with 1, 20, 50 and 100 mM CsCl at pH 7.5 (mean ± SEM, n= 4); (**E**) The only *SLAH1* injected oocyte that showed $CsNO_3$ mediated outward currents when perfusing with various concentration of external $CsNO_3$ (n=1). (**F**) The only *SLAH1* injected oocyte that showed CsCl mediated outward currents when perfusing with various concentration of external CsCl (n=1). Data were presented without water subtraction.

4.3.1.2.3 AtSLAH1 might be activated when co- expressed with a protein kinase in *X. laevis* oocytes

As the AtSLAH1 homolog, AtSLAC1, was also electrically silent in oocytes and required the expression of *OST1* (*SnRK2.6*) to be functional (Geiger *et al*., 2009), it is worthwhile to investigate whether a similar regulatory process was also required for AtSLAH1 to trigger the anion transport in heterologous system. As such, *AtSnRk2.2* and *AtSnRk2.3* were individually co-injected with *AtSLAH1* in *X. laevis* oocytes (AtSnRK2.6 was not tested as it is not highly expressed in roots) (Zheng *et al*., 2010).

When *AtSLAH1* and *AtSnRk2.2* were co-injected in *X. laevis* oocytes, after the experiments were repeated multiple times (41 eggs were clamped from 5 batches of oocytes), no significant anion currents were induced by external $CsNO_3$ or CsCl at various concentrations (1-100 mM). Also, to optimize the co- expression efficiency, different cRNA injection ratios between *AtSLAH1* and *AtSnRK2.2* were tried, such as 1: 0.5 and 1: 0.25 (data not shown). Manipulating the ratio between *AtSLAH1* and *AtSnRK2.2* did not result in any evident anion currents.

AtSnRk2.3 cRNA was also co-injected with *AtSLAH1* cRNA in oocytes, and the anion transport properties were examined following the same conditions as described before. No response was detected in water injected oocytes to a change in the bath solutions (Figure 4.4 C). With increasing the NO_3^- concentration in the bath solution, large *SLAH1-SnRK2.3* mediated anion currents were detected (Figure 4.4 A). Upon the increase of nitrate concentration in bath solution, the reversal potential shifted negative. A 50-fold change in nitrate concentration resulted in a -57 mV shift of reversal potential, which is less negative than the estimated reversal potential shift (around -99-108 mV) (Figure 4.4 A). Both outward and inward currents were increased with increasing nitrate concentration. Similar results were obtained when the *SLAH1-SnRK2.3* injected oocytes was examined in a bath solution with the presence of external Cl^- (Figure 4.4 B). Both outward and inward currents were increased upon increasing chloride concentration (Figure 4.4 B). The reversal potential shifted negative by -55 mV upon a 100-fold increase of external chloride concentration, which is less than the estimated reversal shift (around -115 mV). This result might suggest that AtSnRk2.3 can activate AtSLAH1's function in oocyte and also the SLAH1-SnRk2.3 complex can facilitate nitrate and chloride currents. The current density at – 140 mV was also compared when

same strength (50 mM) of substrate ($CsCl/CsNO_3$) was presented in the media (Figure 4.4 D), suggesting that the SLAH1-SnRk2.3 complex can generated greater nitrate but not chloride related currents, however the differences was not statistically significant.

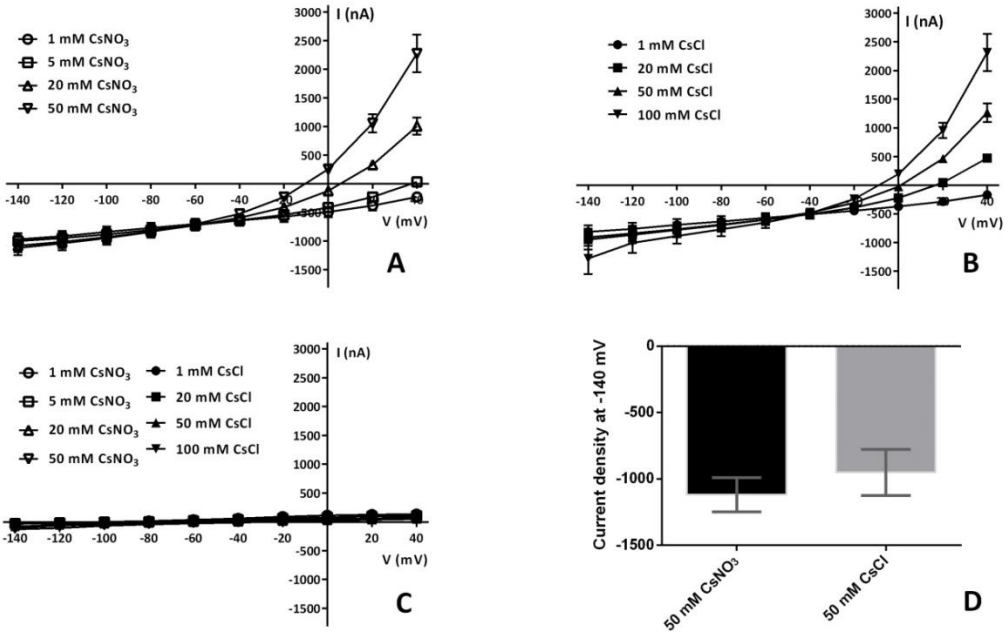

Figure 4.4 Electrophysiolocal characterization of *SLAH1-SnRk2.3* injected *X. laevis* oocytes. (**A-C**) Whole cell currents (steady states) in response to 3 second voltage pluses from +40 mV to -140 mV for *SLAH1-SnRk2.3* cRNA and RNA-free water injected oocytes were recorded. (**A**) SLAH1-SnRK2.3 complex injected oocytes perfused with 1, 5, 20 and 50 mM $CsNO_3$ at pH 7.5 (mean ± SEM, n= 5); (**B**) *SLAH1-SnRK2.3* injected oocytes perfused with 1, 20, 50 and 100 mM CsCl at pH 7.5 (mean ± SEM, n= 5); (**C**) RNA free water injected oocytes perfused with 1, 5, 20 and 50 mM $CsNO_3$ or with 1, 20, 50 and 100 mM CsCl at pH 7.5 (mean ± SEM, n= 3); **(D)** The current density of *SLAH1-SnRK2.3* injected oocytes perfused with 50 mM $CsNO_3$ or CsCl at -140 mV. Data were presented without water subtraction.

4.3.1.2.4 Site-mutated AtSLAH1 was not able to induce anion currents in *X. laevis* oocytes

The transport activity of SLAH3 can be stimulated even when expressed by itself in *X. laevis* oocytes by a mutation ($SLAH3^{T178D}$, termed as ΔSLAH3 in this thesis) that mimics phosphorylation (Geiger *et al*., 2012). To further investigate the anion transport properties of AtSLAH1 in *X. laevis* oocytes, the equivalent predicted phosphorylation site in $SLAH1^{S179D}$ (the protein termed as ΔSLAH1 in this thesis) was mutated and injected into oocytes. First of all, ΔSLAH1 was injected in oocytes and characterized using TEVC with the same protocol as described before. However, no evident anion currents were found when different bath solutions including 100 mM $CsCl/CsNO_3$, 100 mM NaCl and 100 mM NMDG-Cl were used. Therefore, a $^{36}Cl^-$ uptake assay was performed to further examine the Cl^- movement when mutated SLAH1 was injected into the oocytes. No statistically significant differences in mean

$^{36}Cl^-$ were detected in ΔSLAH1 cRNA injected oocytes compared with water-injected controls incubated in 100 mM CsCl (Figure 4.5). No pronounced $^{36}Cl^-$ uptake was found between site-mutated SLAH1 oocytes and controls when 100 mM NaCl or NMDG-Cl was applied to the bath solution.

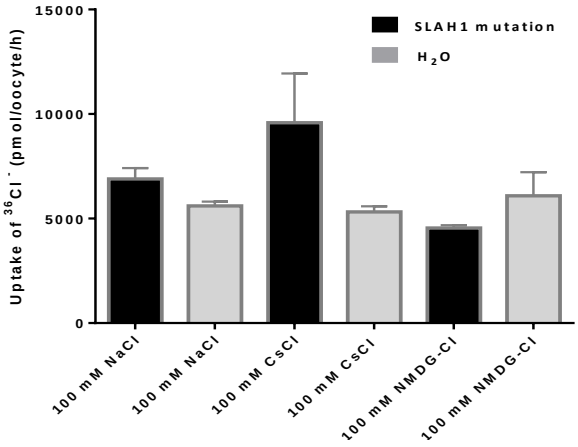

Figure 4.5 $^{36}Cl^-$ Uptake measured in *X. laevis* oocytes injected with either mutated *ΔSLAH1* or water in a background of 100 mM NaCl, CsCl and NMDG-Cl for 1 hour. Results were presented as mean ± SEM, n=10.

4.3.1.3 Functional characterization of *AtSLAH3* in *X. laevis* oocytes

4.3.1.3.1 *AtSLAH3* cRNA injected oocytes leads to greater NO_3^- than Cl^- currents

With presence of 20 mM NO_3^- in the bath solution, *AtSLAH3* cRNA injected oocytes showed nitrate mediated currents and the current density, especially the outward anion currents (i.e. anion movement into the egg), increased when external NO_3^- was increased (Figure 4.6 A black line). When *AtSLAH3* cRNA injected oocyte were perfused with Cl^-, the magnitude of outward currents were significantly reduced (Figure 4.6 A red line). This suggests that when *AtSLAH3* cRNA injected in the *X. laevis* oocyte alone, AtSLAH3 was more selective for NO_3^- over Cl^-. The conductivity was also calculated using the current density at – 140 mV, which was greater for NO_3^- than Cl^- (Figure 4.6 C), also, the conductivity of NO_3^- increased upon the increase of $CsNO_3$, however, with equivalent increase of CsCl, the conductivity of AtSLAH3 to Cl^- did not (Figure 4.6 C). To further investigate the anion selectivity of SLAH3, the current was also measured when both NO_3^- and Cl^- were presented. When additional 50 mM CsCl was mixed with 20 mM or 50 mM $CsNO_3$, the outward currents were reduced however the inward currents were less affected (Figure 4.6 B). For instance, the outward current was reduced by 59 % at 40 mV when extra 50 mM of CsCl was combined with 20 mM of $CsNO_3$ (Figure 4.6 B). The similar reduction (reduced by 52 % at 40 mV) of outward currents were

also seen when $CsNO_3$ and CsCl were both presented at the same concentration (50 mM) (Figure 4.6 D). The conductance was calculated based using the currents at 40 mV, which is showing the NO_3^- conductance in *AtSLAH3* cRNA injected oocytes was reduced (not significant, t- test) when additional CsCl was introduced (Figure 4.6 D).

4.3.1.3.2 DIDS was able to inhibit the NO_3^-- mediated currents in *AtSLAH3* cRNA injected oocytes

An anion channel inhibitor, 4, 4'-Diisothiocyanatostilbene- 2, 2-disulfonic acid disodium salt hydrate (DIDS) has been shown to be an efficient R-type anion channel blocker (Schroeder *et al*., 1993). Recently, it also showed the ability to inhibit the SLAC1-type anion channel in both oocyte and guard cell backgrounds (these are S-type anion channels) (Geiger *et al*., 2009). Therefore, DIDS was used to further investigate the anion selectivity in *AtSLAH3* cRNA injected oocytes. When 10 µM DIDS was added to the bath solution along with different concentrations of $CsNO_3$, the magnitude of nitrate mediated currents (both outward and inward) were reduced (Figure 4.6 E). For instance, the inward currents were reduced by 58 % at – 140 mV when DIDS was combined with 20 mM $CsNO_3$ and 23 % current density reduction was also found when the same strength of DIDS was applied with 50 mM $CsNO_3$ (Figure 4.6 E). The reduction also appeared when *AtSLAH3* cRNA injected oocyte was clamped at 40 mV. After DIDS application, the outward currents were reduced by 84 % and 58 % when 20 mM and 50 mM of $CsNO_3$ were presented within the bath solution (Figure 4.6 E). Although the observed reduction was significant, compared with water injected oocytes (Figure 4.6 F), the inhibition did not completely abolish the anion transport properties as the inhibited current density was still larger than in water-injected controls.

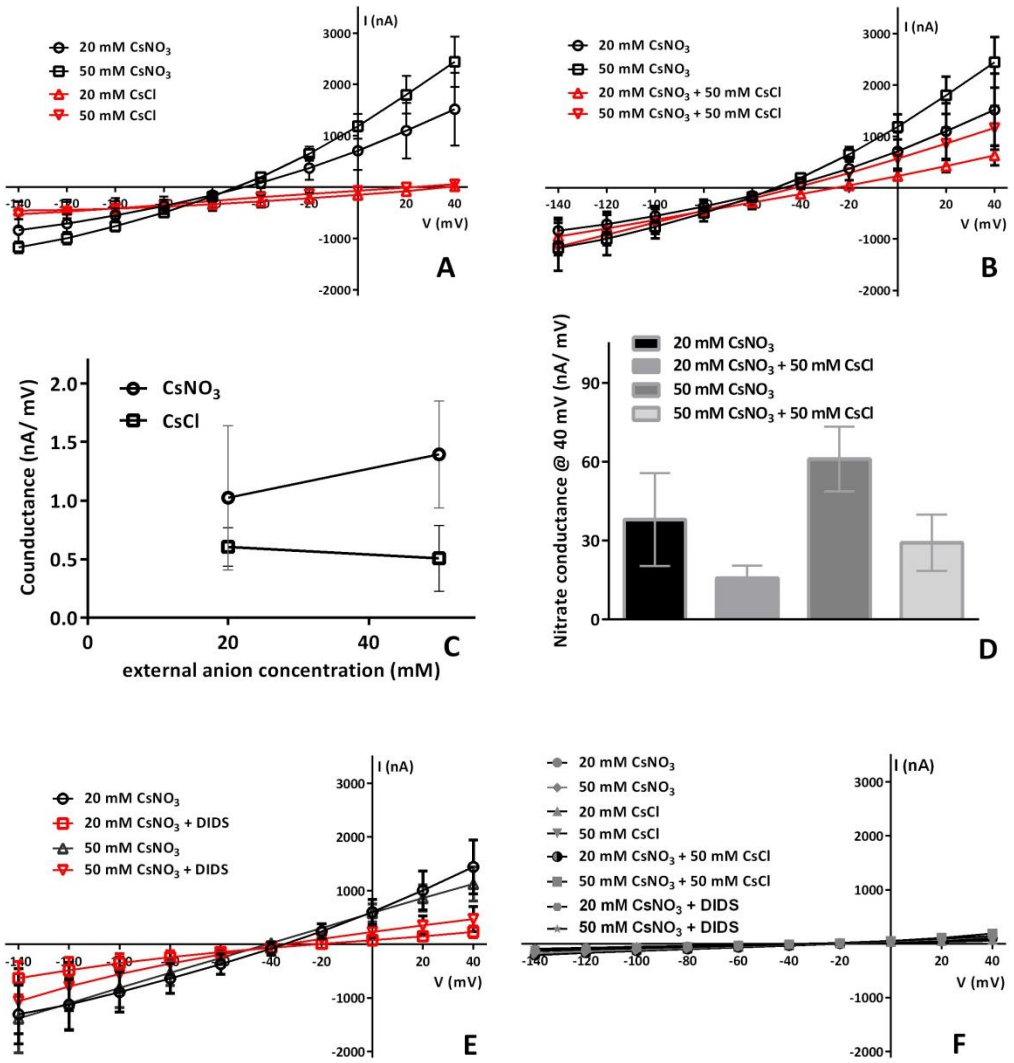

Figure 4.6 Electrophysiolocal characterization of SLAH3 in *X. laevis* oocytes. (**A-D**) Whole cell currents (steady states) in response to 3 second voltage pluses from +40 mV to -140 mV for *SLAH3* cRNA and RNA-free water injected oocytes were recorded. (**A**) *SLAH3* injected oocytes perfused with 20 and 50 mM $CsNO_3$ or CsCl at pH 7.5 (mean ± SEM, n= 3); (**B**) *SLAH3* injected oocytes perfused with 20, 50 mM $CsNO_3$ at pH 7.5; with 20 mM and 50 mM $CsNO_3$ plus 50 mM CsCl (mean ± SEM, n= 3); (**C**) The conductivity of AtSLAH3 to NO_3^- and Cl^-, calculation performed using the values of currents at -140 mV (mean ± SEM, n= 3); (**D**) The conductivity of AtSLAH3 to NO_3^- and Cl^-, calculation performed using the values of currents at 40 mV (mean ± SEM, n= 3); (**E**) *SLAH3* injected oocytes perfused with 20, 50 mM $CsNO_3$ at pH 7.5 plus 0.01 mM DIDS (mean ± SEM, n= 3); (**F**) RNA free water injected oocytes perfused with 20 and 50 mM $CsNO_3$; with 20, 50 mM CsCl at pH 7.5; with 20 mM and 50 mM $CsNO_3$ plus 50 mM CsCl and 20 or 50 mM $CsNO_3$ plus 0.01 mM DIDS (mean ± SEM, n= 4); Data were presented without water subtraction. The t-test was performed between 50 mM $CsNO_3$ and 50 mM $CsNO_3$ plus 50 mM CsCl, $P \leq 0.05$.

4.3.1.4 Functional characterization of *NPF2.4* in *X. laevis* oocytes

NPF2.4 cRNA injected oocytes were able to mediate the Cl^- movement in a Na^+- dependent manner

A proton-dependent oligo-peptide transporter, named as *NPF2.4* has been proposed to be involved in Cl^- xylem loading in Arabidopsis root (Li, 2013). This gene was highly expressed in the root stelar tissue and its expression was decreased upon NaCl or ABA treatments (Figure 3.4 K). I performed electrophysiological characterization of this candidate in oocytes.

Interestingly, the chloride-mediated anion currents were only generated when Na^+ was present in the bath solution (Figure 4.7 A). As no shift in reversal potential was observed when Na^+ concentration was increased, the currents were likely to be due to Cl^- movement not Na^+ (Figure 4.7 A). To further confirm whether the observed inward currents were generated due to Cl^- being transported through NPF2.4, a unidirectional $^{36}Cl^-$ uptake assay for *NPF2.4* and water-injected oocytes was performed by incubation in solutions containing 100 mM NaCl or 100 mM NMDG-Cl mixed with low activities of $^{36}Cl^-$ for 1 hour. *NPF2.4* cRNA injected oocytes exhibited significantly greater uptake of $^{36}Cl^-$ than the water injected oocytes in both NaCl and NMDG-Cl solutions (Figure 4.7 B). The uptake was unaffected by pH as no difference was observed at pH 5.5 or 7.5. *NPF2.4* cRNA injected oocytes were found to have a significantly larger uptake of $^{36}Cl^-$ in the NaCl solution than in the NMDG-Cl solution at both pH values tested (Figure 4.7 B). For further characterizations performed by others see Li *et al*. (2014).

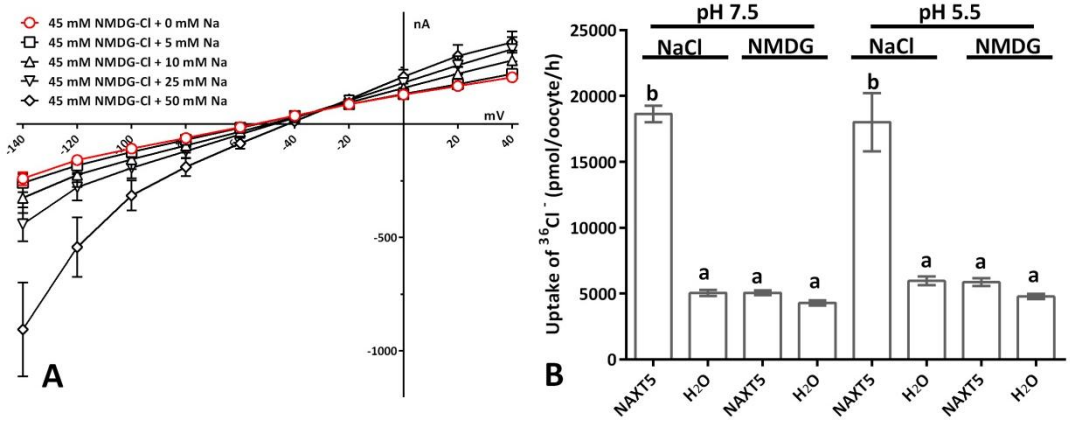

Figure 4.7 Characterization of NPF2.4 in *X. laevis* oocytes with TEVC or unidirectional $^{36}Cl^-$ uptake assay. (A) The whole cell currents of *NPF2.4* injected oocyte were recorded when consistent 45 mM NMDG-Cl and various concentration of Na^+ were presented in the bath solution. (Mean ± SEM, n= 5); **(B)** $^{36}Cl^-$ uptake measured in the oocytes injected with either NPF2.4 cRNA or water, in a background of 100 mM Cl^- for 1 hour. (Mean ± SEM, n = 20). Columns with different letters indicate statistically significant differences ($P \leq 0.05$).

4.3.2 Characterization of GOI anion transport properties in *Saccharomyces cerevisiae*

4.3.2.1 Growth inhibition assay performed on solidified plates

To further investigate the anion transport properties of candidate genes yeast was used as a heterologous expression system. *SLAH1*, *ΔSLAH1*, *SLAH3*, *ΔSLAH3* and *NRT1.5* were reconstituted into a yeast destination vector (pYES-DEST52) and then transformed into wildtype yeast. The empty vector was also transformed into yeast as control. The ability of yeast to grow in the presence of various salts was performed. Fluoride and bromide salts were included as more toxic analogues of chloride. The results are summarized below.

Similar growth phenotypes were observed for *SLAH1, ΔSLAH1*, *SLAH3*, *ΔSLAH3 and NRT1.5* transformed yeast compared to the empty vector yeast on media (both glucose and galactose based) containing 1 mM and 5 mM potassium fluoride (KF) (Figure 4.8 A and C), or sodium fluoride (NaF) (Figure 4.8 B and D). Higher concentration of KF and NaF were tested (data not shown), and a higher dose of KF and NaF (20- 50 mM) resulted in no yeast growth.

SLAH1, ΔSLAH1, *SLAH3*, *ΔSLAH3 and NRT1.5* transformed yeast and the empty vector control yeast showed a growth inhibition phenotype when 500 mM sodium bromide (NaBr), 500 mM sodium chloride (NaCl) or 500 mM sodium nitrate ($NaNO_3$) were presented within the glucose based media (as control) (upper panel of Figure 4.8 E, F and J) which suggests that high concentration of Na^+ is toxic to the yeast cells. *SLAH3*, *ΔSLAH3* and *NRT1.5* transformed yeast showed a slightly greater growth inhibition on galactose-based media containing 500 mM NaBr and 500 mM NaCl compared to *SLAH1, ΔSLAH1* and empty vector control (lower panel of Figure 4.8 E and F). Also, *SLAH1*, *SLAH3*, *ΔSLAH3 and NRT1.5* transformed yeast showed a slightly greater growth inhibition on galactose-based media containing 500 mM $NaNO_3$ (lower panel of Figure 4.8J) compared to *ΔSLAH1* and empty vector transformed yeast.

The toxicity of yeast to K^+ was less pronounced than to equivalent concentration of Na^+ as no significant growth inhibition was identified on glucose based media (as a control) for all the candidate gene transformed yeast and empty vector control yeast when challenged with 500 mM K^+ containing salts unlike when they were challenged with Na^+ (upper panel of Figure 4.8 G, H and I). On the galactose media containing 500 mM potassium bromide (KBr), *SLAH3*, *ΔSLAH3* and *NRT1.5* transformed yeast showed a slightly greater growth inhibition than the

empty vector control (lower panel of Figure 4.8 G). Upon 500 mM potassium chloride (KCl) stress (galactose), *SLAH1*, *SLAH3*, *ΔSLAH3* and *NRT1.5* transformed yeast showed a slightly greater growth inhibition than the *ΔSLAH1* and empty vector control (lower panel of Figure 4.8 H). Also, on the galactose media containing 500 mM potassium nitrate (KNO_3), *SLAH1*, *SLAH3*, *ΔSLAH3* and *NRT1.5* transformed yeast were inhibited compared with the yeast transformed with *ΔSLAH1* and empty vector control (lower panel of Figure 4.8 I). It appeared that *ΔSLAH3* was more sensitive to the high concentration of NO_3^- compared to wild type *SLAH3*. Interestingly, mutated SLAH1 was less affected compared to the original SLAH1 and had a similar phenotype as empty vector control.

In summary (Table 4.6), when glucose was used as a negative control to examine the ion toxicity to the yeast cells, higher concentrations of Na^+ was toxic to the yeast growth (Figure 4.8 E, F and J upper panel). No growth inhibition was observed when KF, NaF, KBr, KCl and KNO3 was applied in all the glucose negative controls (Figure 4.8 A, B, C, D, G, H and I upper panel). When galactose was applied, all of the GOI gave no growth phenotype in yeast exposed to the low concentration of NaF and KF (Figure 4.8 A, B, C and D). A clear growth inhibition was observed for all yeast that grew on the high concentration of NaBr, NaCl and $NaNO_3$ regardless of whether it contained the GOI. However, *SLAH3*, *ΔSLAH3* and *NRT1.5* containing yeast showed a growth inhibition compared to the empty vector control. On the media containing 500 mM K^+ based salts, including KBr, KCl and KNO_3, *NRT1.5* transformed yeast grew the slowest, which suggests that NRT1.5 might be involved in transport of Cl^-, NO_3^- and Br^-; *SLAH1* transformed yeast also exhibited growth inhibition however it was less pronounced than in *NRT1.5* transformed yeast. *ΔSLAH1* transformed yeast did not show a higher degree of growth inhibition compared to wild type *SLAH1,* in contrast, when 500 mM $NaNO_3$ or KNO_3 was applied, it grew better than wild type *SLAH1* transformed yeast, Both *SLAH3* and *ΔSLAH3* transformed yeast showed growth inhibition on media containing 500 mM KBr, KCl and KNO_3, and *ΔSLAH3* transformed yeast showed a more affected growth phenotype especially when the higher concentration of KNO_3 was used, which suggested mutated SLAH3 more effectively transported NO_3^- than wildtype SLAH3.

Table 4.6 Summary of growth inhibition assay performed on solidified plates

		Soulutions									
Constructs	Carbon source	1 mM NaF	5 mM NaF	1 mM KF	5 mM KF	500 mM NaBr	500 mM KBr	500 mM NaCl	500 mM KCl	500 mM $NaNO_3$	500 mM KNO_3
SLAH1	Glucose	NG	NG	NG	NG	— —	NG	— —	NG	— —	NG
	Galactose	NG	NG	NG	NG	— —	—	— —	—	— —	— —
ΔSLAH1	Glucose	NG	NG	NG	NG	— —	NG	— —	NG	— —	NG
	Galactose	NG	NG	NG	NG	— —	—	— —	—	— —	—
SLAH3	Glucose	NG	NG	NG	NG	— —	NG	— —	NG	— —	NG
	Galactose	NG	NG	NG	NG	— —	— —	— —	—	— —	— —
ΔSLAH3	Glucose	NG	NG	NG	NG	— —	NG	— —	NG	— —	NG
	Galactose	NG	NG	NG	NG	— —	— —	— —	—	— —	— —
NRT1.5	Glucose	NG	NG	NG	NG	— —	NG	— —	NG	— —	NG
	Galactose	NG	NG	NG	NG	— —	— —	— —	— —	— —	— —
Empty	Glucose	NG	NG	NG	NG	— —	NG	— —	NG	— —	NG
	Galactose	NG	NG	NG	NG	— —	—	— —	—	— —	—

" NG": no growth inhibition
" —": growth reduction
" — —": more growth reduction

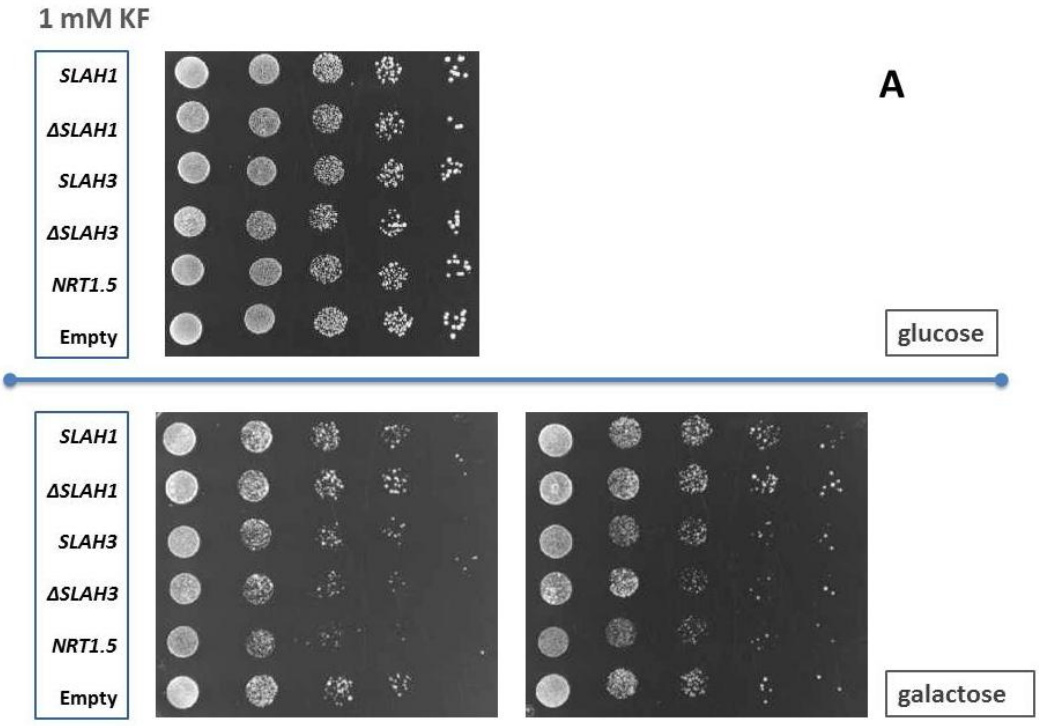

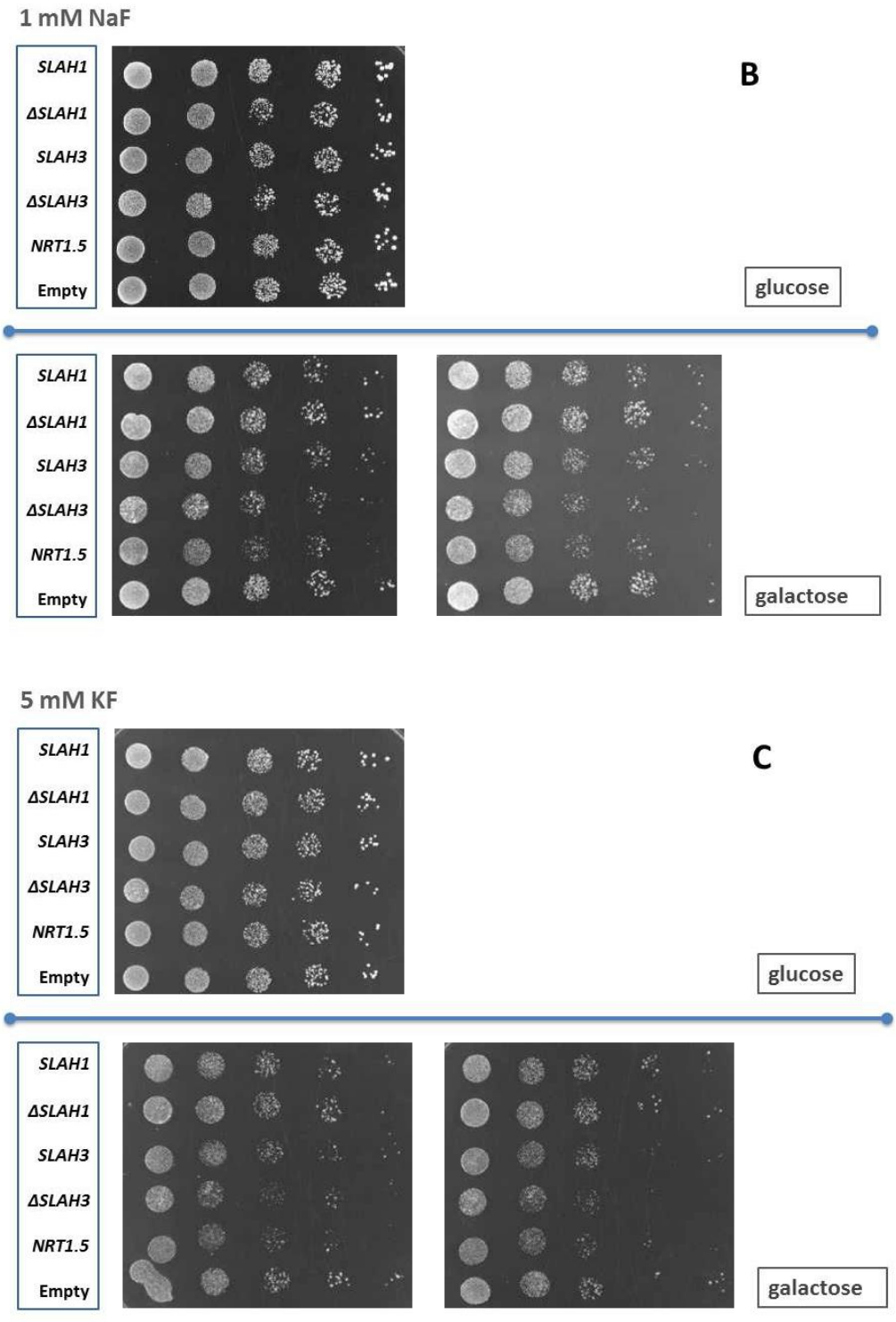
1 mM NaF
SLAH1
ΔSLAH1
SLAH3
ΔSLAH3
NRT1.5
Empty
B
glucose
SLAH1
ΔSLAH1
SLAH3
ΔSLAH3
NRT1.5
Empty
galactose
5 mM KF
SLAH1
ΔSLAH1
SLAH3
ΔSLAH3
NRT1.5
Empty
C
glucose
SLAH1
ΔSLAH1
SLAH3
ΔSLAH3
NRT1.5
Empty
galactose

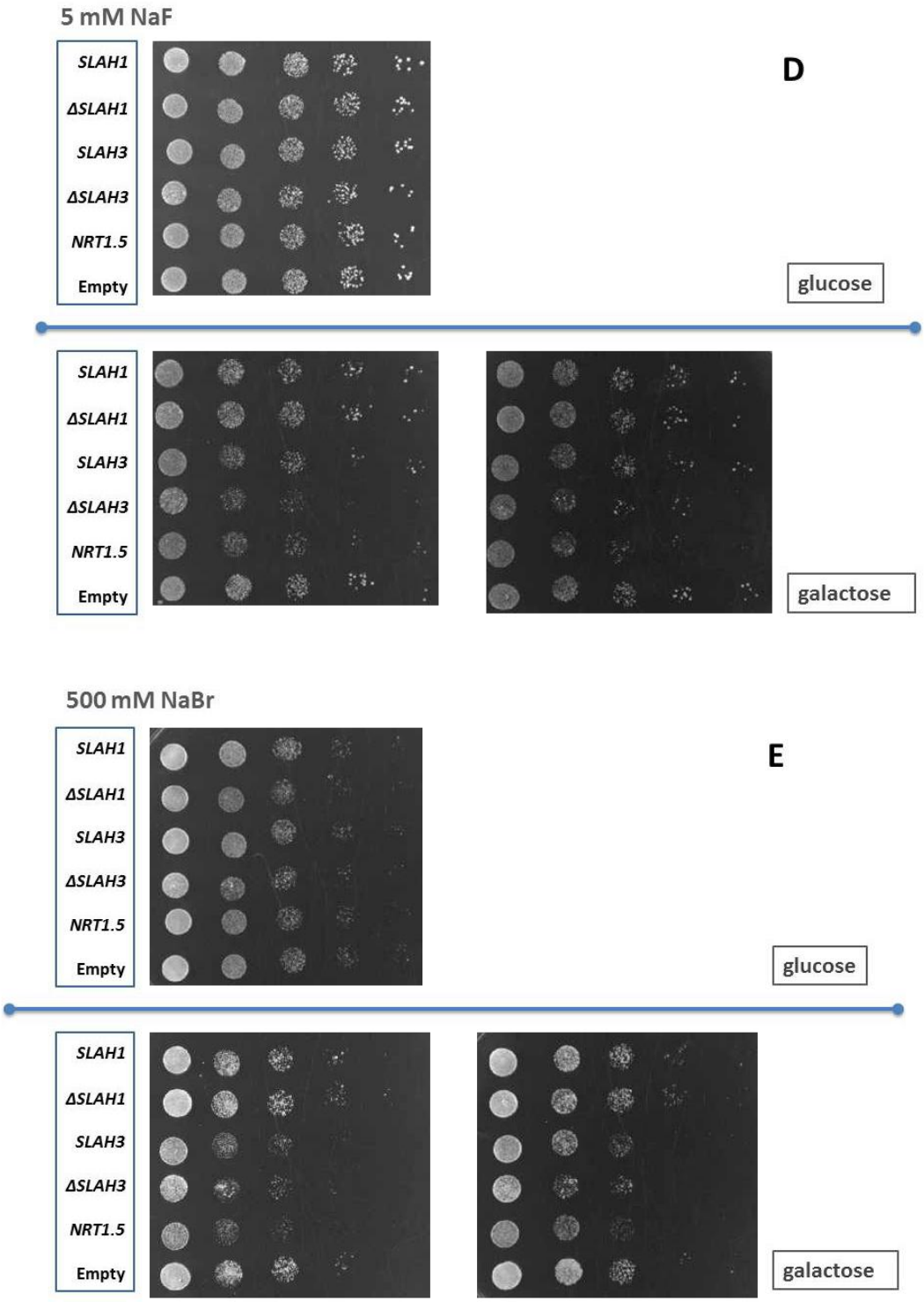
5 mM NaF
SLAH1
ΔSLAH1
SLAH3
ΔSLAH3
NRT1.5
Empty
D
glucose
galactose
500 mM NaBr
E

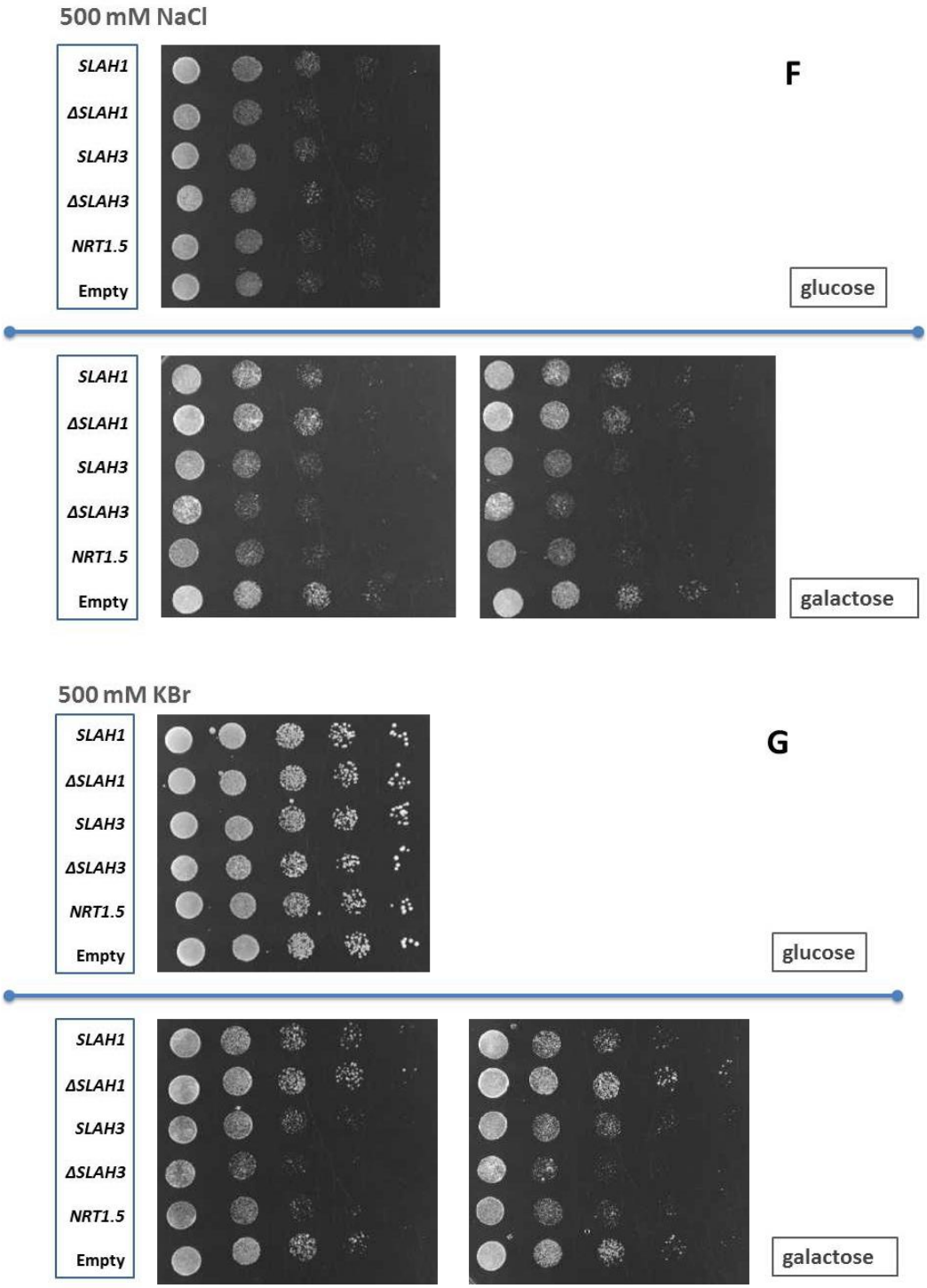
500 mM NaCl
SLAH1
ΔSLAH1
SLAH3
ΔSLAH3
NRT1.5
Empty
F
glucose
SLAH1
ΔSLAH1
SLAH3
ΔSLAH3
NRT1.5
Empty
galactose
500 mM KBr
SLAH1
ΔSLAH1
SLAH3
ΔSLAH3
NRT1.5
Empty
G
glucose
SLAH1
ΔSLAH1
SLAH3
ΔSLAH3
NRT1.5
Empty
galactose

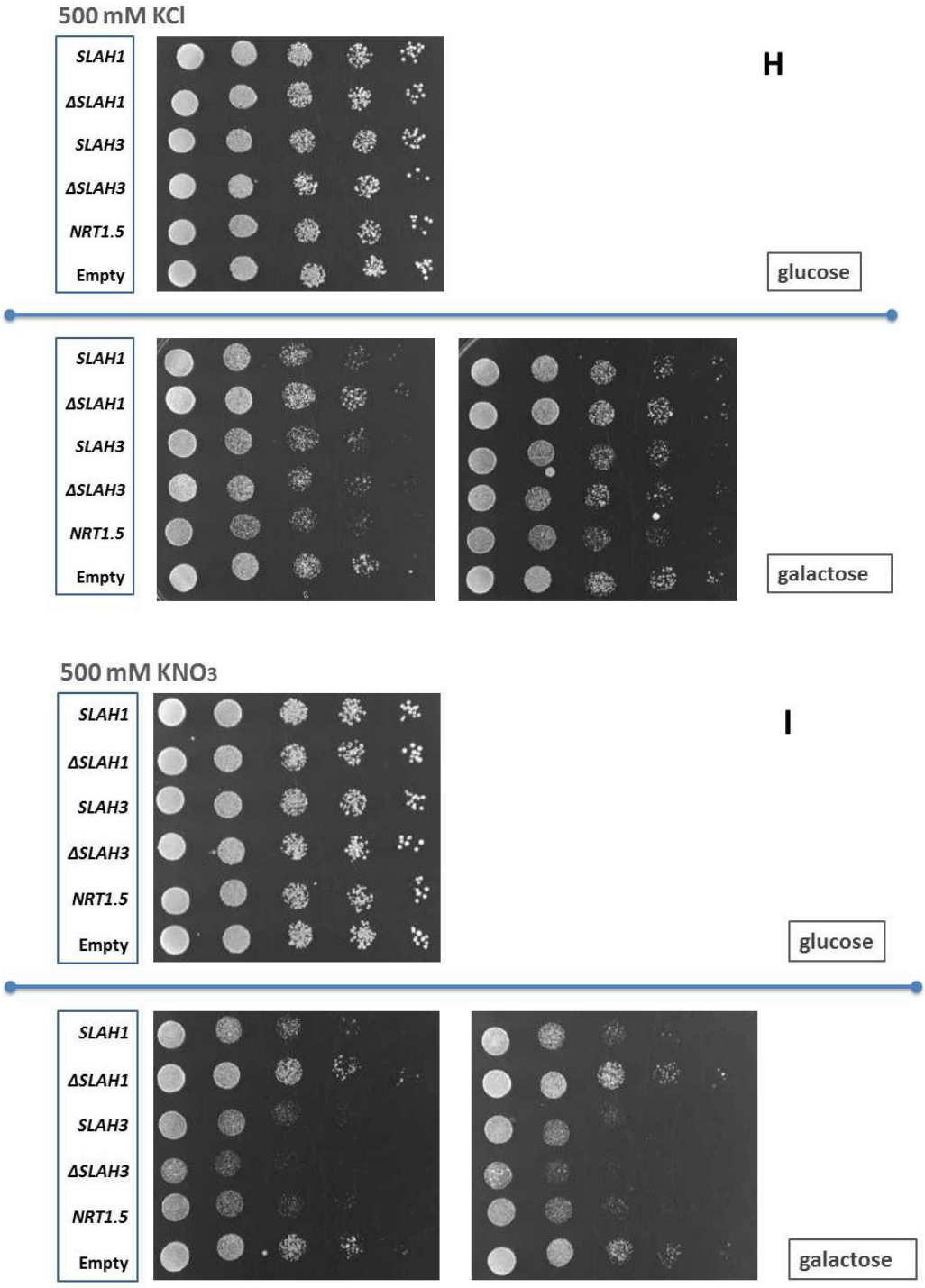
500 mM KCl
SLAH1
ΔSLAH1
SLAH3
ΔSLAH3
NRT1.5
Empty
H
glucose
SLAH1
ΔSLAH1
SLAH3
ΔSLAH3
NRT1.5
Empty
galactose
500 mM KNO3
SLAH1
ΔSLAH1
SLAH3
ΔSLAH3
NRT1.5
Empty
I
glucose
SLAH1
ΔSLAH1
SLAH3
ΔSLAH3
NRT1.5
Empty
galactose

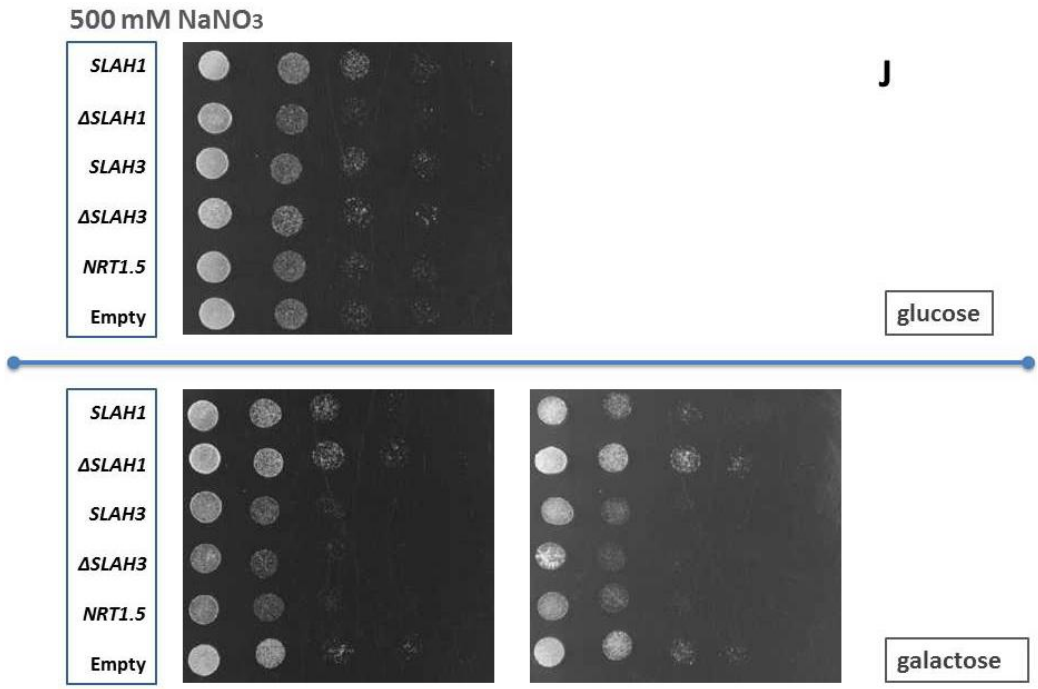

Figure 4.8 *SLAH1*, *ΔSLAH1, SALH3*, *ΔSLAH3*, *NRT1.5* and empty vector (pYES-DEST52) transformed yeast grown on the plate containing various salts (halogen family) with different concentrations of salts. Dilution series of yeast in exponential phase were spotted on medium (-uracil) with 2 % (w/v) glucose (up panel) and galactose (lower panel), 1.67% (w/v) agar and salts as indicated. **(A)** 1 mM KF; **(B)** 1 mM NaF; **(C)** 5 mM KF; **(D)** 5 mM NaF; **(E)** 500 mM NaCl; **(F)** 500 mM NaBr; **(G)** 500 mM KBr; **(H)** 500 mM KCl; **(I)** 500 mM KNO_3; **(J)** 500 mM $NaNO_3$.

4.3.2.2 Growth inhibition assay performed in small volume liquid media

To investigate whether growth assays in liquid would be more sensitive and tease apart the effect of GOI expression on yeast growth when incubated in different salt solutions, a high throughput growth assay was optimized (Section 2.8.1). Previous optimization showed that addition of 20 mM MES was able to maintain the media's pH value at 5.6 (Section 2.8.1), therefore, in following experiments, 20 mM MES was added to all of the testing media for characterizing the GOI's transport properties.

When *NRT1.5* transformed yeast was incubated within the glucose based media for 38 hours, no significant growth difference was observed compared to the empty vector control (Figure 4.9 A). A similar phenotype was found in Figure 4.16 B and C, where 500 mM KCl and KNO_3 was added into the glucose based media. When galactose was applied to trigger the *NRT1.5* expression in the yeast in the control condition, *NRT1.5* transformed yeast spent 15 hours in the lag phase whereas the empty vector control only took 12 hours to enter the log phase,

however, no significant difference in growth rate was found in log phase (Figure 4.9 D, G and H).

When 500 mM KCl was added into the galactose-based media, *NRT1.5* transformed yeast exhibited pronounced growth inhibition compared to the empty vector (Figure 4.9 E). Although *NRT1.5* and empty vector both spent around 20 hours in the lag phase, the growth rate of *NRT1.5* transformed yeast was significantly lower (54 %) than empty vector control (Figure 4.9 G and H). The significant growth rate reduction might suggest that *NRT1.5* was involved in Cl^- transport in yeast. When 500 mM KNO_3 was presented in the media, *NRT1.5* transformed yeast took 5 more hours to enter the log phase (Figure 4.9 G), compared to the empty vector control. Also, a 30 % of the growth rate reduction was discovered in *NRT1.5* transformed yeast when compared to the empty vector control (Figure 4.9 G). In summary, the growth rate of *NRT1.5* transformed yeast was affected by both Cl^- and NO_3^-, which indicates it, may catalyse the transport of both anions.

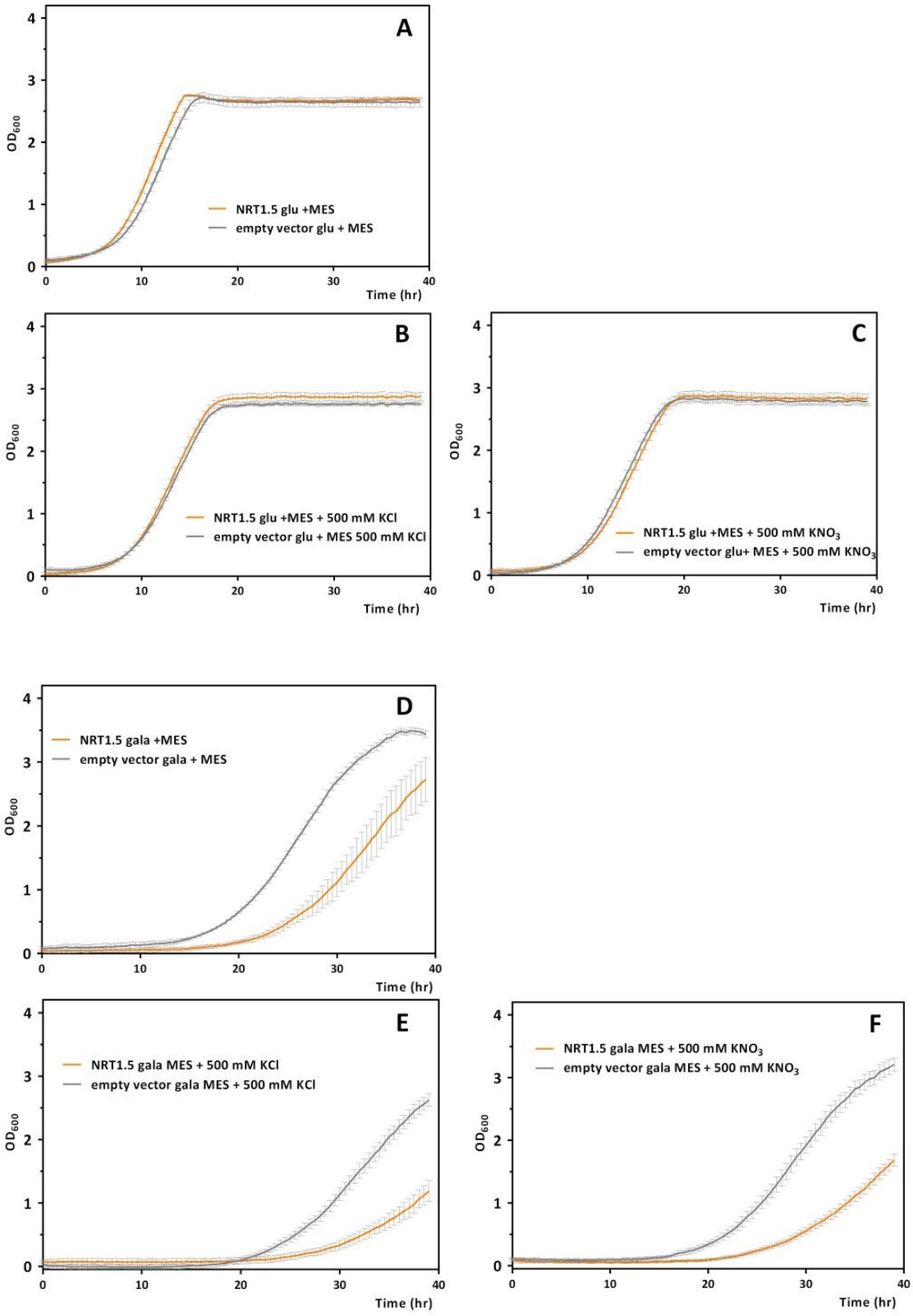
A
NRT1.5 glu +MES
empty vector glu + MES
B
NRT1.5 glu +MES + 500 mM KCl
empty vector glu + MES 500 mM KCl
C
NRT1.5 glu +MES + 500 mM KNO3
empty vector glu+ MES + 500 mM KNO3
D
NRT1.5 gala +MES
empty vector gala + MES
E
NRT1.5 gala MES + 500 mM KCl
empty vector gala MES + 500 mM KCl
F
NRT1.5 gala MES + 500 mM KNO3
empty vector gala MES + 500 mM KNO3
OD600
Time (hr)

Gene	Lag phase time (hour)	Media used
Empty vector	12	Control
NRT1.5	15	Figure D
Empty vector	20	500 mM KCl
NRT1.5	21	Figure E
Empty vector	15	500 mM KNO_3
NRT1.5	20	Figure F

G

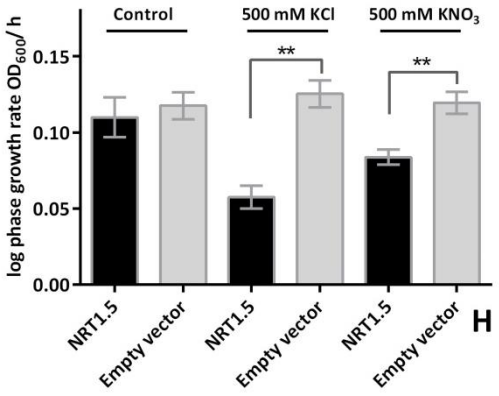

H

Figure 4.9 The growth rate of *NRT1.5* transformed yeast was examined using small-volume liquid assay. Empty vector transformed yeast was used as control. (**A**) Glucose with 20 mM MES; (**B**) Glucose with 20 mM MES plus 500 mM KCl; (**C**) Glucose with 20 mM MES plus 500 mM KNO_3; (**D**) Galactose with 20 mM MES; (**E**) Galactose with 20 mM MES plus 500 mM KCl; (**F**) Galactose with 20 mM MES plus 500 mM KNO_3; (**G**) The time of *NRT1.5* and empty vector transformed yeast spent in lag phase in galactose- based media under control, 500 mM KCl and 500 mM KNO_3 conditions; (**H**) The growth rate of *NRT1.5* and empty vector transformed yeast in log phase when incubated in galactose-based media with various salt stress. Statistical difference was determined by unpaired t test ($P \leq 0.05$); Data were presented as mean ± SEM, n= 4.

No differences were discovered in *SLAH1* and empty vector transformed yeast when grown in the glucose- based media control or 500 mM of KCl/ KNO_3 was applied to the media (Figure 4.10 A, B and C). When glucose was replaced by galactose to trigger the expression of *SLAH1*, no growth differences were found between SLAH1 and empty vector under control (Figure 4.10 D), 500 mM KCl (Figure 4.10 E) or KNO_3 (Figure 4.10 F) conditions, which suggested that SLAH1 may not be able to transport Cl^- or NO_3^- in yeast if it was not targeted to the plasma membrane.

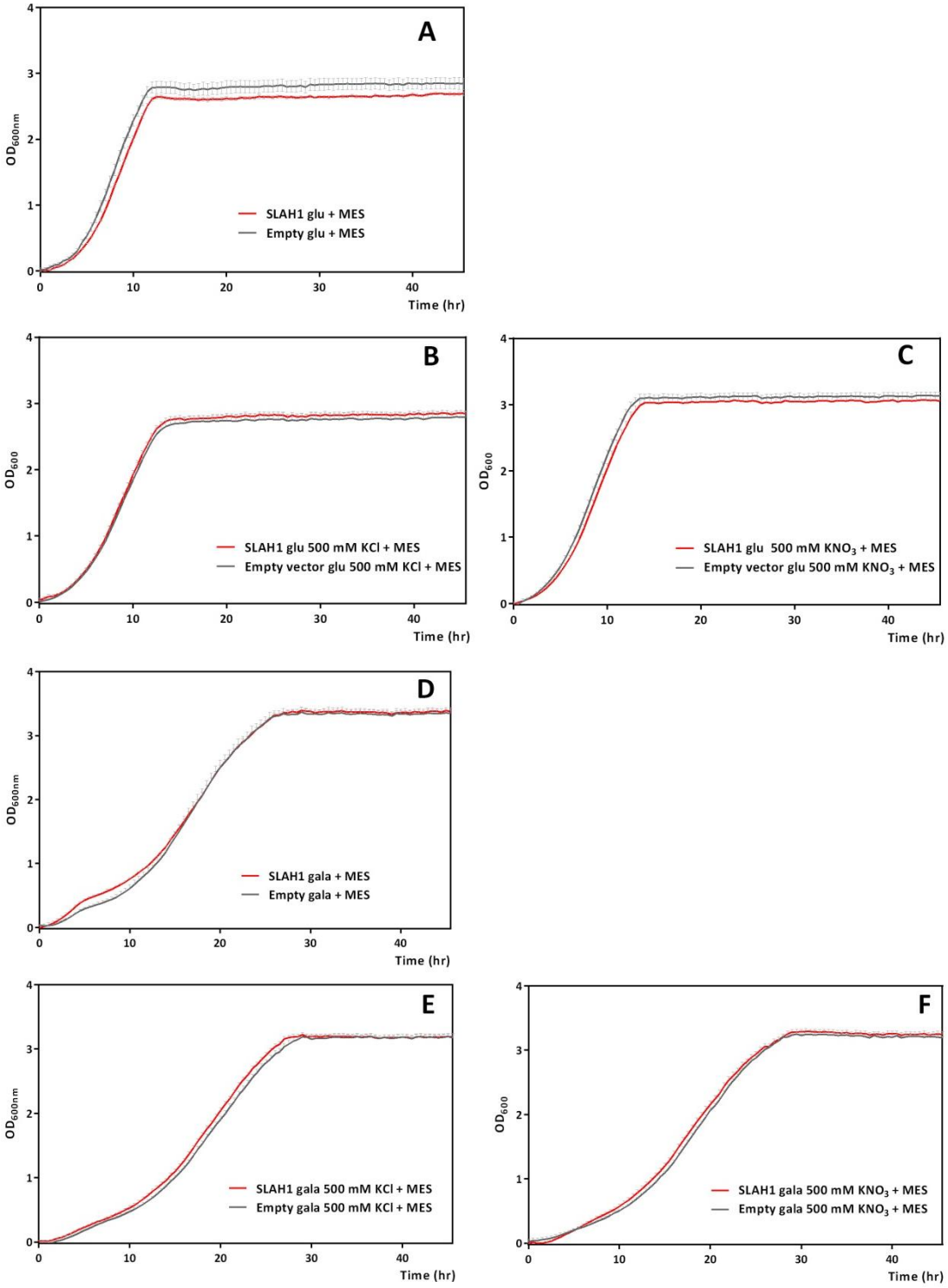

Figure 4.10 The growth rate of *SLAH1* transformed yeast was examined using the small-volume liquid assay. Empty vector transformed yeast was used as control. (**A**) Glucose with 20 mM MES; (**B**) Glucose with 20 mM MES plus 500 mM KCl; (**C**) Glucose with 20 mM MES plus 500 mM KNO_3; (**D**) Galactose with 20 mM MES; (**E**) Galactose with 20 mM MES plus 500 mM KCl; (**F**) Galactose with 20 mM MES plus 500 mM KNO_3. Data were presented as mean ± SEM, n= 4.

SLAH3 transformed yeast did not exhibit growth rate difference when glucose based media was supplied (Figure 4.11 A, B and C). When galactose was used to trigger the gene expression, a slight but non-significant growth rate difference was found in the control conditions (Figure 4.11 D and H). When 500 mM KCl was added into the galactose based media, *SLAH3* and empty vector transformed yeast spent similar lengths of time in lag phase (Figure 4.11 E and G), the *SLAH3* transformed yeast showed an evident growth rate reduction in log phase when compared to the empty vector control (Figure 4.11 E and H), which suggests a potential role of SLAH3 in manipulating Cl^- transport. Under 500 mM KNO_3 treatment, the observed phenotypes were similar to the results identified within 500 mM KCl media. A 33 % reduction in growth rate was found in *SLAH3* transformed yeast in comparison to the empty vector control within the log phase, which indicating that SLAH3 might transport NO_3^- in yeast (Figure 4.11 F and H). The growth assay was also performed in the same sets of media without adding additional of 20 mM MES. Interestingly, without MES present in the media to stabilize the pH, *SLAH3* transformed yeast were less affected under both 500 mM KCl and KNO_3 stress when compared to the empty vector control (Figure 4.11 I and J).

Site- mutated SLAH1 and SLAH3 were also transformed into yeast and tested along with wildtypes within the media containing 500 mM KCl or KNO_3. *SLAH1*, *ΔSLAH1*, *SLAH3* and *ΔSLAH3* and empty vector transformed yeast were firstly tested in glucose based media (Figure 4.12 A) or glucose based media supplied with 500 mM KCl (Figure 4.12 B) and KNO_3 (Figure 4.12 C) and no significant differences were identified, except in the stationary phase cell density at above an OD_{600nm} of above 2 which is likely to be inaccurately measured using a spectrophotometer.

When glucose was replaced by galactose, under 500 mM KCl, *ΔSLAH1* transformed yeast showed a small but significant growth inhibition compared to wildtype, *SLAH1* and empty vector transformed yeast (Figure 4.12 E)

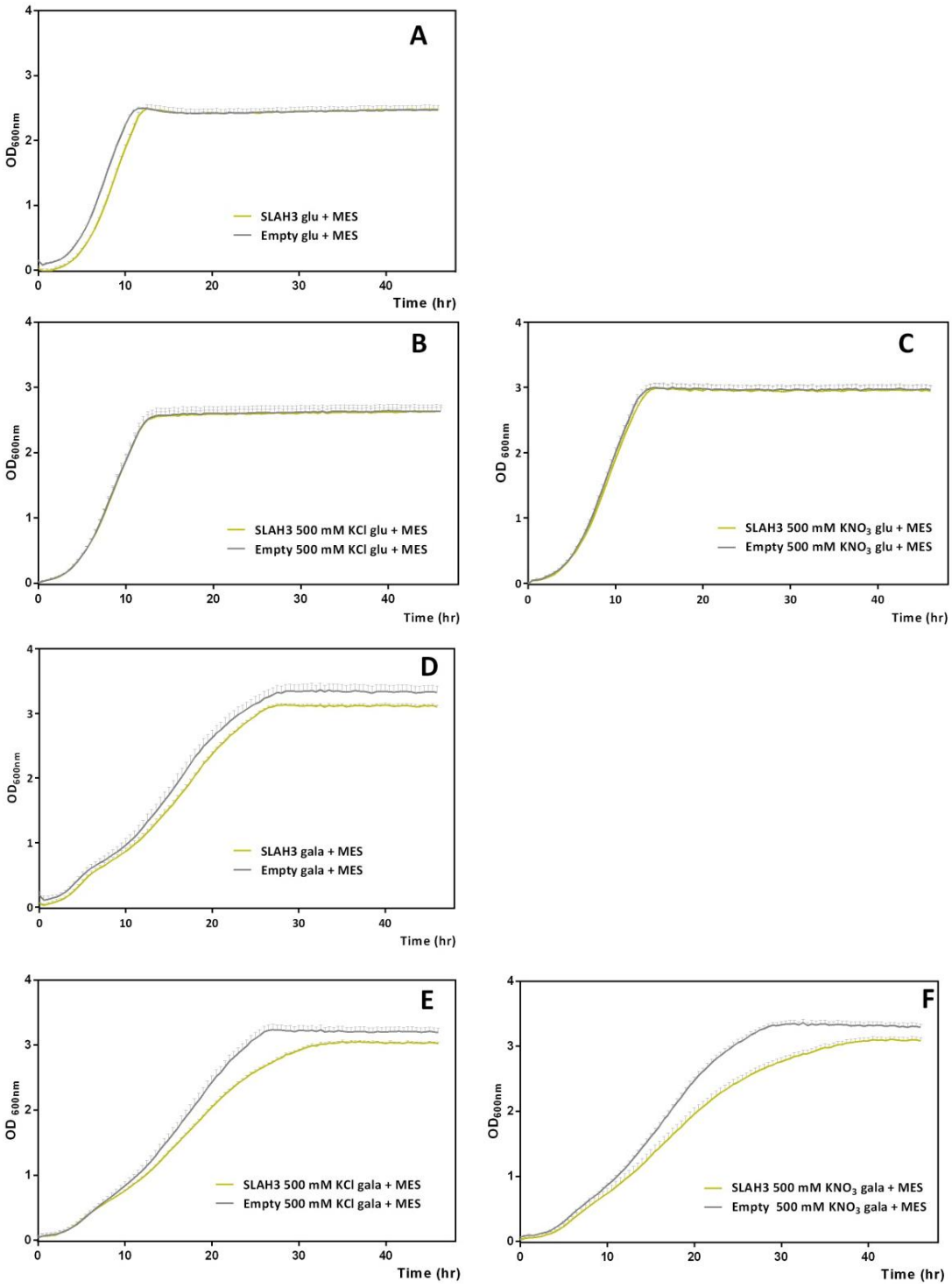
A
OD600nm
SLAH3 glu + MES
Empty glu + MES
Time (hr)
B
OD600nm
SLAH3 500 mM KCl glu + MES
Empty 500 mM KCl glu + MES
Time (hr)
C
OD 600nm
SLAH3 500 mM KNO3 glu + MES
Empty 500 mM KNO3 glu + MES
Time (hr)
D
OD600nm
SLAH3 gala + MES
Empty gala + MES
Time (hr)
E
OD 600nm
SLAH3 500 mM KCl gala + MES
Empty 500 mM KCl gala + MES
Time (hr)
F
OD600nm
SLAH3 500 mM KNO3 gala + MES
Empty 500 mM KNO3 gala + MES
Time (hr)

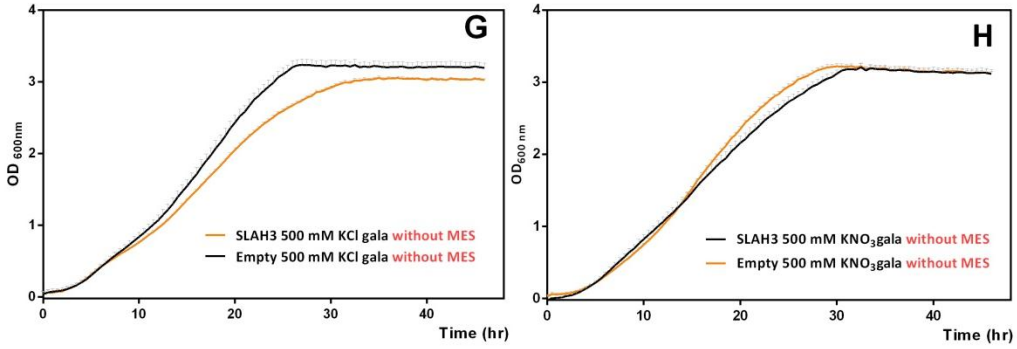

Figure 4.11 The growth rate of SLAH3 transformed yeast was examined using small-volume liquid assay. Empty vector transformed yeast was used as control. (**A**) Glucose with 20 mM MES; (**B**) Glucose with 20 mM MES plus 500 mM KCl; (**C**) Glucose with 20 mM MES plus 500 mM KNO_3; (**D**) Galactose control with 20 mM MES; (**E**) Galactose with 20 mM MES plus 500 mM KCl; (**F**) Galactose with 20 mM MES plus 500 mM KNO_3. (**G**) Galactose without 20 mM MES plus 500 mM KCl; (**H**) Galactose without 20 mM MES plus 500 mM KNO_3. Data were presented as mean ± SEM, n= 4.

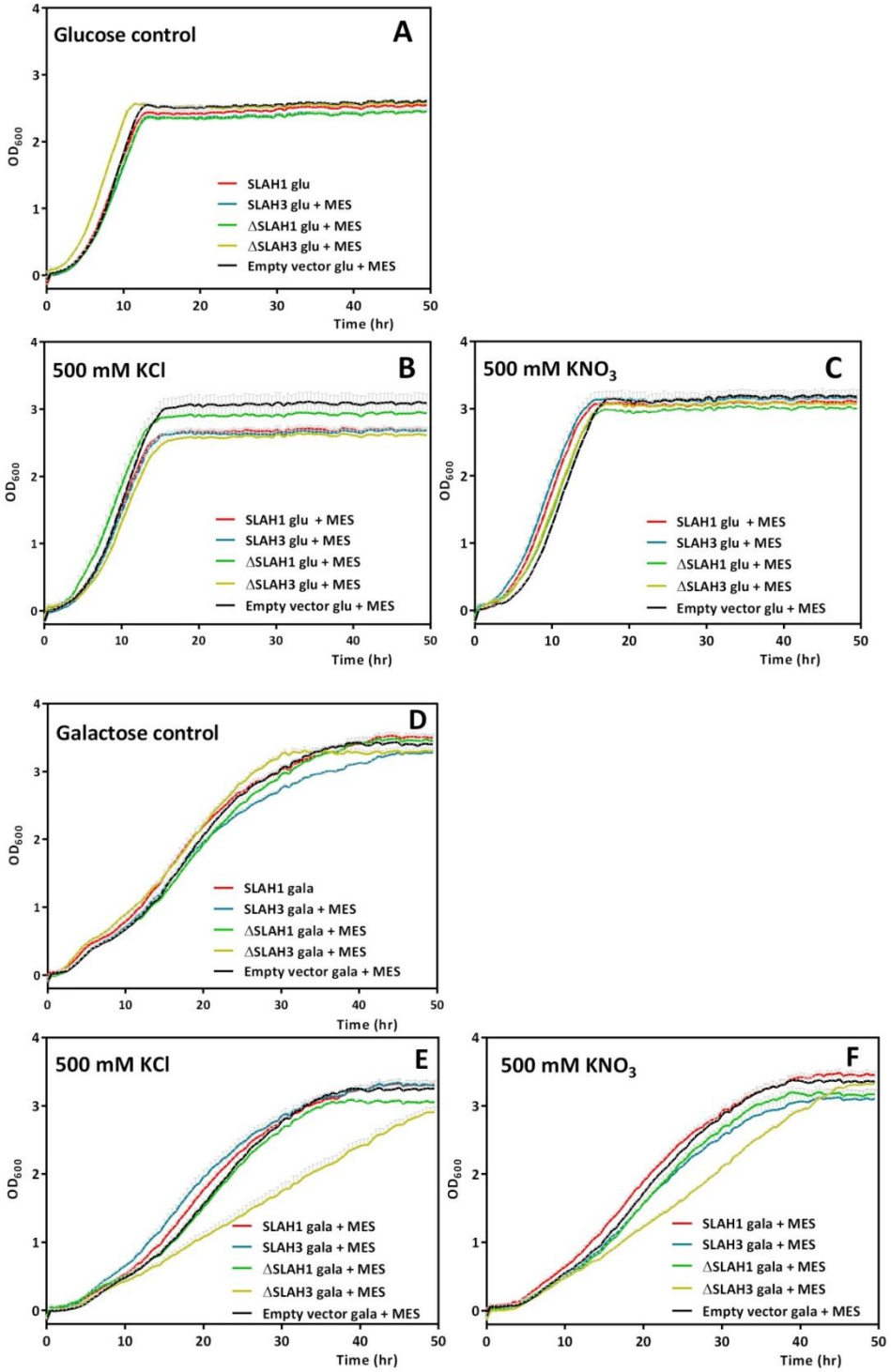

Figure 4.12 The growth rate of *SLAH1*, *ΔSLAH1*, *SLAH3* and *ΔSLAH3* transformed yeast were examined using small-volume liquid assay. Empty vector transformed yeast was used as control. (**A**) Glucose or glucose with 20 mM MES; (**B**) Glucose or glucose with 20 mM MES plus 500 mM KCl; (**C**) Glucose or glucose with 20 mM MES plus 500 mM KNO_3; (**D**) Galactose or galactose with 20 mM MES; (**E**) Galactose or galactose with 20 mM MES plus 500 mM KCl; (**F**) Galactose or galactose with 20 mM MES plus 500 mM KNO_3; Data were presented as mean ± SEM, n= 3.

4.3.3 Examine the potential interaction between SLAH1 and SnRk2.2/2.3 in Arabidopsis mesophyll protoplasts using BiFC

The bimolecular fluorescent complementation (BiFC) assay has been widely employed to identify putative protein-protein interactions (Waadt *et al*., 2008; Walter *et al*., 2004). Although it has been reported that this system is subject to false positives, it is still valuable to supply some clues regarding the potential interactions between proteins. To test the putative interaction between SLAH1 and SnRK2.2 or SnRK2.2.3, or ΔSLAH1 and SnRK2.2 or SnRK2.2.3, the BiFC destination vectors, pUC-SPYNE/GW (with the split N-terminal YFP) and pUC-SPYCE/GW (with the split N-terminal YFP) were used. The co-expression of *SLAH1* or *ΔSLAH1* and potential regulating kinases was performed but resulted in low level YFP signals in all cases (Figure 4.13 A-D). However, by comparing the localization to the plasma membrane maker, the weak YFP signals that were observed in all combinations were unlikely to localize to the plasma membrane, which suggested in this experiment, no strong interaction was found between SLAH1 or its point mutant and SnRK2.2 or SnRK2.3.

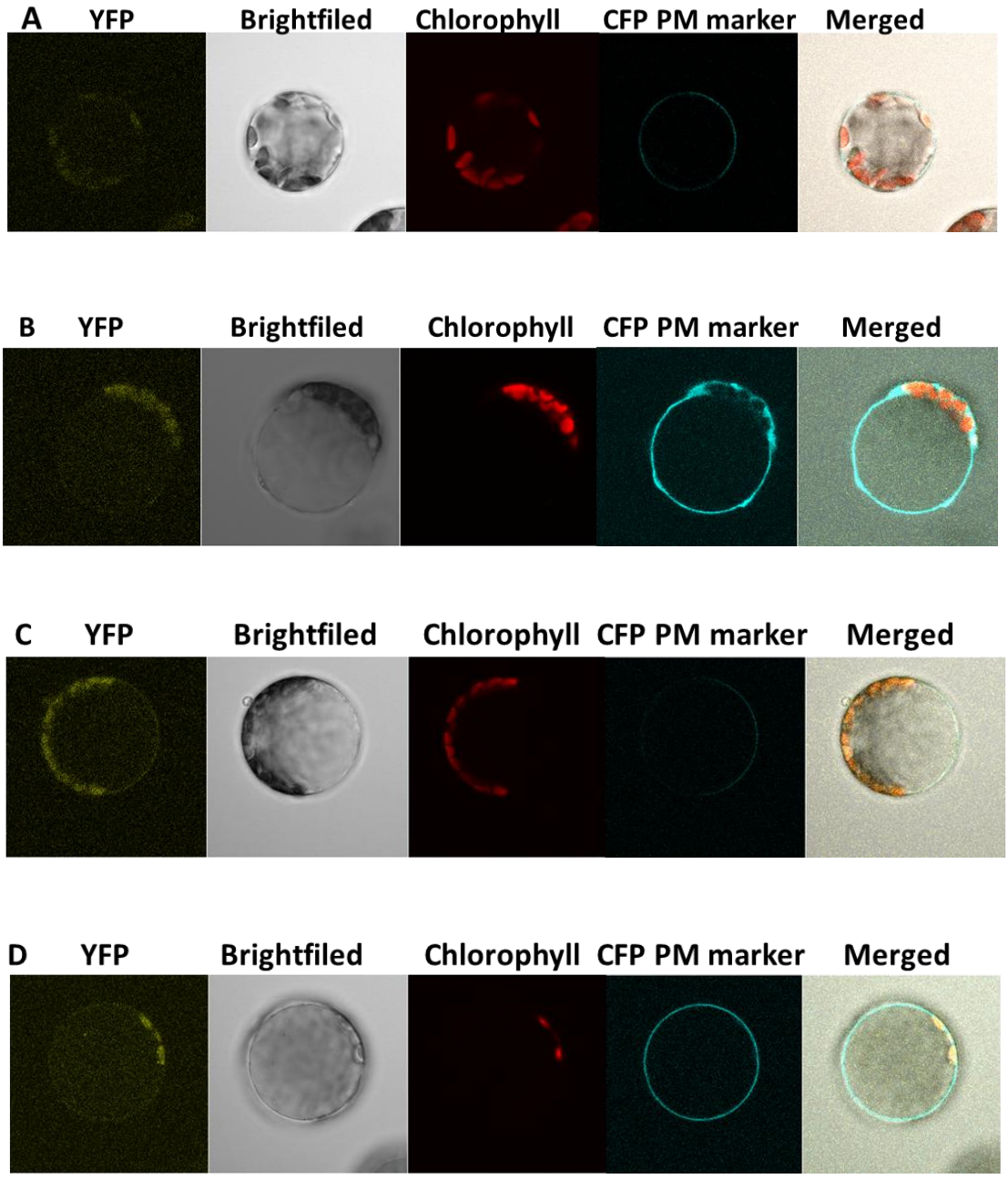

Figure 4.13 Subcellular localisation of SLAH1 and SnRk2.2 or SnRK2.3, or ΔSLAH1 and SnRk2.2 or SnRK2.3 in Arabidopsis mesophyll protoplasts. Confocal images transiently expressing pUC-SPYNE-*SLAH1*: pUC-SPYCE *SnRK2.2/2.3* complex in Arabidopsis (5-6 weeks old) mesophyll protoplasts. (**A**) pUC-SPYNE-SLAH1 :pUC-SPYCE SnRk2.2 complex; (**B**) pUC-SPYNE-SLAH1 :pUC-SPYCE SnRk2.3 complex; (**C**) pUC-SPYNE-ΔSLAH1 :pUC-SPYCE SnRk2.2 complex; (**D**) pUC-SPYNE-ΔSLAH1 :pUC-SPYCE SnRk2.3 complex; The fluorescence was obtained by sequential scanning for YFP (excitation = 514 nm, emission = 520-550 nm) and chlorophyll autofluorescence (excitation = 488 nm, emission = 640-740 nm) by Leica SP5, scale bars = 20 µm.

4.4 Discussion

4.4.1 AtSLAH1 is not directly involved in Cl^- and NO_3^- transport in heterologous systems

So far there is no positive data that supports the hypothesis that AtSLAH1 is involved in anion transport using heterologous systems as no anion mediated currents were identified from *AtSLAH1* cRNA injected oocytes, in *AtSLAH1* co- injected with potential protein kinase SnRK2.2/SnRK2.3 oocytes or in oocytes injected with the site- mutated SLAH1. The yeast data is less definitive as a mild phenotype was observed in K salt on solid containing media for both SLAH1 and the SLAH1 mutant. However, these phenotypes could not be replicated in liquid media. There are a number of factors that may be responsible for the observed results. First of all, the protein concentration of SLAH1 in oocytes/yeast is unknown; no Western blot was performed to confirm the protein transcription in all tested systems. Secondly, it is very likely that SLAH1 needs to be phosphorylated and is activated by a protein kinase, drawing from the evidence from other members of the protein family. When SLAC1 was expressed in *X. Laevis* oocytes alone no clear anion currents were generated (Vahisalu *et al*., 2008). Later, a protein kinase OST1 (also known as SnRk2.6) was found to activate SLAC1 by phosphorylation of multiple serines in the SLAC1 hydrophilic N-terminal sequence (Geiger *et al*., 2009; Lee *et al*., 2009; Vahisalu *et al*., 2010). This evidence further confirmed that a regulatory component is important for activating the S-type anion channels (Schmidt *et al*., 1995). Although co-expression of either *SnRk2*.2 or *2.3* with *SLAH1* was attempted in *X. Laevis* oocyte and Arabidopsis mesophyll protoplasts, there was no strong evidence for an interaction between SnRK2.2 and SnRk2.3 with SLAH1. While an attempt was made to produce a mutated SLAH1 which did not require phosphorylation to be active, the selection of the protein kinases and mutation site were deducted from a review rather than an experimental result (Dreyer *et al*., 2011). It is therefore possible that SLAH1 could be activated by an unknown protein kinase. To address this issue, a high throughput screening system, such as Split-Ubiquitin Membrane Yeast Two-Hybrid System (MYTH), to identify potential interacting proteins from a large protein library might help us to find putative interaction partners of SLAH1. For example, OST1 was fused to the bait for several PP2Cs in an activation vector and then expressed in the yeast cell, which showed the strong interaction between OST1 and ABI1/2 (Lee *et al*., 2009). Additionally the analysis of the protein crystal structure of SLAH1 would also be helpful to reveal the important amino acids at the anion gating/selectivity filter thus providing information on the ions transported by the protein. For example, by revealing the crystal structure of the CLC chloride channel, the

Cl^- binding site was discovered and the anion gating was altered when the binding site was mutated (Dutzler *et al*., 2002). Finally, although a number of attempts were made to improve the experimental setup; more optimization of the protocols may be required. For instance, a wider range of chloride/nitrate, such as HCl and HNO_3 can be selected to further characterize SLAH1's potential function in *X. laevis* oocytes.

Regardless of the fact that SLAH1 is one of the homologs of SLAC1, which codes a slow-type anion channel and involving in chloride and nitrate transport (Negi *et al*., 2008; Vahisalu *et al*., 2008), it is still not clear whether SLAH1 has the same function. Evolutional analysis suggested that SLAH2/3 is classified in the same group of proteins while SLAH1/4 belongs to another group (Dreyer *et al*., 2012). SLAH2 and SLAH3 have been successfully functional characterized in heterologous expression systems and these results suggested that both of them are involved in nitrate transport (Geiger *et al*., 2011; Maierhofer *et al*., 2014). However, the other homologs of SLAC1, including SLAH1 and 4, still remain to be characterized. In comparison with the amino acid sequence of SLAH3, SLAH1 has fewer N/C-terminal residues, and the first trans-membrane domain has a different predicted structure (Dreyer *et al*., 2012). It has been shown that the N-terminal is important to SLAC1 and SLAH3, as it contains several key residues to which protein kinase bind and activates channel function (Vahisalu *et al*., 2010; Geiger *et al*., 2009; Geiger *et al*., 2011). This might suggest that SLAH1 is not directly linked with Cl^- and NO_3^- transport as it lacking the potential phosphorylation sites in the N-terminal region. On the other hand, SLAH1 might be involved in transporting other ions, such as malic acid, as its protein sequence is highly conserved to C4-dicarboxylate/malic acid transporters from plant pathogens (Dreyer *et al*., 2012). Alternatively, it may not be a transporter at all and regulate the transport of other proteins. For instance, an analogous of the Arabidopsis shaker-like ion channel family, AtKC1, was localized to plasma membrane and involved in silencing K^+ transports in root hair (Reintanz *et al*., 2002).

4.4.2 AtSLAH3 is involved in likely to transport both Cl^- and NO_3^- in heterologous systems

AtSLAH3 has been characterized as a protein underlying the S-type anion channel conductance (Geiger *et al*., 2012; Demir *et al*., 2013; Zheng *et al*., 2014). Results showed that SLAH3 was involved in nitrate transport in oocytes when the external nitrate was used as a substrate (Geiger *et al*; 2011) and exhibits higher preference to nitrate than to chloride (Dreyer *et al*., 2012). In this study, *AtSLAH3* cRNA injected oocytes showed nitrate mediated currents and the current density, especially the outward anion currents, increased when

external NO_3^- was increased (Figure 4.6 A). Less Cl^- elicited currents were observed when the same concentration of NO_3^- or Cl^- was used (Figure 4.6 A), which is identical to the findings in previous studies (Geiger *et al*., 2011). The measured conductivity to NO_3^- and Cl^- was confirmed that *AtSLAH3* cRNA injected oocytes were more selective to NO_3^- than Cl^- when the same strength of anions was available in the bath solutions (Figure 4.6 B). The *AtSLAH3* transformed yeast showed significant growth inhibition when 500 mM KCl or KNO_3 was present within the media (Figure 4.8 H and I), which is consistent with SLAH3 being permeable to both Cl^- and NO_3^-. A high- throughput small volume yeast liquid assay was performed and also showed similar results that SLAH3's growth rate (log phase) was significantly affected by high concentration of KCl or KNO_3 (Figure 4.11 E, F and H). A previous study showed that *ΔSLAH3* (the site was mutated to mimic the phosphorylation) cRNA injected oocytes produced significantly greater anion currents than SLAH3 in the absence of CPK21 (Geiger *et al*., 2012). However, the effect of site mutation was not tested in chloride based solution, which leaves the question whether the mutation is also important for gating Cl^- within the oocytes. My results suggested that in *ΔSLAH3* injected oocytes, both NO_3^- and Cl^- mediated currents were increased when external anion concentration was increased (Appendix 2), however, the higher preference to NO_3^- remained. Interestingly, there is a hint that the selectivity may be different in *ΔSLAH3* transformed yeast with it being more clearly more sensitive to Cl^- than SLAH3 (Figure 4.12 E and F).

There are a number of factors which may be responsible for the observed results. First of all, the yeast strain that used in this project may not be ideal for characterization of anion transport. High accompanying cation concentrations were intentionally used in these yeast assays as the cation (Na^+ and K^+) transporters, such as NSC1, Ena1p and Tok1p that are responsible for maintaining ion homeostasis, localized to the yeast plasma membrane (Ke *et al*., 2013), would mean that Na^+ and K^+ entry will depolarize the plasma membrane and allow the anions to enter the cell down their electrochemical gradient. Also, it also been suggested that under a slightly acidic environment, the activation of Ena1p increased and significantly accelerated the membrane depolarization (Ke *et al*., 2013). However, K^+ and Na^+ influx into the yeast cells *per se* through the cation transporter (Ke *et al*., 2013) may have other and confounding effects on the assay. Therefore, the processes that happened natively within the yeast could affect the observed results. Secondly, the pH environment might be important for characterizing SLAH3 function in yeast. For example, when 20 mM of MES that was used to maintain the pH (around 5.6) was added into the media, an evident growth inhibition was

found in both 500 mM KCl and KNO_3 media (Figure 4.11 E and F) and the difference disappeared without additional MES (pH 3-4) (Figure 4.11 G and H). These results might indicate that the pH is crucial for characterization of SLAH3 in yeast. Although no similar results were revealed when characterized the SLAH3 in heterologous systems, recent work performed on the *Atslah3* mutant showed a significant root length reduction under a low pH environment (pH below 5), which suggesting SLAH3 is sensitive to pH or its reduction is caused by increased ammonium (Zheng *et al*., 2014). This may be related to the role that anion efflux out of cells has on the control of the H^+-ATPase and membrane potential? To minimize the factors that could affect the results in the future, yeast strain with specific anion transporter disabled can be used to characterize the GOI. For example, a *Saccharomyces cerevisiae* knock out strain (Gef1p), was successfully used for characterizing the potential chloride channel (Gaxiola *et al*., 1998). Regardless, it appears that *SLAH3* and *ΔSLAH3* transformed yeast are consistent with results obtained by myself and other groups with *X. laevis* oocytes, so can be thought of as a validation of the assay.

As NO_3^- and Cl^- both exist in the soil solution in the environment, and previous results indicate that a high concentration Cl^- would inhibit the NO_3^- uptake. The transport of anions through AtSLAH3 in a combined solution was studied. Additional 50 mM of CsCl was significantly inhibited AtSLAH3s conductivity to NO_3^- (Figure 4.6 C), around 50- 60% of inward currents were reduced. These results suggested that competition existed between NO_3^- and Cl^- when transported through the AtSLAH3.

To identify whether a pharmacological approach could help tease apart the identity of particular anion transporters in plants and their role in long distance transport a blocker to ion transport was used. If a blocker is effective on a protein expressed in a heterologous system then it could be used as a tool to test the role of that protein within the plant (although it is no guarantee that this blocker is selective for a particular protein). DIDS has been used previously to reduce Cl^- accumulation in shoots of barley (Tavakkoli *et al*., 2012). To test whether DIDS could reduce the SLAH3 activity, and therefore may be a route by which DIDS reduces Cl^- loading to the shoot, DIDS was applied to *X. Laevis* oocytes expressing *SLAH3*. Both inward and outward anion currents were reduced by 70- 80 % (Figure 4.6 E), so may indicate the role of similar transporters in long distance anion transport to shoots. Although DIDS has been widely used to characterize the activity of anion channels in many studies (Schroeder *et al*., 1993; Geiger *et al*., 2009; Brandt *et al*., 2012), its mode of action is

still unknown as is the identity of all proteins on which it acts. It would be valuable to discover how DIDS acts in oocytes or plants.

4.4.3 AtNRT1.5 might be involved in both Cl^- and NO_3^- transport

Previous functional characterization of AtNRT1.5 in *X. laevis* oocytes suggested that it is a low-affinity, pH-dependent bidirectional nitrate transporter (Lin *et al*., 2008). Our results suggested that when *AtNRT1.5* cRNA was injected into the oocyte, no significant anion currents were mediated under both low and high pH environment (Figure 4.2), which is not consistent with the previous findings. The potential factors may be: **1)** the currents detected by Lin *et al*. (2008) were very small and near the limit of detection with two-electrode voltage clamp. It is possible that the resolution of my assay was not high enough; **2)** AtNRT1.5 may require activation by a protein kinase, like other NRTs, and so *AtNRT1.5* was expressed alone in oocytes, currents could not be detected. For example, NRT1.1, another member of NRT family can be converted into a high-affinity nitrate transporter when CIPK23 phosphorylated NRT1.1 at T101 site (Ho *et al*., 2009); **3)** co-expression with another nitrate transporter from the same protein family may increase AtNRT1.5 activity. For instance, when *NAR2.1* was co-expressed *NRT2.2* and *NRT2.5* in oocytes together, nitrate uptake was significantly increased (Kotur *et al*., 2012; Krapp *et al*., 2014). The identification of NRT1.1's crystal structure has revealed important phosphorylation sites that regulate the affinity in NRT1.1 (Sun *et al*., 2014; Tsay 2014). To further identify the transport properties of NRT1.5 in oocytes, a few methods such as the identity of the crystal structure (or at least modeling on the NRT1.1 crystal structure), and co-expression of other NRTs with NRT1.5 in the oocytes could be used in the future.

When AtNRT1.5 was transformed into the yeast, an evident growth inhibition was observed under high NO_3^- or Cl^- conditions (Figure 4.8 I and H; Figure 4.8 E, F and H), which indicated a role in both NO_3^- and Cl^- transport. The phenotypes observed in yeast should be interpreted carefully as the yeast strain that was used in this experiment for the reasons explained in section 4.4.2. In addition, when NRT1.5 transformed yeast was incubated under control conditions in galactose based media, there was a difference in lag phase. Clearly NRT1.5 expression affects this length of this state in yeast so may have other confounding effects on the yeast. This result was specific to AtNRT1.5 and not to other GOIs. The expression of *AtNRT1.5*, which compared to the other anion transporters assayed here, is likely to have a higher affinity for anion transport may legitimately affect the growth of yeast in low anion

media because of the availability of substrates in the media that AtNRT1.5 can readily transport. It is known that many NRT can transport a range of amino acids and other compounds such as hormones. *AtNRT1.5* expression may trigger endogenous ion regulation mechanisms and therefore become hypersensitive to other ions that existed in the media (such as Mg^{2+}, Cu^{2+} and SO_4^{2-}). Any ionic imbalance caused by the excessive uptake of an AtNRT1.5 transported substrate may result in the observed increase in lag phase (Figure 4.9 D). In addition, the NO_3^- concentration in the media alone may cause a problem to *AtNRT1.5* expressing yeast. Further assays in media with different compositions may help define what the source of the increased lag phase may be. Alternatively, a specific yeast strain that is defective in nitrate transport can be used to characterize the AtNRT1.5. For instance, there is a mutant strain of *Hansenula polymorpha* yeast, *ynt1*, which is compromised in its ability to take up NO_3^-; wildtype *H. polymorpha* can grow on NO_3^- as the sole N source but *ynt1* cannot grow on low NO_3^- concentrations. This yeast could be used to further characterise the transport activity of AtNRT1.5 (Machin *et al*., 2004).

Chapter 5 Functional characterization of long-distance anion transport candidates *in planta*

5.1 Introduction

It was proposed that *AtSLAH1*, *AtSLAH3* and *AtNRT1.5* may be involved in anion loading into the root xylem vessels of Arabidopsis (Chapter 3). Before investigating the roles of candidate genes in plants, the activity of all genes of interest (GOI) were examined at a protein level in heterologous systems including *X. laevis* oocytes and yeast (Chapter 4). Results from these chapters suggested, **i)** AtSLAH1 did not catalyse chloride/nitrate movement in both oocytes and yeast; **ii)** AtSLAH3 had greater permeability to NO_3^- than Cl^- in both oocytes and yeast; **iii)** AtNRT1.5 was not able to generate chloride/nitrate-mediated anion currents in xenopus oocytes; and, **iv)** *AtNRT1.5* transformed yeast showed pronounced growth inhibition compared to the empty vector transformation when high concentration of KCl or KNO_3 was present in the media (Chapter 4). These results, although indicative of transport capacity by some candidates, are not sufficient to make conclusions about their function *in planta*. As such, more direct evidence was required to test the hypothesis that any of the GOIs are responsible for root-to-shoot long distance anion transport in plants (Teakle and Tyerman, 2010). Therefore, it was deemed worthwhile to examine the function of these GOI through various means of misexpression depending upon availability and time constraints (i.e. artificial microRNA knock-down, knockout, constitutive over-expression and cell type specific over-expression). In this chapter, multiple transgenic plants were generated to test the effect of altering the expression of the GOI on anion (Cl^- and NO_3^-) accumulation in the shoot under different Cl^- regimes. Previous studies suggested that some anion transporter/channels have the ability to transport both Cl^- and NO_3^- (Barbier-Brygoo *et al*., 2011), therefore competition between Cl^- and NO_3^- transport is commonly reported (Buwalda and Smith, 1991). Based on this, misexpression of the GOI should be expected to alter the ratio of shoot Cl^- and NO_3^- accumulation in shoots. In this chapter, an anion blocker (DIDS) was used to further investigate the finding that it can block root-to-shoot Cl^- transport (Tavakkoli *et al*., 2011). As this original finding was performed we barley I tested its impact on both the accumylation of Cl^- and NO_3^- in Arabidopsis shoots.

5.2 Materials and Methods

5.2.1 Generation of constitutive over- expression lines

To investigate the effect of constitutive increased GOI expression on shoot anion (Cl^- and NO_3^-) accumulation under various salt treatments, the CaMV 35S promoter was fused to the coding region of a GOI to overexpress them in Arabidopsis (Col-0). The full length cDNA of *AtNRT1.5*, *AtSLAH1* and *AtSLAH3* was amplified from Arabidopsis root cDNA using high-fidelity Phusion® Taq polymerase and cloned into the Gateway enabled pCR8 entry vector following the description in (Section 2.5.4). All the plasmids containing the GOI were sequenced and examined by restriction digestion, to confirm insertion of the GOI and its orientation with in the plasmid, before being further transformed into a destination vector. Using Gateway® LR Clonase® II Enzyme Mix (Invitrogen), all GOIs were transferred from pCR8 to binary vector pMDC32, which contains a *2X35S* promoter (Curtis and Grossniklaus, 2003). The cloning procedures were was described in (Section 2.5). Transformation of 5-6 week-old Arabidopsis (Col-0) was performed using Agrobacteria-mediated transformation (Chapter 2). Seeds harvested from the dipped Arabidopsis were collected and germinated on growth media containing Hygromycin B (25 mg/mL) in order to select the putative transformants. The survivors (T_1) were then transferred to standard growth media for further growth. PCR was also performed on gDNA harvested from the putative T_1 transformants to assess whether the construct had successfully inserted. The primers used for genotyping and the expected results are listed in Table 5.1. Southern-blotting (described in (Section 2.7.2) was performed on T_1 plant's gDNA to examine the insertion's copy number. Transgenic (T_1) plants with the least number of copies of the insert were selected to grow up to the T_2 generation. Positive transgenic plants were allowed to go to produce T_2 seeds. The Southern-blotting results are shown in Figure 5.2.

5.2.2 Generation of *AtSLAH1*-amiRNA lines

5.2.2.1 *AtSLAH1*-Artificial micro RNA design and cloning

As no T-DNA insertional lines were readily available from SALK, or other Arabidopsis stock centres, artificial micro RNAs (amiRNAs) were genetically engineered to produce transgenic Arabidopsis with reduced expression level of *AtSLAH1* specifically in the root. The specific amiRNAs were designed against the *AtSLAH1* mRNA sequence using Micro RNA Designer (http://wmd3.weigelworld.org/cgi-bin/webapp.cgi), and following the description of Schwab *et al.* (2006). Two *SLAH1-amiRNA* (*SLAH1-amiRNA_1* and *SLAH1-amiRNA_2*) sequences were

selected to produce two independent *SLAH1-amiRNA* lines. In brief, first of all, two sets of four oligonucleotide sequences (I-IV) were designed from the output of WMD3 designer, these sequences correspond to a region of the mRNA of the gene to be knocked down, but have SNP mutations introduced at key points in the primer; secondly, a plasmid that contains the miR319a precursor, pRS300 was used as PCRs templates; thirdly, a series of overlapping PCRs were performed to produce the amiRNA containing precursor following the guide (http://wmd3.weigelworld.org/downloads/Cloning_of_artificial_microRNAs.pdf). For each *SLAH1-amiRNA*, three PCR products (named a, b and c) were amplified with a different combination of primers. The PCR products were initially examined on a gel and then isolated. All the three isolated PCR products were purified and mixed together as the template to amplify the full-length *SLAH1-amiRNA.* All the primers that were used and the expected products are listed in Table 5.2. The final PCR product (full-length *SLAH1-amiRNA*) was A-tailed and cloned into a pCR8 entry vector. Before being transferred into pMDC32 through the LR reaction, the direction of insertion was examined by restriction digestion and full-length sequencing. (Appendix 3)

5.2.2.2 Production of *AtSLAH1*-amiRNA lines

The two independent destination constructs, *AtSLAH1*-amiRNA_1 and *AtSLAH1*-amiRNA_2 in pMDC32 were transferred into Arabidopsis (Col-0) through Agrobacteria transformation (Section 2.6). In order to acquire T_2 transgenic plants that contained few insertions the same selection methods, including genotyping PCRs and southern-blotting, were performed as described in (Section 2.7.2).

5.2.3 Generation of cell type-specific over-expression lines

To specifically over-express the GOIs in the root stelar tissue, an Arabidopsis enhancer trap line (E2568, in Col-0 background) was used to generate the cell type-specific over-expression lines (Møller *et al*., 2009). All the full length GOIs were cloned from the Arabidopsis root cDNA and transferred into a pTOOL5 destination vector containing the GAL4 promoters that drives the target gene to specifically over express in root stelar tissue. The cloning protocol was described in Section 2.5. To confirm a successful insertion, restriction digest and sequencing were performed. Confirmed constructs were transformed into E2586 Arabidopsis using Agrobacteria mediated transformation as described in Section2.6. The seeds from transformed plants were harvested and germinated in soil. When the seedling had 2–4 true

leaves, 20 mg/L BASTA was sprayed on the seedlings to kill the plants without the insertion. The survivors were transferred to soils without BASTA for further growth. PCR was also performed using gDNA from surviving plants as a template to confirm the insertion. The isolated T_1 plants were grown in the soil and the seeds were then harvested. Due to low efficiency of BASTA selection, only a few plants were eventually confirmed as containing an insert (Table 5.1). Therefore, southern-blotting was not performed to examine the copy number.

5.2.3 DIDS treatment

In order to examine whether transport of Cl^- and NO_3^- could be altered under salt stress, a specific anion inhibitor, 4,4'-Diisothiocyanatostilbene-2,2'-disulfonic acid disodium salt hydrate (DIDS) was applied to five-week old Arabidopsis growing in hydroponics. The DIDS stock (100 mM) was completely dissolved in 0.1 M potassium bicarbonate and added into BNS solution to make a final concentration at 0.7 mM before the pH value was adjusted to 5.6 with 1 M KOH. For the salt plus DIDS treatments, 50 mM, 100 mM NaCl and 0.07 mM DIDS was combined with the BNS before adjusting the pH value. All the treatments lasted for 7 days within the same growth conditions described in Section2.1.3. In this experiment, DIDS was ordered from Sigma and Invitrogen and will be mentioned in the correspondent results.

5.2.3 Plant growth conditions

The plant growth conditions were used the methods that detailed described in Chapter 2 (Section 2.1).

5.2.4 Phenotyping transgenic plants

5.2.4.1 Chloride assay

To identify the chloride content of Arabidopsis, 20–30 mg of freeze-fried tissue was digested in 500 µL 1 % nitric acid at 80 °C overnight. The chloride analyzer (Model 926, Sherwood Scientific, Cambridge, UK) was used to examine the chloride concentration. Before the measurement, 1 L of acid buffer (Glacial Acetic, Nitric acids and gelatine) and 100 mg/L chloride standards were prepared. The measuring procedure strictly followed the manufacturers' instructions. The chloride concentration was calculated from dried tissue with the units expressed as mg/kg dry weight (DW).

5.2.4.2 Nitrate assay

The nitrate was extracted from freeze dried plant tissue using a water extraction method following the description in Section 2.9. A nitrate assay was modified (Chapter 2, Section 2.9.1) and used in this chapter to measure the shoot nitrate concentration.

5.2.4.3 Chlorophyll assay

The chlorophyll assay was followed the description by Warren (2008). In brief, Arabidopsis shoot materials were harvested and freeze dried. Dried tissue (10-20 mg) was placed in a 2 mL centrifuge tube to which 1 mL methanol (95 %) was added. The tube was shaken for 2 minutes before being centrifuged at maximum speed (16,000 × *g*) in a desktop microcentrifuge for 2 minutes. The supernatant was removed into a fresh tube. Another 1 mL of methanol was added to the first tube containing the pellet and the centrifugation process was repeated for re-extraction. In total, 2 mL of supernatant was isolated and combined in the second 2 mL centrifuge tube. The chlorophyll extract (200 µL) was transferred into a 96-well clear flat- bottom microplate (Greiner Bio-one). The sample absorbance was measured at two wavelengths, 655 nm and 665 nm using a FLUOstar Optima microplate reader (BMG LABTECH). The reading values were separately recorded and calculated using following equations:

Chlorophyll *a* (µg/mL) = $-8.0962\ A_{652,\ 1\ cm} + 16.5169\ A_{665,\ 1\ cm}$

Chlorophyll *b* (µg/mL) = $27.4405\ A_{652,\ 1\ cm} - 12.1688\ A_{665,\ 1\ cm}$

Chlorophyll content (µg/mg) = 2 × (Chlorophyll *a* + Chlorophyll *b*) / fresh weight (mg)

5.3 Results

5.3.1 Selection of positive transformants

Seed harvested from floral-dipped (T_0) plants were initially germinated on a MS media plate containing appropriate selection media (Table 5.1). The surviving plants were selected and transferred to a MS plate without antibiotics following the descriptions in Section 2.7.1. To further confirm the presence of the insert, PCR was performed on gDNA extracted from surviving putative transformants (Section2.3.1) with primers specific to the GOI and the appropriate construct. The number of resistant plants found to hygromycin B and BASTA and the results of the PCR confirmation are listed in Table 5.3. The selective ratio of resistant plants in the first round using antibiotic selection was low (0.5 %- 4.5 %), however, the number of these confirmed as transformants by PCR was high. Additionally, in order to

minimise potential effects caused by multiple insertions, southern-blotting was performed with a pMDC32 backbone- specific DIG- labelled probe on all T_1 transgenic plants confirmed through selection and PCR (Section 2.6). The plants with fewer than three insertions (preferably one) were selected to generate T_2 plants for further characterization (Figure 5.2). In total, 11 independent transgenic lines (not including cell- type specific over-expression constructs) were selected and carried through to the T_2 generation for phenotyping and genotyping. Plants genotyped in the T_2 generation contained both segregate null lines (devoid of an insert) and transformed lines that still contained the insert DNA (Section 2.7).

Table 5.1 The antibiotic and herbicide used for selecting T_1 transgenic plants and the resistant rate.

Promoter: GOI	Destination vector	Antibiotic/herbicide used for selection		Antibotic resistence rate positive seedlings/ total seeds	PCR confirmation resisten rate PCR confirmed/ selected
amiRNA:AtSLAH1	pMDC 32	Hygromycin B (25 mg/mL) in MS media plate	Applied	9/250	7/9
35S:AtSLAH1				6/200	5/6
35S:AtSLAH3				5/200	5/5
35S:AtNRT1.5				9/200	7/9
GAL4:AtSLAH1	pTOOL5	BASTA (20 mg/mL) soil	Sprayed	3/600	2/3
GAL4:AtSLAH3				5/500	3/5
GAL4:AtNRT1.5				4/500	4/4

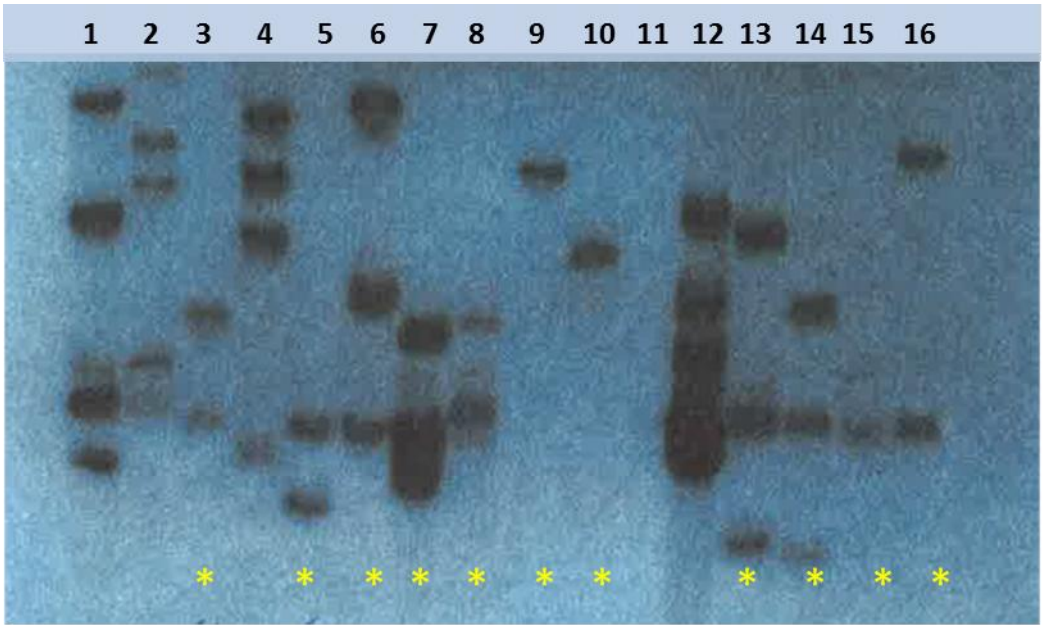

Figure 5.2 Southern-blotting was performed on T_1 mutant plant gDNA to examine the insert copy number. Lane 3, 5, 6 and 7: amiRNA:*AtSLAH1*_1-1,1-2,1-3 and 1-4; Lane 8- 9: *35S:AtSLAH1*_1 and 2; Lane 10 and 13: *35S:AtSLAH3*_1 and 2; Lane 14-16: *35S:AtNRT1.5*_1, 2 and 3. All the selected individuals were carried on to the next generation. A DIG- labelled DNA probe that was specific to the pMDC32 destination vector backbone was used to determine the copy number. Probe sequence: AGTACTAAAATCCAGATCC. Lanes not given a header number contain labelled DNA from T_1 plants from each genotype that were not selected due to their high insert number.

5.3.2 *AtSLAH1* amiRNA knock down lines (T_2) showed low chloride accumulation in the shoot under low Cl^- supply

To investigate the role of *AtSLAH1 in planta*, *AtSLAH1* expression knockdown was attempted using amiRNA constructs driven by a 2×*35S* promoter and transformed into plants using *Agrobacterium*. Four independent amiRNA-*AtSLAH1* mutant lines were used with confirmed insertion and limited copy numbers, these were named amiRNA-*AtSLAH1*_1 (2 inserts), amiRNA-*AtSLAH1*_2 (2 inserts), amiRNA-*AtSLAH1*_3 (3 inserts) and amiRNA-*AtSLAH1*_4 (2 inserts). Under low salt conditions (2 mM NaCl), qRT-PCR analysis showed that the transcript level of *AtSLAH1* in the root was considerably down-regulated in all amiRNA independent lines by more than 22- fold when compared to nulls ($P < 0.005$) (Figure 5.3 A). The shoot chloride contents were shown to be significantly lower in all amiRNA-*AtSLAH1* mutant lines compared to nulls ($P < 0.005$) (Figure 5.3 B). The shoot Cl^- accumulation was reduced by 30%, 43%, 44% and 47% in amiRNA-*AtSLAH1*_1, amiRNA-*AtSLAH1*_2, amiRNA-*AtSLAH1*_3 and amiRNA-*AtSLAH1*_4, respectively in comparison to nulls. To further identify whether the reduced Cl^- accumulation was correlated with decreased expression of *AtSLAH1*, the expression level was plotted against shoot Cl^- contents (Figure 5.3 C). There was a positive relationship between the level of *SLAH1* transcript and shoot Cl^- concentration, with an R^2 of 0.8879, indicating that the relationship between decreased Cl^- accumulation and transcript level in this experiment was highly significant.

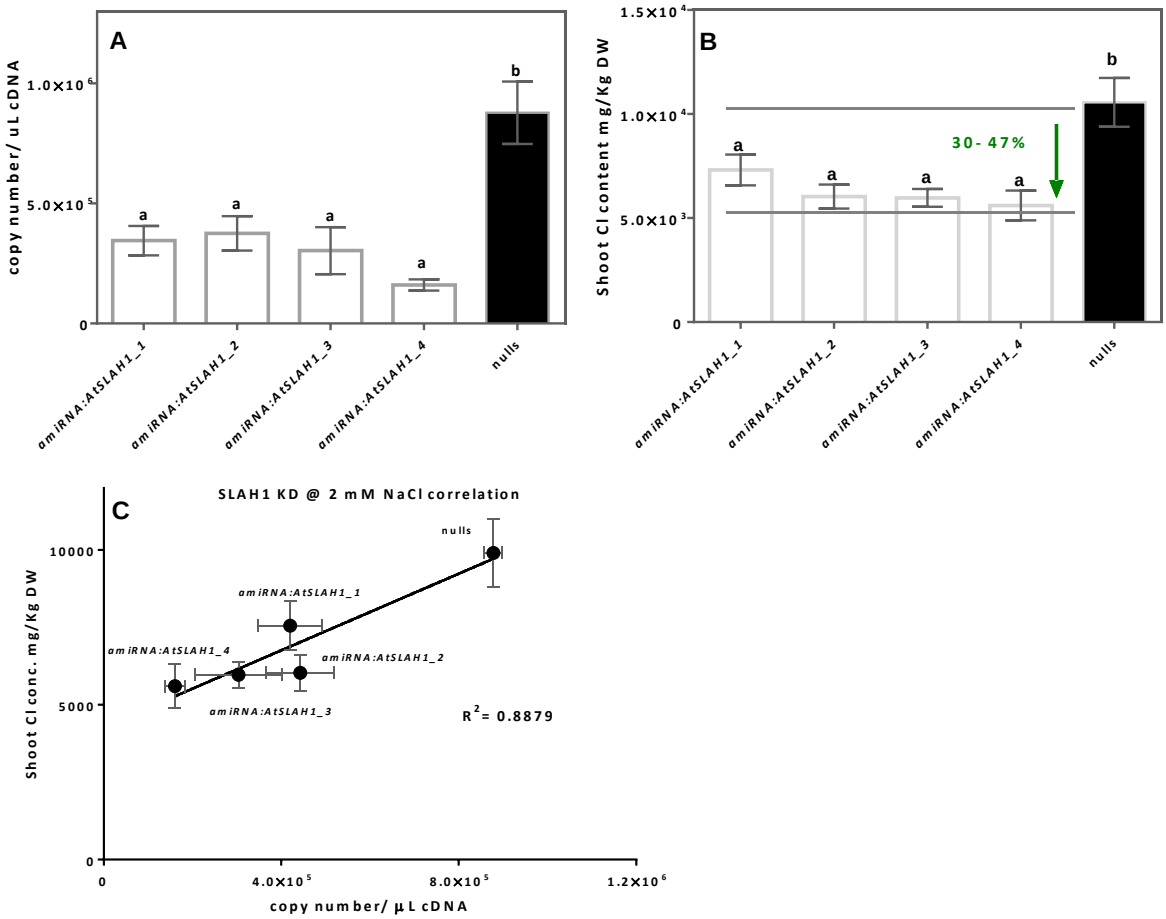

Figure 5.3 The transcript level of amiRNA-*AtSLAH1* lines (T_2), the shoot Cl^- concentration and the correlation between transcript level and shoot Cl^- concentrations under low Cl^- conditions. Hydroponically grown plants (6 weeks old) supplied with BNS that containing 2 mM NaCl (low Cl^- conditions) were harvested at the same time point. **(A)** *AtSLAH1* transcript levels were determined in the root of all amiRNA-*AtSLAH1* mutants (amiRNA-*AtSLAH1*_1, 2, 3 and 4) and nulls. **(B)** Shoot Cl^- accumulation of amiRNA-*AtSLAH1* mutants and nulls under low Cl^- conditions. **(C)** Correlation between transcript level of *AtSLAH1* and shoot Cl^- contents was established. Results were presented as mean ± SEM (n> 8). The transcript level and Cl^- accumulation of wildtype plants were also tested, however not included due to sample contamination. Statistical difference was determined by one-way ANOVA ($P \leq 0.005$). a and b represent data groups that are statistically different from each other.

5.3.3 *AtSLAH1* amiRNA containing lines (T_2) did not result in a shoot chloride accumulation change under high Cl^- supply compared to null lines

Hydroponically grown plants were supplied with BNS containing 2 mM NaCl for 5 weeks and treated with 75 mM NaCl for another 7 days before harvest. After treatment with 75 mM NaCl, in comparison to nulls, the transcript level of *AtSLAH1* in null lines and all amiRNA-*AtSLAH1* mutant lines were significantly repressed ($P \leq 0.005$) compared to control conditions

by about 1.5-2.2 fold, as indicated using the qRT-PCR analysis (Figure 5.4 A vs Figure 5.3 A). However, the alteration of *AtSLAH1* expression did not result in significant Cl^- accumulation differences between all amiRNA-*SLAH1* mutants and null (Figure 5.4 B). The NaCl treatment increased Cl^- levels in all lines to a similar degree (Figure 5.4B).

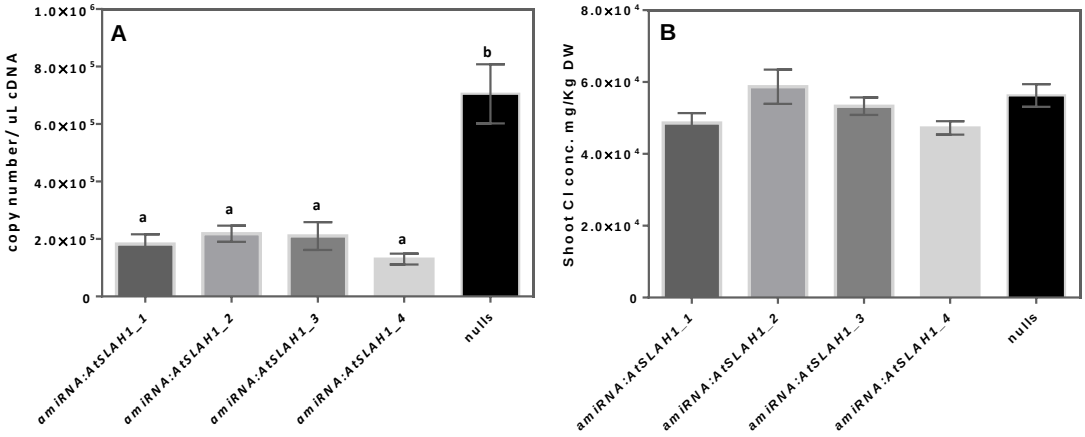

Figure 5.4 The transcript level of *AtSLAH1* amiRNA containing lines (T_2) and shoot Cl^- concentration under high salt stress. Hydroponically grown plants (5 weeks old) were treated with 75 mM NaCl (high salt stress) for 7 days before harvest. **(A)** *AtSLAH1* transcript levels were determined in the root of all amiRNA-*AtSLAH1* mutants (amiRNA-*AtSLAH1*_1, 2, 3 and 4) and nulls. **(B)** Shoot Cl^- accumulation of amiRNA-*AtSLAH1* mutants and nulls under high Cl^- conditions. The transcript level and Cl^- accumulation of wildtype plants were also tested, however not included due to sample contamination. Results were presented as mean ± SEM (n> 10). Statistical difference was determined by one-way ANOVA ($P \leq 0.005$). a and b represent data groups that are statistically different from each other.

5.3.4 *AtSLAH1* amiRNA containing lines (T_2) did not affect the shoot nitrate accumulation after exposure to low and high Cl^-

The effect of reduced abundance of *AtSLAH1* on shoot NO_3^- accumulation was tested in both high and low NaCl treatments (Figure 5.5 A and B). Under both conditions, no differences were found in shoot NO_3^- accumulation between all the amiRNA-*AtSLAH1* mutants and nulls. When 75 mM NaCl was applied to the plant, the overall NO_3^- concentration in all plant shoots was significantly decreased compared to plants in the low salt treatment. The shoot NO_3^-/Cl^- ratios under both low and high Cl^- were also indicated in Figure 5.6 A and B. Results indicated that all amiRNA-*AtSLAH1* mutants showed a higher NO_3^-/Cl^- ratio than nulls under low Cl^- conditions, suggesting that down-regulation of *AtSLAH1* was able to reduce the shoot Cl^- accumulation as it not affect NO_3^- concentration (Figure 5.6 A). However, when plants treated with 75 mM NaCl, as a large amount of Cl^- was accumulated in the shoot, the NO_3^-/Cl^- ratio was dramatically decreased in all amiRNA-*AtSLAH1* mutants and nulls (Figure 5.6 B).

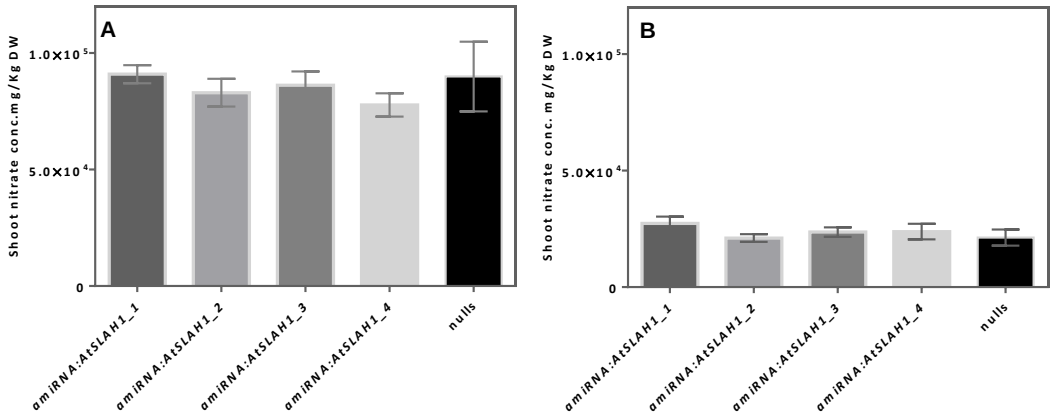

Figure 5.5 The shoot NO_3^- concentration of amiRNA-*AtSLAH1* mutant lines (T_2) under low and high Cl^- supply. Hydroponically grown plants were treated with BNS (2 mM NaCl) or 75 mM NaCl for 7 days before harvest. **(A)** Shoot NO_3^- contents determined in all amiRNA-*AtSLAH1* mutants and nulls with 2 mM Cl^-. **(B)** Shoot NO_3^- contents determined in all amiRNA-*AtSLAH1* mutants and nulls with 75 mM Cl^-. Results were presented as mean ± SEM (n> 10).

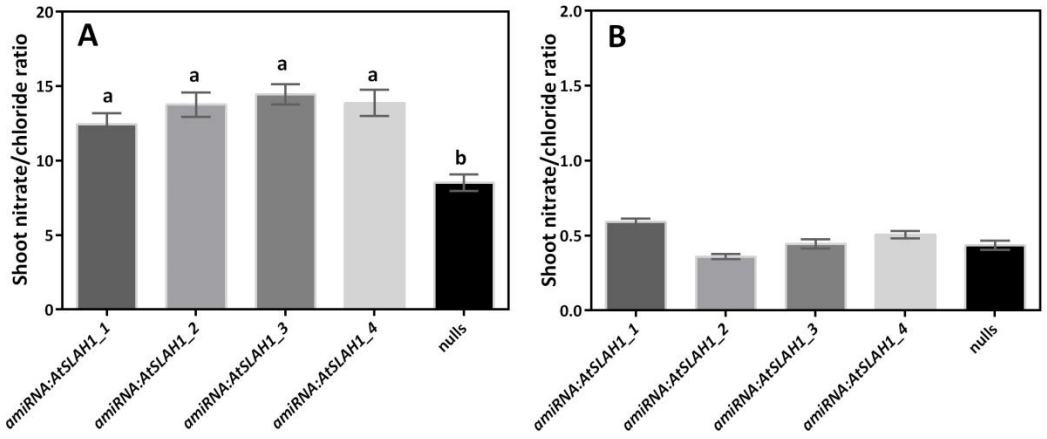

Figure 5.6 The shoot NO_3^-/Cl^- ratio was determined in amiRNA-*AtSLAH1* mutant lines and null under low (A) and high Cl^- supply (B). Results were presented as mean ± SEM (n> 10). Statistical difference was determined by One-way ANOVA ($P \leq 0.005$). a and b represent data groups that are not statistically different from each other.

5.3.5 The *35S:AtSLAH1* transgenic lines (T_2) accumulated high Cl^- in shoot under high salt (75 mM) when compared to nulls

To further investigate whether AtSLAH1 had a role in the accumulation of Cl^- and NO_3^- in the shoot, plants were generated containing *2x35S:AtSLAH1* in an attempt to over-express *AtSLAH1* and these were brought to the T_2 generation. Two independent mutants, termed as

*35S:AtSLAH1*_1 and *35S:AtSLAH1*_2 were grown in hydroponics for 5 weeks before being supplied with 2 mM or 75 mM NaCl for a further 7 days.

Results suggested that both *35S:AtSLAH1*_1 and *35S:AtSLAH1*_2 plants accumulated a significantly higher Cl^- concentration than nulls when 75 mM NaCl was applied ($p< 0.05$) (Figure 5.7 A). No significant differences were found between the two independent mutant lines in Cl^- content, both lines had significantly more Cl^- than null lines, and *35S:AtSLAH1*_1, was significantly different from wildtype, whereas *35S:AtSLAH1*_2 was not. Under low Cl^- conditions (2 mM), less Cl^- was accumulated in the shoot and no significant difference was found between all mutant lines, nulls and wildtypes (Figure 5.7 B).

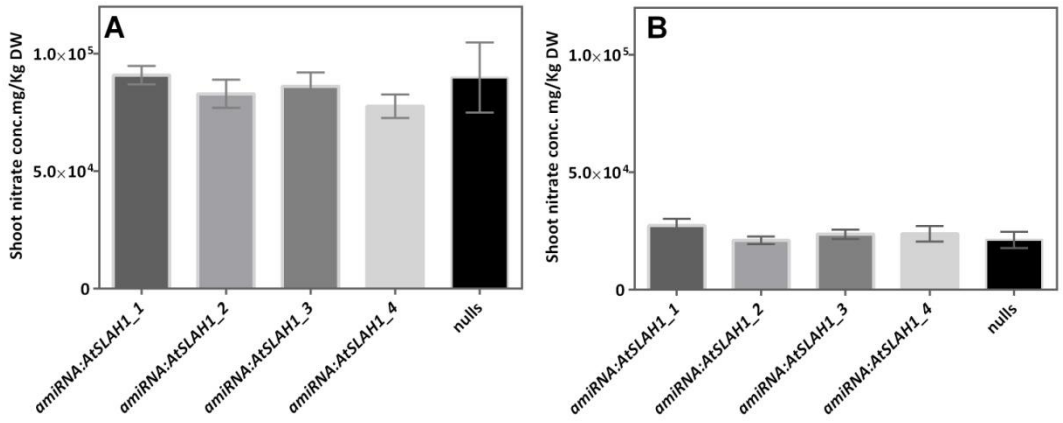

Figure 5.7 The shoot Cl^- concentration of *35S:AtSLAH1* transgenic plants (T_2) under high and low Cl^- conditions. Hydroponically grown plants (5 weeks old) were treated with 75 mM or BNS containing 2 mM (low) NaCl for 7 days before harvest. **(A)** Cl^- contents was determined in the shoot of the *35S:AtSLAH1* mutant lines and nulls treated with 75 mM NaCl. **(B)** Shoot Cl^- content was determined in the shoot of the *35S:AtSLAH1* mutant lines and nulls grown under low Cl^- conditions. Results were presented as mean ± SEM (n> 10). Statistical significance was determined by one-way ANOVA ($P \leq 0.005$). a, b and c represent data groups that are not statistically different from each other.

5.3.6 The *35S:AtSLAH1* transgenic lines (T_2) accumulated low NO_3^- in shoot under low chloride (2 mM) conditions

The shoot NO_3^- contents were also examined in *35S:AtSLAH1* transgenic lines under both low and high Cl^- conditions. High salt stress affected the accumulation of NO_3^- in the shoot with a low and similar NO_3^- concentration identified in all mutants, nulls and wildtype (Figure 5.8 A). Under the low salt conditions, higher NO_3^- contents was observed in all *35S:AtSLAH1* transgenic lines, nulls and wildtype compared to high salt conditions (Figure 5.8 B). Interestingly, both *35S:AtSLAH1*_1 and *35S:AtSLAH1*_2 showed significantly lower NO_3^-

concentration compared to nulls by 31% and 26% respectively. However, such significance was not discovered between the mutants and wildtype. The shoot NO_3^-/Cl^- ratio was also calculated in all plants that grown under both low and high Cl^- environment. The results indicated when less Cl^- was available in the growth solution, more NO_3^- instead of Cl^- was accumulated in the shoot. Only *35S:AtSLAH1*_1 plants showed significantly lower NO_3^-/Cl^- ratio compared to nulls and controls under low Cl^- conditions, but not in *35S:AtSLAH1*_2 (Figure 5.9 A). The NO_3^-/Cl^- ratio was increased when plants were challenged with a high dose of Cl^- (75 mM NaCl) (Figure 5.9 B). Both *35S:AtSLAH1* mutant lines accumulated larger concentrations of Cl^- over NO_3^- when compared to nulls but not wildtype.

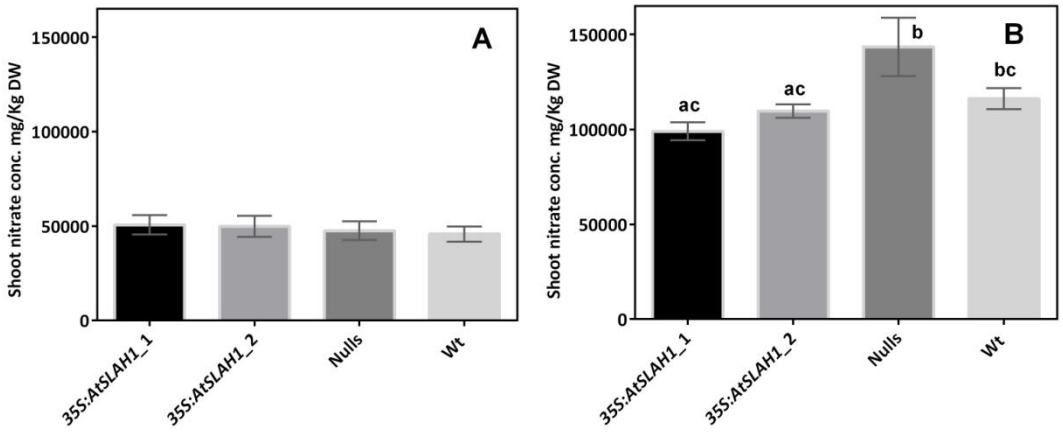

Figure 5.8 The shoot NO_3^- concentration of *35S:AtSLAH1* transgenic plants (T_2) under high and low Cl^- conditions. Hydroponically grown plants (5 weeks old) were treated with 75 mM or BNS containing 2 mM NaCl for 7 days before harvest. **(A)** Shoot NO_3^- level was determined in the shoot of the *35S:AtSLAH1* mutant lines, nulls and wildtype treated with 75 mM NaCl. **(B)** Shoot NO_3^- level was determined in the shoot of the *35S:AtSLAH1* mutant lines, nulls and wildtype grown under low Cl^- conditions. Results were presented as mean ± SEM (n> 10). Statistical significance was determined by one-way ANOVA ($P \leq 0.05$). a, b and c represent data groups that are not statistically different from each other.

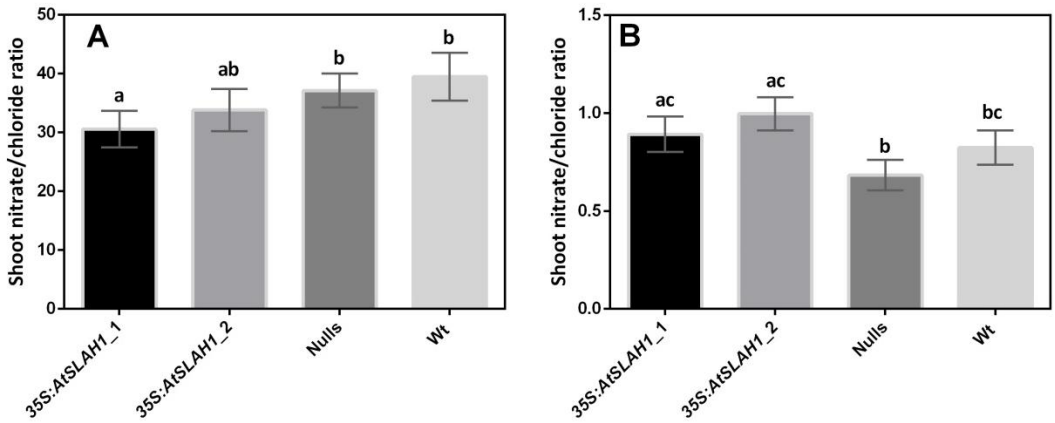

Figure 5.9 The shoot NO_3^-/Cl^- ratio was determined in *35S:AtSLAH1* mutant lines and null under low (A) and high Cl^- supply (B). Results were presented as mean ± SEM (n> 10). Statistical difference was determined by one-way ANOVA ($P < 0.05$). a, b and c represent data groups that are not statistically different from each other.

5.3.7 The 35S:*AtSLAH3* transgenic lines (T_2) accumulated low Cl^- in the shoot under both high and low salt conditions

To investigate whether AtSLAH3 also had a role in the accumulation of Cl^- and NO_3^- in the shoot, plants were generated containing *2x35S:AtSLAH3* in an attempt to over-express *AtSLAH3* and these were brought to the T_2 generation. Two independent mutants, termed as *35S:AtSLAH3*_1 and *35S:AtSLAH3*_2, were grown in hydroponics for 5 weeks before being supplied with 2 mM or 75 mM NaCl for a further 7 days.

After treatment with 75 mM NaCl, significantly less Cl^- was accumulated in both mutants compared to nulls, also, *35S:AtSLAH3*_2 mutant also exhibited Cl^- contents reduction compared to wildtype, but not *35S:AtSLAH3*_1 (Figure 5.10 A). When lower salt was applied, the overall shoot Cl^- content was significantly reduced compared to plants treated with high concentration of salt. Interestingly, low shoot Cl^- accumulation was also observed in mutant plants compared to the nulls but not to wildtype (Figure 5.10 B).

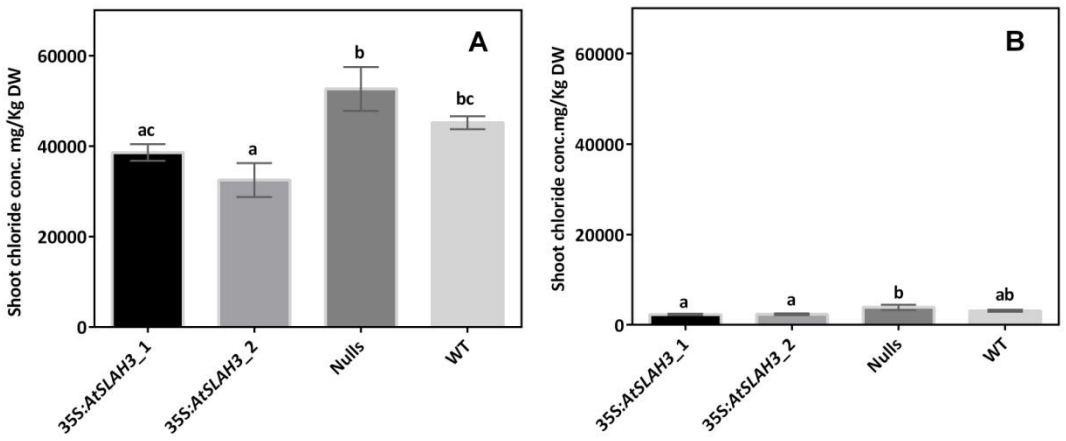

Figure 5.10 The shoot Cl^- concentration of *35S:AtSLAH3* transgenic plants (T_2) under high and low Cl^- conditions. Hydroponically grown plants (5 weeks old) were treated with 75 mM or BNS containing 2 mM NaCl for 7 days before harvest. **(A)** Cl^- contents was determined in the shoot of the *35S:AtSLAH3* mutant lines and nulls treated with 75 mM NaCl. **(B)** Shoot Cl^- content was determined in the shoot of the *35S:AtSLAH3* mutant lines and nulls grown under low Cl^- conditions. Results were presented as mean ± SEM (n> 9). Statistical significance was determined by one-way ANOVA ($P \leq 0.05$). a, b and c represent data groups that are not statistically different from each other.

5.3.8 The 35S:*AtSLAH3* transgenic lines (T_2) accumulated high NO_3^- in shoot under high salt (75 mM) conditions

Under high Cl^- stress, the shoot NO_3^- accumulation in *35S:AtSLAH3*_1 was significantly increased compared to the wildtypes but not nulls (Figure 5.11 A). Under low salt conditions, there was no significant difference for NO_3^- between both mutants compared to nulls and wildtype plants (Figure 5.11 B). The shoot NO_3^- / Cl^- ratio was also calculated in all plants that were grown under both low and high Cl^- environments. When high concentrations of Cl^- were applied to the plant, the NO_3^- / Cl^- ratio was significantly higher in both *35S:AtSLAH3* mutants compared to nulls and wildtype (Figure 5.12 A), which suggesting that overall more NO_3^- was transported to the shoot and less Cl^- accumulated in the shoot. Under low Cl^- conditions, a significantly higher NO_3^- / Cl^- ratio was discovered in both mutants when compared to nulls but not wildtypes (Figure 5.12 B), indicating that more NO_3^- was accumulated within the shoot when less Cl^- was available.

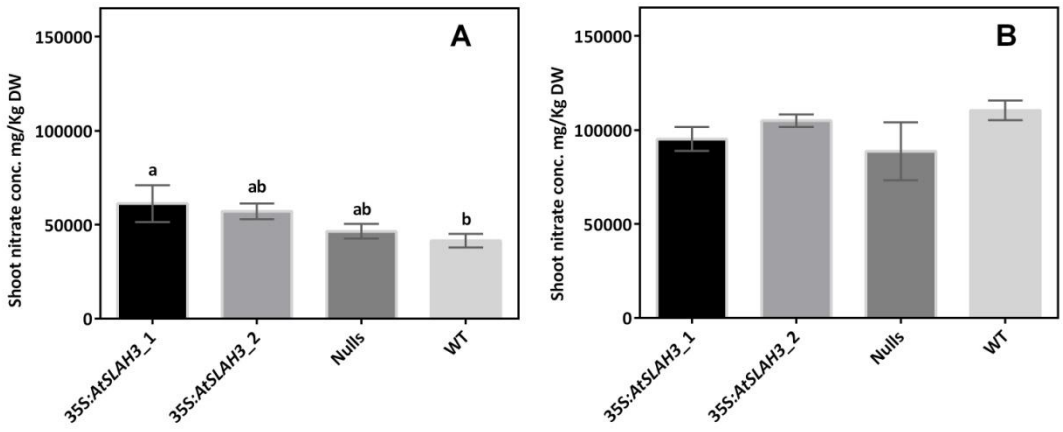

Figure 5.11 The shoot NO_3^- concentration of *35S:AtSLAH3* transgenic plants (T_2) under high and low Cl^- conditions. Hydroponically grown plants (5 weeks old) were treated with 75 mM or BNS containing 2 mM NaCl for 7 days before harvest. **(A)** Shoot NO_3^- level was determined in the shoot of the *35S:AtSLAH3* mutant lines, nulls and wildtype treated with 75 mM NaCl. **(B)** Shoot NO_3^- level was determined in the shoot of the *35S:AtSLAH3* mutant lines, nulls and wildtype grown under low Cl^- conditions. Results were presented as mean ± SEM (n > 9). Statistical significance was determined by One-way ANOVA ($P \leq 0.05$). a and b represent data groups that are not statistically different from each other.

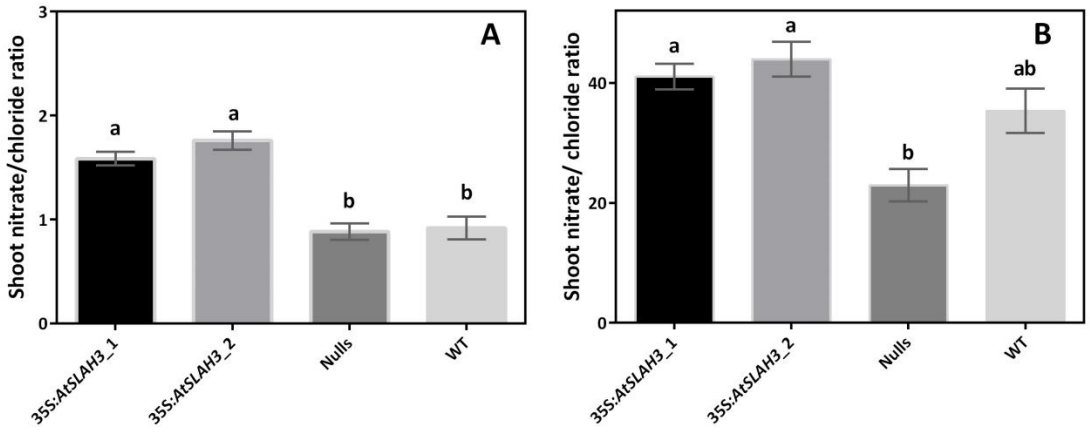

Figure 5.12 The shoot NO_3^-/ Cl^- ratio was determined in *35S:AtSLAH3* mutant lines and null under high Cl^- supply (A) and low Cl^- supply (B). Results were presented as mean ± SEM (n > 9). Statistical difference was determined by one-way ANOVA ($P \leq 0.05$). a, b, c, d and d represent data groups that are not statistically different from each other.

5.3.9 The 35S:*AtNRT1.5* transgenic lines (T_2) accumulated low Cl^- in shoot under high Cl^- conditions

To further investigate whether AtNRT1.5 had a role in the accumulation of Cl^- and NO_3^- in the shoot, plants were generated containing *2x35S:AtNRT1.5* in an attempt to over-express *AtNRT1.5* and these were brought to the T_2 generation. Three independent mutants, termed as *35S:AtNRT1.5*_1, *35S:AtNRT1.5*_2 and *35S:AtNRT1.5*_3 was grown in hydroponics for 5 weeks before being supplied with 2 mM or 75 mM NaCl for a further 7 days.
Under high salt conditions, significant lower concentration of Cl^- was accumulated in *35S:AtNRT1.5*_1 and *35S:AtNRT1.5*_2 compared to nulls but not wildtype (Figure 5.13 A). Only *35S:AtNRT1.5*_1 showed significant higher shoot Cl^- contents than nulls and wildtypes under low Cl^- conditions and no differences were discovered in the other two mutant lines (Figure 5.13 B).

The tissue amount taken for measurement in this experiment was not enough to perfectly fit in the measuring range of the chloridometer. Therefore, the overall shoot Cl^- concentration measured in this experiment was much lower (3- 4 folds) than other experiments. However, the relatively differences that were observed between the samples are valuable to help us understand the shoot anion accumulation in the mutant plants under various Cl^- conditions.

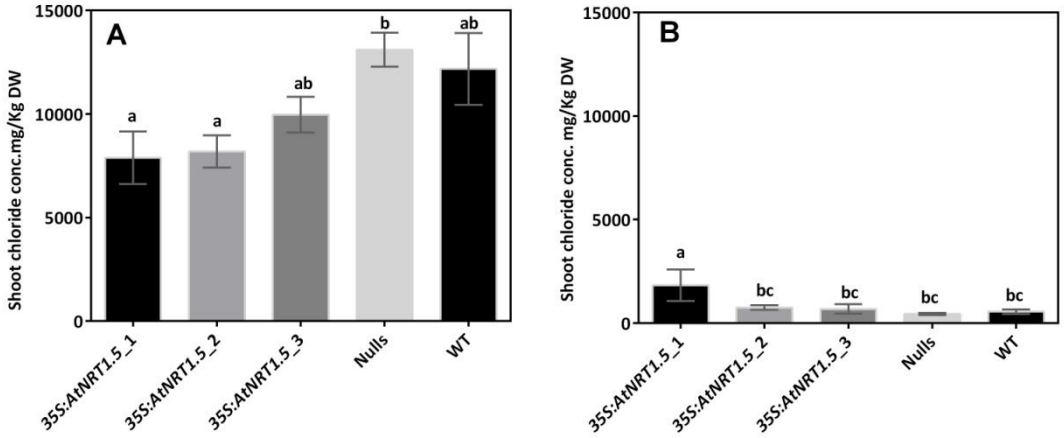

Figure 5.13 The shoot Cl^- concentration of *35S:AtNRT1.5* transgenic plants (T_2) under high and low Cl^- conditions. Hydroponically grown plants (5 weeks old) were treated with 75 mM or BNS containing 2 mM NaCl for 7 days before harvest. **(A)** Cl^- contents was determined in the shoot of the *35S:AtNRT1.5* mutant lines and nulls treated with 75 mM NaCl. **(B)** Shoot Cl^- content was determined in the shoot of the *35S:NRT1.5* mutant lines and nulls grown under low Cl^- conditions. Results were presented as mean ± SEM (n> 7). Statistical significance was determined by one-way ANOVA ($P < 0.05$). a, b and c represent data groups that are not statistically different from each other.

5.3.10 35S:*AtNRT1.5* transgenic lines (T_2) did not have significantly altered shoot NO_3^- accumulation under both high and low Cl^- conditions

The NO_3^- contents were also examined in in all the *35S:AtNRT1.5* mutants and nulls under both high and low Cl^- treatments. After treated with 75 mM NaCl for 7 days, the average NO_3^- levels in all mutants were not significantly different from the nulls (Figure 5.14 A). Under low Cl^- conditions, although the mean NO_3^- levels were higher than plants under high Cl^- conditions, no significant difference was found between mutant plants and nulls/ wildtypes (Figure 5.14 B). The shoot NO_3^-/ Cl^- ratio was determined in *35S:AtNRT1.5* mutant lines and null under high and low Cl^- conditions (Figure 5.15 A and B). Although no significant NO_3^- content difference was discovered under high Cl^- supply, all the mutants showed an higher NO_3^-/ Cl^- ratio than nulls but not wildtypes except *35S:AtNRT1.5*_2 (Figure 5.15 A), which suggested that more NO_3^- was accumulated within the shoot when large proportion of Cl^- was available in the environment. Under control conditions (2 mM Cl^-), a lot more NO_3^- and less Cl^- was found within the shoot, therefore a much higher NO_3^-/ Cl^- ratio was exhibited. No significant difference was found between mutants and nulls except the *35S:AtNRT1.5*_1 (Figure 5.15 B).

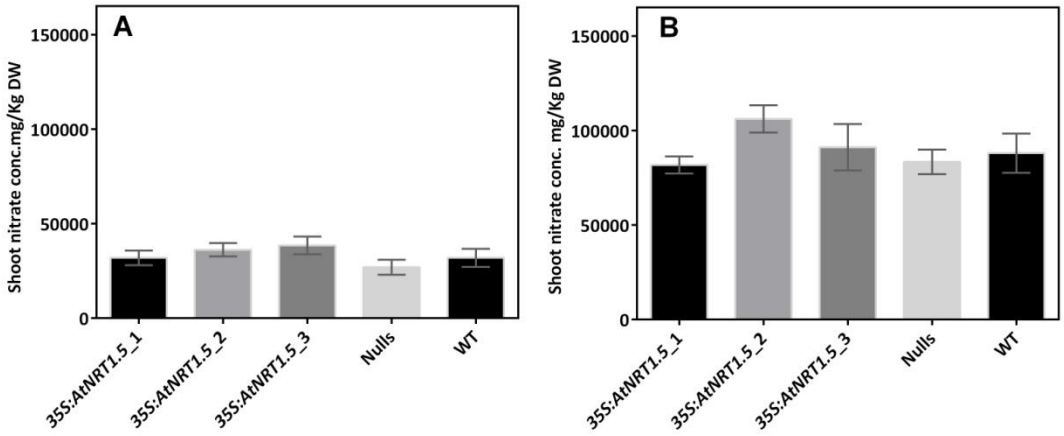

Figure 5.14 The shoot NO_3^- concentration of *35S:AtNRT1.5* transgenic plants (T_2) under high and low Cl^- conditions. Hydroponically grown plants (5 weeks old) were treated with 75 mM or BNS containing 2 mM NaCl for 7 days before harvest. **(A)** Shoot NO_3^- level was determined in the shoot of the *35S:AtNRT1.5* mutant lines, nulls and wildtype treated with 75 mM NaCl. **(B)** Shoot NO_3^- level was determined in the shoot of the *35S:AtNRT1.5* mutant lines, nulls and wildtype grown under low Cl^- conditions. Results were presented as mean ± SEM (n > 7). No statistical significance was determined using a one-way ANOVA ($P \leq 0.05$).

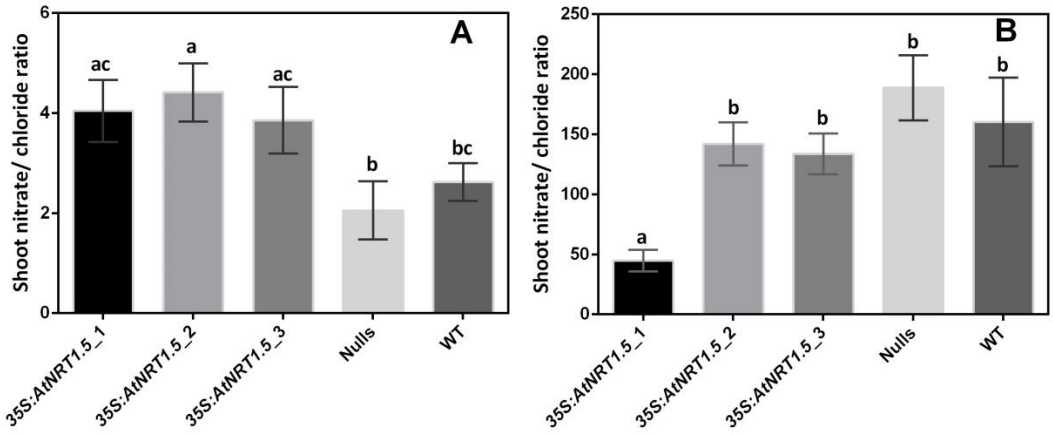

Figure 5.15 The shoot NO_3^-/ Cl^- ratio was determined in *35S:AtNRT1.5* mutant lines and null under high Cl^- supply (A) and low Cl^- supply (B). Results were presented as mean ± SEM (n > 7). Statistical difference was determined by one-way ANOVA ($P \leq 0.05$). a, b and c represent data groups that were statistically different from each other.

5.3.11 DIDS treatment affected the anion accumulation in the Arabidopsis shoot

To study the effect of DIDS on anion accumulation in Arabidopsis especially under salt stress, DIDS was applied to the 5-week-old Arabidopsis for 7 days in hydroponics with or without additional NaCl. After the treatment, the shoot Cl^- and NO_3^- concentrations were tested and shoot biomass and chlorophyll content were also determined to further discover the

physiological effects of DIDS to Arabidopsis

In the first experiment, when NaCl was applied alone, the shoot Cl^- level was significantly increased with increasing NaCl concentration (Figure 5.16 A). When DIDS (from Sigma) was applied along with 2 mM NaCl, no evident Cl^- content difference was found compared to the control. Interestingly, significant less Cl^- was accumulated in shoot under high salt conditions (50 mM) when DIDS was also presented in the growth solution compared to the plants that treated with same strength of salt alone. The shoot NO_3^- concentration was also determined in all plants under various treatments. Increasing salt stress significantly inhibited the NO_3^- accumulation in the shoot (Figure 5.16 B). For instance, only one third of the NO_3^- was detected in plants that were treated with 100 mM NaCl compared to the plants that grew under normal conditions (Figure 5.16 B). The NO_3^- concentration was not altered under low salt conditions when DIDS was applied. When additional DIDS was present in the growth solution containing 50 mM NaCl, the NO_3^- level was less affected by the salt stress and showed a significant higher level than plants that were treated with 50 mM NaCl alone. The NO_3^-/ Cl^- ratio was also calculated and the results further confirmed that high concentration of Cl^- significantly inhibited the NO_3^- uptake from root to shoot. Also, additional DIDS significantly increased the NO_3^-/ Cl^- ratio under low Cl^- supply. It appears that additional DIDS significantly (t-test) increased the NO_3^-/ Cl^- ratio under 50 mM Cl^- conditions (Figure 5.16 C).

To confirm the results, the same experiment was repeated, the only difference being that the DIDS was ordered from Life Technologies as Sigma had no stock left. The shoot anion concentration was also examined after 7 days treatment. Similar to the first experiment, the shoot Cl^- concentration was increased upon salt stress (Figure 5.17 A). When DIDS was added into the growth solution containing 2 mM NaCl, no Cl^- content difference was found with those plants without DIDS treatment. When NaCl concentration was increased to 50 mM, plants with the addition of DIDS had a decreased Cl^- content compared to plants treated with 50 mM NaCl alone. A similar level of reduction on shoot Cl^- content was also discovered in plants that treated with 75 mM NaCl plus DIDS compared to the plants that under salt stress alone (Figure 5.17 A). The NO_3^- concentration was also examined in all plants of this experimental run. Consistent with the previous experiment (Figure 5.16 B), when increased NaCl was applied alone, the shoot NO_3^- concentration was decreased. When DIDS was added into growth solution containing 2 mM NaCl, 50 mM and 75 mM NaCl the NO_3^- concentration was the same compared to the plants that were treated with same concentration of salt

without DIDS (Figure 5.17 B). The NO_3^-/ Cl^- ratio also suggested that high salt stress significantly inhibited the NO_3^- transfer from root to shoot, whereas additional DIDS did not alter the ratio under any treatments (Figure 5.17 C). The shoot biomass (fresh weight) was measured and no significant difference was discovered, which was suggesting that salt stress negatively affected the plant growth despite adding same concentration of DIDS (Figure 5.17 D).

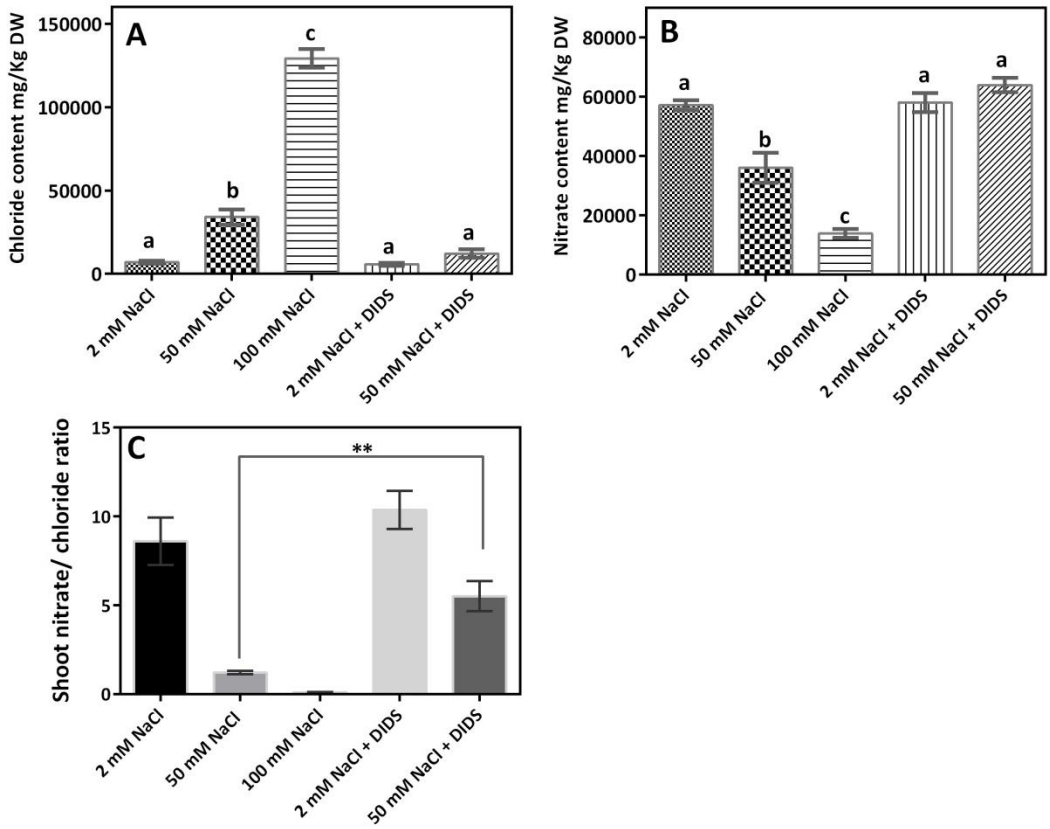

Figure 5.16 Effect of DIDS on shoot accumulation of Cl^- (A), NO_3^- (B) and NO_3^-/ Cl^- ratio (C) in the Arabidopsis under salt stress. Hydroponically Arabidopsis (Col-0) (5 weeks old) were treated with 2 mM, 50 mM and 100 mM NaCl alone or with additional 0.7 mM DIDS plus various concentration of salt for 7 days before harvest. Results were presented as mean ± SEM (n=3). Statistical difference was determined by one-way ANOVA ($P \leq 0.05$). a, b and c represent data groups that were statistically different from each other. Unpaired t test was performed in figure **(C)**. The DIDS used in this experiment was ordered from Sigma (catalog: D3514).

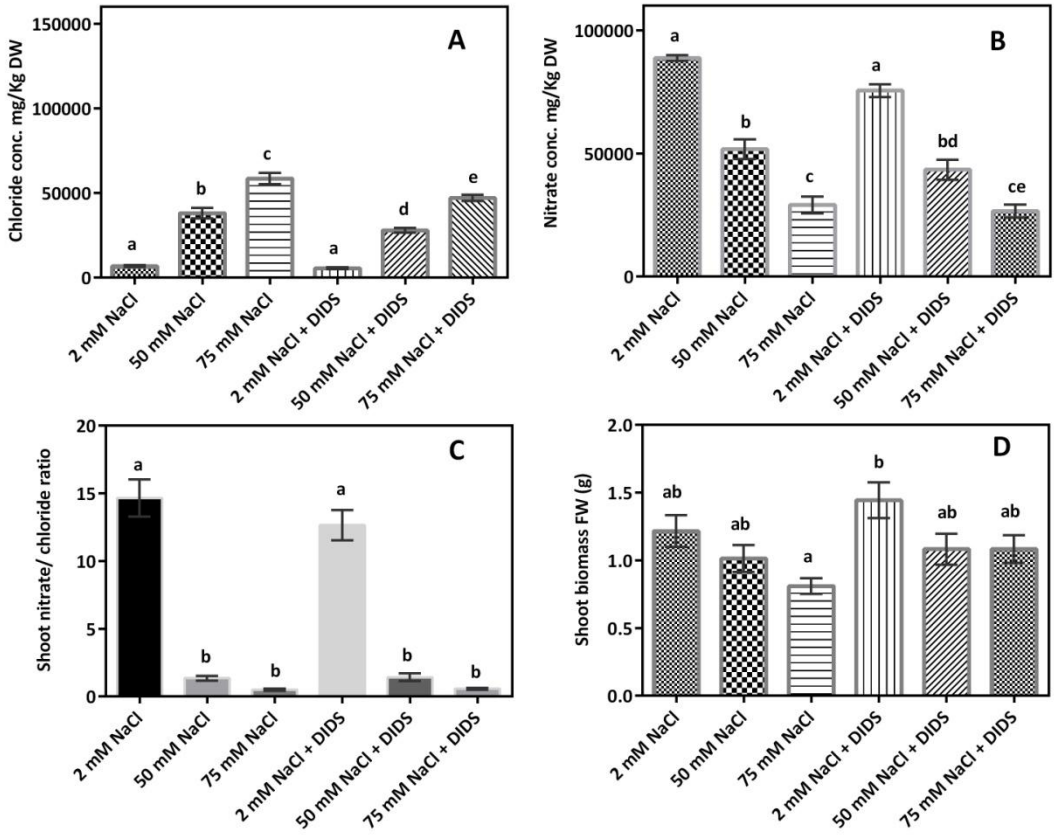

Figure 5.17 Effect of DIDS on shoot accumulation of Cl^- (A), NO_3^- (B), NO_3^-/ Cl^- ratio (C) and shoot biomass (D) in the Arabidopsis under salt stress. Hydroponically Arabidopsis (Col-0) (5 weeks old) were treated with 2 mM, 50 mM and 100 mM NaCl alone or with additional 0.7 mM DIDS plus various concentration of salt for 7 days before harvest. Results were presented as mean ± SEM (n > 6). Statistical difference was determined by one-way ANOVA ($P \leq 0.05$). a, b, c and d represent data groups that were statistically different from each other. The DIDS used in this experiment was ordered form Life technologies (catalog: D-337).

The results gained from first experiment were not fully replicated in the second experiment; therefore, to further test the effects of DIDS on anion accumulation in Arabidopsis shoot, a new batch of DIDS ordered from sigma was used to repeat the experiment again.

In this experiment, DIDS was able to reduce the shoot Cl^- contents under high salt treatment but not with 2 mM Cl^- (Figure 5.18 A) – this was consistent across all 3 experiments. Also, similar to that identified in the first experiment, the NO_3^- level was significantly increased under high salt stress when DIDS was used (Figure 5.18 B). The shoot NO_3^-/ Cl^- ratio was also significantly increased when DIDS was applied under high salt conditions (Figure 5.18 C). I also examined the biomass in this experiment and it appears that the application of DIDS was able to significantly (t test) increase the shoot biomass under both salt conditions (Figure

5.18 D). After 7 days treatments, it appeared by eye that there was a slight difference in the Arabidopsis shoot colour of plants treated with or without DIDS (data not shown). Therefore, the chlorophyll contents were examined but, no chlorophyll concentration differences were identified in all plants that under various treatments (Figure 5.18 E).

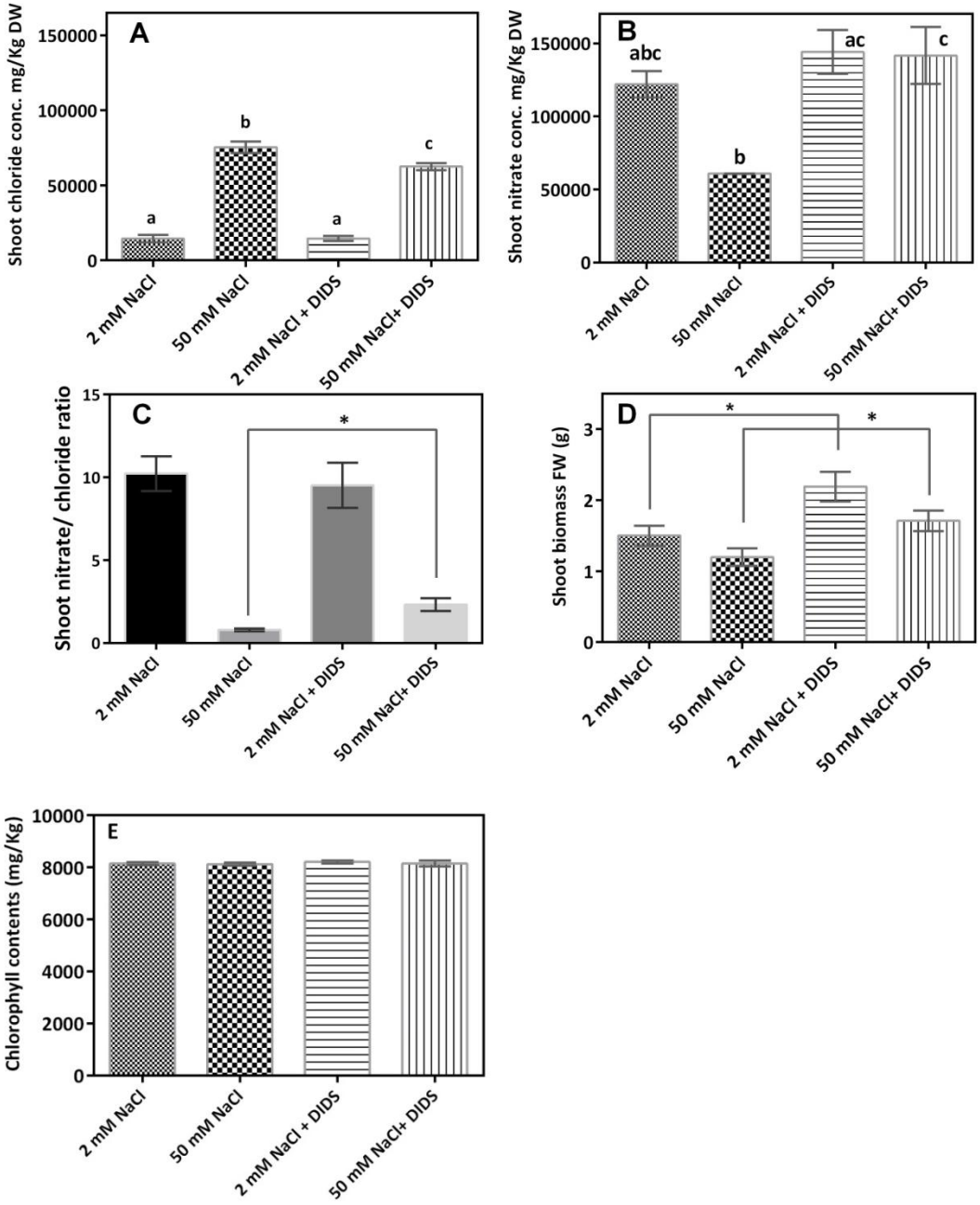

Figure 5.18 Effect of DIDS on shoot accumulation of Cl^- (A), NO_3^- (B), NO_3^-/ Cl^- ratio (C), shoot biomass (D) and chlorophyll contents (E) in the Arabidopsis under different salt treatments. Hydroponically Arabidopsis (Col-0) (5 weeks old) were treated with 2 mM and 50 mM NaCl alone or with an additional 0.7 mM DIDS plus various concentration of salt for 7 days before harvest. Results were presented as mean ± SEM (n=6). S Statistical difference was determined by one-way ANOVA ($P \leq 0.05$). a, b and c represent data groups that were statistically different from each other. Unpaired t test was used in Figure (C) and (D). The DIDS used in this experiment was ordered form Sigma (catalog: D3514).

5.4 Discussion

5.4.1 AtSLAH1 regulates Arabidopsis shoot anion accumulation

To investigate whether AtSLAH1 was involved in root-to-shoot Cl^- transport, different Arabidopsis mutants with an increase or decrease in expression were generated. The *AtSLAH1* knockout lines (SALK lines) were ordered from ABRC. Homozygous lines were successfully identified; however, RT-PCR performed using *AtSLAH1*-specific primers suggested the expression of *AtSLAH1* was not abolished in those SALK lines (Appendix 4). Therefore, four amiRNA-*AtSLAH1* mutant lines were generated to further study the role of AtSLAH1 in plants. Under low Cl^- supply (2 mM NaCl), the reduced expression of *AtSLAH1* resulted in lower Cl^- accumulation in the shoot (Figure 5.3 A and B), which suggests that *AtSLAH1* might play important role in regulating Cl^- transport from root-to-shoot by affecting net loading of xylem vessels in the root. Despite the strong positive correlation between expression levels and shoot Cl^- the large difference in Cl^- contents between the amiRNA-*AtSLAH1* mutants and null lines (and a lack of intermediate points) suggests some caution should be exercised when interpreting this data (Figure 5.3 C). The shoot Cl^- contents were also examined in all amiRNAi-*SLAH1* mutants exposed to high salt stress and no Cl^- concentration differences were found between mutants and nulls (Figure 5.4 B). *AtSLAH1* expression is naturally decreased under high concentrations of NaCl (Figure 3.4 A), therefore, it is reasonable to suggest that the unchanged Cl^- contents in these plants was probably due to the endogenous down-regulation of *AtSLAH1* that was caused by high salinity stress. In the future, it would be worth examining *SLAH1* function in Cl^- sensitive plant species. For example, *SLAH1* (*CcSLAH1*) was identified in a *Citrus* rootstocks *Carrizo citrange* (sensitive to Cl^-) and the transcript level was down- regulated by high strength of NaCl (Brumós *et al*., 2010). Therefore, it would be interesting to test the shoot anion accumulation when *CcSLAH1* expression level was decreased to further examine whether other *SLAH1* genes are involved in root-to -shoot Cl^- transport.

The nitrate level was also examined in all amiRNA-*AtSLAH1* mutants shoot under different Cl^- supply. When the *AtSLAH1* knockdowns were exposed to low and high Cl^-, the NO_3^- level was not significantly altered when compared to nulls (Figure 5.5). The NO_3^-/Cl^- ratio (Figure 5.6 A) suggested that the reduction of *AtSLAH1* expression led to an decreased shoot NO_3^-/Cl^- ratio, resulting from less Cl^- and more NO_3^- accumulation. In salt tolerance studies, the shoot K^+/Na^+ ratio is widely used to evaluate plant's salt tolerance (Tester and Davenport 2003).

Higher value of K^+/Na^+ ratio normally indicates a better salinity tolerance. Therefore, it is reasonable to suggest that higher the NO_3^-/Cl^- ratio, in susceptible plants might be beneficial for improving salt tolerance due to the down- regulation of *AtSLAH1*.

The 35S:AtSLAH1 mutant lines exhibited significantly increased shoot Cl^- concentration under high salt stress (75 mM NaCl) when compared to nulls (Figure 5.7 A), which suggested that *AtSLAH1* might be involved in xylem Cl^- loading. However, under low salt conditions, no significant Cl^- change was observed (Figure 5.7 B); this may have been below a threshold external Cl^- concentration for the overexpression to have an effect. Due to time constraints the expression level of *AtSLAH1* in all the over-expression lines was not checked, despite the material being collected. This will be checked before submitting this work for publication. This will allow the results to be refined by eliminating the lines that do not have altered expression. Although the NO_3^- level was slightly decreased in one of the over-expression lines under low salt conditions, it is difficult to suggest that AtSLAH1 is involved in NO_3^- transport.

To further study the function of AtSLAH1 and avoid potential problems caused by non-targeted over expression in all cell types, stelar type specific over expression lines were generated following the method outlined by Møller *et al*. 2009. However, again, due to the time limitation, the genotyping and phenotyping was not carried out during this project.

5.4.2 AtSLAH3 was able to regulate Arabidopsis shoot anion accumulation

It has been reported that AtSLAH3 was involved in NO_3^- movement in *X. laevis* oocytes (Geiger *et al*., 2011). Therefore, the shoot NO_3^- concentration might have been expected to change when *SLAH3* transcript level was increased. Interestingly, no significant NO_3^- concentration differences were found in any *35S:AtSLAH3* lines under both low and high salt conditions compared to nulls and wildtypes (Figure 5.11). The overall shoot NO_3^- concentration was significantly decreased in all plants (mutants, nulls and wildtypes) under high Cl^- conditions compared to plants treated under low Cl^- conditions (Figure 5.11). Such a reduction was probably due to the high Cl^- that presented within the solution therefore inhibiting root uptake of NO_3^- and transfer from root to shoot.

Although SLAH3 was suggested not to be directly involved in Cl^- transport (Geiger *et al*., 2011), shoot Cl^- content reductions were discovered in all *35S:AtSLAH3* lines compared to

nulls when plants treated with 75 mM or 2 mM NaCl for 7 days (Figure 5.10). Also, under high Cl^- conditions, the Cl^-/ NO_3^- ratio was significantly decreased compared to nulls and wildtypes (Figure 5.12 A), indicating relatively less Cl^- and more NO_3^- was accumulated within the shoot, which might indicate an increased salt tolerance when *SLAH3* transcript level was increased. Under low Cl^- conditions, all *35S:AtSLAH3* lines showed a significantly increased NO_3^-/ Cl^- ratio (Figure 5.12 B), which suggesting Cl^- was less accumulated and more NO_3^- was remained in shoot. If shoot Cl^- contents were changed upon the manipulation of *SLAH3* transcript level this might suggest that SLAH3 has an effect on the root to shoot transfer of Cl^- transport. There are numerous factors that might explain why only the Cl^- contents in the shoot were affected but not NO_3^-. Firstly, root NO_3^- contents were not examined in this study. It is possibly that *35S:AtSLAH3* lines had greater NO_3^- contents and this inhibited root uptake of Cl^-, resulting in less Cl^- being transferred to the shoot. As NO_3^- contents is tightly regulated in shoots it may have been less affected by *35S:AtSLAH3* expression. Secondly, as one of the homologs of the SLAC1 family, SLAH3 shares 57 % identity in amino acid with SLAH2 (Zheng *et al*., 2014) (a nitrate permeable anion channel, not permeable to chloride (Maierhofer *et al*., 2014)). Also, SLAH1, SLAH2 and SLAH4 were all found highly expressed in Arabidopsis root tissue (Negi *et al*. 2008; Geiger *et al*. 2011 and Lee *et al*. 2009); therefore it is reasonable to hypothesize that all members in SLAC/SLAH family are involved in nitrate fluxes and translocation in roots (Zheng *et al*., 2014). Although the aim was to overexpress *SLAH3* in Arabidopsis, the transcript level of other anion transporters, especially transporters/channels from SLAC/SLAH family are likely to be manipulated by expression of *SLAH3*. Similar responses have been seen when family members of other ion transporters have been manipulated (Conn *et al.*, 2011). As a consequence, the ratio between Cl^- and NO_3^- might be controlled by more than one transporter. Thirdly, besides the potential effects from SLAC1/SLAH family, the change of *SLAH3* transcript level might also affect other native anion transporters within the Arabidopsis root. For example, there are other three major nitrate transport families including NRT1/PTR (NPF; nitrate transporter 1/peptide transporter family, 53 members), NRT2 (seven members) and CLC (chloride channels, seven members) that are believed to be involved in nitrate transport (Krapp *et al*., 2014). The anion transport phenotype that is caused by altering *SLAH3* expression may be covered up by the altered expression and activity of other native anion transporters resulting in shoot NO_3^- homeostasis.

As the expression level of *SLAH3* was not identified in this experiment, more experiments will

be required to further test the function of SLAH3 in Arabidopsis. Also, the cell type specific over expression lines were generated, which will be a helpful resource.

5.4.3 AtNRT1.5 was able to regulate Arabidopsis shoot anion accumulation

It has been reported that the disruption of *AtNRT1.5* in Arabidopsis increased salt tolerance (Chen *et al*., 2012). Research showed that the *nrt1.5* knockout maintained lower NO_3^- concentration in the shoot but higher NO_3^- concentration in the roots compared to the control. However, the Cl^- concentration was not checked. To identify whether AtNRT1.5 was involved in Cl^- movement, three independent 35S:*AtNRT1.5* mutant lines were also generated to determine shoot anion contents were examined. Results showed that under a high salinity environment, two of third of the mutant lines accumulated significantly less Cl^- in the shoot (Figure 5.13 A), which might indicate the potential role of *AtNRT1.5* in regulating Cl^- movement. Unfortunately, no evidence was observed for an NO_3^- change in the shoots under both high and low salt conditions, except *35S:AtNRT1.5*-2 showed a slight increase of NO_3^- in shoot under a low salt environment (Figure 5.11). From this, there is not solid evidence to support the hypothesis that AtNRT1.5 is directly involved in anion xylem loading. However, analogous to the *Atnrt1.5* experiments constitutive overexpression of *AtNRT1.5* might result in greater influx of NO_3^- into roots and greater $NO3^-$ contents in roots. This may result, as similarly hypothesized for the *35S:AtSLAH3* lines, with lower Cl^- influx into roots and a lower amount of Cl^- transfer to shoots. A hypothesis that root NO_3^- contents is important in regulating Cl^- transfer to shoots requires future work to check NO_3^- contents in roots of all plants.

Alternatively, there are a few other potential reasons that might help to explain the difference in shoot Cl^- without a difference in shoot NO_3^-: 1) the non-specific over expression of *AtNRT1.5* could disrupt the native regulation process; 2) there are a number of other anion transporters/channels, such as NRT1.8, ClCc, CCC and NPF2.4 that have been identified in Arabidopsis that play roles in anion transport (Krapp *et al*., 2014). Without studying the effects on other anion transporters it might be difficult to interpret the results; 3) When *AtNRT1.5* cRNA was injected into Xenopus oocyte, we were not able to detect any significant anion currents, which probably suggested that *AtNRT1.5* might not be directly involved in anion transport and an unknown and complicated activation mechanism is yet unrevealed.

5.4.4 DIDS affected anion accumulation in Arabidopsis

Three independent DIDS experiments were performed to test the effect of DIDS on shoot anion accumulation. Two out of three experiments suggested that DIDS was able to reduce the Cl^- accumulation and also able to increase the NO_3^- contents under high salt stress. The other experiments showed a similar DIDS regulation on shoot Cl^- accumulation when salt stress was increased, however, not for NO_3^-. As an anion channel blocker, DIDS has been widely used as a pharmacological approach to test the anion transport ability *in vivo* and *in vitro* (Schwartz *et al*., 1995; Tavares *et al*., 2010; Kurusu *et al*., 2013). The ultimate goal of this thesis was to reduce Cl^- accumulation in the shoot and meanwhile maintain a high availability of NO_3^- in the shoot to improve nitrate use efficiency. My data suggested that DIDS has the ability to regulate the shoot anion accumulation, especially under saline environments. However, the mechanisms underlying the observed phenotypes are unknown. Research has shown DIDS is effective in blocking both R-type and S-type anion channels. As AtSLAH1 and AtSLAH3 were classified as S-type anion channels; it is possible that the DIDS blocks currents through these channels. Also, my results suggested that the application of DIDS was able to regulate both Cl^-/ NO_3^-simultaneously. However, other studies showed that DIDS was more efficient in blocking NO_3^- not Cl^-. For example, studies showed DIDS was able to block at least 70% of NO_3^-currents in *AtSLAC1* expressed oocytes (Geiger *et al*., 2009) and a similar level for NO_3^-currents of SLAH3 (Figure 4.10 E). Also, the net Cl^- uptake blocking efficiency of DIDS was much lower than anthracene-9-carboxylic acid (A-9-C) in barley seedlings (Kawachi *et al*., 2002). A potential explanation is that DIDS may only effectively block fluxes for one of the anions, and due to the reduction in competition between the fluxes, transport of the other anion will be less inhibited. However, more experiments are required to further understand how DIDS regulates the anion accumulation under the salt stress in different parts of the plants. For example, both root and shoot anion contents should be examined to help discriminate how anion flux to the shoot is affected when DIDS is applied.

Chapter 6 General Discussion

6.1 Aims of this project

Plants have developed various adaptive progresses to help them cope with salinity (NaCl) stress (Roy *et al*., 2014; Roy and Tester 2012). Compared with the mechanisms of Na^+ tolerance, which are comparatively well-studied (Munns and Tester, 2008), how plants tolerate Cl^- are less well researched (Teakle and Tyerman, 2010). Previous research has proposed that reducing Cl^- accumulation in the shoot through restricting xylem Cl^- loading is important to improve plant salt tolerance (Teakle and Tyerman, 2010); however the molecular determinants of this – the focus of this thesis – are poorly described in the literature. This project aimed to study putative Cl^- transport mechanisms through identifying candidate genes encoding anion channels/ transporters that might be responsible for Cl^- xylem loading in Arabidopsis. The functional characterization of these candidate proteins was examined in both heterologous systems and *in planta*. The ultimate aim is that with an increased understanding gained through this project it may be possible to develop crop plants which were better able to survive and maintain good yields under saline environments, either through a conventional breeding or genetic engineering.

In this project, three candidate genes, *AtSLAH1*, *AtSLAH3* and *AtNRT1.5* were found to be down regulated by salt stress and ABA so were selected as genes of interest (GOI) (Chapter 3). All the candidate genes were functional characterized in *X. laevis* oocytes and *S. cerevisiae* for examining the anion transport properties and selectivity (Chapter 4). The GOI's functions were also investigated in Arabidopsis mutant plants where the transcript level was either decreased or over-expressed (Chapter 5). This general discussion will summarize the key results gained in this project and the future plans aiming at further enhancing plant salinity tolerance through manipulation of Cl^- transport.

6.2 Summary of work accomplished in this thesis

6.2.1 *AtSLAH1* misexpression affects shoot Cl^- accumulation in Arabidopsis

As one of the homologs of SLAC1 (slow anion channel 1), SLAH1 was found localized to the plasma membrane (Negi *et al*., 2008) and highly expressed in Arabidopsis roots (Chapter 3).

qRT-PCR also suggested that *AtSLAH1* was strongly down-regulated by NaCl and ABA treatments (Chapter 3), which meets the predicted characteristics of a gene encoding an anion channel and involved in xylem Cl^- loading. No significant anion currents were elicited from the *SLAH1* cRNA injected oocytes and no significant growth inhibition was found when *SLAH1* transformed yeast was challenged with high concentrations (500 mM) of Cl^- or NO_3^- (Chapter 4). This may have been due to a lack of the knowledge on how SLAH1 could be regulated (an unknown signaling component or phosphorylation sites), or that it is not an ion transporter (Chapter 4). However, SLAH1 was characterized in the plant where its potential regulators partners would be present (Chapter 5). Interestingly, T_2 amiRNA-*AtSLAH1* mutant lines had reduced transcription of *SLAH1* which resulted in significantly lower shoot Cl^- accumulation compared to null lines when grown on low Cl^- (2 mM). No significant effect of reducing *SLAH1* expression was found on shoot NO_3^- accumulation, so the decreased shoot Cl^- and unaffected NO_3^- level resulted in a significant increased shoot NO_3^-/Cl^- ratio (Chapter 5). Moreover, all *35S:AtSLAH1* mutant plants accumulated a significantly higher Cl^- concentration than nulls when high Cl^- (75 mM) was applied and resulted in an increase in NO_3^-/Cl^- ratio. Unfortunately, the increase in shoot Cl^- accumulation did not alter the growth phenotype. These results indicate that *SLAH1* affects Cl^- but not NO_3^- transport in plants.

6.2.2 *AtSLAH3* might transport both NO_3^- and Cl^- in heterologous systems and in *planta*

AtSLAH3 cRNA injected oocytes showed a stronger selectivity to NO_3^- than to Cl^- (Chapter 4), which is consistent with previous findings (Geiger *et al*., 2012; Demir *et al*., 2013). The ability to distinguish ion selectivity between NO_3^- and Cl^- using a yeast growth is likely to be less sensitive than when using *X. laevis* oocytes, however, a similar growth inhibition was observed in *SLAH3* transformed yeast grown on both NO_3^- and Cl^- containing solutions compared to vector control transformed yeast (Chapter 4). It also appeared that maintaining a pH (around 5.6) is crucial for the anion transport ability of SLAH3 in yeast. SLAH3 has been well-characterized in several recent studies and suggested to be involved in NO_3^- transport (Geiger *et al*., 2011; Zheng *et al*., 2014). However, less work has been performed *in planta*. In this study, *35S:AtSLAH3* transgenic lines were developed and treated with different concentrations of NaCl. Interestingly, under both low (2 mM) and high (75 mM) Cl^- supply, no significant difference was found in shoot NO_3^- accumulation between *35S:AtSLAH3* transgenic lines and nulls. Significantly less Cl^- was accumulated in shoot in *35S:AtSLAH3* mutant lines when compared to nulls under high Cl^- (75 mM) supply. These results might

suggest that SLAH3 was involved in Cl^- but not NO_3^- transport in plant or that root NO_3^- levels might impact Cl^- uptake and transfer to the shoot (Chapter 5). Compared to the phenotype observed for *35S:AtSLAH1* mutant lines (which accumulated more Cl^- in shoot under high Cl^- supply), *35S:AtSLAH3* mutant lines exhibited an opposite phenotype with less Cl^-accumulated in shoot suggesting that SLAH1 and SLAH3 have a distinct and different functions in the plant. This is backed up by the fact that *SLAH3* increases expression in the root upon a salt stress whereas *SLAH1* decreases expression (Figure 3.8). However, as the root anion concentration wasn't examined in this experiment, it is difficult to conclude whether the change that observed in shoot is also affected by the root anion accumulation.

6.2.3 NRT1.5 might regulate both NO_3^- and Cl^- transport

Although NRT1.5 is proposed to be a nitrate transporter (Lin *et al*., 2008), there were difficulties found in detecting any Cl^- or NO_3^- related anion currents in NRT1.5 cRNA injected oocytes in this project (Chapter 4). When NRT1.5 was expressed in yeast, a significant growth inhibition was identified when the yeast was grown in high concentrations (500 mM) of KCl or KNO_3 (Chapter 4). This suggests that NRT1.5 might have the ability to transport both Cl^- and NO_3^-. When *35S:AtNRT1.5* transgenic plants were treated with high concentrations of Cl^- (75 mM), significantly less Cl^- was accumulated in the shoot. Interestingly, no difference in shoot NO_3^- content was identified in all mutants that were treated either with low (2 mM) or high (75 mM) NaCl. These results show that NRT1.5 was involved in altering Cl^- accumulation in the plant under salinity stress and that over- expressing *NRT1.5* might improve the salinity tolerance of plants as the shoot NO_3^-/ Cl^- ratio was significantly improved. This result seemingly contradicts previous findings that the absence of *NRT1.5* expression in the roots enhanced the salt tolerance of plants (Chen *et al*., 2012). Taken with the observation of *NRT1.5* transformed yeast responding to both Cl^- and NO_3^- it may suggests that NRT1.5 could be involved in both NO_3^- and Cl^- regulation *in planta*. More work, however, needs to be done to further confirm whether the lower shoot Cl– accumulation phenotype is caused by over-accumulation of NO_3^- in root (as may have occurred in the *nrt1.5* knockout), which prevents the uptake of Cl^- from root to shoot.

6.3 Future work

Several key research questions remain to be answered in this project, future plans will be discussed to help us further understand the long distance root- to- shoot Cl^- transport mechanisms and consequently improve plant salt tolerance under saline environments.

6.3.1 Future directions for characterizing candidate protein transport properties in heterologous systems

Results in Chapter 4 suggested that SLAH1 and NRT1.5 cRNA injected oocytes were not able to produce significant anion elicited currents, while the results gained from characterization in Arabidopsis indicated that SLAH1 and NRT1.5 might have a role in anion transport (Chapter 5). This raises the question as to why it was difficult to characterize SLAH1 and NRT1.5 in oocytes. The most likely explanation would be lack of knowledge regarding how these proteins are regulated. Do they require interaction with other proteins, such as kinases, which are not present in heterologous systems? Several attempts were made (Chapter 4) to examine whether SLAH1 can be activated in oocytes by the co-expression of the kinases SnRK2.2/ 2.3. An attempt was also made to mutate potential phosphorylation sites in SLAH1 to permanently activate the protein. These attempts, however, were not successful either because SLAH1 is activated through an unknown mechanism, or is not a transporter. To investigate this further there are several approaches that can be used to demonstrate a potential SLAH1/ NRT1.5 activation mechanism or protein phosphorylation network.

A first approach would be to determine which protein kinase would potentially interact with the protein of interest. A split-ubiquitin based Membrane Yeast Two- Hybrid (MYTH) system, a high throughput and efficient approach, which allows the identification of interactions between full-length membrane proteins and cytosolic or membrane-bound partners in many organisms (Lyer *et al*., 2005, Sinder *et al*., 2010) can be used to screen the candidate protein kinases. The protein of interest (bait) could be fused to the C- terminal half of yeast ubiquitin (C_{Ub}) following an artificial transcription factor, while the potential protein kinase (prey) will be fused to the N- terminal of yeast ubiquitin moiety ($N_{Ub}G$). The positive interaction partner will result in reconstitution of ubiquitin, which leads to a proteolytic cleavage and subsequent release of a transcription factor. The reporter gene can then be triggered (Lyer *et*

al., 2005, Sinder *et al*., 2010). This method can be used to quickly narrow down the candidate protein kinases, which are likely to interact with SLAH1 or NRT1.5. The selection of prey can be chosen from the protein kinase that has already shown to have positive interactions with other proteins that come from the same family. For instance, SLAC1 has shown can be activated by OST1 (a calcium-independent SnRK2- type kinase), CPK23 (calcium- dependent protein kinase) and CPK21 through phosphorylation when ABA was present (Geiger *et al*., 2009; Lee *et al*., 2009; Vahisalu *et al*., 2010). The activation of SLAC1 and SLAH3 were also triggered when CBL1/9 (calcineurin B–like calcium sensor) forms a complex with a CIPK23 (calcium- independent protein kinase) (Maierhofer *et al*., 2014). Similar activation was also found for NRT1.1, which was activated by a CIPK23/CBL9 complex (Hashimoto *et al*., 2012). Therefore, candidate protein kinases could be primarily selected from CPKs, CIPKs and SnRK2s family. Also, the public microarray database, such as GENEVESTIGATOR (Zimmermann *et al*., 2004) and Membrane-protein Interaction Network Database (MIND) (Lalonde *et al*., 2010) would also be very helpful for selecting the candidate interacting partners (these were continuously checked throughout my candidature but did not yield any results as to potential interactors). All the potential interaction between protein of interest and candidate protein kinase will be firstly tested using MYTH method. The protein kinases showed positive interaction in the MYTH system will be then examined using split- YPF system in Arabidopsis mesophyll protoplasts or in in *N. benthamiana* epidermal cells. Once the physical interaction is confirmed, the candidate protein kinase will be co-expressed with protein of interest in the oocyte for examination of the anion transport ability in order to determine whether the protein kinase is able to activate the anion channel/ transporter or alter the anion transport properties *in vitro*.

Strategies described above are focused on determining the protein kinase that has a physical interaction with the protein of interest. Under some circumstances, significant anion currents may still not be constantly detected when the protein of interest and interacting protein kinase (as shown by the MYTH/ BiFC systems) are co- expressed in oocytes due to a lack of knowledge in regard to the molecular activation mechanisms. For instance, when OST1 was co- expressed with SLAC1 in oocytes, only 25 % of injected oocytes showed anion elicited currents (Geiger *et al*., 2009). Further investigation suggests OST1 activated SLAC1 function through phosphorylation at a specific phosphorylation site (Geiger *et al*., 2009). Therefore, determination of the phosphorylation site in both the channel and in the potential protein kinase is also crucial in understanding the anion channel/ transporter regulation

mechanisms. CelluSpots peptide arrays, site-directed mutagenesis and *In vitro* kinase assay are widely used for investigating and confirming the phosphorylation sites (Geiger *et al*., 2009, Lee *et al*., 2009, Geiger *et al*., 2010, Brandt *et al*., 2012). In brief, peptide arrays have been used to locate the phosphorylation region within the N- and C- terminal (located in the cytosol) of SLAC1 and three regions (N- terminal: 41- 60, 101- 130; C- terminal: 506- 525) showed high phosphorylation signals (Geiger *et al*., 2009). Alternatively, the *in vitro* kinase assay can also be used to identify the important activation regions in protein of interest. For example, with the use of [γ^{32}] ATP radio-labeling, OST1 was found to be phosphorylated in the N- terminus of SLAC1 but not C- terminus (Geiger *et al*., 2009). Site-directed mutagenesis then can be performed to replace the predicted serine/threonine phosphorylation sites (using phosphorylation site prediction software) with residues that simulate constitutive phosphorylation or dephosphorylation before functional testing. Moreover, phosphoproteomics using liquid chromatography – tandem mass spectrometry provides the opportunity to investigate the *in vivo* phosphorylation in an efficient manner (Schirber *et al*., 2008). Previous studies have used this approach to investigate the Arabidopsis protein phosphorylation network in the ABA signaling pathway and provided valuable information regarding to the ABA controlled regulation (Umezawa *et al*., 2013, Wang *et al*., 2013). These methods can be used in the future to massively identify proteins that are phosphorylated by a master protein kinase, such as SnRK2s and CPKs.

Another aspect into investigating the anion channel/transporter activation is to determine the crystal structure of a candidate protein. The discovery of the NRT1.1 crystal structure was used to explain how NRT1.1's dual affinity of nitrate transport was controlled through phosphorylation (Liu and Tsay 2003, Sun *et al*., 2014, Tsay *et al*., 2014). It was shown that the T101 phosphorylation, located on the N terminus of the transmembrane helix 3 (TMH3), is crucial for NRT1.1 to switch its affinity (from low to high). It is interesting to note that this site is highly conserved in other nitrate transporters that have been shown to feature dual-affinity control (Liu and Tsay 2003). Although no SLAC1 crystal structure has been revealed, a bacterial structural homolog of SLAC1 was discovered, HiTehA, which helped to identify several important sites that controlling chloride transport (Chen *et al*., 2010). The transmembrane (TM) domain of AtSLAC1 (residues 188-504) was aligned (structure- based) to HiTehA and highly conserved residues that located in the central pore were selected to build up a conceptual model of AtSLAC1 (Chen *et al*., 2010). The predicted structure of AtSLAC1 was than compared to the HiTehA's crystal structure and the F450 residue was

found to locate on TM9 and blocks the central pore, suggesting its importance in controlling anion selectivity (Chen *et al*., 2010). When mutated AtSLAC1 (F450A) cRNA was injected into oocytes, large chloride related currents were observed and the current was larger when OST1, a known activator was co- expressed with SLAC1 (Sun *et al*., 2010, Chen *et al*., 2010). In conclusion, the research in structural analysis is a powerful approach to study the regulation mechanism of anion channels/transporters. The application of such approaches can lead to the identification of sites that are predicted to be important and the mutation of these sites will be useful to further discover the function of the protein.

In conjunction with finding a specific protein kinase or phosphorylation site to activate the GOI protein's function, another alternative scenario is that some transporters can be activated by another protein from same gene family though forming a heteromeric complex in a membrane. For example, AtNAR2.1 (AtNRT3.1) was found to be important in regulating high- affinity nitrate transport in Arabidopsis (Okamoto *et al*., 2006). When AtNAR2.1 forms a 150-kDa PM complex with AtNRT2.1, nitrate uptake was increased (Li *et al*., 2007). Similar increases in nitrate uptake were also found when *NAR2.1* was co- expressed with *NRT2.2* or *NRT2.5* in oocytes (Kotur *et al*., 2012; Krapp *et al*., 2014). Therefore, it would be interesting to co- express *SLAH1* and *SLAH3* in oocyte and examine whether SLAH1 can be activated.

6.3.2 Future directions for characterizing GOI transport properties *in planta*

In this project, amiRNA knockdown and constitutive overexpression plants were generated to study the GOI function in Arabidopsis. To further investigate the GOI function in plants, several future plans will be discussed below.

In this project, GOIs that express in stelar cells surrounding the vasculature were selected and hypothesized to be involved in anion xylem loading. Several studies have shown that genes expressed in cell type- specific manner contribute to salinity tolerance, whereas the same genes expressed in a constitutive manner may decrease salt tolerance (Møller *et al*., 2009). Therefore, it may be necessary to manipulate anion transport in a cell type- specific manner (Møller *et al*., 2009). The cell type- specific over expression mutant lines that can be used for this approach, containing *GAL4: AtSLAH1*, *GAL4: AtSLAH3* and *GAL4: AtNRT1.5* that are driven by the *GAL4* promoter were produced, however, due to the time constrains the T_2 plants were not phenotyped or genotyped under various treatments. The shoot anion

accumulation should be tested in all cell type- specific mutant lines to further determine the role of these GOI.

Furthermore, in this project, all the phenotyping was focused on shoot, it would be interesting to examine anion accumulation in the root as the anion movement in plants is highly dynamic. For instance, although SLAH3 and NRT1.5 have been proposed to be involved in NO_3^- transport, no significant shoot NO_3^- change were identified in both *35S:AtSLAH3* and *35S:AtNRT1.5* mutant line shoots under various salt treatments (Chapter 5). By testing the root anion contents it would be helpful to explain whether the phenotype (altered shoot Cl^- but not NO_3^-) was caused by increased NO_3^- compartmentation in root and therefore alters Cl^- transfer from root to shoot.

Results suggested that both *amiRNA: AtSLAH1* and *35S: AtSLAH1* transgenic plants had altered shoot Cl^- accumulation, however, they did not result in any significant growth phenotype and biomass change (Chapter 5). Similar shoot anion accumulation was also observed in *amiRNA: AtNPF2.4* mutants where only Cl^- but not NO_3^- change was observed (Li 2014). It is possible that SLAH1 and NPF2.4 are both involved in Cl^- transport to the shoot. However, neither pathway may be dominant; therefore, the generation of a double mutant line, such as double over-expression or double knockdown line would help to further understand the anion transport ability of both transporters and also the anion regulation network in general. This approach was successfully used for characterization redundant ABA-activated protein kinase where the triple mutant, *snrk2.2/2.3/2.6* showed significant greater growth defects and difficulties in seed development than single or double mutation, which suggests all of them are involved in ABA signaling (Nakashima *et al*., 2009, Fujii and Zhu, 2011). Furthermore, to see whether a modification in anion transport to the shoot results in a phenotype longer time courses for salt treatment of single and double gene mutant plants could be performed.

6.3.3 Other candidate genes

Two genes identified in the microarray mined in Chapter 3 were an amino acid permease 3 (*AAP3*, At1g77380), and ABC transporter 14 (*AtABCB14*, At1g28010). Both genes were highly expressed in the Arabidopsis root stele (compared to cortex) and up-regulated by NaCl (Evrard 2013), but these genes were not further characterized in the current project (Figure

3.8). However, a QTL map generated from Bay-0 × Shahdara recombinant inbred lines (RIL) suggested that these two genes are also located near two Cl^--related QTL (CL 3.1 and CL 3.2) (Loudet *et al*., 2003). AAP3 is located under chromosome 1 marker MSAT1.13, whereas AtABCB14 is located under chromosome 1 marker MSAT1.10 (Loudet *et al*., 2003). Evidence obtained from microarray and QTL indicates that AAP3 and AtABCB14 are possibly involved in Cl^- transport.

Previous research demonstrated that AAP3 is expressed in the phloem of roots and localized to the plasma membrane, as well as the nuclear membrane, ER, Golgi and endosomal vesicles (Okumoto *et al*., 2004). It has been hypothesized to play a role in the retrieval of amino acid leaked from the phloem. AtABCB14 is expressed mainly in guard cells and localizes at the plasma membrane. It was suggested that AtABCB14 modulates stomatal movement by transporting malate from the apoplast into guard cells (Lee *et al*., 2008), however, as mRNA transcripts of this gene were identified in root cells it can be hypothesized that there may be another role for this gene. Although current evidence suggested that AtABCB14 is responsible for malate transport, it raises the possibility that AtABCB14 may also be able to transport Cl^- through the same pathway, as malate is another common anion and share the same anion conductance with Cl^- in plant (Roberts 2006). As chloride transport to the shoot is likely to be a multigenic trait (Henderson *et al.*, 2014), the exploration of the function of multiple genes will be needed to discover the various genes involved in root-to-shoot transfer of Cl^-. Therefore, both these other candidates could warrant further exploration as to their role in this process.

6.3.4 Would forward genetics also be helpful in improving plant salinity tolerance?

This project used reverse genetics not a forward genetics approach to select the candidate genes that are believed to be involved in long distance anion transport. However, this approach is risky if the candidates are difficult to characterize or turn out not to have a function in the mechanism being studied. Forward genetics could also be applied to identify anion transporter genes involved in improving plant salinity tolerance. One approach is using a bi-parental mapping population that is generated by crossing ecotypes that have large genetic and environmental variation to identify QTLs that may responsible for the phenotype

of interest. This approach was used to successfully isolate a novel gene, *AtCIPK16* (Calcineurin B- like- interacting protein kinase 16), a protein kinase has been shown important to improve the salinity tolerance of Arabidopsis and barley (Roy *et al*., 2013). In brief, a significant QTL for shoot Na^+ exclusion was identified on chromosome 2 in an Arabidopsis Bay-0 × Shahdara mapping population (Loudet *et al*. 2002), which was fine mapped to *AtCIPK16* (Roy *et al*., 2013). Characterization of *AtCIPK16* further confirmed the hypothesis that this gene was capable of increasing salinity tolerance in Arabidopsis (Roy *et al*., 2013).

Another aspect of using forward genetics is to rely on genome-wide association (GWAS) studies (Atwell *et al*., 2010), which can be used to identify regions of the genome at which genetic variation is linked to the phenotype of interest. For example, this method led to the conclusion that AtHKT1;1 was involved in Na^+ transport (Baxter *et al*., 2010). In brief, a set of 360 accessions of Arabidopsis were phenotyped using ICP-MS and genotyped using a Affymetrix SNP-tilling array to read the variations for producing SNPs (this can now be performed by Genotyping-by-sequencing or whole genome sequencing). Then the SNPs were correlated with leaf Na^+ contents and one SNP that found to be associated with the phenotype that was used to locate the region in the genome. The advantage of this approach over bi-parental mapping is that GWAS relies on linkage disequilibrium and the interval of the QTL is usually a location that is a couple of cM in size (typical of bi-parental mapping). *AtHKT1;1* was found under the single strong peak where the SNP were located (Baxter *et al*., 2010).

6.3.5 Using functional genomic to identify the candidate anion transporters

The forward genetic approaches described have been widely used to identify novel genes. Functional genomics, such as transcriptome, metabolome, proteome and ionomics have also been used to interpret gene responses and the role of specific gene networks in response to abiotic stress (Cramer *et al*., 2011). For example, Figure 6.1 proposed a modified strategy to improve the screening efficiency of such approaches that combines variants screening with systems biology, another strategy to specifically identify novel genes in response to abiotic stress (Sheldon and Roessner 2013).

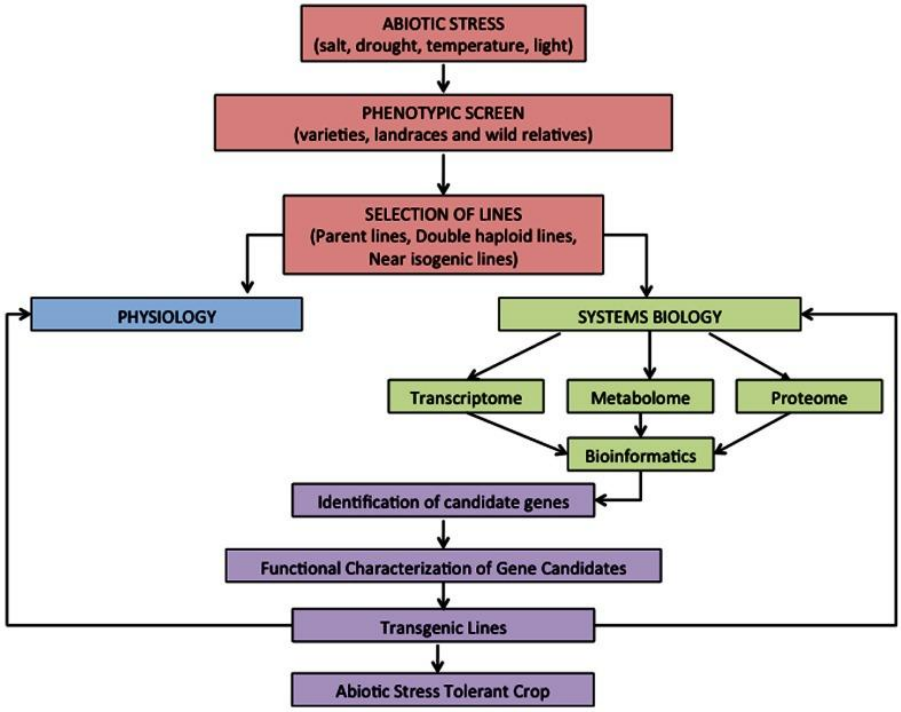

Figure 6.1 Proposed strategies for the integration of physiology and systems biology to gain insights into abiotic stress responses in cereals and the future development of abiotic stress tolerant crops (Adapted from Sheldon and Roessner 2013).

6.3.6 Is it possible to improve the salinity tolerance of a crop using a gene from another plant species?

The ultimate goal of this research is to improve crop plant's salinity tolerance and maintain the crop yield under salt stress using the molecular identities found in Arabidopsis. To achieve this goal, one way is to take advantage of the results of such studies and apply it to an economically important crop plant. For example, *AtCIPK16* misexpression resulted in altered Na^+ accumulation in Arabidopsis and improved salt tolerance as determined by vegetative biomass (Roy *et al*., 2013). Later, when *AtCIPK16* was constitutively over-expressed in barley (Golden Promise) it also resulted in reduced shoot Na^+ accumulation and increased salinity tolerance (also indicated by increased vegetative biomass under saline conditions) (Roy *et al*., 2013). AVP1, an Arabidopsis vacuolar proton pumping pyrophosphatase (H^+-PPase) has been shown to improve salinity tolerance in transgenic Arabidopsis (Gaxiola *et al*., 2001), rice (Zhao *et al.*, 2006) and alfalfa (Bao *et al*., 2009). When *AVP1* was over- expressed in barley, the shoot biomass was increased under saline conditions in the field (Schilliing *et al*., 2014). This strategy would potentially increase crop plant's

salinity tolerance and increase the grain yield.

Another way is to improve the salinity tolerance is by direct manipulation of the GOI's homologs in the crop plant. For instance, SLAH1 was also identified in other species including barley (*HvSLAH1*) (Liu *et al*., 2014), grapevine (*VvSLAH1*) (Henderson *et al*., 2014), citrus (*CcSLAH1*) (Brumos *et al*., 2010) and other crop plants (Dreyer *et al*., 2012, Liu *et al*., 2014). Preliminary research results have suggested that the up- regulation of *HvSLAH1* is correlated with the higher barley yield (Liu *et al*., 2014), however, no direct link between CcSLAH1 and salinity tolerance has been established. Taken together, it would be interesting to discover whether orthologous genes in sequence play similar roles in different plant species? To answer this question, cross-referencing phylogenetic analyses (e.g. Dreyer et al., 2012) and protein functional analysis in specific plant species would be very helpful and may lead to a route to improving crop productivity.

References

Apse, M.P., Aharon, G.S., Snedden, W.A.and Blumwald, E. (1999) Salt tolerance conferred by overexpression of a vacuolar Na^+/H^+ antiport in Arabidopsis. *Science*, **285**, 1256-1258.

Apse, M.P.and Blumwald, E. (2007) Na^+ transport in plants. *FEBS Lett.*, **581**, 2247-2254.

Atwell, S., Huang, Y.S., Vilhjalmsson, B.J., Willems, G., Horton, M., Li, Y., Meng, D., Platt, A., Tarone, A.M., Hu, T.T., Jiang, R., Muliyati, N.W., Zhang, X., Amer, M.A., Baxter, I., Brachi, B., Chory, J., Dean, C., Debieu, M., de Meaux, J., Ecker, J.R., Faure, N., Kniskern, J.M., Jones, J.D.G., Michael, T., Nemri, A., Roux, F., Salt, D.E., Tang, C., Todesco, M., Traw, M.B., Weigel, D., Marjoram, P., Borevitz, J.O., Bergelson, J.and Nordborg, M. (2010) Genome-wide association study of 107 phenotypes in Arabidopsis thaliana inbred lines. *Nature*, **465**, 627-631.

Barbier-Brygoo, H., De Angeli, A., Filleur, S., Frachisse, J.-M., Gambale, F., Thomine, S.and Wege, S. (2011) Anion Channels/Transporters in Plants: From Molecular Bases to Regulatory Networks. In *Annual Review of Plant Biology, Vol **62*** (Merchant, S.S., Briggs, W.R.and Ort, D. eds), pp. 25-51.

Barragan, V., Leidi, E.O., Andres, Z., Rubio, L., De Luca, A., Fernandez, J.A., Cubero, B.and Pardo, J.M. (2012) Ion Exchangers NHX1 and NHX2 Mediate Active Potassium Uptake into Vacuoles to Regulate Cell Turgor and Stomatal Function in Arabidopsis. *Plant Cell*, **24**, 1127-1142.

Bassil, E., Tajima, H., Liang, Y.-C., Ohto, M.-a., Ushijima, K., Nakano, R., Esumi, T., Coku, A., Belmonte, M.and Blumwald, E. (2011) The arabidopsis Na^+/H^+ antiporters NHX1 and NHX2 control vacuolar pH and K^+ homeostasis to regulate growth, flower development, and reproduction (vol 23, pg 3482, 2011). *Plant Cell*, **23**, 4526-4526.

Baxter, I., Hosmani, P.S., Rus, A., Lahner, B., Borevitz, J.O., Muthukumar, B., Mickelbart, M.V., Schreiber, L., Franke, R.B.and Salt, D.E. (2009) Root suberin forms an extracellular barrier that affects water relations and mineral nutrition in arabidopsis. *PLoS Genet.*, **5**, 12.

Bergsdorf, E.-Y., Zdebik, A.A.and Jentsch, T.J. (2009) Residues important for nitrate/proton coupling in plant and mammalian CLC transporters. *J. Biol. Chem.*, **284**, 11184-11193.

Blumwald, E., Aharon, G.S.and Apse, M.P. (2000) Sodium transport in plant cells. *Biochim. Biophys. Acta-Biomembr.*, **1465**, 140-151.

Bo Li. (2014) POT proteins are important for chloride transport in Arabidopsis. PhD thesis,

University of Adelaide.

Brandt, B., Brodsky, D.E., Xue, S., Negi, J., Iba, K., Kangasjarvi, J., Ghassemian, M., Stephan, A.B., Hu, H.and Schroeder, J.I. (2012) Reconstitution of abscisic acid activation of SLAC1 anion channel by CPK6 and OST1 kinases and branched ABI1 PP2C phosphatase action. *Proceedings of the National Academy of Sciences of the United States of America*, **109**, 10593-10598.

Brumos, J., Colmenero-Flores, J.M., Conesa, A., Izquierdo, P., Sanchez, G., Iglesias, D.J., Lopez-Climent, M.F., Gomez-Cadenas, A.and Talon, M. (2009) Membrane transporters and carbon metabolism implicated in chloride homeostasis differentiate salt stress responses in tolerant and sensitive Citrus rootstocks. *Funct. Integr. Genomics*, **9**, 293-309.

Brumos, J., Talon, M., Bouhlal, R.and Colmenero-Flores, J.M. (2010) Cl^- homeostasis in includer and excluder citrus rootstocks: transport mechanisms and identification of candidate genes. *Plant Cell and Environment*, **33**, 2012-2027.

Burton, R.A., Wilson, S.M., Hrmova, M., Harvey, A.J., Shirley, N.J., Stone, B.A., Newbigin, E.J., Bacic, A.and Fincher, G.B. (2006) Cellulose synthase-like CslF genes mediate the synthesis of cell wall (1,3;1,4)-beta-D-glucans. *Science*, **311**, 1940-1942.

Byrt, C.S., Platten, J.D., Spielmeyer, W., James, R.A., Lagudah, E.S., Dennis, E.S., Tester, M.and Munns, R. (2007) HKT1;5-like cation transporters linked to Na^+ exclusion loci in wheat, Nax2 and Kna1. *Plant Physiology*, **143**, 1918-1928.

Byrt, C.S., Xu, B., Krishnan, M., Lightfoot, D.J., Athman, A., Jacobs, A.K., Watson-Haigh, N.S., Plett, D., Munns, R., Tester, M.and Gilliham, M. (2014) The Na^+ transporter, TaHKT1;5-D, limits shoot Na^+ accumulation in bread wheat. *Plant Journal*, **80**, 516-526.

Cataldo, D.A., Haroon, M., Schrader, L.E.and Youngs, V.L. (1975) Rapid colorimetric determination of nitrate in plant-tissue by nitration of salicylic-acid. *Commun Soil Sci Plan*, **6**, 71-80.

Chen, Y.-h., Hu, L., Punta, M., Bruni, R., Hillerich, B., Kloss, B., Rost, B., Love, J., Siegelbaum, S.A.and Hendrickson, W.A. (2010) Homologue structure of the SLAC1 anion channel for closing stomata in leaves. *Nature*, **467**, 1074-U1157.

Churchill, K.A.and Sze, H. (1984) Anion-sensitive, H^+-pumping ATpase of oat roots-direct effects of Cl^-, NO_3^- and a disulfonic stilbene. *Plant Physiology*, **76**, 490-497.

Colmenero-Flores, J.M., Martinez, G., Gamba, G., Vazquez, N., Iglesias, D.J., Brumos, J.and Talon, M. (2007) Identification and functional characterization of cation-chloride

cotransporters in plants. *Plant Journal*, **50**, 278-292.

Conn, S.and Gilliham, M. (2010) Comparative physiology of elemental distributions in plants. *Ann. Bot.*, **105**, 1081-1102.

Conn, S.J., Hocking, B., Dayod, M., Xu, B., Athman, A., Henderson, S., Aukett, L., Conn, V., Shearer, M.K., Fuentes, S., Tyerman, S.D.and Gilliham, M. (2013) Protocol: optimising hydroponic growth systems for nutritional and physiological analysis of Arabidopsis thaliana and other plants. *Plant Methods*, **9**.

Cram, W.J.and Pitman, M.G. (1972) Action of abscisic acid on ion uptake and water flow in plant roots. *Aust J Biol Sci*, **25**, 1125-1132.

Cramer, G.R. (2002) Response of abscisic acid mutants of Arabidopsis to salinity. *Funct. Plant Biol.*, **29**, 561-567.

Cramer, G.R., Urano, K., Delrot, S., Pezzotti, M.and Shinozaki, K. (2011) Effects of abiotic stress on plants: a systems biology perspective. *Bmc Plant Biol*, **11**.

Crawford, N.M.and Glass, A.D.M. (1998) Molecular and physiological aspects of nitrate uptake in plants. *Trends in Plant Science*, **3**, 389-395.

Curtis, M.D.and Grossniklaus, U. (2003) A gateway cloning vector set for high-throughput functional analysis of genes in planta. *Plant Physiology*, **133**, 462-469.

Davenport, R., James, R.A., Zakrisson-Plogander, A., Tester, M.and Munns, R. (2005) Control of sodium transport in durum wheat. *Plant Physiology*, **137**, 807-818.

Davenport, R.J., Munoz-Mayor, A., Jha, D., Essah, P.A., Rus, A.and Tester, M. (2007) The Na^+ transporter AtHKT1;1 controls retrieval of Na^+ from the xylem in Arabidopsis. *Plant Cell and Environment*, **30**, 497-507.

Davenport, R.J.and Tester, M. (2000) A weakly voltage-dependent, nonselective cation channel mediates toxic sodium influx in wheat. *Plant Physiology*, **122**, 823-834.

De Angeli, A., Monachello, D., Ephritikhine, G., Frachisse, J.M., Thomine, S., Gambale, F.and Barbier-Brygoo, H. (2006) The nitrate/proton antiporter AtCLCa mediates nitrate accumulation in plant vacuoles. *Nature*, **442**, 939-942.

De Angeli, A., Monachello, D., Ephritikhine, G., Frachisse, J.M., Thomine, S., Gambale, F.and Barbier-Brygoo, H. (2009) CLC-mediated anion transport in plant cells. *Philos. Trans. R. Soc. B-Biol. Sci.*, **364**, 195-201.

De Angeli, A., Moran, O., Wege, S., Filleur, S., Ephritikhine, G., Thomine, S., Barbier-Brygoo, H.and Gambale, F. (2009) ATP Binding to the C Terminus of the Arabidopsis thaliana Nitrate/Proton Antiporter, AtCLCa, Regulates Nitrate Transport into Plant Vacuoles. *J. Biol. Chem.*, **284**, 26526-26532.

De Angeli, A., Thomine, S., Frachisse, J.-M., Ephritikhine, G., Gambale, F.and Barbier-Brygoo, H. (2007) Anion channels and transporters in plant cell membranes. *Febs Letters*, **581**, 2367-2374.

Demir, F., Horntrich, C., Blachutzik, J.O., Scherzer, S., Reinders, Y., Kierszniowska, S., Schulze, W.X., Harms, G.S., Hedrich, R., Geiger, D.and Kreuzer, I. (2013) Arabidopsis nanodomain-delimited ABA signaling pathway regulates the anion channel SLAH3. *Proceedings of the National Academy of Sciences of the United States of America*, **110**, 8296-8301.

Dluzniewska, P., Gessler, A., Dietrich, H., Schnitzler, J.P., Teuber, M.and Rennenberg, H. (2007) Nitrogen uptake and metabolism in Populus x canescens as affected by salinity. *New Phytologist*, **173**, 279-293.

Downes, M.T. (1978) Improved hydrazine reduction method for automated-determination of low nitrate levels in freshwater. *Water Res*, **12**, 673-675.

Downton, W.J.S., Loveys, B.R.and Grant, W.J.R. (1990) Salinity Effects on the Stomatal Behaviour of Grapevine. *New Phytol.*, **116**, 499-503.

Dreyer, I., Gomez-Porras, J.L., Riano-Pachon, D.M., Hedrich, R.and Geiger, D. (2012) Molecular evolution of slow and quick anion channels (SLACs and QUACs/ALMTs). *Front Plant Sci*, **3**.

Dreyer, I., Horeau, C., Lemaillet, G., Zimmermann, S., Bush, D.R., Rodriguez-Navarro, A., Schachtman, D.P., Spalding, E.P., Sentenac, H.and Gaber, R.F. (1999) Identification and characterization of plant transporters using heterologous expression systems. *Journal of Experimental Botany*, **50**, 1073-1087.

Dreyer, I., Lucia Gomez-Porras, J., Mauricio Riano-Pachon, D., Hedrich, R.and Geiger, D. (2012) Molecular evolution of slow and quick anion channels (SLACs and QUACs/ALMTs). *Front Plant Sci*, **3**.

Dutzler, R., Campbell, E.B., Cadene, M., Chait, B.T.and MacKinnon, R. (2002) X-ray structure of a CIC chloride channel at 3.0 angstrom reveals the molecular basis of anion selectivity. *Nature*, **415**, 287-294.

Edwards, K., Johnstone, C.and Thompson, C. (1991) A simple and rapid method for the preparation of plant genomic DNA for PCR analysis. *Nucleic Acids Research*, **19**, 1349-1349.

Evrard, A. (2013) Cell type-specific transcriptional responses of plants to salinity. Adelaide, Australia: The University of Adelaide.

Estevez, R.and Jentsch, T.J. (2002) CLC chloride channels: correlating structure with function.

Current Opinion in Structural Biology, **12**, 531-539.

Felle, H.H. (1994) The H^+/Cl^- symporter in root-hair cells of *Sinapis alba Plant Physiol.*, **106**, 1131-1136.

Fort, K.P., Lowe, K.M., Thomas, W.A.and Walker, M.A. (2013) Cultural conditions and propagule type influence relative chloride exclusion in grapevine rootstocks. *American Journal of Enology and Viticulture*, **64**, 241-250.

Fujii, H., Verslues, P.E.and Zhu, J.-K. (2011) Arabidopsis decuple mutant reveals the importance of SnRK2 kinases in osmotic stress responses in vivo. *Proceedings of the National Academy of Sciences of the United States of America*, **108**, 1717-1722.

Gamba, G. (2005) Molecular physiology and pathophysiology of electroneutral cation-chloride cotransporters. *Physiological Reviews*, **85**, 423-493.

Gaxiola, R.A., Li, J.S., Undurraga, S., Dang, L.M., Allen, G.J., Alper, S.L.and Fink, G.R. (2001) Drought- and salt-tolerant plants result from overexpression of the AVP1 H^+-pump. *Proceedings of the National Academy of Sciences of the United States of America*, **98**, 11444-11449.

Gaxiola, R.A., Yuan, D.S., Klausner, R.D.and Fink, G.R. (1998) The yeast CLC chloride channel functions in cation homeostasis. *Proceedings of the National Academy of Sciences of the United States of America*, **95**, 4046-4050.

Gaymard, F., Pilot, G., Lacombe, B., Bouchez, D., Bruneau, D., Boucherez, J., Michaux-Ferriere, N., Thibaud, J.B.and Sentenac, H. (1998) Identification and disruption of a plant shaker-like outward channel involved in K^+ release into the xylem sap. *Cell*, **94**, 647-655.

Geiger, D., Maierhofer, T., Al-Rasheid, K.A.S., Scherzer, S., Mumm, P., Liese, A., Ache, P., Wellmann, C., Marten, I., Grill, E., Romeis, T.and Hedrich, R. (2011) Stomatal Closure by Fast Abscisic Acid Signaling Is Mediated by the Guard Cell Anion Channel SLAH3 and the Receptor RCAR1. *Science Signaling*, **4**.

Geiger, D., Scherzer, S., Mumm, P., Marten, I., Ache, P., Matschi, S., Liese, A., Wellmann, C., Al-Rasheid, K.A.S., Grill, E., Romeis, T.and Hedrich, R. (2010) Guard cell anion channel SLAC1 is regulated by CDPK protein kinases with distinct $Ca2^+$ affinities. *Proceedings of the National Academy of Sciences of the United States of America*, **107**, 8023-8028.

Geiger, D., Scherzer, S., Mumm, P., Stange, A., Marten, I., Bauer, H., Ache, P., Matschi, S., Liese, A., Al-Rasheid, K.A.S., Romeis, T.and Hedrich, R. (2009) Activity of guard cell anion channel SLAC1 is controlled by drought-stress signaling kinase-phosphatase

pair. *Proceedings of the National Academy of Sciences of the United States of America*, **106**, 21425-21430.

Gietz, R.D.and Schiestl, R.H. (2007) High-efficiency yeast transformation using the LiAc/SS carrier DNA/PEG method. *Nat. Protoc.*, **2**, 31-34.

Gilliham, M.and Tester, M. (2005) The regulation of anion loading to the maize root xylem. *Plant Physiology*, **137**, 819-828.

Gong, H., Blackmore, D., Clingeleffer, P., Sykes, S., Jha, D., Tester, M.and Walker, R. (2011) Contrast in chloride exclusion between two grapevine genotypes and its variation in their hybrid progeny. *Journal of Experimental Botany*, **62**, 989-999.

Greenway, H.and Munns, R. (1980) Mechanisms of salt tolerance in non-halophytes. *Annual Review of Plant Physiology and Plant Molecular Biology*, **31**, 149-190.

Gutermuth, T., Lassig, R., Portes, M.-T., Maierhofer, T., Romeis, T., Borst, J.-W., Hedrich, R., Feijo, J.A.and Konrad, K.R. (2013) Pollen Tube Growth Regulation by Free Anions Depends on the Interaction between the Anion Channel SLAH3 and Calcium-Dependent Protein Kinases CPK2 and CPK20. *Plant Cell*, **25**, 4525-4543.

Hackenberg, M., Shi, B.-J., Gustafson, P.and Langridge, P. (2012) A Transgenic Transcription Factor (TaDREB3) in Barley Affects the Expression of MicroRNAs and Other Small Non-Coding RNAs. *Plos One*, **7**.

Harrison, S.J., Mott, E.K., Parsley, K., Aspinall, S., Gray, J.C.and Cottage, A. (2006) A rapid and robust method of identifying transformed Arabidopsis thaliana seedlings following floral dip transformation. *Plant Methods*, **2**.

Hauser, F.and Horie, T. (2010) A conserved primary salt tolerance mechanism mediated by HKT transporters: a mechanism for sodium exclusion and maintenance of high K^+/Na^+ ratio in leaves during salinity stress. *Plant Cell and Environment*, **33**, 552-565.

Hedrich, R. (2012) ION CHANNELS IN PLANTS. *Physiological Reviews*, **92**, 1777-1811.

Henderson, S.W., Baumann, U., Blackmore, D.H., Walker, A.R., Walker, R.R.and Gilliham, M. (2014) Shoot chloride exclusion and salt tolerance in grapevine is associated with differential ion transporter expression in roots. *Bmc Plant Biol*, **14**. 921-929

Henderson, S.W., Wege, S., Qiu, J., Blackmore, DH., Walker, AR., Tyerman, S., Walker, R. and Gilliham, M. (2015) Grapevine and Arabidopsis cation-chloride cotransporters localise to the Golgi and trans-Golgi network and indirectly influence long-distance ion homeostasis and plant salt tolerance. *Plant Phyiols.* **15**. 499-512

Ho, C.-H.and Frommer, W.B. (2014) Fluorescent sensors for activity and regulation of the nitrate transceptor CHL1/NRT1.1 and oligopeptide transporters. *Elife*, **3**.

Hofgen, R.and Willmitzer, L. (1988) Storage of competent cells for agrobacterium transformation. *Nucleic Acids Research*, **16**, 9877-9877.

Iyer, K., Burkle, L., Auerbach, D., Thaminy, S., Dinkel, M., Engels, K.and Stagljar, I. (2005) Utilizing the split-ubiquitin membrane yeast two-hybrid system to identify protein-protein interactions of integral membrane proteins. *Science's STKE : signal transduction knowledge environment*, **2005**, pl3-pl3.

Izawa, S., Heath, R.L.and Hind, G. (1969) Role of chloride ion in photosynthesis. 3. Effect of artificial electron donors upon electron transport. *Biochimica Et Biophysica Acta*, **180**, 388-398.

James, R.A., Davenport, R.J.and Munns, R. (2006) Physiological characterization of two genes for Na^+ exclusion in durum wheat, *Nax1* and *Nax2*. *Plant Physiology*, **142**, 1537-1547.

Jha, D., Shirley, N., Tester, M.and Roy, S.J. (2010) Variation in salinity tolerance and shoot sodium accumulation in Arabidopsis ecotypes linked to differences in the natural expression levels of transporters involved in sodium transport. *Plant Cell and Environment*, **33**, 793-804.

Johnston, M., Flick, J.S.and Pexton, T. (1994) Multiple mechanisms provide rapid and stringent glucose repression of *GAL* gene-expression in *saccharomyces-cerevisiae*. *Molecular and Cellular Biology*, **14**, 3834-3841.

Joshi-Saha, A., Valon, C.and Leung, J. (2011) A Brand New START: Abscisic Acid Perception and Transduction in the Guard Cell. *Science Signaling*, **4**.

Jossier, M., Kroniewicz, L., Dalmas, F., Le Thiec, D., Ephritikhine, G., Thomine, S., Barbier-Brygoo, H., Vavasseur, A., Filleur, S.and Leonhardt, N. (2010) The Arabidopsis vacuolar anion transporter, AtCLCc, is involved in the regulation of stomatal movements and contributes to salt tolerance. *Plant Journal*, **64**, 563-576.

Kawachi, T., Nishijo, C., Fujikake, H., Abdel-Latif, S., Ohtake, N., Sueyoshi, K., Ohyama, T., Shigeta-Ishioka, N., Watanabe, S., Osa, A., Sekine, T., Matsuhashi, S., Ito, T., Mizuniwa, C., Kume, T., Hashimoto, S., Uchida, H.and Tsuji, A. (2002) Effects of anion channel blockers on xylem nitrate transport in barley seedlings. *Soil Science and Plant Nutrition*, **48**, 271-277.

Ke, R., Ingram, P.J.and Haynes, K. (2013) An Integrative Model of Ion Regulation in Yeast. *Plos Computational Biology*, **9**.

Kiegle, E., Moore, C.A., Haseloff, J., Tester, M.A.and Knight, M.R. (2000) Cell-type-specific calcium responses to drought, salt and cold in the Arabidopsis root. *Plant Journal*, **23**,

267-278.

Kilian, J., Whitehead, D., Horak, J., Wanke, D., Weinl, S., Batistic, O., D'Angelo, C., Bornberg-Bauer, E., Kudla, J.and Harter, K. (2007) The AtGenExpress global stress expression data set: protocols, evaluation and model data analysis of UV-B light, drought and cold stress responses. *Plant Journal*, **50**, 347-363.

Kohler, B.and Raschke, K. (2000) The delivery of salts to the xylem. Three types of anion conductance in the plasmalemma of the xylem parenchyma of roots of barley. *Plant Physiol.*, **122**, 243-254.

Kohler, E., Mohring, R.H.and Schilling, H. (2005) Acceleration of shortest path and constrained shortest path computation. In *Experimental and Efficient Algorithms, Proceedings* (Nikoletseas, S.E. ed, pp. 126-138.

Kolbe, M., Besir, H., Essen, L.O.and Oesterhelt, D. (2000) Structure of the light-driven chloride pump halorhodopsin at 1.8 angstrom resolution. *Science*, **288**, 1390-1396.

Kollist, H., Jossier, M., Laanemets, K.and Thomine, S. (2011) Anion channels in plant cells. *Febs Journal*, **278**, 4277-4292.

Kotur, Z., Mackenzie, N., Ramesh, S., Tyerman, S.D., Kaiser, B.N.and Glass, A.D.M. (2012) Nitrate transport capacity of the Arabidopsis thaliana NRT2 family members and their interactions with AtNAR2.1. *New Phytologist*, **194**, 724-731.

Koyama, M.L., Levesley, A., Koebner, R.M.D., Flowers, T.J.and Yeo, A.R. (2001) Quantitative trait loci for component physiological traits determining salt tolerance in rice. *Plant Physiology*, **125**, 406-422.

Krapp, A., David, L.C., Chardin, C., Girin, T., Marmagne, A., Leprince, A.-S., Chaillou, S., Ferrario-Mery, S., Meyer, C.and Daniel-Vedele, F. (2014) Nitrate transport and signalling in Arabidopsis. *Journal of Experimental Botany*, **65**, 789-798.

Kulik, A., Wawer, I., Krzywinska, E., Bucholc, M.and Dobrowolska, G. (2011) SnRK2 Protein Kinases-Key Regulators of Plant Response to Abiotic Stresses. *Omics-a Journal of Integrative Biology*, **15**, 859-872.

Lauchli, A., James, R.A., Huang, C.X., McCully, M.and Munns, R. (2008) Cell-specific localization of Na^+ in roots of durum wheat and possible control points for salt exclusion. *Plant Cell and Environment*, **31**, 1565-1574.

Lee, L.Y.and Gelvin, S.B. (2008) T-DNA binary vectors and systems. *Plant Physiology*, **146**, 325-332.

Lee, S.C., Lan, W., Buchanan, B.B.and Luan, S. (2009) A protein kinase-phosphatase pair interacts with an ion channel to regulate ABA signaling in plant guard cells.

Proceedings of the National Academy of Sciences of the United States of America, **106**, 21419-21424.

Leran, S., Varala, K., Boyer, J.-C., Chiurazzi, M., Crawford, N., Daniel-Vedele, F., David, L., Dickstein, R., Fernandez, E., Forde, B., Gassmann, W., Geiger, D., Gojon, A., Gong, J.-M., Halkier, B.A., Harris, J.M., Hedrich, R., Limami, A.M., Rentsch, D., Seo, M., Tsay, Y.-F., Zhang, M., Coruzzi, G.and Lacombe, B. (2014) A unified nomenclature of NITRATE TRANSPORTER 1/PEPTIDE TRANSPORTER family members in plants. *Trends in Plant Science*, **19**, 5-9.

Leung, J.and Giraudat, J. (1998) Abscisic acid signal transduction. *Annual Review of Plant Physiology and Plant Molecular Biology*, **49**, 199-222.

Li, J.Y., Fu, Y.L., Pike, S.M., Bao, J., Tian, W., Zhang, Y., Chen, C.Z., Li, H.M., Huang, J., Li, L.G., Schroeder, J.I., Gassmann, W.and Gonga, J.M. (2010) The Arabidopsis Nitrate Transporter NRT1.8 Functions in Nitrate Removal from the Xylem Sap and Mediates Cadmium Tolerance. *Plant Cell*, **22**, 1633-1646.

Lin, S.H., Kuo, H.F., Canivenc, G., Lin, C.S., Lepetit, M., Hsu, P.K., Tillard, P., Lin, H.L., Wang, Y.Y., Tsai, C.B., Gojon, A.and Tsay, Y.F. (2008) Mutation of the Arabidopsis NRT1.5 Nitrate Transporter Causes Defective Root-to-Shoot Nitrate Transport. *Plant Cell*, **20**, 2514-2528.

Linder, B.and Raschke, K. (1992) A slow anion channel in guard-cells, activating at large hyperpolarization, may be principal for stomatal closing. *Febs Letters*, **313**, 27-30.

Lisal, J.and Maduke, M. (2008) The ClC-0 chloride channel is a 'broken' $Cl(^{-})/H(^{+})$ antiporter. *Nature Structural & Molecular Biology*, **15**, 805-810.

Liu, K.H.and Tsay, Y.F. (2003) Switching between the two action modes of the dual-affinity nitrate transporter *CHL1* by phosphorylation. *Embo Journal*, **22**, 1005-1013.

Lorenzen, I., Aberle, T.and Plieth, C. (2004) Salt stress-induced chloride flux: a study using transgenic Arabidopsis expressing a fluorescent anion probe. *Plant Journal*, **38**, 539-544.

Loudet, O., Gaudon, V., Trubuil, A.and Daniel-Vedele, F. (2005) Quantitative trait loci controlling root growth and architecture in Arabidopsis thaliana confirmed by heterogeneous inbred family. *Theoretical and Applied Genetics*, **110**, 742-753.

Maas, E.V.and Hoffman, G.J. (1977) Crop salt tolerance - current assessment. *Journal of the Irrigation and Drainage Division, American Society of Civil Engineers*, **103**, 115-134.

Maathuis, F.J.M.and Amtmann, A. (1999) K^{+} nutrition and Na^{+} toxicity: The basis of cellular K^{+}/Na^{+} ratios. *Ann. Bot.*, **84**, 123-133.

Machin, F., Medina, B., Navarro, F.J., Perez, M.D., Veenhuis, M., Tejera, P., Lorenzo, H., Lancha, A.and Siverio, J.M. (2004) The role of *YNT1* in nitrate and nitrite transport in the yeast *Hansenula polymorpha*. *Yeast*, **21**, 265-276.

Maierhofer, T., Diekmann, M., Offenborn, J.N., Lind, C., Bauer, H., Hashimoto, K., Al-Rasheid, K.A.S., Luan, S., Kudla, J., Geiger, D.and Hedrich, R. (2014) Site- and kinase-specific phosphorylation-mediated activation of *SLAC1*, a guard cell anion channel stimulated by abscisic acid. *Science Signaling*, **7**.

Maierhofer, T., Lind, C., Huettl, S., Scherzer, S., Papenfuss, M., Simon, J., Al-Rasheid, K.A.S., Ache, P., Rennenberg, H., Hedrich, R., Mueller, T.D.and Geiger, D. (2014) A single-pore residue renders the arabidopsis root anion channel *SLAH2* highly nitrate selective. *Plant Cell*, **26**, 2554-2567.

Maresova, L.and Sychrova, H. (2010) Genetic interactions among the *ARL1* GTPase and intracellular Na^+/H^+ antiporters in pH homeostasis and cation detoxification. *Fems Yeast Research*, **10**, 802-811.

Marschner, H., Kirkby, E.A.and Cakmak, I. (1995) Effect of mineral nutritional status on shoot-root partitioning of photoassimilates and cycling of mineral nutrients. *Journal of Experimental Botany*, **47**, 1255-1263.

Miller, A.J., Fan, X.R., Orsel, M., Smith, S.J.and Wells, D.M. (2007) Nitrate transport and signalling. *Journal of Experimental Botany*, **58**, 2297-2306.

Moller, I.S., Gilliham, M., Jha, D., Mayo, G.M., Roy, S.J., Coates, J.C., Haseloff, J.and Tester, M. (2009) Shoot Na^+ exclusion and increased salinity tolerance engineered by cell type-specific alteration of Na^+ transport in arabidopsis. *Plant Cell*, **21**, 2163-2178.

Moller, I.S.and Tester, M. (2007) Salinity tolerance of Arabidopsis: a good model for cereals? *Trends Plant Sci.*, **12**, 534-540.

Moya, J.L., Gomez-Cadenas, A., Primo-Millo, E.and Talon, M. (2003) Chloride absorption in salt-sensitive Carrizo citrange and salt-tolerant Cleopatra mandarin citrus rootstocks is linked to water use. *Journal of Experimental Botany*, **54**, 825-833.

Munns, R. (2002) Comparative physiology of salt and water stress. *Plant Cell and Environment*, **25**, 239-250.

Munns, R., James, R.A., Xu, B., Athman, A., Conn, S.J., Jordans, C., Byrt, C.S., Hare, R.A., Tyerman, S.D., Tester, M., Plett, D.and Gilliham, M. (2012) Wheat grain yield on saline soils is improved by an ancestral Na^+ transporter gene. *Nat. Biotechnol.*, **30**, 360-U173.

Munns, R.and Tester, M. (2008) Mechanisms of salinity tolerance. *Annu. Rev. Plant Biol.*, **59**,

651-681.

Munns, R. and Gilliham, M. (2015) Salinity tolerance of crops – what is the cost?. New Phytol, **208**: 668–673.

Nakashima, K., Ito, Y.and Yamaguchi-Shinozaki, K. (2009) Transcriptional regulatory networks in response to abiotic stresses in arabidopsis and grasses. *Plant Physiology*, **149**, 88-95.

Negi, J., Matsuda, O., Nagasawa, T., Oba, Y., Takahashi, H., Kawai-Yamada, M., Uchimiya, H., Hashimoto, M.and Iba, K. (2008) CO2 regulator *SLAC1* and its homologues are essential for anion homeostasis in plant cells. *Nature*, **452**, 483-U413.

Okamoto, M., Kumar, A., Li, W.B., Wang, Y., Siddiqi, M.Y., Crawford, N.M.and Glass, A.D.M. (2006) High-affinity nitrate transport in roots of Arabidopsis depends on expression of the NAR2-like gene *AtNRT3.1*. *Plant Physiology*, **140**, 1036-1046.

Okumoto, S., Koch, W., Tegeder, M., Fischer, W.N., Biehl, A., Leister, D., Stierhof, Y.D.and Frommer, W.B. (2004) Root phloem-specific expression of the plasma membrane amino acid proton co-transporter *AAP3*. *Journal of Experimental Botany*, **55**, 2155-2168.

Pilot, G., Gaymard, F., Mouline, K., Cherel, I.and Sentenac, H. (2003) Regulated expression of Arabidopsis Shaker K^+ channel genes involved in K^+ uptake and distribution in the plant. *Plant Molecular Biology*, **51**, 773-787.

Pineros, M.A., Magalhaes, J.V., Alves, V.M.C.and Kochian, L.V. (2002) The physiology and biophysics of an aluminum tolerance mechanism based on root citrate exudation in maize. *Plant Physiology*, **129**, 1194-1206.

Pitman, M.G. (1982) Transport across plant roots. *Q. Rev. Biophys.*, **15**, 481-554.

Plett, D.C.and Moller, I.S. (2010) Na plus transport in glycophytic plants: what we know and would like to know. *Plant Cell and Environment*, **33**, 612-626.

Preuss, C.P., Huang, C.Y.and Tyerman, S.D. (2011) Proton-coupled high-affinity phosphate transport revealed from heterologous characterization in Xenopus of barley-root plasma membrane transporter, *HvPHT1;1*. *Plant Cell and Environment*, **34**, 681-689.

Reintanz, B., Szyroki, A., Ivashikina, N., Ache, P., Godde, M., Becker, D., Palme, K.and Hedrich, R. (2002) *AtKC1*, a silent Arabidopsis potassium channel alpha-subunit modulates root hair K^+ influx. *Proceedings of the National Academy of Sciences of the United States of America*, **99**, 4079-4084.

Ren, Z.H., Gao, J.P., Li, L.G., Cai, X.L., Huang, W., Chao, D.Y., Zhu, M.Z., Wang, Z.Y., Luan, S.and Lin, H.X. (2005) A rice quantitative trait locus for salt tolerance encodes a

sodium transporter. *Nature Genet.*, **37**, 1141-1146.

Rengasamy, P. (2006) World salinization with emphasis on Australia. *Journal of Experimental Botany*, **57**, 1017-1023.

Rengasamy, P. (2010) Soil processes affecting crop production in salt-affected soils. *Funct. Plant Biol.*, **37**, 613-620.

Roberts, S.K. (2006) Plasma membrane anion channels in higher plants and their putative functions in roots. *New phytologist*, **169**, 647-666.

Roberts, S.K.and Snowman, B.N. (2000) The effects of ABA on channel-mediated K^+ transport across higher plant roots. *Journal of Experimental Botany*, **51**, 1585-1594.

Roelfsema, M.R.G., Hedrich, R.and Geiger, D. (2012) Anion channels: master switches of stress responses. *Trends in Plant Science*, **17**, 221-229.

Roelfsema, M.R.G., Levchenko, V.and Hedrich, R. (2004) ABA depolarizes guard cells in intact plants, through a transient activation of R- and S-type anion channels. *Plant Journal*, **37**, 578-588.

Rogers, M.E., Noble, C.L., Halloran, G.M.and Nicolas, M.E. (1997) Selecting for salt tolerance in white clover (*Trifolium repens*): Chloride ion exclusion and its heritability. *New phytologist*, **135**, 645-654.

Rognes, S.E. (1980) Anion regulation of lupin asparagine synthetase-chloride activation the glutamine-utilizing reactions. *Phytochemistry*, **19**, 2287-2293.

Roy, S.J., Gilliham, M., Berger, B., Essah, P.A., Cheffings, C., Miller, A.J., Davenport, R.J., Liu, L.H., Skynner, M.J., Davies, J.M., Richardson, P., Leigh, R.A.and Tester, M. (2008) Investigating glutamate receptor-like gene co-expression in Arabidopsis thaliana. *Plant Cell and Environment*, **31**, 861-871.

Roy, S.J., Huang, W., Wang, X.J., Evrard, A., Schmoeckel, S.M., Zafar, Z.U.and Tester, M. (2013) A novel protein kinase involved in Na plus exclusion revealed from positional cloning. *Plant Cell and Environment*, **36**, 553-568.

Roy, S.J., Negrao, S.and Tester, M. (2014) Salt resistant crop plants. *Curr. Opin. Biotechnol.*, **26**, 115-124.

Roy, S.J., Tucker, E.J.and Tester, M. (2011) Genetic analysis of abiotic stress tolerance in crops. *Current Opinion in Plant Biology*, **14**, 232-239.

Roy, S.J. and Tester, M. (2012) Approaches for increasing salinity tolerance of crops, in Encyclopedia of sustainable science and Technology, R.A. Meyers, ed, Springer, New York, USA

Rudiger, M.and Oesterhelt, D. (1997) Specific arginine and threonine residues control anion

binding and transport in the light-driven chloride pump halorhodopsin. *Embo Journal*, **16**, 3813-3821.

Rus, A., Lee, B.H., Munoz-Mayor, A., Sharkhuu, A., Miura, K., Zhu, J.K., Bressan, R.A.and Hasegawa, P.M. (2004) *AtHKT1* facilitates Na^+ homeostasis and K^+ nutrition in planta. *Plant Physiology*, **136**, 2500-2511.

Sanchez, D.H., Siahpoosh, M.R., Roessner, U., Udvardi, M.and Kopka, J. (2008) Plant metabolomics reveals conserved and divergent metabolic responses to salinity. *Physiol Plantarum*, **132**, 209-219.

Sanders, D. (1980) The mechanism of Cl^- transport at the plasma-membrane of *Chara Corallina*. I. Cotranport with H^+. *Journal of Membrane Biology*, **53**, 129-141.

Schilling, R.K., Marschner, P., Shavrukov, Y., Berger, B., Tester, M., Roy, S.J.and Plett, D.C. (2014) Expression of the Arabidopsis vacuolar H plus - pyrophosphatase gene (*AVP1*) improves the shoot biomass of transgenic barley and increases grain yield in a saline field. *Plant Biotechnol. J.*, **12**, 378-386.

Schmidt, C., Schelle, I., Liao, Y.J.and Schroeder, J.I. (1995) Strong regulation of slow anion channels and abscisic-acid signaling in guard-cells by phosphorylation and dephosphorylation events. *Proceedings of the National Academy of Sciences of the United States of America*, **92**, 9535-9539.

Schroeder, J.I., Delhaize, E., Frommer, W.B., Guerinot, M.L., Harrison, M.J., Herrera-Estrella, L., Horie, T., Kochian, L.V., Munns, R., Nishizawa, N.K., Tsay, Y.F.and Sanders, D. (2013) Using membrane transporters to improve crops for sustainable food production. *Nature*, **497**, 60-66.

Schroeder, J.I.and Hagiwara, S. (1989) Cytosolic calcium regulates ion channels in the plasma-membrane of vicia-faba guard-cells. *Nature*, **338**, 427-430.

Schroeder, J.I., Schmidt, C.and Sheaffer, J. (1993) Identification of high-affinity slow anion channel blockers and evidence for stomatal regulation by slow anion channels in guard-cells. *Plant Cell*, **5**, 1831-1841.

Schulz, P., Herde, M.and Romeis, T. (2013) Calcium-dependent protein kinases: hubs in plant stress signaling and development. *Plant Physiology*, **163**, 523-530.

Segonzac, C., Boyer, J.-C., Ipotesi, E., Szponarski, W., Tillard, P., Touraine, B., Sommerer, N., Rossignol, M.and Gibrat, R. (2007) Nitrate efflux at the root plasma membrane: Identification of an Arabidopsis excretion transporter. *Plant Cell*, **19**, 3760-3777.

Shelden, M.C.and Roessner, U. (2013) Advances in functional genomics for investigating salinity stress tolerance mechanisms in cereals. *Front Plant Sci*, **4**.

Shi, H.Z., Lee, B.H., Wu, S.J.and Zhu, J.K. (2003) Overexpression of a plasma membrane Na^+/H^+ antiporter gene improves salt tolerance in Arabidopsis thaliana. *Nat. Biotechnol.*, **21**, 81-85.

Sigel, E. (1990) Use of xenopus oocytes for the functional expression of plasma-membrane proteins. *Journal of Membrane Biology*, **117**, 201-221.

Skerrett, M.and Tyerman, S.D. (1994) A channel that allows inwardly direxted fluxes of anions in protoplasts derived from wheat roots. *Planta*, **192**, 295-305.

Snider, J., Kittanakom, S., Curak, J.and Stagljar, I. (2010) Split-ubiquitin based membrane yeast two-hybrid (MYTH) system: a powerful tool for identifying protein-protein interactions. *Journal of visualized experiments : JoVE*.

Southern, E. (2006) Southern blotting. *Nat. Protoc.*, **1**, 518-525.

Storey, R., Schachtman, D.P.and Thomas, M.R. (2003) Root structure and cellular chloride, sodium and potassium distribution in salinized grapevines. *Plant Cell and Environment*, **26**, 789-800.

Storey, R.and Walker, R.R. (1999) Citrus and salinity. *Sci. Hortic.*, **78**, 39-81.

Sun, J., Dai, S., Wang, R., Chen, S., Li, N., Zhou, X., Lu, C., Shen, X., Zheng, X., Hu, Z., Zhang, Z., Song, J.and Xu, Y. (2009) Calcium mediates root K^+/Na^+ homeostasis in poplar species differing in salt tolerance. *Tree Physiology*, **29**, 1175-1186.

Tavakkoli, E., Fatehi, F., Coventry, S., Rengasamy, P.and McDonald, G.K. (2011) Additive effects of Na^+ and Cl^- ions on barley growth under salinity stress. *Journal of Experimental Botany*, **62**, 2189-2203.

Tavares, B., Domingos, P., Dias, P.N., Feijo, J.A.and Bicho, A. (2011) The essential role of anionic transport in plant cells: the pollen tube as a case study. *Journal of Experimental Botany*, **62**, 2273-2298.

Taylor, M.A., Johnson, A.D.and Smith, L.D. (1985) Growing xenopus oocytes have spare translational capacity. *Proceedings of the National Academy of Sciences of the United States of America*, **82**, 6586-6589.

Teakle, N.L., Flowers, T.J., Real, D.and Colmer, T.D. (2007) Lotus tenuis tolerates the interactive effects of salinity and waterlogging by 'excluding' Na^+ and Cl^- from the xylem. *J. Exp. Bot.*, **58**, 2169-2180.

Teakle, N.L., Real, D.and Colmer, T.D. (2006) Growth and ion relations in response to combined salinity and waterlogging in the perennial forage legumes Lotus corniculatus and Lotus tenuis. *Plant and Soil*, **289**, 369-383.

Teakle, N.L.and Tyerman, S.D. (2010) Mechanisms of Cl^- transport contributing to salt

tolerance. *Plant Cell and Environment*, **33**, 566-589.

Tester, M. (1997) Techniques for studying ion channels: An introduction. *Journal of Experimental Botany*, **48**, 353-359.

Tester, M.and Davenport, R. (2003) Na^+ tolerance and Na^+ transport in higher plants. *Ann. Bot.*, **91**, 503-527.

Tester, M.and Langridge, P. (2010) Breeding Technologies to Increase Crop Production in a Changing World. *Science*, **327**, 818-822.

Thomine, S.and Barbier-Brygoo, H. (2010) STRUCTURAL BIOLOGY A peep through anion channels. *Nature*, **467**, 1058-1059.

Tregeagle, J.M., Tisdall, J.M., Blackmore, D.H.and Walker, R.R. (2006) A diminished capacity for chloride exclusion by grapevine rootstocks following long-term saline irrigation in an inland versus a coastal region of Australia. *Australian Journal of Grape and Wine Research*, **12**, 178-191.

Tsay, Y.-F. (2014) PLANT SCIENCE How to switch affinity. *Nature*, **507**, 44-45.

Tsay, Y.F., Chiu, C.C., Tsai, C.B., Ho, C.H.and Hsu, P.K. (2007) Nitrate transporters and peptide transporters. *Febs Letters*, **581**, 2290-2300.

Tyerman, S.D. (1992) Anion channels in plants. *Annual Review of Plant Physiology and Plant Molecular Biology*, **43**, 351-373.

Umezawa, T., Sugiyama, N., Takahashi, F., Anderson, J.C., Ishihama, Y., Peck, S.C.and Shinozaki, K. (2013) Genetics and phosphoproteomics reveal a protein phosphorylation network in the abscisic acid signaling pathway in arabidopsis thaliana. *Science Signaling*, **6**.

Undurraga, S.F., Santos, M.P., Paez-Valencia, J., Yang, H., Hepler, P.K., Facanha, A.R., Hirschi, K.D.and Gaxiola, R.A. (2012) Arabidopsis sodium dependent and independent phenotypes triggered by H^+-PPase up-regulation are *SOS1* dependent. *Plant Sci.*, **183**, 96-105.

Uozumi, N., Kim, E.J., Rubio, F., Yamaguchi, T., Muto, S., Tsuboi, A., Bakker, E.P., Nakamura, T.and Schroeder, J.I. (2000) The Arabidopsis *HKT1* gene homolog mediates inward Na^+ currents in Xenopus laevis oocytes and Na^+ uptake in Saccharomyces cerevisiae. *Plant Physiol.*, **122**, 1249-1259.

Vahisalu, T., Kollist, H., Wang, Y.F., Nishimura, N., Chan, W.Y., Valerio, G., Lamminmaki, A., Brosche, M., Moldau, H., Desikan, R., Schroeder, J.I.and Kangasjarvi, J. (2008) *SLAC1* is required for plant guard cell S-type anion channel function in stomatal signalling. *Nature*, **452**, 487-U415.

Vahisalu, T., Puzorjova, I., Brosche, M., Valk, E., Lepiku, M., Moldau, H., Pechter, P., Wang, Y.-S., Lindgren, O., Salojarvi, J., Loog, M., Kangasjarvi, J.and Kollist, H. (2010) Ozone-triggered rapid stomatal response involves the production of reactive oxygen species, and is controlled by *SLAC1* and *OST1*. *Plant Journal*, **62**, 442-453.

Vanfleet, D.S. (1961) Histochemistry and function of the endodermis. *Botanical Review*, **27**, 165-220.

Waadt, R., Schmidt, L.K., Lohse, M., Hashimoto, K., Bock, R.and Kudla, J. (2008) Multicolor bimolecular fluorescence complementation reveals simultaneous formation of alternative *CBL/CIPK* complexes in planta. *Plant Journal*, **56**, 505-516.

Walker, R.R., Blackmore, D.H., Clingeleffer, P.R.and Correll, R.L. (2002) Rootstock effects on salt tolerance of irrigated field-grown grapevines (Vitis vinifera L. cv. Sultana). 1. Yield and vigour inter-relationships. *Australian Journal of Grape and Wine Research*, **8**, 3-14.

Walker, R.R., Blackmore, D.H., Clingeleffer, P.R.and Iacono, F. (1997) Effect of salinity and Ramsey rootstock on ion concentrations and carbon dioxide assimilation in leaves of drip-irrigated, field-grown grapevines (Vitis vinifera L. cv. Sultana). *Australian Journal of Grape and Wine Research*, **3**, 66-74.

Walter, M., Chaban, C., Schutze, K., Batistic, O., Weckermann, K., Nake, C., Blazevic, D., Grefen, C., Schumacher, K., Oecking, C., Harter, K.and Kudla, J. (2004) Visualization of protein interactions in living plant cells using bimolecular fluorescence complementation. *Plant Journal*, **40**, 428-438.

Wang, P., Xue, L., Batelli, G., Lee, S., Hou, Y.-J., Van Oosten, M.J., Zhang, H., Tao, W.A.and Zhu, J.-K. (2013) Quantitative phosphoproteomics identifies SnRK2 protein kinase substrates and reveals the effectors of abscisic acid action. *Proceedings of the National Academy of Sciences of the United States of America*, **110**, 11205-11210.

Wang, Y.-F., Triin, V., Julian, S., Jaakko, K., Hannes, K., Noriyuki, N., Wai-Yin, C., Gabriel, V., Lamminmaki, A., Mikael, B., Heino, M.and Radhika, D. (2008) *SLAC1* is required for plant guard cell S-type anion channel function in stomatal signalling. *Plant Biology (Rockville)*, **2008**, 120-120.

Wang, Y.-Y., Hsu, P.-K.and Tsay, Y.-F. (2012) Uptake, allocation and signaling of nitrate. *Trends in Plant Science*, **17**, 458-467.

Wege, S., De Angeli, A., Droillard, M.-J., Kroniewicz, L., Merlot, S., Cornu, D., Gambale, F., Martinoia, E., Barbier-Brygoo, H., Thomine, S., Leonhardt, N.and Filleur, S. (2014) Phosphorylation of the vacuolar anion exchanger AtCLCa is required for the stomatal

response to abscisic acid. *Science Signaling*, **7**.

Wege, S., Jossier, M., Filleur, S., Thomine, S., Barbier-Brygoo, H., Gambale, F.and De Angeli, A. (2010) The proline 160 in the selectivity filter of the Arabidopsis $NO3^-/H^+$ exchanger AtCLCa is essential for nitrate accumulation in planta. *Plant Journal*, **63**, 861-869.

White, P.J.and Broadley, M.R. (2001) Chloride in soils and its uptake and movement within the plant: A review. *Ann. Bot.*, **88**, 967-988.

Winter, D., Vinegar, B., Nahal, H., Ammar, R., Wilson, G.V.and Provart, N.J. (2007) An "Electronic Fluorescent Pictograph" Browser for Exploring and Analyzing Large-Scale Biological Data Sets. *Plos One*, **2**.

Xu, G.H., Magen, H., Tarchitzky, J.and Kafkafi, U. (2000) Advances in chloride nutrition of plants. In *Advances in Agronomy, Vol 68*. San Diego: Academic Press Inc, pp. 97-150.

Yeo, A.R., Yeo, M.E.and Flowers, T.J. (1987) The contribution of an apoplastic pathway to soudium uptake by rice roots in saline conditions. *J. Exp. Bot.*, **38**, 1141-1153.

Yoo, S.D., Cho, Y.H.and Sheen, J. (2007) Arabidopsis mesophyll protoplasts: a versatile cell system for transient gene expression analysis. *Nat. Protoc.*, **2**, 1565-1572.

Zheng, X., He, K., Kleist, T., Chen, F.and Luan, S. (2015) Anion channel SLAH3 functions in nitrate-dependent alleviation of ammonium toxicity in Arabidopsis. *Plant Cell and Environment*, **38**, 474-486.

Zheng, Z., Xu, X., Crosley, R.A., Greenwalt, S.A., Sun, Y., Blakeslee, B., Wang, L., Ni, W., Sopko, M.S., Yao, C., Yau, K., Burton, S., Zhuang, M., McCaskill, D.G., Gachotte, D., Thompson, M.and Greene, T.W. (2010) The protein kinase SNRK2.6 mediates the regulation of sucrose metabolism and plant growth in arabidopsis. *Plant Physiology*, **153**, 99-113.

Zhu, J.-K. (2003) Regulation of ion homeostasis under salt stress. *Current Opinion in Plant Biology*, **6**, 441-445.

Zimmermann, P., Hirsch-Hoffmann, M., Hennig, L.and Gruissem, W. (2004) Genevestigator. Arabidopsis microarray database and analysis toolbox. *Plant Physiology*, **136**, 2621-2632.

Appendix 1

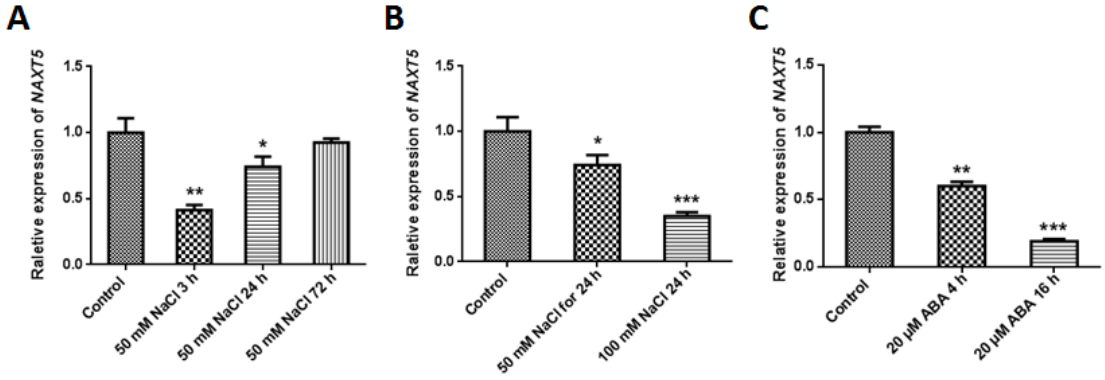

Figure A1. *AtNPF2.4* expression is down-regulated by both salt (NaCl) and ABA. Four-week old Col-0 Arabidopsis plants were treated with NaCl or ABA as indicated before (Section 3.8). Whole roots were harvested for qRT-PCR analysis. (A) *NPF2.4* transcripts detected in the root of plants treated with 50 mM NaCl for 3 h, 24 h, or 72 h. Control plants were treated with 2 mM NaCl for 3 h. (B) *NPF2.4* transcripts detected in the root of plants treated with 2 mM (control), 50 mM or 100 mM NaCl for 24 h. (C) *NPF2.4* transcripts detected in the root of plants treated with 20 µM +/– cis, trans ABA for 4 h or 16 h. Results are presented as mean ± SEM (n = 4 or 5), expression levels were normalized to controls. Significance is indicated by the asterisks (one way ANOVA and Tukey test, *$P \leqslant 0.0.5$; **$P \leqslant 0.01$;***$P \leqslant 0.001$).

This data was included in a submitted manuscript “Bo Li, et al. (2015) NPF2.4 facilitates chloride loading of the xylem in Arabidopsis”

Further results I contributed to this submitted manuscript were shown in Figure 4.13 (Chapter 4).

Appendix 2

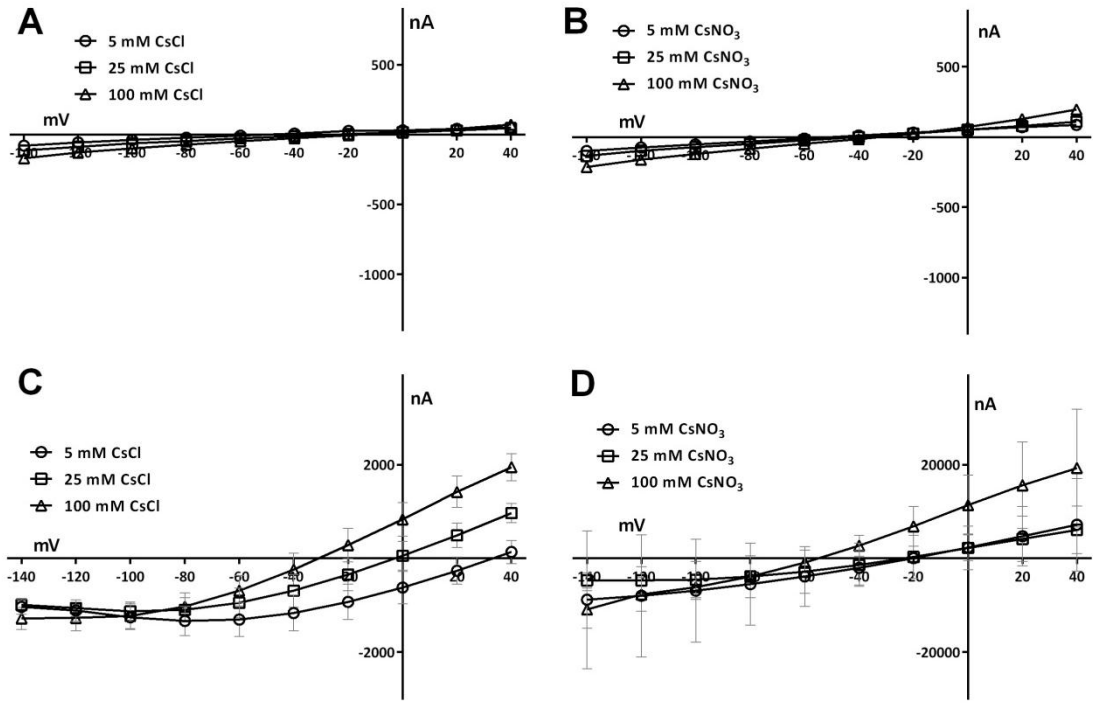

Figure A2. Electrophysiolocal characterization of ΔSLAH3 in *X. laevis* oocytes. (**A-D**) Whole cell currents (steady states) in response to 3 second voltage pluses from +40 mV to -140 mV for ΔSLAH3 cRNA and RNA-free water injected oocytes were recorded. (**A**) RNA free water injected oocytes perfused with 5, 25 and 100 mM CsCl at pH 7.5 (mean ± SEM, n= 3); (**B**) RNA free water injected oocytes perfused with 5, 25 and 100 mM $CsNO_3$ at pH 7.5; (mean ± SEM, n= 3); (**C**) *ΔSLAH3* injected oocytes perfused with 5, 25 and 100 mM CsCl at pH 7.5 (mean ± SEM, n= 6); (**D**) *ΔSLAH3* injected oocytes perfused with 20 and 50 mM $CsNO_3$; with 20, 50 mM CsCl at pH 7.5; with 5, 25 and 100 mM $CsNO_3$ (mean ± SEM, n= 6); Data were presented without water subtraction.

Appendix 3

These are the vectors that I used in this project, including entry vector (pCR8 Gateway), destination vector, pGEMHE (*X.laevis* oocytes expression), pTOOL5 (GAL4 cell-type specific over expression), pMDC32 (35S over expression), pYEST-DEST52 (Yeast expression), pUC-SPYCE, pUC-SPYNE (BiFC) and pR300 (amiRNA).

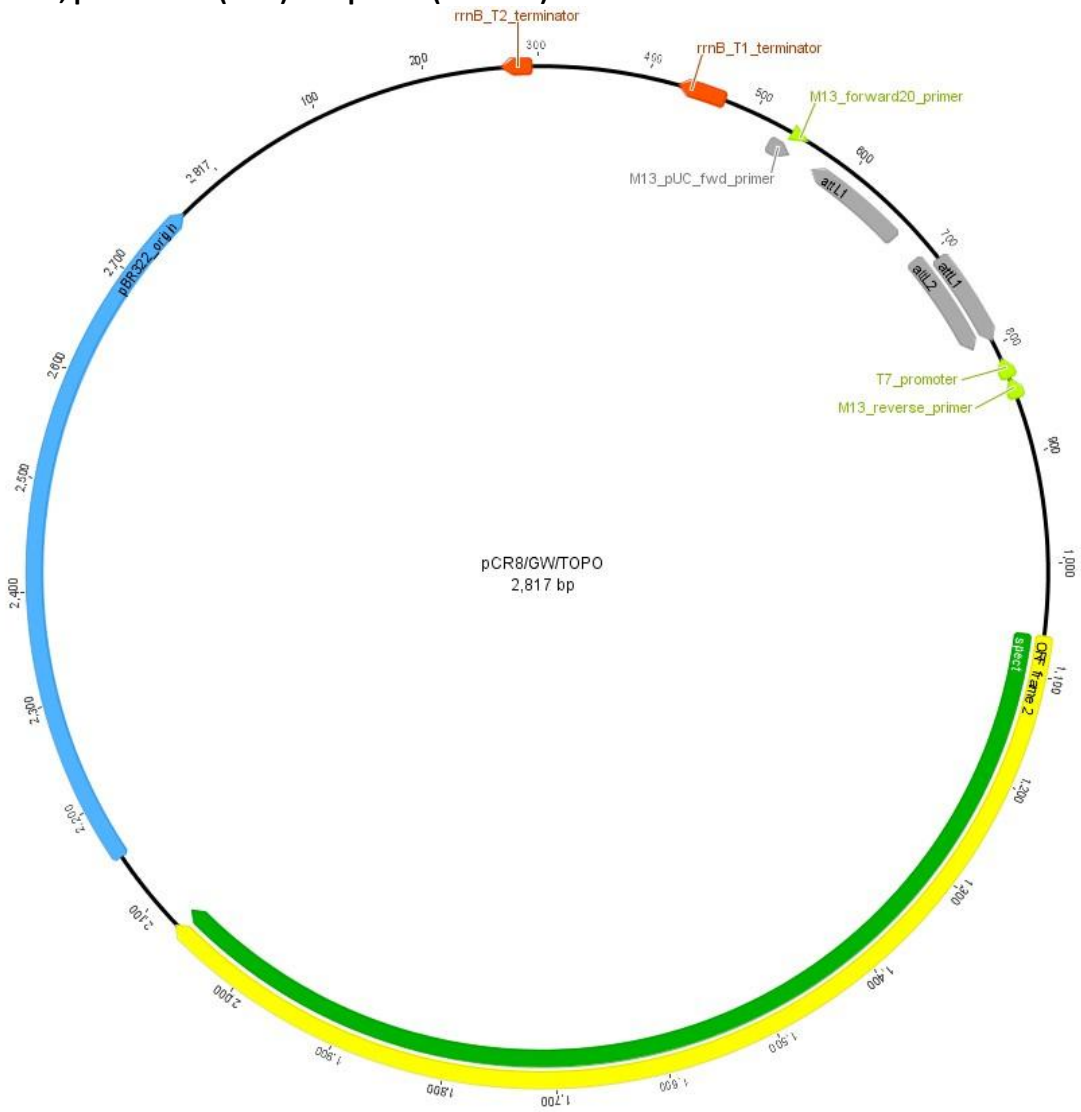

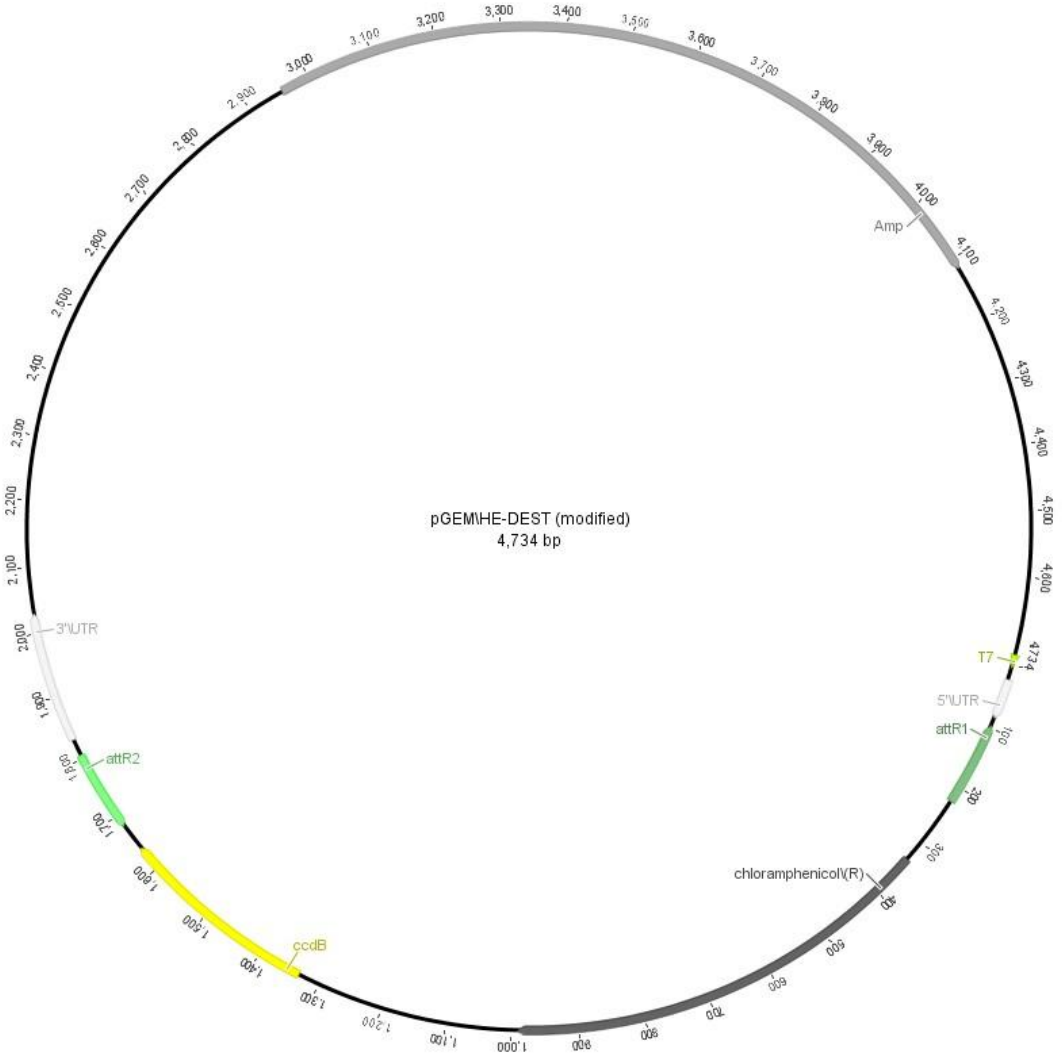
pGEM\HE-DEST (modified)
4,734 bp
Amp
T7
5'\UTR
attR1
chloramphenicol\(R)
ccdB
attR2
3'\UTR

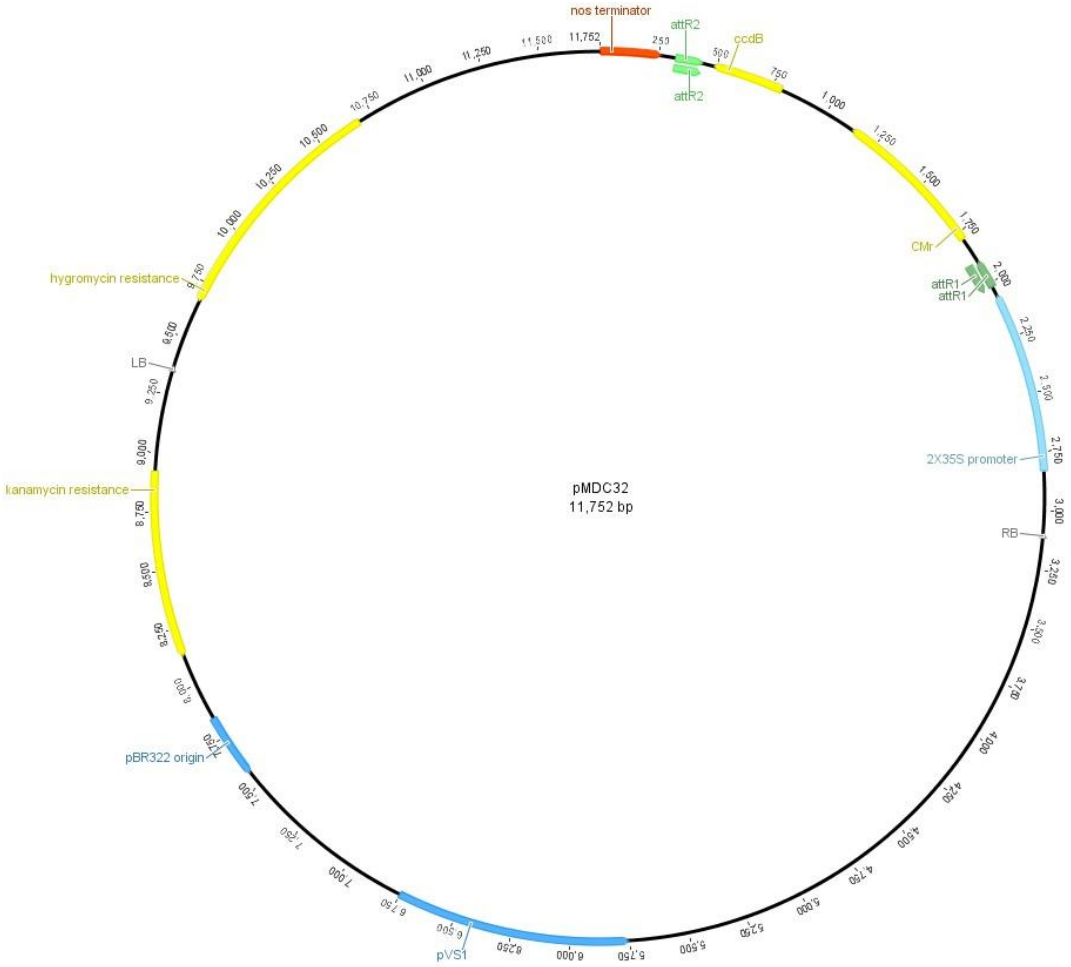
nos terminator
attR2
attR2
ccdB
CMr
attR1
attR1
2X35S promoter
RB
pVS1
pBR322 origin
kanamycin resistance
LB
hygromycin resistance
pMDC32
11,752 bp

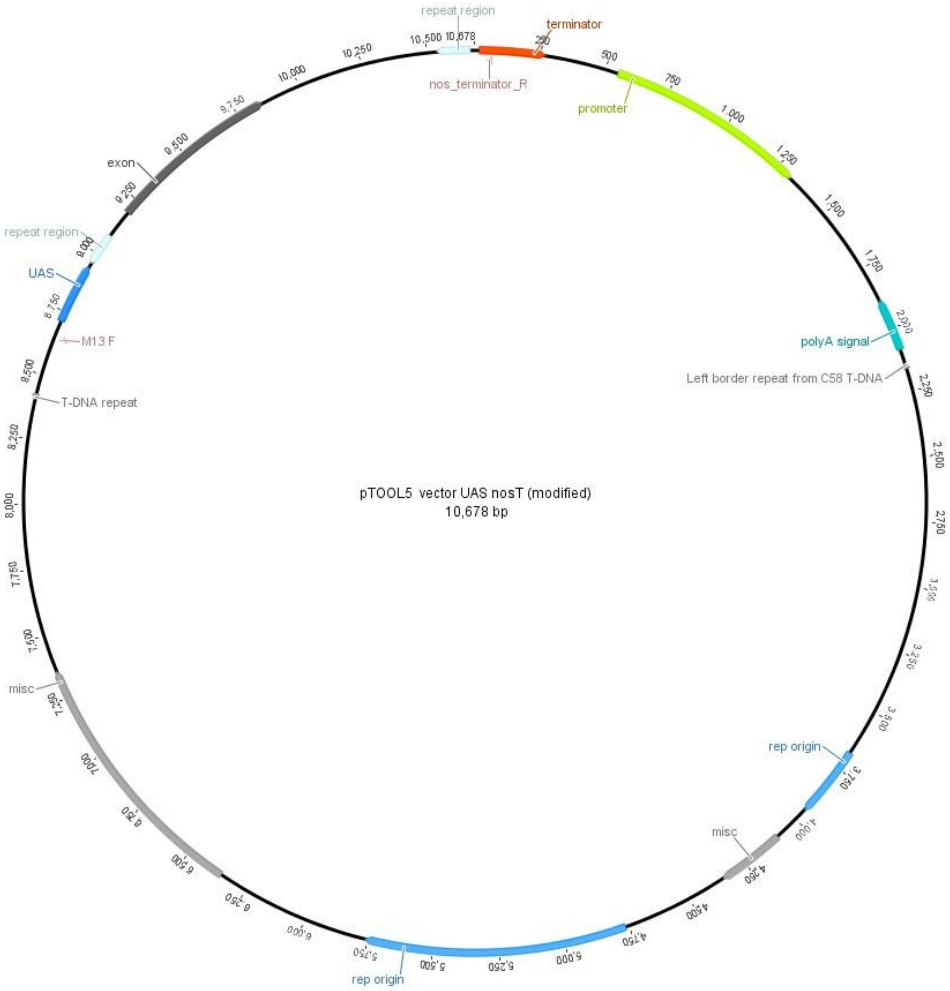
repeat region
terminator
nos_terminator_R
promoter
exon
repeat region
UAS
M13 F
T-DNA repeat
polyA signal
Left border repeat from C58 T-DNA
misc
rep origin
misc
rep origin
pTOOL5 vector UAS nosT (modified)
10,678 bp

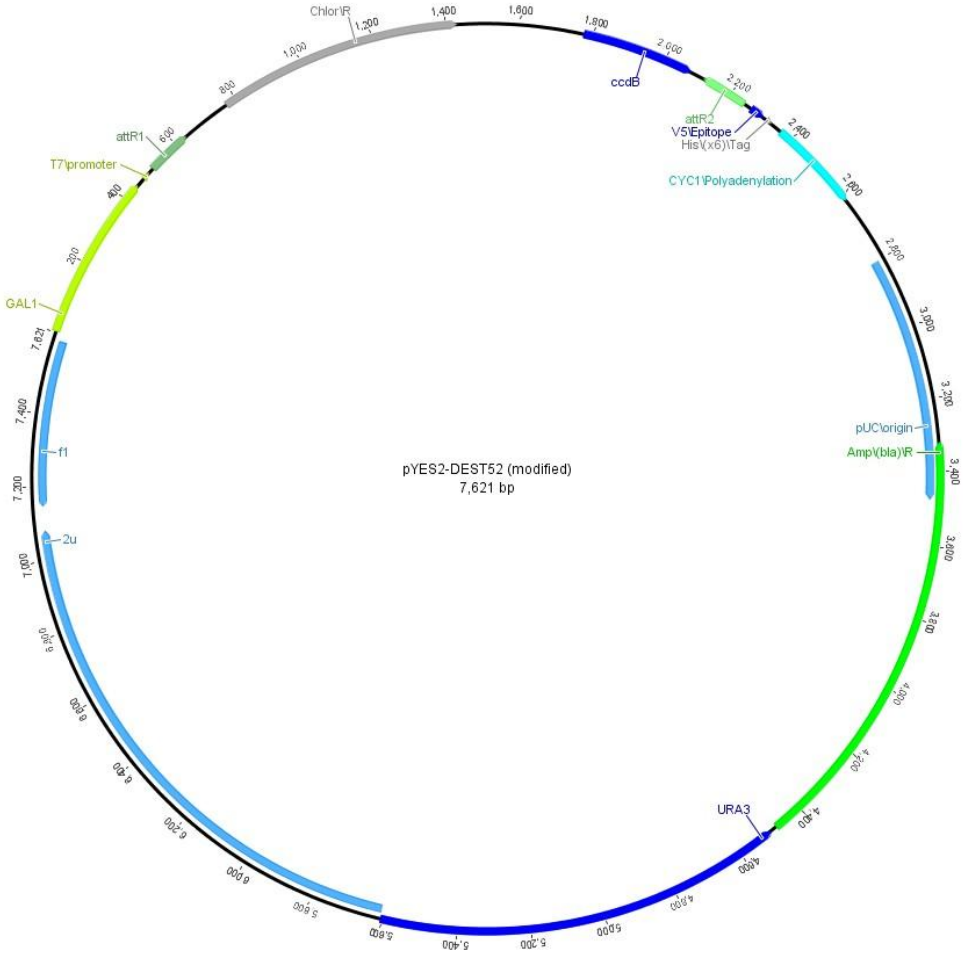
pYES2-DEST52 (modified)
7,621 bp
Chlor\R
ccdB
attR2
V5\Epitope
His\(x6)\Tag
CYC1\Polyadenylation
pUC\origin
Amp\(bla)\R
URA3
2u
f1
GAL1
T7\promoter
attR1

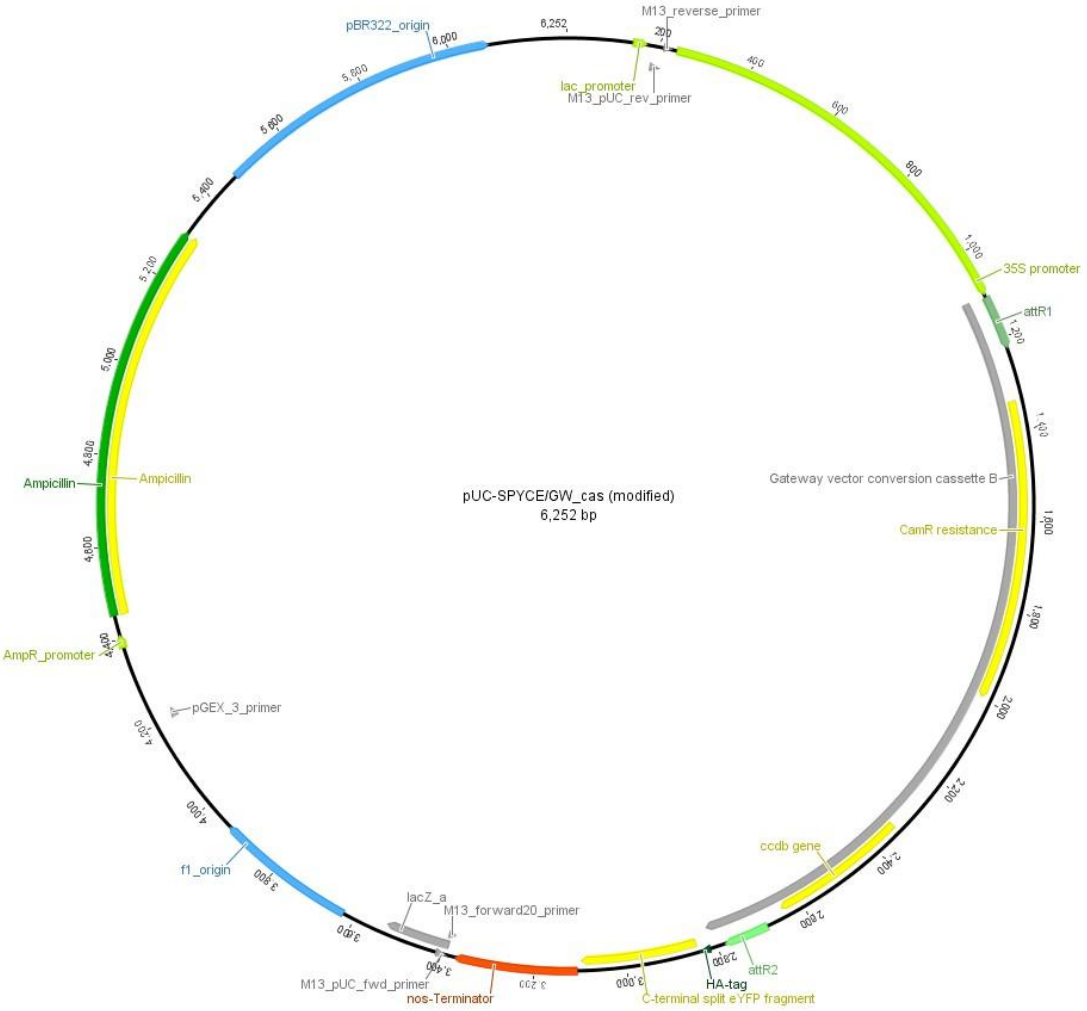
pUC-SPYCE/GW_cas (modified)
6,252 bp
M13_reverse_primer
pBR322_origin
lac_promoter
M13_pUC_rev_primer
35S promoter
attR1
Gateway vector conversion cassette B
CamR resistance
ccdb gene
attR2
HA-tag
C-terminal split eYFP fragment
lacZ_a
M13_forward20_primer
M13_pUC_fwd_primer
nos-Terminator
f1_origin
pGEX_3_primer
AmpR_promoter
Ampicillin
Ampicillin

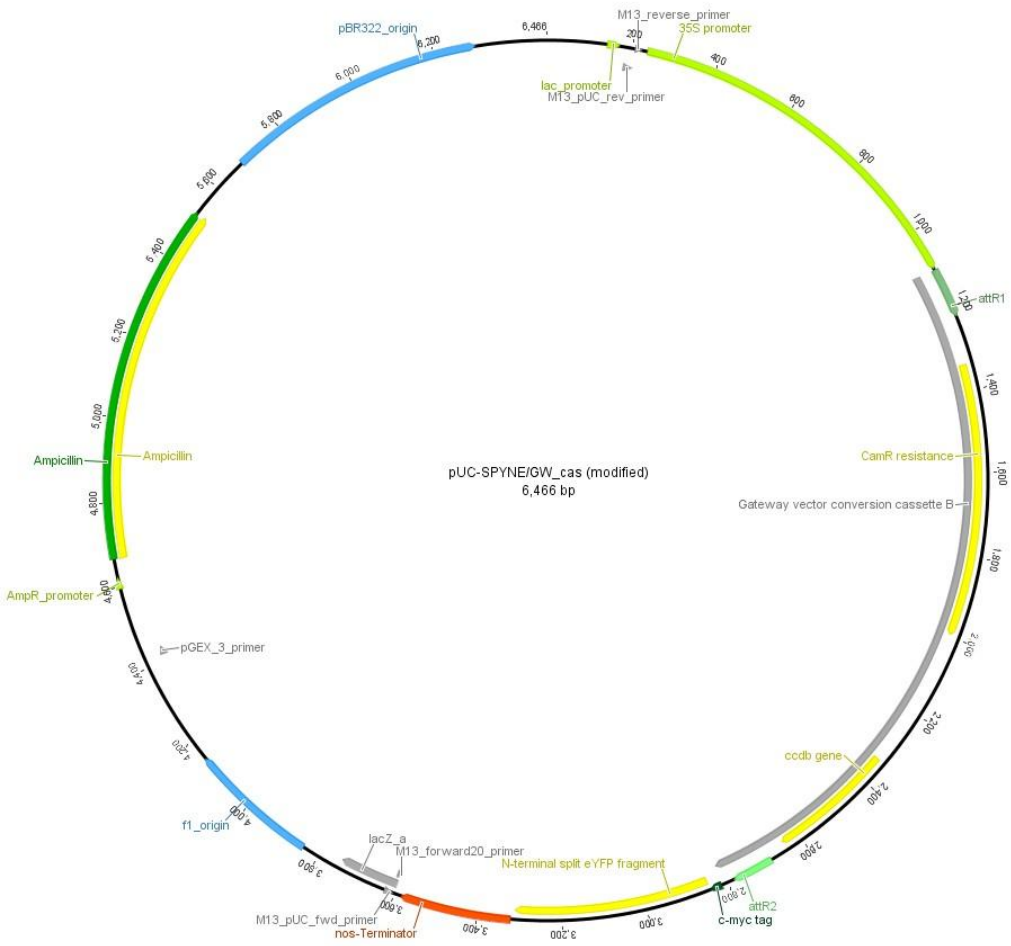
pUC-SPYNE/GW_cas (modified)
6,466 bp
M13_reverse_primer
35S promoter
lac_promoter
M13_pUC_rev_primer
attR1
CamR resistance
Gateway vector conversion cassette B
ccdb gene
attR2
c-myc tag
N-terminal split eYFP fragment
lacZ_a
M13_forward20_primer
M13_pUC_fwd_primer
nos-Terminator
f1_origin
pGEX_3_primer
AmpR_promoter
Ampicillin
Ampicillin
pBR322_origin

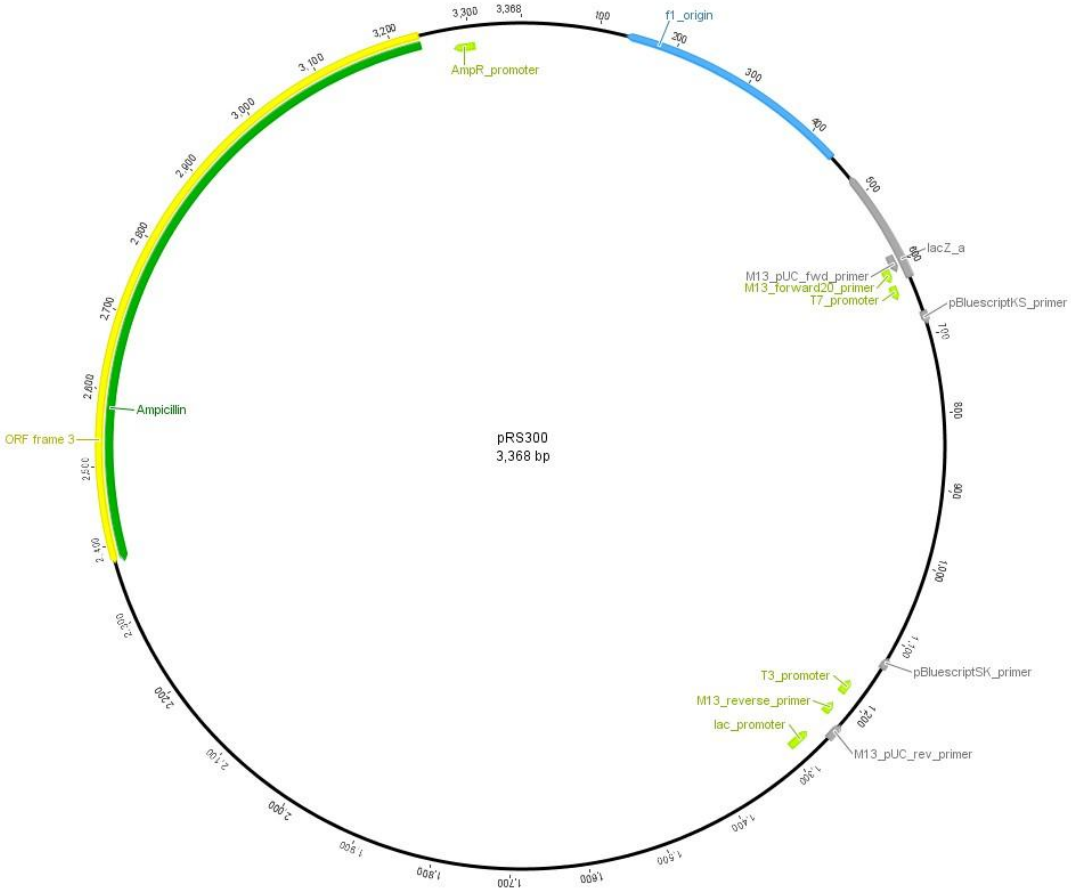
pRS300
3,368 bp
AmpR_promoter
f1_origin
lacZ_a
M13_pUC_fwd_primer
M13_forward20_primer
T7_promoter
pBluescriptKS_primer
Ampicillin
ORF frame 3
T3_promoter
M13_reverse_primer
lac_promoter
pBluescriptSK_primer
M13_pUC_rev_primer

Appendix 4

Table A1. T-DNA knock out lines ordered from NASC

GOI	AGI	SALK Line	other T-DNA insertion lines	Name on NASC
AtCLCc	At5g49890		GABI_633B04	N460688
AtNRT1.5	At1g32450	SALK_063393C		N675535
AtNRT1.8	At4g21680		GABI_756D01	N472517
			GABI_725B08	N469524
AtNRT1.9	At1g18880		GABI_099B01	N409421
			GABI_284B09	N427189
			GABI_457G09	N443857
SLAC1	At1g12480	SALK_099145C		N664784
		SALK_137265		N637265
SLAH1	At1g62280	SALK_039811C		N679554
		SALK_039811		N539811
SLAH2	At4g27970		GABI_414C04	N439676
		SALK_130318		N630318
SLAH4	At1g62262	SALK_144196		N644196
		SALK_091937C		N676198
AtABCB14	At1g28010	SALK_016005 C		N516005
		SALK_026876C		N654111
AtAAP3	At1g77380	SALK_148822C		N669236

Appendix 5

Method optimizations

1 Optimization of yeast growth in small volumes of liquid media

In addition to examine the GOI function by performing the yeast serial dilutions on solid media, the comparison of yeast growth rate differences of empty vector control and GOI expressing yeast in liquid growth media is also widely employed in characterizing the GOI function. The conventional method for determining the growth rate is to grow the yeast transformants in 10 mL SD galactose liquid media and the OD_{600nm} value of each replicates are measured every few hours. The overall growth rate is plotted using the OD_{600nm} value against time. This method is ideal for characterizing the gene that has profound differences in growth rate compared to the empty vector control. However, we cannot expect that all the candidate genes to necessarily have such a pronounced phenotype. Therefore, a modified liquid assay method, that more frequently measures the OD value over the whole time course might help us to distinguish a smaller difference between GOI and control yeast growth. A microplate reader (BMG LABTECH, Germany) available in our lab enables the recording of the OD value continually in a 96-well plate and this was used to characterize the yeast growth rate in a small volume. Meanwhile, compared to the traditional liquid assay which is time consuming and cumbersome, the assay performed in the microplate offers an opportunity to test more replicates in an efficient and productive way.

Yeast with the GOI expressed was cultured in SD glucose media as described above. The yeast cells were harvested at the exponential growth stage and resuspended in SD media. Instead of growing the yeast culture in 10 mL with a start OD_{600nm} value at 0.2, 200 µL of culture was transferred to each well of the microplate and the OD_{600nm} value was adjusted to 0.01. The OD value was recorded every 15 minutes over 40 hours. However, we found that it was difficult to show consistent results even with the same experimental settings (Figure 2.2). For instance, to test the transport properties of AtSLAH1, yeast expressed with *AtSLAH1* was cultured in galactose based liquid media (with/without 250 mM KCl) and empty vector expressed yeast was used as the control. In Figure 1 A and B, the growth rate of SLAH1 expressed yeast was decreased when 250 mM KCl was presented, however, when the experiment was repeated under same conditions (Figure 1 C and D), the results were inconsistent with previous data. In order to acquire repeatable and reliable results, several

optimizations were performed, as described below, to improve the small volume liquid assay.

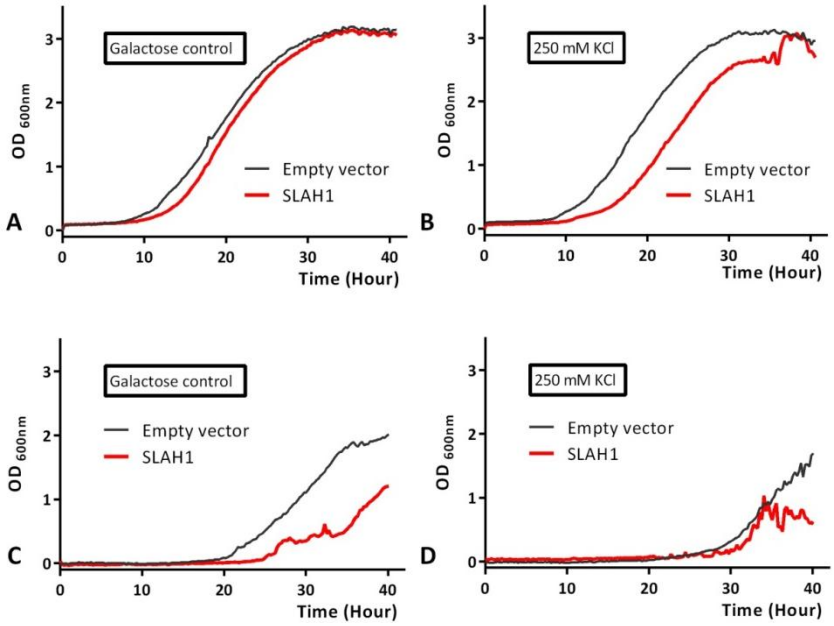

Figure 1 A-D Initial results from yeast growth inhibition assay when expressing the empty vector (pYES2-DEST52) and *SLAH1* were cultured in the small volumes of liquid media. A and **B**, first experiment; **C** and **D** the repeat; both experiments have same experimental settings. **A** and **C**, yeast grown in galactose liquid media; **B** and D, yeast grown in galactose liquid media with 250 mM KCl.

1.1 Maintaining consistent pH is vital for yeast growth in small liquid volumes

The pH value is adjusted to 5.6 with NaOH or KOH in the SD yeast growth media, which provides an ideal pH (pH 5.6- 6.5) for yeast growth. However, during yeast growth the pH value in the media may change due to H^+ release; this may differ between control and GOI expressing yeast due to the interaction of gain of transporter function and H^+ release. If the pH is changed significantly it may no longer be suitable for yeast growth and development, and lead to an observed phenotype that is not directly related to the GOI function. Therefore, to maintain a consistent pH during the measurement period, 20 mM MES (2-N-morpholino ethane-sulfonic acid) was used to buffer the pH between 5.5- 5.6 (Marešová*et et al*., 2007). Figure 2 showed that with 20 mM MES, the pH value of media was maintained at 5-6 after 40 hours incubation (Figure 2 B, D and F). In contrast, the pH value dropped to 3-4 within the media without MES after 40 hours (Figure 2 A, C and E). The results suggested that with additional MES present in the media, the pH value was stable and the yeast growth rate was less variable. Therefore, 20 mM MES was added to the liquid media as a pH buffer before the media pH value was adjusted to 5.6 with 1 M KOH.

	Control	500 mM KCl	500 mM KNO_3
Without MES	pH 3-4 (Fig. A)	pH 3-4 (Fig. C)	pH 3-4 (Fig. E)
With MES	pH 5-6 (Fig. B)	pH 5-6 (Fig. D)	pH 5-6 (Fig. F)

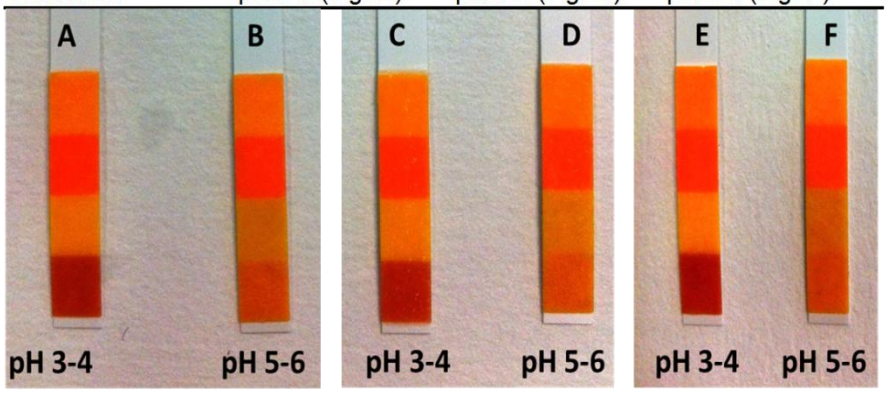

Figure 2 The pH value was measured in *NRT1.5* expressed yeast in galactose based liquid media (with/without 20 mM MES) with 500 mM KCl or 500 mM KNO_3 after 40 hours incubation. (A) galactose control media; **(B)** galactose control media with 20 mM MES; **(C)** galactose media with 500 mM KCl; **(D)** galactose media with 500 mM KCl plus 20 mM MES; **(E)** galactose media with 500 mM KNO_3; **(F)** galactose media with 500 mM KNO_3 plus 20 mM MES.

1.2 Pre-incubation before testing

In order to characterize the GOI transport properties in yeast, high concentrations of salt such as 500 mM NaCl and KCl were added into the growth media. If the growth rate was affected by the additional salt, it would be consistent with a role for that gene in ion transport. However, high concentrations of salt will also raise the media's osmolality and stress the yeast cell. Although the yeast strain we used is not sensitive to some of ions such as potassium, the growth rate will still be decreased due to the osmotic shock. To avoid the complication of measuring a combined osmotic shock with any GOI transport related phenotype when salt was initially applied, both control and GOI transformed yeast were pre-incubated in the testing growth media (i.e. with salt) for a few hours, but glucose was used as carbon source to avoid GOI expression. The yeast cell were harvested when the growth reached to the exponential stage and resuspended in testing media (with galactose). The OD value was adjusted to 0.01 and 200 µL of culture was transferred to microplate.

1.3 Optimizing incubation conditions

In the conventional yeast liquid assays cultures are shaken to keep the yeast cells in suspension. The microplate assay protocol initially included regular shaking. However, it was interesting to observe that the growth rate fluctuated between the sampling points, when shaking was applied, which resulted in large errors among the replicates. Shaking of the solution may led to aggregations of yeast cells within the wells, particularly at the cell wall,

and as absorbance is measured the bottom of the well, inaccurate OD value may have been measured. When the shaking process was completely removed, the deviation between the sampling points was reduced and the growth curve was smoother than before. When the micro-plate was incubated with shaking the OD value of empty vector expressed yeast incubated in glucose media reduced after 30 hours incubation (Figure 3 red line), which must be artifactual because the cell density cannot decrease over time. When the shaking was removed (Figure 3black line), the OD value was maintained at the similar value during the stationary phase. Therefore, for the yeast growth rate assay to be optimal when using small liquid volumes in the plate reader it is best not to use shaking.

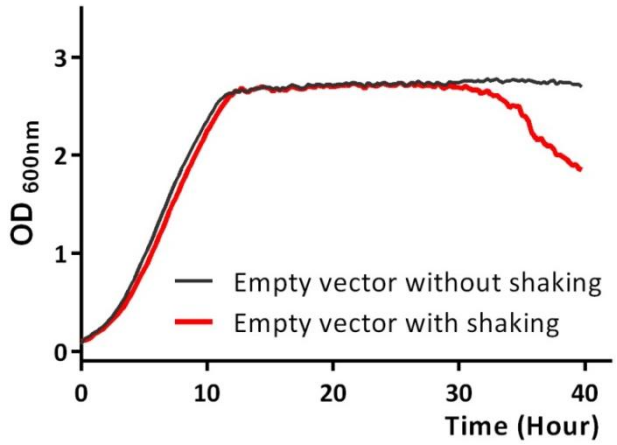

Figure 3 The growth rate of empty vector expressed yeast difference at the platform stage with (red line) or without shaking (black line).

2 Optimization of the hydrazine reduction method for nitrate analysis

2. 1 Modified hydrazine reduction nitrate analysis

Reagents were prepared strictly following the previous protocol (Downes *et al*., 1978) including 2 mM copper sulfate ($CuSO_4$), 211.34 µM hydrazine sulfate ($H_6N_2O_4S$), 1 M sodium hydroxide (NaOH), 2.5% (w/v) sulphanilamide and 0.5% (w/v) N-Naphthyl ethylenediamine ($C_{12}H_{14}N_2$). Various concentrations of KNO_3 were used as standards. Standards were prepared fresh before the experiment.

In a previous study, the nitrate assay was performed using an Autoanalyzer, which automatically added reagents in order. Samples and reagents then were well- mixed through a series of filtering and heating processes. The absorbance of the solution was recorded and evaluated by comparing with a calibration curve. Here, a Microplate Reader ((BMG LABTECH, Germany) that enables the reading of absorbance was employed for quick and accurate measurement of the $OD_{540\,nm}$ value. The nitrate concentration was then calculated using a previously established standard curve. Briefly, 25 µL of nitrate extraction was added to a transparent flat- bottom 96- well plate (Greine, Sigma) followed by adding 15 µL of 2 mM

$CuSO_4$ and 10 µL hydrazine sulfate. Mixtures were incubated at 37°C for 5 minutes. Before shaking the plate for 60 seconds, 15 µL of Sodium hydroxide (2 M) was added. When the mixture was mixed by vortex, the plate was incubated at 37 °C for 10 minutes. While the mixture was incubated, sulphanilamide (0.1 % w/v) and N-Naphthyl ethylenediamine (2 % w/v) was mixed in a 1:1 volume ratio and kept in the dark. Once the incubation was finished, 100 µL of sulphanilamide and *N*-Naphthyl ethylenediamine mixture was added into the plate, followed by 10 minutes incubation at room temperature. The absorbance of each sample in the plate was measured at $OD_{540\ nm}$. The calculation of nitrate concentration was based on the linear regression equation generated using a standard curve.

2.2 Standards

To analyse the Arabidopsis shoot nitrate concentration, a standard curve which was within the range of the samples concentration was generated. Initially, a serial of known concentrations of potassium nitrate (KNO_3) were used as standards which ranged from 0 mM– 5 mM. A standard curve was constructed according to the relationship between KNO_3 concentrations and measured optical density ($OD_{540\ nm}$). However, the curve was not linear when KNO_3 concentration was lower than 1 mM or higher than 4 mM (R^2= 0.9037), which was not ideal for accurately determining the concentration of an unknown sample. After excluding the non-linear region from the previous standard curve, a linear standard curve was given (R^2= 0.9979). By altering the KNO_3 concentrations used in the standard curve a reliable linear relationship was observed between 0.6 mM to 3.0 mM (R^2= 0.9937).

2.3 Dilution factors

For accurate determination of the nitrate concentration it was necessary to control the sample concentration within range of the standard curve. Previous studies showed that Arabidopsis shoot nitrate concentration various from 2-20 mM depends on the availability of nitrate/ammonium in the growth conditions (Krapp *et al.*, 2014), which could exceed the detection limitations of this protocol. In addition, Arabidopsis grown under control conditions (low NaCl) showed significantly higher nitrate concentration than those grown under salt (high NaCl) treatment. Therefore, a dilution of the Arabidopsis shoot nitrate extract was performed. Typically, a five- fold dilution was normally applied to the nitrate extractions that isolated Arabidopsis (Col-0) grown under BNS (control) growth media, whereas no dilution was applied to extract from plants treated with 75 mM NaCl for 7 days.

2.4 Recovery test

The method (Downes *et al*., 1978) was designed for measuring the nitrate in water and sewage. To confirm its accuracy and sensitivity, several different ions such as Cl^-, Ca^+ and Mg^{2+} that are commonly found in water sources were tested for potential interference in measuring procedures (Downes *et al*., 1978). Compared to water or sewage, Arabidopsis shoot nitrate extraction not only contains those ions but also contains chlorophyll and other substances that might affect the testing accuracy. Therefore, a recovery test was performed to examine whether there was any interference from these factors.

First of all, the nitrate extraction solution isolated from 10 mg freeze- dried shoot tissue (Arabidopsis, Col-0) was diluted by 4, 8 and 10 fold with MQ water. The amount of nitrate in the tissues was determined following the protocol described above. $OD_{540\ nm}$ values were recorded and the nitrate concentration was calculated according to the linear regression equation generated from the standard curve. Once the Arabidopsis shoot nitrate concentration was known for a particular sample, the same amount of KNO_3 was combined with the original dried powder of the test sample to determine array's the recovery rate. For example, if the data indicated that the nitrate concentration for a particular 10 mg of dried Arabidopsis shoot tissue (Col-0) was 7.42 mM, the original dried tissue powder was diluted in 1 mL of 7.42 mM of KNO_3 (instead of in 1 mL MQ water) and another nitrate extraction performed. Theoretically, the nitrate concentration value should be double because of extra input of KNO_3. The data, shown in Table 1, indicated the KNO_3 recovery ranged from 98.9-101.4 %. As such, this modified protocol was determined suitable for measuring Arabidopsis shoot nitrate.

Table 1 The recovery test performed using one sample with different dilution factors.

Original		Recovery			
Dilution factor	Nitrate con.(mM)	KNO_3 added (mM)	Dilution factor	Nitrate con. (mM)	Recovery (%)
4	7.875	7.8	8	15.758	100.05
8	7.418	7.4	16	14.991	101.04
10	7.641	7.6	20	15.121	98.95

The optimized hydrazine reduction nitrate analysis method described above was able to determine the Arabidopsis shoot nitrate concentration accurately. However, due to a limited linear range for the final determination, most of samples required multiple fold dilutions, which become time consuming especially when dealing with large amount of samples. Also, some chemical reagents that were used in the protocol were expensive. Therefore, another rapid nitrate assay method was selected and optimized for measuring the Arabidopsis shoot

nitrate content.

2.5 Optimizing the colorimetric determination of nitrate by nitration of salicylic acid

This method uses salicylic acid to form a chromophore with nitrate that absorbs maximally at 410 nm under alkaline conditions (pH > 12) (Cataldo *et al*., 1975). Compared to the hydrazine reduction method, this protocol has its advantages, firstly, only simple chemicals are employed in the reaction including salicylic acid, sulphuric acid and sodium hydroxide; secondly, this protocol has a wider measurement range than the previous method, from 0–60 mM NO_3^- (Cataldo *et al*., 1975).

2.5.1 Identifying nitrate concentration in small sample volumes

The main optimization performed was reducing the reaction size per sample in order to determine the NO_3^- concentrations on limited amount of Arabidopsis shoot tissue, and so the assay could be performed in a 96- well microplate in the Microplate Reader. In a previous study (Okamoto *et al*., 2006), 100 mg of freeze- dried Arabidopsis tissue was used as several samples were mixed before measurement. While I'm working with individual plant, therefore a smaller size is required. Due to the nature of Arabidopsis shoot size, only limited tissue is available per each plant. Therefore, there was a need to scale-down all aspects of this protocol. It is suggested that the ratio between the SA-H_2SO_4 and water input (3:1) is crucial for maintaining the testing accuracy. Consequently, all the chemical reagents were reduced to maintain the ratios between chemicals. In detail, 3– 5 mg of Arabidopsis dried tissue was dissolved in 0.5 mL deionized water, and 0.05 mL of extraction was incubated with 0.2 mL of 5% (w/v) SA-H_2SO_4. After finishing the incubation, only 0.05 mL of mixture was transferred into a fresh tube, and 0.95 mL of 2N NaOH was added. When the mixture was fully cooled down, a 0.2 ml of aliquot was transferred to a transparent 96-well plate for reading the absorbance at OD_{410nm}.

2.5.2 Recovery test

Dried Arabidopsis tissue (10 mg) was used in this assay, and the original concentration was shown in Table 2. The same concentration of KNO_3 was made and used to dissolve another 10 mg of dried tissue from same sample batch. A new nitrate extraction was performed and the concentration was examined following the exactly same procedures. Results showed that the recovery was ranging from 99.8-100.8 %. The recovery rate was similar compared to the published protocol (cataldo *et al*., 1975), which confirmed the accuracy of this rapid nitrate

assay protocol.

Table 2 The recovery test

	Original		Recovery		
	OD $_{410\ nm}$	**con. (mM)**	**KNO_3 added (mM)**	**Nitrate con. (mM)**	**Reovery (%)**
Sample 1	0.27	7.07	7	14.12	99.8585573
Sample 2	0.036	1.69	1.7	3.41	100.887574